Filtering and Model Predictive Control of Networked Nonlinear Systems

by

Huiping Li
B.Eng., Northwestern Polytechnical University, 2006
M.Sc., Northwestern Polytechnical University, 2009

A Dissertation Submitted in Partial Fulfillment of the
Requirements for the Degree of

DOCTOR OF PHILOSOPHY

in the Department of Mechanical Engineering

Filtering and Model Predictive Control of Networked Nonlinear Systems

by

Huiping Li
B.Eng., Northwestern Polytechnical University, 2006
M.Sc., Northwestern Polytechnical University, 2009

Supervisory Committee

Dr. Yang Shi, Supervisor
(Department of Mechanical Engineering)

Dr. Daniela Constantinescu, Departmental Member
(Department of Mechanical Engineering)

Dr. Wu-Sheng Lu, Outside Member
(Department of Electrical and Computer Engineering)

Supervisory Committee

Dr. Yang Shi, Supervisor
(Department of Mechanical Engineering)

Dr. Daniela Constantinescu, Departmental Member
(Department of Mechanical Engineering)

Dr. Wu-Sheng Lu, Outside Member
(Department of Electrical and Computer Engineering)

ABSTRACT

Networked control systems (NCSs) present many advantages such as easy installation and maintenance, flexible layouts and structures of components, and efficient allocation and distribution of resources. Consequently, they find potential applications in a variety of emerging industrial systems including multi-agent systems, power grids, tele-operations and cyber-physical systems. The study of NCSs with nonlinear dynamics (i.e., nonlinear NCSs) is a very significant yet challenging topic, and it not only widens application areas of NCSs in practice, but also extends the theoretical framework of NCSs with linear dynamics (i.e., linear NCSs). Numerous issues are required to be resolved towards a fully-fledged theory of industrial nonlinear NCS design. In this dissertation, three important problems of nonlinear NCSs are investigated: The robust filtering problem, the robust model predictive control (MPC) problem and the robust distributed MPC problem of large-scale nonlinear systems.

In the robust filtering problem of nonlinear NCSs, the nonlinear system model is subject to uncertainties and external disturbances, and the measurements suffer from time delays governed by a Markov process. Utilizing the Lyapunov theory, the algebraic Hamilton-Jacobi inequality (HJI)-based sufficient conditions are established for designing the $\mathcal{H}_\infty$ nonlinear filter. Moreover, the developed results are specialized

for a special type of nonlinear systems, by presenting the HJI in terms of matrix inequalities.

For the robust MPC problem of NCSs, three aspects are considered. Firstly, to reduce the computation and communication load, the networked MPC scheme with an efficient transmission and compensation strategy is proposed, for constrained nonlinear NCSs with disturbances and two-channel packet dropouts. A novel Lyapunov function is constructed to ensure the input-to-state practical stability (ISpS) of the closed-loop system. Secondly, to improve robustness, a networked min-max MPC scheme are developed, for constrained nonlinear NCSs subject to external disturbances, input and state constraints, and network-induced constraints. The ISpS of the resulting nonlinear NCS is established by constructing a new Lyapunov function. Finally, to deal with the issue of unavailability of system state, a robust output feedback MPC scheme is designed for constrained linear systems subject to periodical measurement losses and external disturbances. The rigorous feasibility and stability conditions are established.

For the robust distributed MPC problem of large-scale nonlinear systems, three steps are taken to conduct the studies. In the first step, the issue of external disturbances is addressed. A robustness constraint is proposed to handle the external disturbances, based on which a novel robust distributed MPC algorithm is designed. The conditions for guaranteeing feasibility and stability are established, respectively. In the second step, the issue of communication delays are dealt with. By designing the waiting mechanism, a distributed MPC scheme is proposed, and the feasibility and stability conditions are established. In the third step, the robust distributed MPC problem for large-scale nonlinear systems subject to control input constraints, communication delays and external disturbances are studied. A dual-mode robust distributed MPC strategy is designed to deal with the communication delays and the external disturbances simultaneously, and the feasibility and the stability conditions are developed, accordingly.

Contents

List of Tables

List of Figures

Acronyms

NCS Networked control system

ISS Input-to-state stability

ISpS Input-to-state practical stability

RPI Robust positively invariant

RHOMPC Receding horizon open-loop MPC

RHE Moving horizon estimation

RCI Robust control invariant

RHC Receding horizon control

HJI Hamilton-Jacobi inequality

LMI Linear matrix inequality

BMI Bilinear matrix inequality

LSCD Linear subsystems with coupled dynamics

LSDD Linear subsystems with decoupled dynamics

NSCD Nonlinear subsystems with coupled dynamics

NSDD Nonlinear subsystems with decoupled dynamics

LMPC Lyapunov-based model predictive control

MPC Model predictive control

S-C Sensor-to-controller

C-A Controller-to-actuator

TCP Transmission Control Protocol

UDP User Datagram Protocol

TS Time-stamped

GPC Generalized predictive control

EKF Extended Kalman filter

UKF Unscented Kalman filter

ACKNOWLEDGEMENTS

I first would like to express my sincerest thanks to my advisor Dr. Yang Shi, for his continuous and intensive guidance, encouragement and support during the last four years. His vision and knowledge on networked control systems is remarkable, steering me in the right direction; his thoughts and suggestions to academic problems are insightful and inspirational, providing me valuable resources to solve challenging problems; his sense and passion of conducting world-class research is really encouraging, driving me to achieve better and higher. Dr. Yang Shi is not only a great mentor but also a trusted friend to me. He always provided me friendship-like encouragement and support whenever I was frustrated, and has been offering constructive advice to my career development since the beginning of the Ph.D. program. I greatly appreciate him and feel so proud and fortunate under his supervision.

Next, I would like to thank the thesis committee members, Dr. Wu-Sheng Lu and Dr. Daniela Constantinescu for their constructive comments and valuable suggestions to improve the quality of this dissertation. In particular, I would like to give my special thanks to Dr. Wu-Sheng Lu for his guidance and instruction on optimization, which inspired me to work out a robust distributed MPC algorithm.

I am so privileged to have had such excellent colleagues and friends in the research group at the University of Victoria. I am particularly grateful to Dr. Jian Wu for his helps on computer softwares and mathematics, to Ji Huang for the discussions with him on NCSs and Markov process, to Dr. Hui Zhang for sharing his experiences on LMIs with me, and to Xiaotao Liu for his discussions on MPC. I also greatly thank Mingxi Liu, Binxian Mu, Yanjun Liu, Wenbai Li, Fuqiang Liu, Ping Cheng, Sina Doroudgar, Yang Lin, Qiao Zhang, Yuanye Chen, Cao Shen, Yiming Zhao, Xue Zhang, Kevin Lorette, Peter Lu, Dr. Yingyan Zhao, Dr. Fang Fang, Dr. Zexu Zhang and Dr. Le Wei, for their valuable discussions and suggestions during the group meetings, which have improved me. In addition, I would like to thank Patrick Chang, who provided a lot of helps in my TA jobs and daily life.

Finally, I gratefully acknowledge the financial support from the Chinese Scholarship Council (CSC), the Natural Sciences and Engineering Research Council of Canada (NSERC), Canada Foundation for Innovation (CFI), the Department of Mechanical Engineering and the Faculty of Graduate Studies (FGS) at the University of Victoria, the IEEE Control System Society (CSS), Mr. Alfred Smith and Mrs. Mary Anderson Smith Scholarship and Dr. Esme Foord Graduate Scholarship.

To my wife and my parents.

Chapter 1

Introduction

1.1 Networked Control Systems

Networked control systems (NCSs) play essential roles in many emerging industrial applications such as intelligent transportation systems, power grids, water distributed systems, cyber-physical systems, sensor network systems, tele-operation and haptics systems, and multi-agent systems. Broadly speaking, the NCSs are referred to as control systems among which the information (data) is transmitted or shared via communication networks. So far, the research direction of NCSs can be divided into three categories [173, 164]: (1) control of communication networks, (2) control over communication networks, and (3) networked multi-agent systems.

- **Control of communication networks** [42]: This type of research is mainly focused on how to design efficient and real-time communication networks, such as networking protocol design, network congestion management and routing control.

- **Control over communication networks** [173, 42]: This type of study is concerned with the problems on designing feedback control laws an/or filtering strategies to (adapt to) unreliable communication networks such that the closed-loop system is stabilized or achieves certain control performance, which is the focus of the dissertation.

- **Networked multi-agent systems** [164, 173]: The research effort is devoted to designing network topologies, distributed control laws and/or filtering strategies to address the changes of network connections and network imperfections,

such that some global control objective can be achieved. This problem is also investigated in the dissertation. An example of a networked multi-agent system consisting of eight mobile robots (i.e., agents or subsystems) is demonstrated in Figure 1.1. In this multi-agent system, the information can be exchanged among these robots via communication networks to achieve expected global control and/or filtering objectives.

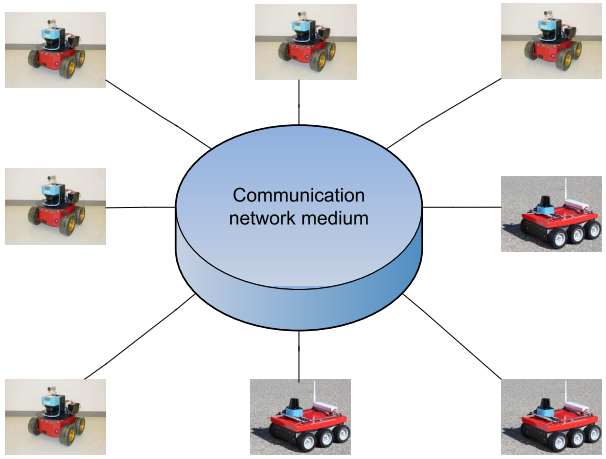

Figure 1.1: An example of a networked multi-agent system.

In comparison with traditional control systems, NCSs enable spatial distribution and placement of components through multi-purpose networks, offering many advantages:

- **Reducing system cost**: In NCSs, all information is transmitted through shared communication networks, and thus multiple system wirings among sensors, controllers and actuators can be simplified by a simple communication link or even a wireless communication link. As a result, great amounts of system wirings are reduced and the power consumption may also be reduced accordingly, resulting in a significant decrease of system cost, especially for large-scale systems.

- **Easing installation and maintenance**: Due to the communication networks, the controllers, sensors and actuators can be freely installed in a large space unlike traditional control systems in which the controllers, sensors and actuators are generally located together in a limited space. The distributed NCS structure also facilitates fault detections and isolations. For example, if an NCS does not

work or fails, one can easily isolate the controller, sensor and actuator, test them one by one, and replace the malfunctioned one conveniently.

- **Increasing structural flexibility and facilitating resource allocations**: The communication networks also bring flexibility in optimizing the locations of controllers, which leads to compact and efficient system design, saving space and system resources. In addition, the remote connection and flexible structure between the controller and plant fits particularly well with the requirements of some special applications such as tele-operation systems, space operation and control systems, and remote control in nuclear plants.

When taking a look at the other side of the "coin", however, the deployment of communication networks also brings unreliability and uncertainty in the control loop, posing great challenges for NCS design and its applications. To overcome these obstacles, two types of measures can be taken. On the one hand, the infrastructure of the communication channels and communication protocols should be improved or redesigned, which falls within the research on control of networks. On the other hand, the control methodologies for NCSs should be developed and enhanced to remedy imperfections induced by the communication networks. It has been reported that the latter aspect is of significant importance towards building reliable, robust and effective NCSs, and thus has received tremendous attention during last decade; see, e.g., the survey papers in [42, 1, 169, 47] and references therein.

The main issues induced by imperfect communication networks are recognized as three aspects: (1) network-induced time delays; (2) data losses or packet dropouts; (3) sampling errors and quantization issues.

- **Networked-induced delays**: Time delays in NCSs are very likely to occur mainly due to bandwidth limits and network traffic congestions, especially in large-scale and shared networks. In general, the time delays can be modeled as deterministic and random ones.

    a. Deterministic delays: In this type of delay characterizations, the delays are further modeled as constant time delays, such as [178, 152] and time-varying delays, e.g., [106, 48]. To deal with time delays, two types of sufficient conditions for guaranteeing closed-loop system stability have been proposed. The first type is called delay-independent conditions which are

irrelevant to time-delay characteristics, for example, [98, 38, 49]. In contrast, the second type of conditions are named as delay-dependent conditions which are explicitly dependent on delay characteristics; see, e.g., [43, 92, 58]. The delay-dependent conditions facilitate the efficient use of delay information, thus reducing conservatism.

b. Random delays: For the random time delays, three methods of delay modeling are available. In the first case, the occurrence of time delays is characterized as a Bernoulli process [137]. Since the Bernoulli process is only able to model two random states and it ignores mutual effects of delays among different time instants, Markov chains have been utilized to model random delays capturing more information; see, e.g., [108, 53, 141, 140]. The third type of random model of time delays is semi-Markov processes [10], which are of more general features. Yet, the system analysis and design become more complicated.

- **Packet dropouts**: Packet dropout is also called data loss or data missing in the literature, which is another critical network-induced constraint in NCS design. The packet dropouts may bring undesired phenomena such as oscillations and erratic behaviors, and even destabilize the closed-loop system. In a digital network, it has been reported in [42] that the packet dropouts are mainly caused by physical link failures, buffer overflowing and long time delays. There are several different ways of modeling packet dropouts, which are summarized in the following.

  a. Consecutive and constant packet dropouts. This is the simplest way of modeling packet dropouts, which is suitable for periodical physical link failures and data errors; see, e.g., [72].

  b. Bernoulli-type packet dropouts. In this model, the packet dropouts occur according to a certain probability $0 < p < 1$ and the data is transmitted successfully with the probability $1 - p$. This modeling is able to capture stochastic properties of the packet dropouts, and is also mathematically easy to deal with. Thus, it is widely employed in NCSs [47, 157, 175, 142].

  c. Markov chain-type packet dropouts. In this type of packet-dropout modeling, the data missing occurs according to a Markov process, which is more informative and practical than the Bernoulli-type model; see, e.g.,

[140, 177, 54].

d. Arbitrary packet dropouts with bounded occurrence length. This type of modeling is particularly useful for many practical applications in which the stochastic model of the packet dropouts is unknown or unavailable, but the maximum number of packet dropouts can be tested. The work that utilizes this type of models can be referred to [113, 119, 74, 73].

- **Sampling error and quantization**: The sampling and quantization error is generated due to signal transmission and transformation over communication networks. In NCSs, the control signal to plant is required to be in a continuous-time format, but the controller is apt to deal with digital signal. Therefore, on the one hand, to transmit measurement signals from sensor (continuous-time signals) to controller over networks, the signal must be sampled and encoded in a digital format before transmission. On the other hand, after the actuator receives the encoded digital signal from controller, it must be decoded and converted to a continuous-time format. Since the sampling rates and the word lengths of a packet are limited, the quantization and sampling errors will be unavoidable. To analyze stability and further improve control performance, a lot of results have been developed for dealing with quantization and sampling errors; see the papers in [37, 167, 172, 149] and references therein.

In addition, there are also some other important issues to deal with towards building reliable, robust, effective and secure NCSs, such as the fault detection and fault-tolerant control of NCSs [12], bandwidth allocation [51], network scheduling [76], real-time control [2], network security [29], and so on.

1.2 Review of Related Literature

This section provides an overview of existing work of NCSs directly related to this dissertation, including three parts: nonlinear filtering and estimation of NCSs, model predictive control (MPC) of NCSs and distributed MPC of large-scale systems.

1.2.1 Nonlinear Filtering and Estimation of NCSs

The filtering and estimation problem is one of the most important issues in the area of systems and control. Filtering can be applied in many problems including output

feedback control, system modeling, and fault-detection and monitoring. The filtering and estimation problem in NCSs has been a very active research area and many promising results have been reported in the literature. In various network environments, the filtering and estimation problem of NCSs with linear system dynamics (i.e., linear NCSs) has been extensively investigated. The readers are referred to the survey papers in [178, 47, 42], the theses in [170, 174] and references therein.

In comparison with the filtering and estimation problem of linear NCSs, the problem of NCSs with nonlinear system dynamics (i.e., nonlinear NCSs) is even more important and interesting, since the nonlinear filtering design can find more applications and may theoretically generalize corresponding linear system results as special cases. However, the design and analysis of nonlinear filters for NCSs is more challenging because the properties of superposition and homogeneity are, in general, not valid for nonlinear systems.

In the literature, one way to studying filtering problem of nonlinear NCSs is based on conventional nonlinear estimation approaches such as Extend Kalman Filter (EKF) and Unscented Kalman Filter (UKF). In this framework, the disturbances are modeled as white noises and the algorithms of EKF and/or UKF are redesigned to accommodate communication constraints induced in NCSs. For example, in [65], Kulge *et al.* has proven the stochastic stability of the EKF with intermittent observations, where the availability of the measurement is modeled as a Bernoulli process and a two-step EKF has been designed. In [52], the stability of EKF with stochastic nonlinearities and multiple missing measurements is investigated and the upper bound of the filtering error covariance is established. The stability of UKF with measurement dropouts is reported in [75].

Another approach to dealing with filtering problem of nonlinear NCSs is the so-called robust filtering scheme. This scheme has two advantages over EKF or/and UKF: (1) it can deal with non-Gaussian disturbances without knowing exact models of disturbances; (2) it highly efficient to handle system parameter uncertainties and network communication constraints. As a result, the robust nonlinear filtering scheme has enjoyed great popularity in NCSs and a lot of results have been reported in studying communication delays, packet dropouts, quantization errors and other issues.

So far, most of these results are developed for special types of nonlinear NCSs, in which the treatment of the nonlinear terms can be converted to dealing with linear terms by utilizing the properties of the involved special nonlinear terms. As a

result, the communication constraints and parameter uncertainties can be efficiently accommodated by borrowing existing methods from linear NCSs. And the linear matrix inequalities (LMI) or/and bilinear matrix inequalities (BMI) techniques can be utilized to design the robust filters.

For example, in [159, 18, 168, 17, 19], the $\mathcal{H}_\infty$ filtering problem of nonlinear NCSs with sector-bounded nonlinearities has been studied and the LMI-based stability conditions have been developed accordingly. Among them, the communication delay has been considered in [19, 168]; the packet-dropout issue has been studied in [18, 168, 17]; the sensor saturation effect has been addressed in [17, 159]. In [161, 139, 20, 138], the robust $\mathcal{H}_\infty$ filters and estimators of nonlinear NCSs with randomly occurring nonlinearities have been designed, and the LMI-based sufficient conditions have been proposed. In these results, the measurement missing problem is dealt with in [161, 138]; the quantization effect is addressed in [139] and the sensor saturation problem is considered in [20]. In [135], the robust distributed $\mathcal{H}_\infty$ filtering has been designed for nonlinear sensor networks with polynomial nonlinearities.

In addition, there are a few results studying the robust $\mathcal{H}_\infty$ filtering problem of general nonlinear NCSs without simplifying models. In [136], Shen *at el.* investigate the robust $\mathcal{H}_\infty$ filtering problem of a class of nonlinear NCSs with packet dropouts, and the nonlinear conditions for guaranteeing stability of the closed-loop system have been developed. In [137], the $\mathcal{H}_\infty$ filtering problem has been investigated for a class of stochastic nonlinear systems with sensor delays modeled by a Bernoulli process and the filtering design conditions have been proposed. In [160], the nonlinear filtering problem is considered in a network environment, where the random packet losses and the quantization effects are incorporated into the filtering design.

To be more informative, the aforementioned results of filtering design of nonlinear NCSs are summarized in the following Table 1.1.

Nonlinear form	Time delay	Data loss	Quantization	Saturation
Sector-bounded	[19][168]	[18][168][17]		[17][159]
Randomly occurring		[161][138]	[139]	[20]
Polynomial			[135]	
General	[137]	[136][160][65] [52][75]	[160]	

Table 1.1: Recent results on filtering of nonlinear NCSs.

1.2.2 MPC-based Control of NCSs

The MPC-based approach to studying NCSs is of appealing features in comparison with other approaches. Firstly, the MPC strategy can generate a sequence of future control signals by optimizing a control performance function at each time instant. The generated future control sequence is particularly effective in compensating for communication constraints in NCSs such as packet dropouts and delays. Secondly, the MPC is capable of handling various system constraints including input constraints and state constraints, which is also desired in many NCS applications. Thirdly, there have been a lot of applications of MPC in many practical industrial systems [95] [115] [116]. Thus, the study of MPC for NCSs would facilitate the modification and advancement of network-based control applications.

In the literature on NCSs, some promising results on MPC have been developed for addressing different communication constraints. Some of the results are documented here in terms of linear NCS design and nonlinear NCS design.

For linear NCSs, an early result is reported in [148], where Tang *et al.* propose a novel generalized predictive control (GPC) algorithm to design the control packets; the compensation strategy including the buffer design is developed to address both the control-to-actuator (C-A) and sensor-to-controller (S-C) delays; the designed algorithm is tested for the control of a dual-axis hydraulic positioning system using an Ethernet-based communication network. But the closed-loop stability is not analyzed in [148]. In [162], Wu *et al.* design an MPC strategy for NCSs with C-A and S-C delays modeled by two independent Markov chains, in which the stability and feasibility issues have been investigated and the LMI-based conditions have been developed. In [171], the modified GPC algorithm is designed for NCSs with two-channel Markov delays and the stability analysis is conducted. The min-max MPC design problem of wireless sensor networks has been investigated in [13]. In [122], the packetized predictive control problem of stochastic systems over bit-rate limited channels with packet losses has been investigated, where the dropout is modeled by a Bernoulli process, but only the C-A packet dropout is considered. In [37], Goodwin *et al.* investigate the moving horizon control problem of stochastic NCSs with quantization effects in one communication channel.

Furthermore, there is another research line worthwhile to mention. In contrast to the control packets designed by optimizing a control performance function, the control prediction signal is simply generated by designing an observer or a predictor based

on the system model. In this framework, the disturbances and model uncertainties can also be easily accounted by designing $\mathcal{H}_\infty$ control scheme and the LMI-based conditions can be developed for guaranteeing closed-loop stability. For example, the networked predictive controller design problem by considering the random time delays is studied in [79, 80, 153, 154]; both the time delays and packet dropouts are simultaneously addressed in [78, 163].

In comparison with MPC-based control of linear NCSs, the study of nonlinear NCSs using MPC scheme is more attractive, yet more challenging due to intrinsic complexity of nonlinearities. With the help of existing techniques of nonlinear MPC, some promising results of networked nonlinear MPC have been developed in the literature. In [114], Polushin *et al.* develop a model-based approach to studying a class of nonlinear sampled-data systems and they propose a novel strategy to compensate for communication delays. Based on the Lyapunov-based MPC (LMPC) scheme, Muñoz de la Peña *et al.* study the networked state feedback control problem of nonlinear systems subject to data losses in [100], where the networked controller works in a sample-and-hold fashion; they further investigate the corresponding output feedback problem in [102]; the LMPC scheme of nonlinear NCSs with time-varying measurement delays is reported in [85]. In [120], Quevedo *et al.* investigate the discrete-time nonlinear NCSs with disturbances and C-A packet dropouts modeled by a Bernoulli process, and they prove the closed-loop stability in the sense of input-to-state stability (ISS). Furthermore, they extend the result [120] for considering the C-A packet dropouts modeled by a Markov chain in [121, 129]. In [113], Pin *et al.* design a unified framework of MPC-based control strategy for discrete-time nonlinear NCSs, in which the system constraints, the packet dropouts and the time delays are considered, and the recursive feasibility and regional ISS stability of the closed-loop system have been analyzed. Most recently, the MPC-based networked control problem for hybrid systems in presence of packet dropouts is studied and the ISS of the closed-loop system is established in [87].

For the sake of comparison and discussion, the MPC-based results of NCSs are classified in Table 1.2.

1.2.3 Distributed MPC of Large-scale Systems

In the framework of using MPC-based approach to studying large-scale systems, there are three schemes available in the literature, namely, centralized MPC, distributed

Type of systems	Time delay	Data loss	Quantization
Linear NCSs	[148][162] [171][13] [79][80] [153][154][78][163]	[122][78][163]	[37]
Nonlinear NCSs	[114][113]	[100][102][85][120] [121][129][113][87]	

Table 1.2: Recent results on MPC-based control of NCSs.

MPC and decentralized MPC. The centralized MPC treats the whole large-scale system as an ordinary one with high-dimension system states and designs only a central model predictive controller to regulate it. The techniques for centralized MPC algorithm design are trivial by following the well-developed MPC and this scheme is generally too computational expensive to be implemented in practice. On the contrary, the decentralized MPC decouples the whole large-scale system into many independent subsystems, and a local MPC algorithm is designed to regulate each subsystem. The decentralized MPC algorithm design is a direct application of the classical MPC theory. However, it has been shown [127] that the decentralized MPC only works for large-scale systems in which the subsystems are weakly coupled; for these with strong couplings among subsystems, this scheme is likely to lead to an unstable system or unsatisfactory control performance.

In comparison with those two MPC schemes, the distributed MPC treats the whole large-scale system as many subsystems and each subsystem is able to communicate with some other subsystems. A local model predictive controller is designed for each subsystems, but each local controller can exchange information with some other subsystems to account for couplings among them. In this way, the distributed MPC is computationally efficient while achieving comparable control performance to the centralized MPC. It is worth noting that the distributed MPC is heavily dependent on communication networks among subsystems. The design of communication strategies is nontrivial, especially for unreliable communication networks, and the system performance analysis is very challenging.

The last decade has witnessed great progress in distributed MPC addressing many different issues such as state partitioning, nonlinearities, system constraints, disturbances, communication constraints, and so on. In the literature on distributed MPC, one research direction is to design distributed MPC algorithms for large-scale systems in which there are strong coupled system dynamics among subsystems.

Along this line, the results on distributed MPC problem of large-scale linear sys-

tems are reported in [7, 57, 99, 145, 27, 150]. In [7], the authors study the distributed MPC design problem of large-scale systems with subsystems coupled by system states and they propose an approach to partitioning system states and designing the communication mechanism. In [57], the min-max distributed MPC design problem of the same system has been studied. In [99], an optimal partitioning scheme is proposed to group the subsystems by balancing the open-loop controllability and closed-loop stability. In [150], Venkat *et al.* investigate the distributed MPC problem for large-scale systems with both coupled state and control input; the local model predictive controllers are designed to achieve plant-wide objectives through iterative cooperation and communications within a sampling interval; the designed algorithm is applied to the distributed control of a power system. A cooperative distributed MPC scheme is developed for large-scale systems with input constraints in [145]; the solution is proven to converge to the plant-wide Pareto optimum. A non-cooperative distributed MPC algorithm with neighbor-to-neighbor communication is proposed for large-scale linear systems in [27] where the set invariant theory is utilized to analyze the stability of the overall system.

The distributed MPC problem of large-scale nonlinear systems has been studied in [83, 81, 84, 82, 46, 45, 146]. In [83], Liu *at el.* study the distributed MPC problem of a nonlinear system using the LMPC scheme, in which the control input is artificially partitioned into two parts and two local Lyapunov-based model predictive controllers are designed to generate the whole control input. In [81], they extend the result in [83] by considering multiple control inputs partitioning, and both the sequential distributed MPC and iterative distributed MPC schemes are proposed. Furthermore, by considering the occurrence of asynchronous and delayed measurements, they generalize the result in [83] for non-iterative scheme in [84] and for iterative scheme in [82], respectively. Based on these results, the same problem is studied by considering the noises and data losses in the communication channels among the local controllers in [45]; the multi-rate distributed LMPC design is further reported in [46]. In [146], Stewart *et al.* investigate the distributed MPC problem for nonlinear systems with both coupled state and input, wherein the distributed MPC algorithm is designed through distributed gradient projection. In [21], Dunbar designs a distributed MPC strategy for a class of continuous-time nonlinear systems by proposing a consistency constraint to guarantee closed-loop stability.

Another research direction is focused on distributed MPC design for large-scale systems consisting of completely decoupled subsystems (agents) but with coupled

control objective functions and/or system constraints. These large-scale systems are particularly useful to model multi-agent systems such as vehicle platoons, multi-robot systems and even biological systems. Therefore, the design of distributed MPC scheme for such systems has attracted a lot of attention. Specifically, the results in this direction can be further divided into two categories.

- **Cooperative control of multi-agent systems using distributed MPC**. In [130], Richards *et al.* have designed a robust distributed MPC scheme for a group of decoupled linear subsystems subject to disturbances and with coupled system constraints; the communication strategy among subsystems has been designed to satisfy the coupling constraints; comparable control performance has been achieved in comparison with the centralized one. For the systems of discrete-time nonlinear dynamics with coupled control objective functions, the distributed MPC algorithm has been designed in [61]; the closed-loop system stability has been established. In [23], Dunbar and Murray study the vehicle-formation control problem using distributed receding horizon control (RHC) for subsystems with continuous-time nonlinear dynamics and a coupled control objective. In [22], Dunbar further investigates the same problem for a class of vehicle platoons, and analyzes both the stability and string stability. To address communication delays among subsystems, Franco *et al.* study the distributed MPC problem of a group of discrete-time linear systems among which the information is subject to constant delays in [32]; they further investigate the corresponding problem for nonlinear systems in [31]. In these two results, the delayed information is treated as bounded disturbances and the ISS technique is utilized to analyze the closed-loop stability, but the external disturbance of the system is not considered and the communication delays are constant.

- **Consensus of multi-agent systems using distributed MPC**. In [60], Johansson *et al.* study the consensus problem of linear systems with convex input and state constraints; they design a local MPC algorithm for each agent and propose a negotiation algorithm for regulating each local controller that computes an optimal consensus point for the overall system. In [63], Keviczky and Johansson further investigate the convergence properties of the distributed MPC consensus problem for a class of linear systems with input and state constraints. In [28], the consensus problem using MPC strategies is researched for multi-agent systems with subsystems of single- and double-integrator dynamics;

the time-varying communication topologies are considered and the stability is established by using geometric properties of the optimal path.

In summary, the results on distributed MPC of large-scale systems can be classified in Table 1.3, in which the following abbreviations are adopted: LSCD – Linear subsystems with coupled dynamics, LSDD – Linear subsystems with decoupled dynamics, NSCD – Nonlinear subsystems with coupled dynamics, NSDD – Nonlinear subsystems with decoupled dynamics.

System type	Disturbance	No disturbance	Delay	Data loss
LSCD	[57]	[7][99][145][27][150]		
LSDD	[130]	[32][60][63][28]	[32]	
NSCD	[83][81][84][82][46][45]	[21][146]	[84][82]	[45]
NSDD		[61][23][22] [31]	[31]	

Table 1.3: Recent results on distributed MPC of large-scale systems.

1.3 Motivations

It is well known that, in practice, the dynamics of most industrial systems are essentially nonlinear and many nonlinear dynamics cannot be simply characterized by their linearized ones at operation points, especially in high-performance application scenarios. Though great progress has been made on NCS design, most of the results are developed for plant models with linear dynamics; these results of linear NCSs are generally not valid for nonlinear NCSs due to the fact that the properties of superposition and homogeneity cannot be directly applied. In the literature, the problem of nonlinear NCS design has not been fully investigated and the results for general nonlinear NCSs are scarce, even though they are highly desired in many practical applications. This motivates the research of the dissertation to focus on nonlinear NCS design. More specifically, the motivations of the research work are detailed in three aspects as follows.

- **Robust filtering of nonlinear NCSs**. Filtering design plays an essential role in providing state estimate of nonlinear NCSs, which are indispensable to many NCS problems such as networked output feedback control and fault detection. Compared to other filtering approaches, the robust $\mathcal{H}_\infty$ filtering method features three aspects: (1) it is of great efficiency to deal with model uncertainties and

external disturbances, which are frequently encountered challenges in nonlinear NCS design; (2) the error dynamic system can achieve guaranteed disturbance attenuation level and the state estimate is robust against external disturbances; (3) the filtering system achieves proven stability property with zero external disturbances. In the literature, the robust filtering of NCSs has spurred significant interest, but most of the results reported are for linear systems. Even in the available results on nonlinear NCSs, almost all of them are developed exclusively for nonlinear systems of special types of nonlinearities, where the treatment of nonlinearities can be converted into that of linear systems and the approaches of linear NCSs can then be applied. The robust filtering problem of general nonlinear NCSs is still open; the filtering design and analysis of nonlinear NCSs under various communication networks are left unexplored.

In particular, one of the most critical issues faced in NCS design is communication delay, which is likely to occur in a stochastic manner in practice. According to NCS experiments in [108, 140], the Markov process can capture the physical properties of communication delays, matching experimental data of industrial network delays. In addition, the Markov process is more informative and efficient in comparison to Bernoulli process and constant model by incorporating the relationship among delays in different time instants. Therefore, the robust filtering design of general nonlinear systems with disturbances and measurements subject to Markov delays is of theoretical merit and application importance, and it will be investigated in the first part of the dissertation.

- **MPC-based control of nonlinear NCSs**. The MPC-based control strategy is one of the most effective approaches to NCSs, since it can actively compensate for, rather than be passively adapted to communication constraints. In traditional MPC, a sequence of control inputs is generated by optimizing a control objective function at each time instant; the first one in the control sequence is picked up as the current control signal and the others (i.e., the predicted one) for the future time instants are discarded; this procedure is executed iteratively for each time instant. In contrast, the network-based MPC will not discard the predicted control inputs in a control sequence arbitrarily, but make full use of them for the future time instants whenever control input losses or/and delays occur over communication networks. In addition, the MPC under network environments also preserves the advantages of traditional MPC, i.e., capability of

satisfying constraints and achieving optimal control performance.

These features make MPC a desired solution to NCSs and a lot of results have been developed for NCSs based on MPC. But most of the results are proposed for linear systems and the networked MPC design problem of nonlinear systems under various communication constraints has not been fully investigated. In particular, the following questions need to be answered: How to design a unified MPC framework to accommodate all types of communication constraints simultaneously for nonlinear NCSs? How to design robust MPC algorithms and efficient compensation strategies to improve control performance? Additionally, almost all the existing results are reported for designing state feedback MPC algorithms of NCSs, but the study on how to design output feedback MPC of NCSs is still not available. Motivated by these facts, the second part of this dissertation will focus on the design of efficient compensation strategies and robust MPC algorithms for nonlinear NCSs, and the study of networked output feedback MPC problem.

- **Distributed MPC of large-scale nonlinear systems**. The development of network and communication techniques advances the design and implementation of large-scale and multi-agent systems. The distributed MPC is one of the most promising control strategies for large-scale systems. It not only inherits the advantages of traditional MPC in handling system constraints and achieving suboptimal control performance, but also provides a unique feature with similar computational efficiency as decentralized MPC while achieving comparable control performance to centralized MPC. These advantages provided by distributed MPC is highly desired in practical implementations and have rendered it an active topic in the research area of MPC. Though many interesting results have been reported, most of them are restricted to the design of distributed MPC strategies for large-scale linear systems and/or systems without disturbances. Few results have been proposed to design robust distributed MPC of large-scale nonlinear systems subject to external disturbances which is unavoidable in practical design and implementation.

  On the other hand, the distributed MPC heavily relies on communication networks, through which information among subsystems is exchanged to address their couplings and the desired control performance. However, most of the current results are developed under the assumption that the communication

networks are perfectly reliable, which is not valid in many practical large-scale systems, especially in large-scale wireless networks shared by great amounts of subsystems. So far, little attention has been paid to the distributed MPC problem in unreliable communication networks. This motivates the third part of this dissertation: The investigation of the robust distributed MPC problem of large-scale nonlinear systems with communication delays and external disturbances.

1.4 Contributions

The robust filtering and MPC-based control problem of nonlinear NCSs, and the distributed MPC problem of large-scale nonlinear systems are investigated in the dissertation. The main contributions of this dissertation are summarized as follows.

- **Design robust filters of nonlinear NCSs with measurements subject to Markov delays**. A robust $\mathcal{H}_\infty$ filtering design approach is proposed for a class of general networked nonlinear systems. The proposed approach is capable of dealing with model uncertainties, disturbances and Markov delays in measurements simultaneously, which serves an effort towards a unified robust filtering design framework of industrial networked nonlinear systems. In particular, the Markov process has been proven to be more effective in characterizing the physical properties of the real network delays compared to the deterministic modeling, which makes the developed results more efficient and practical than the existing filtering results. Furthermore, in this work, a Markov mode-dependent algebraic Hamilton-Jacobi inequality (HJI) is developed as a sufficient condition to designing the robust filter, generalizing the classic algebraic HJI for non-networked control systems. The stability conditions of the filtering system are proposed and the $\mathcal{H}_\infty$ performance is analyzed. Finally, the results are specialized for corresponding networked linear systems and the bilinear matrix inequality (BMI)-based conditions are derived for designing the robust linear filter.

- **Design robust MPC algorithms and efficient compensation strategies of NCSs**. Firstly, an improved MPC strategy is designed for a class of nonlinear systems subject to two-channel packet dropouts, system constraints and external disturbances. A novel compensation strategy is proposed such that the

frequencies of the packet transmission can be reduced and the network resources can be efficiently utilized; a new approach is developed to prove the closed-loop stability by constructing a novel ISpS-type Lyapunov function. This work provides a potential solution to efficient MPC-based nonlinear NCS design.

Secondly, a min-max MPC scheme is designed for a class of nonlinear NCSs with delays, packet dropouts, disturbances and systems constraints. This scheme can explicitly incorporate the disturbances into the controller design, which improves the robustness and control accuracy of the closed-loop system in comparison with the existing results of NCSs. A novel Lyapunov function is proposed to establish the ISpS of the resulting closed-loop system. This work offers a useful tool to improving the robustness of nonlinear NCSs.

Finally, a robust output feedback MPC algorithm is designed for constrained linear systems with periodical measurement dropouts. More specifically, a novel observer is first designed such that the estimate error converges to a compact set even when disturbed by disturbances and measurement dropouts. The networked robust output MPC algorithm is then developed based on the tightening technique and set-invariant theory; the feasibility of the algorithm and the stability of the closed-loop system are studied; the convergence sets of the system state under the designed controller are developed as well. This work is particularly useful for the networked system in which the system state is not directly measurable, and it takes a first step towards studying quantitative effects of disturbances and packet dropouts.

- **Design novel robust distributed MPC of large-scale nonlinear systems considering disturbances and communication delays**. First of all, a novel distributed MPC scheme is designed for large-scale nonlinear systems subject to bounded disturbances. A robustness constraint is integrated into the optimization problem in order to address the effects of external disturbances. In this framework, the feasibility conditions of the designed algorithm and the stability conditions of the closed-loop systems are developed, respectively. It is shown that the stability of the closed-loop system is affected by the sampling period, the parameters of the robustness constraint and the bounds of disturbances. The system state rendered by the designed control law is proven to converge to a compact set. The contribution of this work mainly lies in the fact that it not only provides a novel scheme to deal with external disturbances,

but also lays a foundation for studying large-scale nonlinear systems subject to communication delays.

Second, a novel distributed MPC scheme of large-scale nonlinear systems with communication delays but without disturbances is developed. The conditions that guarantee the feasibility and stability are also developed accordingly. It is shown that the stability of the closed-loop system is related to the sampling period and the communication delays; the state of the closed-loop system converges to the equilibrium point. This work provides an effective tool for addressing communication delays of large-scale nonlinear systems in noiseless environments.

Finally, based on the aforementioned two pieces of work, the robust distributed MPC problem of large-scale nonlinear systems subject to bounded disturbances and communication delays is studied. A robust distributed MPC algorithm, which can simultaneously accommodate communication delays and external disturbances are developed by designing the robustness constraint and the waiting mechanism. The sufficient conditions for guaranteeing the feasibility and stability are developed, respectively. It is shown that the closed-loop stability is dependent on the sampling period, the bound of the disturbances, the communication delays and the parameters of the robustness constraint; the system state is stabilized into a convergence set containing zero. This work not only provides a feasible robust distributed MPC method for practitioners, but also gives insights into understanding how the disturbances and communication delays affect system stability.

1.5 Organizations of The Dissertation

The remainder of the dissertation is organized as follows. In **Chapter 2**, the robust $\mathcal{H}_\infty$ filtering problem of uncertain nonlinear systems subject to Markov delays is studied.

The MPC-based control problems of NCSs are presented in **Chapter 3**, **4** and **5**. In **Chapter 3**, the results on designing MPC strategy for nonlinear NCSs with two-channel packet dropouts is presented; in **Chapter 4**, the min-max MPC problem of nonlinear NCSs subject to time delays and packet dropouts is investigated; the design of output feedback model predictive controller of linear constrained NCSs

with periodical measurement dropouts is reported in **Chapter 5**.

The distributed MPC problems of large-scale nonlinear systems are studied in **Chapter 6**, **7** and **8**. **Chapter 6** investigates the robust distributed MPC problem of large-scale nonlinear systems subject to disturbances; **Chapter 7** studies the distributed MPC design problem of large-scale nonlinear systems by considering communication delays; **Chapter 8** is concerned with the robust distributed MPC design for large-scale nonlinear systems subject to both communication delays and external disturbances.

Finally, in **Chapter 9**, a summary of the dissertation is presented and the future research directions are stated.

Chapter 2

Robust Nonlinear $\mathcal{H}_\infty$ Filtering of NCSs with Measurement Subject to Markov Delays

2.1 Introduction

In a control system, the system state is the foundation to design a controller. However, in many practical control systems, the system states may not directly available, and only the state information (likely coupled with noises) can be measured by sensors. The filtering problem is to design an estimator (i.e., observer) to estimate the system state by using information from the sensor measurement and the system model. Like conventional control systems, the filtering problem is also a very important issue in NCSs. One of the most efficient filtering techniques is the robust $\mathcal{H}_\infty$ filtering approach which has demonstrated noticeable advantages in simultaneously tackling time delays and model uncertainties. It is found to be robust against energy-bounded disturbances without knowing exact statistical properties. There are generally three types of $\mathcal{H}_\infty$ filtering design approaches, i.e., the linear matrix inequality based method [35, 111, 165, 16], the Riccati based method [158, 112], and the polynomial based approach [176, 117, 34, 33]. When considering the delay systems, there are delay-independent filtering design [165, 176], and delay-dependent design [117, 34, 180, 35] for the purpose of reducing the conservatism. Nevertheless, all these results mentioned above are for linear systems or special types of nonlinear systems which can be dealt with using the similar design techniques for linear

systems.

Due to the intrinsic nonlinear characteristics, the well developed filtering methodologies for linear system cannot be directly extended to nonlinear systems. Compared to the rich literature on linear system filtering, there are only relatively few results on $\mathcal{H}_\infty$ filtering of nonlinear systems. Shaked and Berman [134] develop an $\mathcal{H}_\infty$ filtering technique for nonlinear stochastic systems based on the linearization method. Further, the nonlinear filtering for sampled-data systems is studied in [105]. Based on the HJI, the $\mathcal{H}_\infty$ filtering for the continuous-time nonlinear system with an Itô-type stochastic differential equation model is investigated in [179]. For corresponding discrete-time nonlinear systems, Berman *et al.* [5] design an $\mathcal{H}_\infty$ controller by solving an algebraic HJI. Alternatively, the Carleman approximation approach is employed to deal with the filtering problem for nonlinear stochastic systems in [36]. It is worth noting that these approaches for the nonlinear filtering problem did not consider the time delays and model uncertainties.

It is well known that the time delays and model uncertainties are frequently encountered in many practical engineering systems. Thus, how to address the time delays and uncertainties in the nonlinear $\mathcal{H}_\infty$ filtering problem is of both theoretical and practical merits. However, only few results on this topic are available in the literature. An $\mathcal{H}_\infty$ filtering design for a special type of stochastic nonlinear systems with state delays is proposed in [166]; the nonlinearity is modeled as a perturbation to the linear system which is quite special, and the time delay is assumed to be bounded and time-varying. Based on the algebraic HJI, a nonlinear $\mathcal{H}_\infty$ filtering with time-varying measurement delays is studied in [137], where the time delay is assumed to satisfy the Bernoulli distribution, but uncertainties are not considered.

It is practically demanding, yet more challenging, to investigate the $\mathcal{H}_\infty$ filtering problem for nonlinear stochastic systems with random delays. On the one hand, under the deterministic framework, the delay can be modeled as a constant [91] or a time-varying one [166, 180]. On the other hand, it has been shown that the time delays occur randomly [107], and it is more desirable to incorporate the delay's random properties into the design. One way of modeling the random delays is the Bernoulli distribution [137]. Yet, the Bernoulli-type delay only takes two possible values with known probabilities, which may not fully characterize the statistic feature of delays. Further, it cannot reflect the relationship between delays at different time instants. Another way of modeling random delays is the finite state Markov chains method [107, 140, 177]. By summarizing all the discussions above, to the best of au-

thors' knowledge, the $\mathcal{H}_\infty$ filtering problem for a class of general nonlinear stochastic systems with model uncertainties and random time delays modeled by Markov chains has not been investigated, which motives this study.

In this chapter, the nonlinear system under investigation is modeled as a type of *general* stochastic nonlinear process. The time delays occurring in measurements are governed by discrete-time Markov chains with finite states, and the model uncertainties are time-varying but norm-bounded. The main contribution is three-fold:

- Establish a general algebraic HJI for nonlinear stochastic systems with model uncertainties and random time delays governed by Markov chains.
- Develop a set of sufficient conditions for the nonlinear stochastic filtering system to achieve the stochastic stability and the prescribed disturbance attenuation level.
- Develop a set of sufficient conditions expressed in terms of matrix inequalities for a special class of nonlinear stochastic systems, which can be conveniently applied to design the $\mathcal{H}_\infty$ filter.

The remainder of this chapter is organized as follows. The problem formulation and preliminaries are presented in Section 2.2. In Section 2.3, the derivation of the general algebraic HJI is given first, and the sufficient conditions for guaranteeing the stochastic stability and the prescribed disturbance attenuation level are presented for the synthesis of the $\mathcal{H}_\infty$ filter. In Section 2.4, the $\mathcal{H}_\infty$ filter design for a special class of nonlinear stochastic systems is discussed. Simulation studies and comparisons are illustrated in Section 2.5. The concluding remarks are addressed in Section 2.6.

The notation in this chapter is fairly standard. The superscripts "T" and "-1" stand for the matrix transposition and the matrix inverse, respectively. $\mathbb{R}^n$ denotes the n-dimensional Euclidean space and $\mathbb{R}^{n\times m}$ stands for $n \times m$-dimensional real matrix. I is the identity matrix with appropriate dimension and the notation $P > 0$ means that P is real symmetric and positive definite. $l_2[0,\infty)$ refers to the space of square summable vector sequences over $[0,\infty)$. Tr means the trace of a matrix; col$\{.\}$ is the operation of stacking vectors or matrices in the column direction. $\|\cdot\|$ refers to the Euclidean norm for vectors and the induced 2-norm for matrices. $\mathbb{E}(\cdot)$ stands for the mathematical expectation operator.

2.2 Problem Formulation and Preliminaries

Consider the following nonlinear stochastic system:

$$\begin{cases} x_{k+1} &= \varphi(x_k) + \Delta\varphi(x_k) + [\phi(x_k) \\ & \quad + \Delta\phi(x_k)]\,\nu_k + \vartheta(x_k)\omega_k^1 + \theta(x_k)\nu_k\omega_k^2, \\ \tilde{y}_k &= l(x_k) + \Delta l(x_k) + \kappa(x_k)\nu_k, \\ z_k &= \rho(x_k), \quad y_k = \tilde{y}_{k-d_k}, \end{cases} \tag{2.1}$$

where $\{x_k\}_{k\geq 0}$ is the solution to (2.1), with an initial value x_0, and vector x_k is $\mathbb{R}^n$-valued; $\{\nu_k\}_{k\geq 0}$ is the exogenous disturbance and $\{\omega_k\}_{k\geq 0} \triangleq \{[(\omega_k^1)^{\mathrm{T}}(\omega_k^2)^{\mathrm{T}}]^{\mathrm{T}}\}_{k\geq 0}$ is an $\mathbb{R}^{l+1}$-valued, independent component, zero-value white-noise sequence, defined on a probability space $(\Omega, \Im, \mathrm{P})$, with covariance $\mathbb{E}\left\{\omega_k\omega_k^{\mathrm{T}}\right\} = \mathrm{diag}\left\{r_1, r_2, \cdots, r_l, r_s\right\} = \mathrm{diag}\left\{R, R_s\right\}$, $\mathbb{E}\left\{\omega_k^1(\omega_k^1)^{\mathrm{T}}\right\} = R$ and $\mathbb{E}\left\{\omega_k^2(\omega_k^2)^{\mathrm{T}}\right\} = R_s$, respectively. In the sequel, let$(\Omega, \Im, \{\Im_k\}_{k\geq 0}, \mathrm{P})$ be a filtered probability space, where $\{\Im_k\}_{k\geq 0}$ is the family of sub σ-algebras of $\Im$ generated by $\{\omega_k\}_{k\geq 0}$. Furthermore, $\Im_k$ is assumed to be the minimal σ-algebras generated by $\{\omega_i\}_{0\leq i\leq k-1}$ and $\Im_0$ is assumed to be some given sub σ-algebra of $\Im$, independent of $\Im_k$; $\{\nu_k\}_{k\geq 0}$ is assumed to be a nonanticipative, $\mathbb{R}^m$-valued, stochastic process defined on $(\Omega, \Im, \{\Im_k\}_{k\geq 0}, \mathrm{P})$, which belongs to $l_2[0, \infty)$ and satisfies $\mathbb{E}\{\sum_{k=0}^{N} \|\nu_k\|^2\} < \infty, \forall N \geq 0$; $\{z_k\}_{k\geq 0}$ is the sequence of state combinations to be estimated, with z_k $\mathbb{R}^p$-valued; $\{\tilde{y}_k\}_{k\geq 0}$ is the sequence of ideal output, with $\tilde{y}_k$ $\mathbb{R}^q$-valued and $\{y_k\}_{k\geq 0}$ is the actual measurement output sequence with y_k $\mathbb{R}^q$-valued. $\{d_k\}_{k\geq 0}$ is the homogenous discrete-time Markov chain defined on the state-space $\bar{N} \triangleq \{0, 1, \cdots, d-1\}$ with the one-step transition matrix $(\pi_{ij})_{d\times d}$ and the initial distribution π_0, where $d > 0$ is a fixed integer.

For the nonlinear system in (2.1), functions $\varphi : \mathbb{R}^n \to \mathbb{R}^n$, $\phi : \mathbb{R}^n \to \mathbb{R}^{n\times m}$, $\vartheta : \mathbb{R}^n \to \mathbb{R}^{n\times l}$, $\theta : \mathbb{R}^n \to \mathbb{R}^{n\times m}$, $\rho : \mathbb{R}^n \to \mathbb{R}^p$, $l : \mathbb{R}^n \to \mathbb{R}^q$, and $\kappa : \mathbb{R}^n \to \mathbb{R}^{q\times m}$ are assumed to be time-invariant continuous mappings with initial conditions $\varphi(0) = 0$, $\phi(0) = 0$, $\theta(0) = 0$, $\vartheta(0) = 0$, $\rho(0) = 0$, $l(0) = 0$ and $\kappa(0) = 0$. It is also assumed that functions $\Delta\varphi : \mathbb{R}^n \to \mathbb{R}^n$, $\Delta\phi : \mathbb{R}^n \to \mathbb{R}^{n\times m}$, and $\Delta l : \mathbb{R}^n \to \mathbb{R}^q$ are uncertain continuous mappings, satisfying the following assumptions: $\Delta\varphi(x_k) = E_1(x_k)\delta_1(x_k)$, $\Delta\phi(x_k) = \phi(x_k)\delta_0(x_k)$ and $\Delta l(x_k) = E_2(x_k)\delta_2(x_k)$. Here functions $E_1(x_k) \in \mathbb{R}^n$ and $E_2(x_k) \in \mathbb{R}^q$ are assumed to be known, time-invariant, continuous mappings, and $\delta_0(x_k)$, $\delta_1(x_k)$,$\delta_2(x_k) \in \mathbb{R}$, are unknown functions, for which it is assumed that there exist scalar functions such that $\|\delta_i(x_k)\| \leq M_i(x_k)$ with $M_i(x_k) \geqslant 0$ for $i = 0, 1, 2$. The uncertainties are said to be admissible if they satisfy the above conditions. Define the

random variable $\mathbb{E}_x\left(V(X,Y,Z)\right) \triangleq \int_{\mathbb{R}^{n_x}} V(x,Y,Z)d\mathrm{P}_x(x)$, and $\mathbb{E}_{y,x}\left(V(X,Y,Z)\right) \triangleq \int_{\mathbb{R}^{n_y}}\int_{\mathbb{R}^{n_x}} V(x,y,Z)d\mathrm{P}_x(x)d\mathrm{P}_y(y)$, where X, Y, and Z are $\mathbb{R}^{n_x}$-valued, $\mathbb{R}^{n_y}$-valued and $\mathbb{R}^{n_z}$-valued random variables defined on $(\Omega, \Im, \mathrm{P})$ respectively, and the function is the mapping: $V:\ \mathbb{R}^{n_x}\times\mathbb{R}^{n_y}\times\mathbb{R}^{n_z}\to\mathbb{R}$, P_x and P_y are the probability distributions of X and Y, respectively.

Remark 2.1. *The nonlinear system under investigation in (2.1) has simultaneously incorporated both model uncertainties ($\Delta\varphi(x_k)$, $\Delta\phi(x_k)$ and $\Delta l(x_k)$) and the measurement time delays. The nonlinear filtering problem was investigated for the same type of continuous-time nonlinear stochastic system [179] and the corresponding discrete-time case [5], but neither of them considered the uncertainties and time delays. Further, the Bernoulli-distributed delays were considered in [137]; however, the uncertainty issue was not addressed. Technically, these aforementioned methods cannot be directly applied to solve the filtering problem for the system in (2.1). In fact, the method developed in this chapter needs to build a Markov chain-related Hamilton-Jacobi inequality, and construct a Markovian mode-dependent positive function, which will be different from the techniques used in [5, 137, 179]. Moreover, the results developed for the systems with Markov delays can capture those for systems with Bernoulli-distributed delays as special cases.*

By considering the measurement time delays existing in the nonlinear system in (2.1), the system states and external disturbances can be augmented as follows: $\bar{x}_k = \mathrm{col}\{x_k^{\mathrm{T}}, x_{k-1}^{\mathrm{T}}, \cdots, x_{k-(d-1)}^{\mathrm{T}}\}$ and $\bar{\nu}_k = \mathrm{col}\{\nu_k^{\mathrm{T}}, \nu_{k-1}^{\mathrm{T}}, \cdots, \nu_{k-(d-1)}^{\mathrm{T}}\}$, then it follows:

$$\begin{cases} \bar{x}_{k+1} &= \bar{\varphi}(\bar{x}_k) + \Delta\bar{\varphi}(\bar{x}_k) + \big[\bar{\phi}(\bar{x}_k) \\ & \quad + \Delta\bar{\phi}(\bar{x}_k)\big]\,\bar{\nu}_k + \bar{\vartheta}(\bar{x}_k)\omega_k^1 + \bar{\theta}(\bar{x}_k)\bar{\nu}_k\omega_k^2, \\ \bar{y}_k &= \bar{l}(\bar{x}_k) + \Delta\bar{l}(\bar{x}_k) + \bar{\kappa}(\bar{x}_k)\bar{\nu}_k, \\ z_k &= \bar{\rho}(\bar{x}_k), \quad y_k = C_{d_k}\bar{y}_k, \end{cases} \tag{2.2}$$

where $\bar{\varphi}(\bar{x}_k) = \mathrm{col}\ \{\ \varphi(x_k)^{\mathrm{T}},\ x_k^{\mathrm{T}},\ \cdots,\ x_{k-(d-2)}^{\mathrm{T}}\}$, $\Delta\bar{\varphi}(\bar{x}_k) = \mathrm{col}\ \{\ \Delta\varphi(x_k)^{\mathrm{T}},\ 0^{\mathrm{T}},\ \cdots,\ 0^{\mathrm{T}}\ \}$, $\bar{\phi}(\bar{x}_k) = \mathrm{diag}\ \{\ \phi(x_k),\ 0,\ \cdots,\ 0\ \}$, $\Delta\bar{\phi}(\bar{x}_k) = \mathrm{diag}\ \{\ \Delta\phi(x_k),\ 0,\ \cdots,\ 0\ \}$, $\bar{\vartheta}(\bar{x}_k) = \mathrm{col}\ \{\ \vartheta(x_k)^{\mathrm{T}},\ 0^{\mathrm{T}},\ \cdots,\ 0^{\mathrm{T}}\ \}$, $\bar{\rho}(\bar{x}_k) = \rho(x_k)$, $\bar{l}(\bar{x}_k) = \mathrm{col}\ \{\ l(x_k)^{\mathrm{T}},\ l(x_{k-1})^{\mathrm{T}},\ \cdots,\ l(x_{k-(d-1)})^{\mathrm{T}}\ \}$, $\bar{\theta}(\bar{x}_k) = \mathrm{diag}\ \{\ \theta(x_k),\ 0,\ \cdots,\ 0\ \}$, $\Delta\bar{l}(\bar{x}_k) = \mathrm{col}\ \{\Delta l(x_k)^{\mathrm{T}},\ \Delta l(x_{k-1})^{\mathrm{T}},\ \cdots,\ \Delta l(x_{k-(d-1)})^{\mathrm{T}}\ \}$, $\bar{\kappa}(\bar{x}_k) = \mathrm{diag}\ \{\ \kappa(x_k),\ \kappa(x_{k-1}),\ \cdots,\ \kappa(x_{k-(d-1)})\}$, $\bar{y}_k = \mathrm{col}\ \{\tilde{y}_k^{\mathrm{T}},\ \tilde{y}_{k-1}^{\mathrm{T}},\ \cdots,\ \tilde{y}_{k-(d-1)}^{\mathrm{T}}\ \}$ and $C_{d_k} = [0,\ \cdots,\ 0,\ I,\ 0,\ \cdots,\ 0]$ with i-th block being identity.

For the augmented system in (2.2), we aim to design a filter of the following form:

$$\begin{cases} \hat{x}_{k+1} &= \hat{\varphi}(\hat{x}_k) + \hat{G}(\hat{x}_k, d_k)y_k, \\ \hat{z}_k &= \hat{\rho}(\hat{x}_k), \quad \hat{\varphi}(0) = 0,\ \hat{\rho}(0) = 0, \end{cases} \tag{2.3}$$

where $\hat{x}_k \in \mathbb{R}^{dn}$ represents the filtering states of the stochastic system in (2.2), $\hat{z}_k \in \mathbb{R}^q$ is the combination of the estimated states, and the functions $\hat{\rho}$, $\hat{\varphi}$ and $\hat{G}$, all being smooth functions with appropriate dimensions, are to be designed. By combining (2.2) and (2.3), and defining $X_k = \text{col}\{\bar{x}_k^{\mathrm{T}}, \hat{x}_k^{\mathrm{T}}\}$, the filtering system can be readily derived as

$$\begin{cases} X_{k+1} &= f(X_k) + \Delta f(X_k) + [g(X_k) + \Delta g(X_k)] \\ & \quad \times\bar{\nu}_k + h(X_k)\omega_k^1 + s(X_k)\bar{\nu}_k\omega_k^2, \\ \tilde{z}_k &= \bar{\rho}(x_k) - \hat{\rho}(\hat{x}_k), \end{cases} \tag{2.4}$$

where

$$\begin{aligned} s(X_k) =& \text{col}\{\bar{\theta}(\bar{x}_k)^{\mathrm{T}}, 0^{\mathrm{T}}\}, \\ f(X_k) =& \text{col}\{\bar{\varphi}(\bar{x}_k)^{\mathrm{T}}, \hat{\varphi}(\hat{x}_k)^{\mathrm{T}} + [\hat{G}(\hat{x}_k, d_k)C_{d_k}\bar{l}(\bar{x}_k)]^{\mathrm{T}}\}, \\ \Delta f(X_k) =& \text{col}\{\Delta\bar{\varphi}(\bar{x}_k)^{\mathrm{T}}, [\hat{G}(\hat{x}_k, d_k)C_{d_k}\Delta\bar{l}(\bar{x}_k)]^{\mathrm{T}}\}, \\ g(X_k) =& \text{col}\{\bar{\phi}(\bar{x}_k)^{\mathrm{T}}, [\hat{G}(\hat{x}_k, d_k)C_{d_k}\bar{\kappa}(\bar{x}_k)]^{\mathrm{T}}\}, \\ \Delta g(X_k) =& \text{col}\{\Delta\bar{\phi}(\bar{x}_k)^{\mathrm{T}}, 0^{\mathrm{T}}\}, \\ h(X_k) =& \text{col}\{\bar{\vartheta}(\bar{x}_k)^{\mathrm{T}}, 0^{\mathrm{T}}\}. \end{aligned}$$

Definition 2.1. *[5] The system in (2.4) is said to be l_2-gain less than or equal to γ if for all $k \geq 0$, all $\{\bar{\nu}_k\}_{k\geq 0}$ with $\sum_{i=0}^{k}\mathbb{E}\{\|\bar{\nu}_i\|^2\} < \infty$, and for all admissible uncertainties, there exists a positive function $\Xi : \mathbb{R}^n \to \mathbb{R}^+$ with $\mathbb{E}\{\Xi(x_0)\} < \infty$ for every x_0 in an $\Im_0$-measurable random variable set satisfying $\mathbb{E}\{\|x_0\|^2\} < \infty$, such that the following inequality holds: $\sum_{i=0}^{k}\mathbb{E}\{\|\tilde{z}_i\|^2\} \leq \mathbb{E}\{\Xi(x_0)\} + \sum_{i=0}^{k}\gamma^2\mathbb{E}\{\|\bar{\nu}_i\|^2\}$.*

Remark 2.2. *The definition of the l_2-gain less than or equal to γ property for time-varying nonlinear stochastic systems was defined in [5] for a control problem. In light of this, the similar definition to formulate the $\mathcal{H}_\infty$ filtering problem for a class of time-invariant nonlinear stochastic systems is utilized. In fact, if the system in (2.4) holds the l_2-gain less than or equal to γ property according to Definition 2.1, then the following filtering performance can be guaranteed: (1) For a zero-valued exogenous $\bar{\nu}_k$, the zero-solution of the system in (2.4) is stochastic asymptotically stable in the sense of mean square; (2) given a zero-initial condition and for all nonzero exogenous*

disturbance $\bar{\nu}_k$*, the filtering error* $\tilde{z}_i$ *has a prescribed disturbance attenuation level* $\gamma > 0$*, such that* $\sum_{i=0}^{k} \mathbb{E}\{\|\tilde{z}_i\|^2\} \leq \sum_{i=0}^{k} \gamma^2 \mathbb{E}\{\|\bar{\nu}_i\|^2\}$.

In what follows, we aim to design the filtering parametric matrix functions $\hat{\varphi}$, $\hat{G}$ and $\hat{\rho}$ such that the filtering system in (2.4) guarantees the property of l_2-gain less than or equal to γ.

2.3 $\mathcal{H}_\infty$ Filtering Design

In this section, an HJI for the system in (2.4) is first presented, which guarantees the l_2-gain less than or equal to γ criterion for the studied system; then specific sufficient conditions rendering the filtering system in (2.4) of the l_2-gain less than or equal to γ property are developed based on the proposed algebraic HJI.

Before proceeding to the filter design, some preliminary results are important to facilitate the derivations.

Lemma 2.1. *Considering the filtering system in (2.4), if there exists a positive real valued function:* $V : \mathbb{R}^n \times \bar{N} \to \mathbb{R}^+$ *satisfying* $\mathbb{E}\{V(X_0)\} \leq \gamma^2 \mathbb{E}\{\|X_0\|^2\}$ *for all* X_0 *in an* $\Im_0$*-measurable random variable set with* $\mathbb{E}\{\|X_0\|^2\} < \infty$*, for all admissible uncertainties, such that*

$$\begin{aligned} V(X, d_k) \geq \sup_{\bar{\nu} \in \mathbb{R}^n} \big\{ &\|\tilde{z}(X)\|^2 - \gamma^2 \|\bar{\nu}\|^2 \\ &+ \mathbb{E}_{\omega_k, d_{k+1}} \{V[F(X, \bar{\nu}, d_k, \omega_k), d_{k+1}]\} \big\}, d_k \in \bar{N}, \end{aligned} \tag{2.5}$$

where $\gamma > 0$ *and* $F(X, \bar{\nu}, d_k, \omega_k) \triangleq f(X) + \Delta f(X) + [g(X) + \Delta g(X)]\ \bar{\nu} + h(X)\ \omega_k^1 + s(X)\ \bar{\nu}\ \omega_k^2$*, then the system in (2.4) has the* l_2*-gain less than or equal to* γ *property. Furthermore, if there are filtering parametric matrix functions* $\hat{\varphi}$*,* $\hat{G}$ *and* $\hat{\rho}$*, such that the system in (2.4) has the* l_2*-gain less than or equal to* γ *property, for some* $\gamma > 0$ *and for all* $\Im_0$*-measurable random variable* X_0 *with* $\mathbb{E}\{\|X_0\|^2\} < \infty$*, then there exists a positive function* V *satisfying the algebraic HJI in (2.5).*

Proof. This proof can be completed by following the similar line of Corollary 1 in [5] by taking into account the time delay d_k and the model uncertainties. □

Remark 2.3. *It is worth noting that in Lemma 2.1, an extended algebraic HJI (2.5) for the filtering system in (2.4) has been established by considering the time delays* d_k *and uncertainties simultaneously. In fact, Lemma 2.1 reveals that: Satisfying the*

algebraic HJI (2.5) implies achieving the l_2-gain less than or equal to γ property for the filtering system in (2.4). This motivates us to seek an appropriate algebraic HJI (2.5) and a corresponding function V in order for guaranteeing the l_2-gain less than or equal to γ property for the filtering system in (2.4).

Now the following theorem under the standard assumption of $\bar{\kappa}^{\mathrm{T}}(\bar{x}_k)\bar{\kappa}(\bar{x}_k) \equiv I$ (see e.g., [56, 137]) is developed.

Theorem 2.1. *For the filtering system in (2.4) with a given disturbance attenuation level $\gamma > 0$, for all the admissible uncertainties, if there exist two positive scalars α and β and two sets of positive-definite matrices $\tilde{Q}_1(r) = \tilde{Q}_1^T(r) > 0$ and $\tilde{Q}_2(r) = \tilde{Q}_2^T(r) > 0$ for all $r \in \bar{N}$, such that the following conditions hold:*

$$\begin{aligned}
&(1 + M_0(\bar{x}_k))^2 \bar{\phi}^{\mathrm{T}}(\bar{x}_k) Q_1(r) \bar{\phi}(\bar{x}_k) \\
&\qquad + R_s \bar{\theta}^{\mathrm{T}}(\bar{x}_k) Q_1(r) \bar{\theta}(\bar{x}_k) \leq \alpha I, && (2.6)\\
&\hat{G}^{\mathrm{T}}(\hat{x}_k, r) Q_2(r) \hat{G}(\hat{x}_k, r) \leq \beta I, \quad \alpha + \beta < \gamma^2, && (2.7)\\
&\Gamma_1(\bar{x}_k, r) < 0, \quad \Gamma_2(\bar{x}_k, r) < 0, && (2.8)
\end{aligned}$$

where

$$\begin{aligned}
Q_1(r) &\triangleq \sum_{j=0}^{d-1} \tilde{Q}_1(j)\pi_{rj}, \quad Q_2(r) \triangleq \sum_{j=0}^{d-1} \tilde{Q}_2(j)\pi_{rj},\\
\Gamma_1(\bar{x}_k, r) &\triangleq \frac{5((1 + M_0(\bar{x}_k))^2)}{\gamma^2 - \alpha - \beta} \|\bar{\varphi}^{\mathrm{T}}(\bar{x}_k) Q_1(r) \bar{\phi}(\bar{x}_k)\|^2 + \frac{5[(1 + M_0(\bar{x}_k))^2 M_1^2(\bar{x}_k)]}{\gamma^2 - \alpha - \beta}\\
&\quad \times \|E_1^{\mathrm{T}}(\bar{x}_k) Q_1(r) \bar{\phi}(\bar{x}_k)\|^2 - \bar{x}_k^{\mathrm{T}} \tilde{Q}_1(r) \bar{x}_k + 2\|\bar{\rho}(\bar{x}_k)\|^2,\\
&\quad + (\frac{5(M_2(\bar{x}_k))^2 \beta^2}{\gamma^2 - \alpha - \beta} + \beta(M_2(\bar{x}_k))^2) \|E_2^{\mathrm{T}}(\bar{x}_k) C_r^{\mathrm{T}}\|^2 + \bar{\varphi}^{\mathrm{T}}(\bar{x}_k) Q_1(r) \bar{\varphi}(\bar{x}_k)\\
&\quad + \mathrm{Tr}(R^{1/2} \bar{\vartheta}^{\mathrm{T}}(\bar{x}_k) Q_1(r) \bar{\vartheta}(\bar{x}_k) R^{1/2})\\
&\quad + (M_1(\bar{x}_k))^2 E_1^{\mathrm{T}}(\bar{x}_k) Q_1(r) E_1(\bar{x}_k) + (\frac{5\beta^2}{\gamma^2 - \alpha - \beta} + 1 + \beta) \|\bar{l}(\bar{x}_k)^{\mathrm{T}} C_r^{\mathrm{T}}\|^2\\
\Gamma_2(\bar{x}_k, r) &\triangleq 2\|\hat{\rho}(\hat{x}_k)\|^2 - \hat{x}_k^{\mathrm{T}} \tilde{Q}_2(r) \hat{x}_k + (\frac{5}{\gamma^2 - \alpha - \beta} + 1) \|\hat{\varphi}^{\mathrm{T}}(\hat{x}_k) Q_2(r) \hat{G}(\hat{x}_k, r)\|^2\\
&\quad + \hat{\varphi}^{\mathrm{T}}(\hat{x}_k) Q_2(r) \hat{\varphi}(\hat{x}_k),
\end{aligned}$$

$\forall r \in \bar{N}$, then the filtering system in (2.4) achieves the l_2-gain less than or equal to γ property.

Proof. By Applying the triangle inequality, the following inequality can be obtained: $\|\tilde{z}_k\|^2 \leq 2(\|\bar{\rho}(\bar{x}_k)\|^2 + \|\hat{\rho}(\hat{x}_k)\|^2)$. Collectively considering this inequality and (2.8), it is obtained

$$\Gamma(\bar{x}_k, \hat{x}_k, r) \leq \Gamma_1(\bar{x}_k, r) + \Gamma_2(\hat{x}_k, r) < 0, \forall r \in \bar{N}, \tag{2.9}$$

where

$$\begin{aligned}
&\Gamma(\bar{x}_k, \hat{x}_k, r) \\
\triangleq&(\frac{5}{\gamma^2-\alpha-\beta})\{\|\bar{\varphi}^{\mathrm{T}}(\bar{x}_k)Q_1(r)(\bar{\phi}(\bar{x}_k)+\Delta\bar{\phi}(\bar{x}_k))\|^2 + \|\hat{\varphi}^{\mathrm{T}}(\hat{x}_k)Q_2(r)\hat{G}(\hat{x}_k,r)\|^2 \\
&+ \|\bar{l}^{\mathrm{T}}(\bar{x}_k)C_r^{\mathrm{T}}\hat{G}^{\mathrm{T}}(\hat{x}_k,r)Q_2(r)\hat{G}(\hat{x}_k,r)C_r\bar{l}(\bar{x}_k)\|^2 + \|\Delta\bar{\varphi}^{\mathrm{T}}(\bar{x}_k)Q_1(r)(\bar{\phi}(\bar{x}_k)+\Delta\bar{\phi}(\bar{x}_k))\|^2 \\
&+ \|\Delta\bar{l}^{\mathrm{T}}(\bar{x}_k)C_r^{\mathrm{T}}\hat{G}^{\mathrm{T}}(\hat{x}_k,r)Q_2(r)\hat{G}(\hat{x}_k,r)C_r\bar{\kappa}(\bar{x}_k)\|^2\} \\
&+ \bar{\varphi}^{\mathrm{T}}(\bar{x}_k)Q_1(r)\bar{\varphi}(\bar{x}_k) - \hat{x}_k^{\mathrm{T}}Q_2(r)\hat{x}_k + \|\hat{\varphi}^{\mathrm{T}}(\hat{x}_k)Q_2(r)\hat{G}(\hat{x}_k,r)\|^2 + \|\bar{l}(\bar{x}_k)\|^2 \\
&- \bar{x}_k^{\mathrm{T}}Q_1(r)\bar{x}_k + \bar{l}^{\mathrm{T}}(\bar{x}_k)C_r^{\mathrm{T}}\hat{G}^{\mathrm{T}}(\hat{x}_k,r)Q_2(r)\hat{G}(\hat{x}_k,r)C_r\bar{l}(\bar{x}_k) + \|\tilde{z}_k\|^2 \\
&+ \Delta\bar{l}^{\mathrm{T}}(\bar{x}_k)C_r^{\mathrm{T}}\hat{G}^{\mathrm{T}}(\hat{x}_k,r)Q_2(r)\hat{G}(\hat{x}_k,r)C_r\Delta\bar{l}(\bar{x}_k) \\
&+ \mathrm{Tr}(R^{1/2}\bar{\vartheta}^{\mathrm{T}}(\bar{x}_k)Q_1(r)\bar{\vartheta}(\bar{x}_k)R^{1/2}) + \hat{\varphi}^{\mathrm{T}}(\hat{x}_k)Q_2(r)\hat{\varphi}(\hat{x}_k).
\end{aligned}$$

On the other hand, in terms of the conditions in (2.6) and (2.7), we have

$$\Lambda(\bar{x}_k, \hat{x}_k, r) \leq (\gamma^2-\alpha-\beta)^{-1}I, \forall r \in \bar{N},$$

where $\Lambda(\bar{x}_k, \hat{x}_k, r) \triangleq \{\, \gamma^2 I - [\bar{\phi}^{\mathrm{T}}(\bar{x}_k) + \Delta\bar{\phi}^{\mathrm{T}}(\bar{x}_k)]\, Q_1(r)\, [\bar{\phi}(\bar{x}_k) + \Delta\bar{\phi}(\bar{x}_k)] - R_s\, \bar{\theta}^{\mathrm{T}}(\bar{x}_k)\, Q_1(r)\, \bar{\theta}(\bar{x}_k) - \bar{\kappa}^{\mathrm{T}}(\bar{x}_k)\, C_r^{\mathrm{T}}\, \hat{G}^{\mathrm{T}}(\hat{x}_k, d_k)\, Q_2(r)\, \hat{G}(\hat{x}_k, d_k)\, \bar{C}_r\, \kappa(\bar{x}_k)\}^{-1}$. To simplify the expression, define a function as follows:

$$\begin{aligned}
&\mathrm{K}(\bar{x}_k, \hat{x}_k, r) \\
\triangleq&\bar{\varphi}^{\mathrm{T}}(\bar{x}_k)Q_1(r)\bar{\phi}(\bar{x}_k) + \bar{\varphi}^{T}(\bar{x}_k)Q_1(r)\Delta\bar{\phi}(\bar{x}_k) + \hat{\varphi}^{\mathrm{T}}(\hat{x}_k)Q_2(r)\hat{G}(\hat{x}_k)C_r\bar{\kappa}(\bar{x}_k) \\
&+ \bar{l}^{\mathrm{T}}(\bar{x}_k)C_r^{\mathrm{T}}\hat{G}^{\mathrm{T}}(\hat{x}_k)Q_2(r)\hat{G}(\hat{x}_k)C_r\bar{\kappa}(\bar{x}_k) + \Delta\bar{\varphi}^{\mathrm{T}}(\bar{x}_k)Q_1(r)\left[\bar{\phi}(\bar{x}_k) + \Delta\bar{\phi}(\bar{x}_k)\right] \\
&+ \Delta\bar{l}^{\mathrm{T}}(\bar{x}_k)C_r^{\mathrm{T}}\hat{G}^{\mathrm{T}}(\hat{x}_k)Q_2(r)\hat{G}(\hat{x}_k)C_r\bar{\kappa}(\bar{x}_k).
\end{aligned}$$

By combining $\Lambda(\bar{x}_k, \hat{x}_k, r)$ and $\mathrm{K}(\bar{x}_k, \hat{x}_k, r)$, we get

$$\Phi(\bar{x}_k, \hat{x}_k, r) \leq \Gamma(\bar{x}_k, \hat{x}_k, r) < 0, \quad \forall r \in \bar{N},$$

where $\Phi(\bar{x}_k, \hat{x}_k, r) \triangleq \bar{\varphi}^{\mathrm{T}}(\bar{x}_k)\ Q_1(r)\bar{\varphi}(\bar{x}_k) + \mathrm{K}(\bar{x}_k, \hat{x}_k, r)\ \Lambda(\bar{x}_k, \hat{x}_k, r)\ \mathrm{K}^{\mathrm{T}}(\bar{x}_k, \hat{x}_k, r) +$

$\hat{\varphi}^{\mathrm{T}}(\hat{x}_k)\, Q_2(r)\, \hat{\varphi}(\hat{x}_k) + 2\hat{\varphi}^{\mathrm{T}}(\hat{x}_k)\, Q_2(r)\hat{G}^{\mathrm{T}}(\hat{x}_k)\, C_r\, \bar{l}(\bar{x}_k) + \bar{l}^{\mathrm{T}}(\bar{x}_k)C_r^{\mathrm{T}}\hat{G}^{\mathrm{T}}(\hat{x}_k)Q_2(r)\, \hat{G}(\hat{x}_k)C_r$ $\bar{l}(\bar{x}_k) + \Delta\bar{\varphi}^{\mathrm{T}}(\bar{x}_k)\, Q_1(r)\, \Delta\bar{\varphi}(\bar{x}_k) + \Delta\bar{l}^{\mathrm{T}}(\bar{x}_k)\, C_r^{\mathrm{T}}\, \hat{G}^{\mathrm{T}}(\hat{x}_k)\, Q_2(r)\, \hat{G}(\hat{x}_k)\, C_r\, \Delta\bar{l}(\bar{x}_k) + \|\tilde{z}_k\|^2 + \mathrm{Tr}(R^{1/2}\, \bar{\vartheta}^{\mathrm{T}}(\bar{x}_k)\, Q_1(r)\, \bar{\vartheta}(\bar{x}_k)\, R^{1/2}) - \bar{x}_k^{\mathrm{T}}\tilde{Q}_1(r)\bar{x}_k - \hat{x}_k^{\mathrm{T}}\tilde{Q}_2(r)\hat{x}_k$. Here, we take a positive-definite function as

$$V\left(X, d_k\right) = \bar{x}_k^{\mathrm{T}}\tilde{Q}_1(d_k)\bar{x}_k + \hat{x}_k^{\mathrm{T}}\tilde{Q}_2(d_k)\hat{x}_k, \tag{2.10}$$

where $X = \mathrm{col}\{\bar{x}_k^{\mathrm{T}}, \hat{x}_k^{\mathrm{T}}\}$ and $V : \mathbb{R}^{dn\times dn} \times \bar{N} \to \mathbb{R}^+$. In terms of the transition probability of Markov process [131], the right-hand side of (2.5) can be evaluated as

$$\begin{aligned}
\mathrm{A}\left(\bar{x}_k, \hat{x}_k, r\right) \triangleq & \sup_{\bar{\nu}\in\mathbb{R}^n} \left\{\|\tilde{z}(X)\|^2 - \gamma^2\, \|\bar{\nu}\|^2\right. \\
& \left. + \mathbb{E}_{\omega_k, d_{k+1}} \left\{V\left[F\left(X, \bar{\nu}, d_k, \omega_k\right), d_{k+1}\right]|_{d_k=r}\right\}\right\} \\
= & \sup_{\bar{\nu}\in\mathbb{R}^n} \left\{\bar{\nu}^{\mathrm{T}}\left[-\Lambda^{-1}\left(\bar{x}_k, \hat{x}_k, r\right)\right]\bar{\nu} + 2\mathrm{K}\left(\bar{x}_k, \hat{x}_k, r\right)\bar{\nu}\right. \\
& + \|\tilde{z}(X)\|^2 + \bar{\varphi}^{\mathrm{T}}(\bar{x}_k)Q_1(r)\bar{\varphi}(\bar{x}_k) + 2\hat{\varphi}^{\mathrm{T}}(\hat{x}_k)Q_2(r) \\
& \times \hat{G}^{\mathrm{T}}(\hat{x}_k, r)C_r\bar{l}(\bar{x}_k) + \hat{\varphi}^{\mathrm{T}}(\hat{x}_k)Q_2(r)\hat{\varphi}(\hat{x}_k) + \bar{l}^{\mathrm{T}}(\bar{x}_k)C_r^{\mathrm{T}} \\
& \times \hat{G}^{\mathrm{T}}(\hat{x}_k, r)Q_2(r)\hat{G}(\hat{x}_k, r)C_r\bar{l}(\bar{x}_k) \\
& + \Delta\bar{l}^{\mathrm{T}}(\bar{x}_k)C_r^{\mathrm{T}}\hat{G}^{\mathrm{T}}(\hat{x}_k, r)Q_2(r)\hat{G}(\hat{x}_k, r)C_r\Delta\bar{l}(\bar{x}_k) \\
& + \mathrm{Tr}\left(R^{1/2}\bar{\vartheta}^{\mathrm{T}}(\bar{x}_k)Q_1(r)\bar{\vartheta}(\bar{x}_k)R^{1/2}\right) \\
& \left. + \Delta\bar{\varphi}^{\mathrm{T}}(\bar{x}_k)Q_1(r)\Delta\bar{\varphi}(\bar{x}_k)\right\}, \forall r \in \bar{N}.
\end{aligned} \tag{2.11}$$

It is observed that (2.11) is maximized when $\bar{\nu}_{\max} = \Lambda\left(\bar{x}_k, \hat{x}_k, r\right)\mathrm{K}^{\mathrm{T}}\left(\bar{x}_k, \hat{x}_k, r\right)$. Therefore, $\mathrm{A}\left(\bar{x}_k, \hat{x}_k, d_k\right)$ can be accordingly maximized as: $\Phi\left(\bar{x}_k, \hat{x}_k, d_k\right) + \bar{x}_k^{\mathrm{T}}\tilde{Q}_1(d_k)\bar{x}_k + \hat{x}_k^{\mathrm{T}}\tilde{Q}_2(d_k)\hat{x}_k$. By $\Phi\left(\bar{x}_k, \hat{x}_k, r\right)$, the following can be obtained:

$$\begin{aligned}
\mathrm{A}\left(\bar{x}_k, \hat{x}_k, d_k\right) &< \bar{x}_k^{\mathrm{T}}\tilde{Q}_1(d_k)\bar{x}_k + \hat{x}_k^{\mathrm{T}}\tilde{Q}_2(d_k)\hat{x}_k \\
&= V\left(X, d_k\right).
\end{aligned} \tag{2.12}$$

According to Lemma 2.1, we conclude that the filtering system achieves the l_2-gain less than or equal to γ property. The proof is completed. □

Remark 2.4. *A closer look into Theorem 2.1 shows: It can be used not only to verify the stochastic stability in the sense of mean square under zero exogenous disturbance, but also to achieve certain disturbance attenuation for the filtering system. On one hand, if we choose the Lyapunov function as $V(X_k, d_k)$ defined by (2.10), then the difference of the Lyapunov function can be calculated as $\Delta V(X_k, d_k) =$*

$\mathbb{E}(V(X_{k+1}, d_{k+1}|X_k, d_k)\ ) - V(X_k, d_k) = \Phi(\bar{x}_k, \hat{x}_k, d_k) - \mathrm{K}(\bar{x}_k, \hat{x}_k, d_k)\ \Lambda(\bar{x}_k, \hat{x}_k, d_k)\ \mathrm{K}^{\mathrm{T}}(\bar{x}_k, \hat{x}_k, d_k) < 0$. *Therefore, the filtering system in (2.4) is stochastically stable under zero exogenous disturbance. On the other hand, if we set* $X = X_k$ *and* $\bar{\nu} = \bar{\nu}_k$ *in (2.12), and consider that* ω_k, d_k, X_k, *and* $\bar{\nu}_k$ *are independent, the following holds according to (2.12):* $\|\tilde{z}_k\|^2 - \gamma^2\ \|\bar{\nu}_k\|^2 \leq V(X_k, d_k) - \mathbb{E}_{\omega_k, d_{k+1}}\ \{V[\ F(d_k, \omega_k, X_k, \bar{\nu}_k), d_{k+1}]|_{X_k, d_k, \bar{\nu}_k}\}$. *Taking expectation operation on both sides of above inequality gives rise to* $\mathbb{E}(\|\tilde{z}_k\|^2) - \gamma^2\mathbb{E}(\|\bar{\nu}_k\|^2) \leq V\left(X_k, r\right) - \mathbb{E}\left\{V\left(X_{k+1}, d_{k+1}\right)|d_k = r\right\}$, $\forall r \in \bar{N}$. *Under zero initial conditions, we make a summation to both sides of the derived inequality, and obtain* $\sum_{k=0}^{K}\mathbb{E}(\|\tilde{z}_k\|^2) - \gamma^2\sum_{k=0}^{K}\mathbb{E}(\|\bar{\nu}_k\|^2) \leq 0$. *Therefore, the disturbance attenuation level can be guaranteed.*

Corollary 2.1. *For the system in (2.4) with a prescribed disturbance attenuation* $\gamma > 0$, *for all the admissible uncertainties, if there exist two positive scalars* α *and* β *and two positive-definite matrices* $Q_1 = Q_1^{\mathrm{T}} > 0$ *and* $Q_2 = Q_2^{\mathrm{T}} > 0$ *for all* $r \in \bar{N}$, *satisfying the following conditions:*

$$
\begin{aligned}
&(1 + M_0(\bar{x}_k))^2\bar{\phi}^{\mathrm{T}}(\bar{x}_k)Q_1\bar{\phi}(\bar{x}_k) \\
&\qquad + R_s\theta^{\mathrm{T}}(\bar{x}_k)Q_1\theta(\bar{x}_k) \leq \alpha I, \\
&\hat{G}^{\mathrm{T}}(\hat{x}_k, r)Q_2\hat{G}(\hat{x}_k, r) \leq \beta I, \quad \alpha + \beta < \gamma^2, \\
&\bar{\Gamma}_1(\bar{x}_k, r) < 0, \quad \bar{\Gamma}_2(\bar{x}_k, r) < 0,
\end{aligned}
$$

where

$$
\begin{aligned}
\bar{\Gamma}_1(\bar{x}_k, r) \triangleq & \frac{5((1 + M_0(\bar{x}_k))^2)}{\gamma^2 - \alpha - \beta}\|\bar{\varphi}^{\mathrm{T}}(\bar{x}_k)Q_1\bar{\phi}(\bar{x}_k)\|^2 - \bar{x}_k^{\mathrm{T}}Q_1\bar{x}_k \\
& + \frac{5[(1 + M_0(\bar{x}_k))^2M_1^2(\bar{x}_k)]}{\gamma^2 - \alpha - \beta}\|E_1^{\mathrm{T}}(\bar{x}_k)Q_1\bar{\phi}(\bar{x}_k)\|^2 + \bar{\varphi}^{\mathrm{T}}(\bar{x}_k)Q_1\bar{\varphi}(\bar{x}_k) \\
& + (\frac{5(M_2(\bar{x}_k))^2\beta^2}{\gamma^2 - \alpha - \beta} + \beta(M_2(\bar{x}_k))^2)\|E_2^{\mathrm{T}}(\bar{x}_k)C_r^{\mathrm{T}}\|^2 + 2\|\bar{\rho}(\bar{x}_k)\|^2 \\
& + \mathrm{Tr}(R^{1/2}\bar{\vartheta}^{\mathrm{T}}(\bar{x}_k)Q_1\bar{\vartheta}(\bar{x}_k)R^{1/2}) + (\frac{5\beta^2}{\gamma^2 - \alpha - \beta} + 1 + \beta)\|\bar{l}(\bar{x}_k)^{\mathrm{T}}C_r^{\mathrm{T}}\|^2 \\
& + (M_1(\bar{x}_k))^2E_1^{\mathrm{T}}(\bar{x}_k)Q_1E_1(\bar{x}_k) < 0, \\
\bar{\Gamma}_2(\bar{x}_k, r) \triangleq & (\frac{5}{\gamma^2 - \alpha - \beta + 1})\|\hat{\varphi}^{\mathrm{T}}(\hat{x}_k)Q_2\hat{G}(\hat{x}_k, r)\|^2 + \hat{\varphi}^{\mathrm{T}}(\hat{x}_k)Q_2\hat{\varphi}(\hat{x}_k) \\
& - \hat{x}_k^{\mathrm{T}}Q\hat{x}_k + 2\|\hat{\rho}(\hat{x}_k)\|^2 < 0,
\end{aligned}
$$

then the filtering system in (2.4) achieves the l_2*-gain less than or equal to* γ *prop-*

erty.

Proof. This proof can be completed by following the similar line of Theorem 2.1 while summing the total probability of each state in Markov process [131]. □

Remark 2.5. *Without incorporating the Markov model information into the positive function, Corollary 2.1 provides sufficient conditions to guarantee the filtering system in (2.4) satisfying the l_2-gain less than or equal to γ property. These conditions are more conservative than those developed in Theorem 2.1. But, it has only $3d+2$ matrix inequalities to solve compared with $4d+1$ in Theorem 2.1.*

2.4 A Special Case

Now we consider a special case of the stochastic nonlinear system in (2.1): The nonlinear terms appear as uncertainties in the state-space model, as shown in the following:

$$\begin{cases} x_{k+1} &= Ax_k + E_1 x_k \delta_1(x_k) + [B \\ & \quad +B\delta_0(x_k)]\nu_k + C\omega_k^1 + Dx_k\nu_k\omega_k^2, \\ \tilde{y}_k &= Lx_k + E_2 x_k \delta_2(x_k) + K\nu_k, \\ y_k &= \tilde{y}_{k-d_k}, \quad z_k = Px_k, \end{cases} \tag{2.13}$$

where $\delta_i(x_k) \in \mathbb{R}$, $\delta_i \leq m_i$, $m_i > 0$ is known for $i = 0, 1, 2$, and ω_k^1 and ω_k^2 are both one-dimensional white noise, with covariance r_0 and R_s, respectively. Note that this type of system in (2.13) can be employed to model some practical systems, and has been studied for the control [5] and filtering problems [137, 166], respectively.

For this special nonlinear stochastic system, the filter in (2.3) is accordingly designed as the following linear form:

$$\begin{cases} \hat{x}_{k+1} &= \hat{A}\hat{x}_k + \hat{G}(d_k)y_k, \\ \hat{z}_k &= \hat{P}\hat{x}_k. \end{cases} \tag{2.14}$$

Then the system in (2.2) can be simplified as:

$$\begin{cases} \bar{x}_{k+1} &= \bar{A}\bar{x}_k + \bar{E}_1\bar{x}_k\bar{\delta}_1(\bar{x}_k) + [\bar{B} \\ & \quad +\bar{B}\bar{\delta}_0(\bar{x}_k)]\bar{\nu}_k + \bar{C}\bar{x}_k\omega_k^1 + \bar{D}\bar{\nu}_k\omega_k^2, \\ \bar{y}_k &= \bar{L}\bar{x}_k + \bar{E}_2\bar{\delta}_2(\bar{x}_k)\bar{x}_k + \bar{K}\bar{\nu}_k, \\ y_k &= C_{d_k}\bar{y}_k, \quad z_k = \bar{P}\bar{x}_k, \end{cases} \tag{2.15}$$

where $\bar{A}$ is a square matrix with $[1,1]$-th block being A, $[i,i-1]$-th block being I for $i=2$ to d and the other blocks being zero, $\bar{E}_1 = \mathrm{diag}\{E_1, 0, \cdots, 0\}$, $\bar{B} = \mathrm{diag}\{B, 0, \cdots, 0\}$, $\bar{C} = \mathrm{diag}\{C, 0, \cdots, 0\}$, $\bar{D} = \mathrm{diag}\{D, 0, \cdots, 0\}$, $\bar{L} = \mathrm{diag}\{L, \cdots, L\}$, $\bar{E}_2 = \mathrm{diag}\{E_2, E_2, \cdots, E_2\}$, $\bar{K} = \mathrm{diag}\{K, K, \cdots, K\}$, $\bar{P} = [P, 0, \cdots, 0]$, $\bar{\delta}_1(\bar{x}_k) = \delta_1(x_k)$, $\bar{\delta}_0(\bar{x}_k) = \delta_0(x_k)$ and $\bar{\delta}_2(\bar{x}_k) = \delta_2(x_k)$.

Theorem 2.2. *For the filtering system in (2.15), given a prescribed attenuation $\gamma > 0$, for all the admissible uncertainties, if there exist two positive scalars α and β and two sets of positive-definite matrices $\tilde{Q}_1(r) = \tilde{Q}_1^T(r) > 0$, $\tilde{Q}_2(r) = \tilde{Q}_2^T(r) > 0, \forall r \in \bar{N}$, and a set of real matrices $Y(r), \forall r \in \bar{N}$, such that the following matrix inequalities hold:*

$$\begin{bmatrix} -\beta I & Y(r) \\ * & -Q_2(r) \end{bmatrix} < 0, \quad \alpha + \beta < \gamma^2, \tag{2.16}$$

$$\begin{bmatrix} -\alpha I & (1+m_0)\bar{B}^{\mathrm{T}}Q_1(r) & \sqrt{R_s}\bar{D}^{\mathrm{T}}Q_1(r) \\ * & -Q_1(r) & 0 \\ * & * & -Q_1(r) \end{bmatrix} < 0, \tag{2.17}$$

$$\begin{bmatrix} -\tilde{Q}_2(r) & \hat{A}^{\mathrm{T}}Y^{\mathrm{T}}(r) & \hat{A}^{\mathrm{T}} & \hat{P} \\ * & \dfrac{\alpha+\beta-\gamma^2}{5+\gamma^2-\alpha-\beta}I & 0 & 0 \\ * & * & -Q_2(r) & 0 \\ * & * & * & -\frac{I}{2} \end{bmatrix} < 0, \tag{2.18}$$

$$\begin{bmatrix} \Theta(r) & \bar{A}^{\mathrm{T}}Q_1(r)\bar{B} & \bar{E}_1^{\mathrm{T}}Q_1(r)\bar{B} \\ * & \dfrac{\alpha+\beta-\gamma^2}{5(1+m_0)^2}I & 0 \\ * & * & \dfrac{\alpha+\beta-\gamma^2}{5m_1(1+m_0)^2}I \end{bmatrix} < 0, \tag{2.19}$$

where $\Theta(r) = \bar{A}^{\mathrm{T}}Q_1(r)\bar{A} + m_1^2\bar{E}_1^{\mathrm{T}}Q_1(r)\bar{E}_1 + (\frac{5\beta^2 m_2^2}{\gamma^2-\alpha-\beta} + \beta m_2^2)\bar{E}_2^{\mathrm{T}}C_r^{\mathrm{T}}C_r\bar{E}_2 - \tilde{Q}_1(r) + (\frac{5\beta^2}{\gamma^2-\alpha-\beta}+\beta+1)\,\bar{L}^{\mathrm{T}}C_r^{\mathrm{T}}C_r\bar{L} + 2\bar{P}^{\mathrm{T}}\bar{P} + r_0\bar{C}^{\mathrm{T}}Q_1(r)\bar{C}$ with $Q_1(r) \triangleq \sum_{j=0}^{d-1}\tilde{Q}_1(j)\pi_{rj}$ and $Q_2(r) \triangleq \sum_{j=0}^{d-1}\tilde{Q}_2(j)\pi_{rj}, \forall r \in \bar{N}$, then there exists a linear filter in the form of (2.14) guaranteeing that: (1) The filtering system is stochastically stable, and (2) the l_2-gain less than or equal to γ performance is achieved. Furthermore, if the linear filter in (2.14) takes $\hat{A} = \bar{A}$ and $\hat{P} = \bar{P}$, and the matrix inequalities (2.16–2.19) are feasible, then the designed filter parameter $\hat{G}(r)$ is given by $\hat{G}(r) = Q_2(r)^{-1}Y^{\mathrm{T}}(r), r \in \bar{N}$.

Proof. For the filtering system in (2.15), by Theorem 2.1, the following conditions hold: $\alpha + \beta < \gamma^2$, $\hat{G}^{\mathrm{T}}(r)Q_2(r)\hat{G}(r) - \beta I < 0$, $(1+m_0)^2\bar{B}^{\mathrm{T}}Q_1(r)\bar{B} + r\bar{D}^{\mathrm{T}}Q_1(r) -$

$\alpha I < 0$, $(\frac{5}{\gamma^2-\alpha-\beta}+1)\ \hat{A}^{\mathrm{T}}Q_2(r)\hat{G}(r)\hat{G}^{\mathrm{T}}(r)\ Q_2(r)\hat{A} + \hat{A}^{\mathrm{T}}Q_2(r)\hat{A} - \tilde{Q}_2(r) + 2\hat{P}^{\mathrm{T}}\hat{P} < 0$, $(\frac{(1+5m_0)^2}{\gamma^2-\alpha-\beta})\ \bar{A}^{\mathrm{T}}Q_1(r)\bar{B}\bar{B}^{\mathrm{T}}Q_1(r)\bar{A} + \bar{A}^{\mathrm{T}}Q_1(r)\bar{A} + (\frac{5m_1(1+m_0)^2}{\gamma^2-\alpha-\beta})\bar{E}_1^{\mathrm{T}}\ Q_1(r)\bar{B}\bar{B}^{\mathrm{T}}Q_1(r)\bar{E}_1 + m_1^2\bar{E}_1^{\mathrm{T}}Q_1(r)\bar{E}_1 + (\frac{5\beta^2m_0^2}{\gamma^2-\alpha-\beta} + \beta m_2^2)\ \bar{E}_2^{\mathrm{T}}C_r^{\mathrm{T}}C_r\bar{E}_2 - \tilde{Q}_1(r) + r_0\bar{C}^{\mathrm{T}}Q_1(r)\bar{C} + (\frac{5\beta^2}{\gamma^2-\alpha-\beta}+\beta+1)\bar{L}^{\mathrm{T}}C_r^{\mathrm{T}}C_r\bar{L} + 2\bar{P}^{\mathrm{T}}\bar{P} < 0$. By applying Schur's Complement to above inequalities, (2.16-2.19) can be derived directly. Moreover, by setting $\hat{A} = \bar{A}$ and $\hat{P} = \bar{P}$ and defining $Y(r) = \hat{G}^{\mathrm{T}}(r)Q_2(r)$, the solution can be obtained by $\hat{G}(r) = Q_2^{-1}(r)Y^{\mathrm{T}}(r)$. This completes the proof. □

Remark 2.6. *Theorem 2.2 is built on Theorem 2.1 when the general nonlinearities [in Eqn. (2.1)] are reduced to a special case: Only the uncertainty terms have the nonlinear functions [in Eqn. (2.15)]. For this special case, the $\mathcal{H}_\infty$ filter can be conveniently designed by solving a set of matrix inequalities. It is noted that the resulting matrix inequalities are nonlinear, and therefore, we propose to iteratively fix the variables α and β, and then employ the LMI toolbox at each iteration to search for the solution. A detailed algorithm description is illustrated in Algorithm 1.*

Remark 2.7. *Theorem 2.2 establishes the mode-dependent conditions by incorporating the Markov delay information into $V(X, d_k)$ and $\hat{G}(d_k)$; the derived condition includes $4d+1$ matrix inequalities. If the designed filtering parameter $\hat{G}$ and $V(X)$ are independent of d_k, then only $d+4$ matrix inequalities are required to be solved. In this case, the designed filter is called mode-independent. Accordingly, the filter designed by Theorem 2.2 is called mode-dependent. As the Markov delay information is not incorporated, the mode-independent filter will be more conservative than the mode-dependent filter.*

In order to clearly show the procedure of designing the filter (2.14) by using Theorem 2.2, the algorithm description is presented in Algorithm 1.

2.5 An Illustrative Example

In this section, an inverted pendulum example is presented to demonstrate the effectiveness of the developed approach for the system in (2.15); the corresponding filter in (2.14) will be designed by solving a set of matrix inequalities as derived. In [5], the state feedback controller was designed for a single degree-of-freedom inverted pendulum system. Here, we consider the filtering problem for the inverted pendulum system when it has been stabilized with an appropriately pre-designed controller [5]. The

Algorithm 1 Filter Design Algorithm Description

1: Input system parameters for the system in (2.15);
2: Set initial values $\alpha_0 \in (0,\gamma)$, $\beta_0 \in (0,\gamma)$, and interval $\Delta t \in (0,\gamma)$ Partition interval $[\alpha_0,\gamma]$ and $[\beta_0,\gamma]$ into N_α and N_β intervals by Δt
3: **for** $i = 0$ to N_α **do**
4: Set $\alpha = \alpha_i$,
5: **for** $j = 0$ to N_β **do**,
6: Set $\beta = \beta_j$,
7: **if** $\alpha + \beta < \gamma$ **then**
8: Solve (2.16-2.19) using the LMI toolbox,
9: **end if**
10: **if** (2.16-2.19) is feasible **then**
11: Output $Y(r)$, $Q_1(r)$ and $Q_2(r)$,
12: Evaluate $\hat{G}(r) = Q_2^{-1}(r)Y^{\mathrm{T}}(r)$,
13: **end if**
14: **end for**
15: **end for**

model of the inverted pendulum system is given by $ml^2\ddot{\theta} - mgl\sin(\theta) + (\varsigma+\omega)\dot{\theta} + \kappa\theta = u + 2\nu_2$ in [5], where m is the mass and l is the length of the inverted pendulum, g is the gravitation coefficient, θ is the inclination angle, and ς and κ are the spring coefficient and damping parameter, respectively. ω is the white noise for the damping coefficient, ν_2 is the external disturbance, and u is the control input that has been pre-designed as $u = k_1\theta + k_2 ml^2\dot{\theta}$. Two output measurements are $\tilde{y}_1 = \theta + \nu_1$ and $\tilde{y}_2 = ml^2\dot{\theta} + \frac{\sin(ml^2\dot{\theta})}{ml^2 g\dot{\theta}} + \nu_2$, respectively. The regulated output is described by $z = \frac{\theta + ml^2\dot{\theta}}{10}$. Taking $x_1 = \theta$, $x_2 = ml^2\dot{\theta}$, and sampling period as T, the system model can be discretized and realized by the state-space model as follows:

$$\begin{aligned}
\begin{bmatrix} x_{1,k+1} \\ x_{2,k+1} \end{bmatrix} &= \begin{bmatrix} 1 & \frac{T}{ml^2} \\ -\kappa T + Tk_1 & 1 - \frac{T\varsigma}{ml^2} + Tk_2 \end{bmatrix} \begin{bmatrix} x_{1,k} \\ x_{2,k} \end{bmatrix} \\
&\quad + \begin{bmatrix} 0 & 0 \\ Tmgl & 0 \end{bmatrix} \begin{bmatrix} x_{1,k} \\ x_{2,k} \end{bmatrix} \delta_1(x_k) \\
&\quad + \begin{bmatrix} 0 & 0 \\ 0 & 2T \end{bmatrix} \begin{bmatrix} \nu_{1,k} \\ \nu_{2,k} \end{bmatrix} + \begin{bmatrix} 0 & 0 \\ 0 & \frac{-\sqrt{T}}{ml^2} \end{bmatrix} \begin{bmatrix} x_{1,k} \\ x_{2,k} \end{bmatrix} \omega_k,
\end{aligned}$$

where $\delta_1(x_k) = \frac{\sin(x_{1,k})}{x_{1,k}}$. The output measurement equation is discretized as

$$\begin{bmatrix} \tilde{y}_{1,k} \\ \tilde{y}_{2,k} \end{bmatrix} = \begin{bmatrix} 1 & 0 \\ 0 & 1 \end{bmatrix} \begin{bmatrix} x_{1,k} \\ x_{2,k} \end{bmatrix} + \begin{bmatrix} 0 & 0 \\ 0 & \frac{1}{ml^2g} \end{bmatrix} \begin{bmatrix} x_{1,k} \\ x_{2,k} \end{bmatrix} \delta_2(x_k) + \begin{bmatrix} 1 & 0 \\ 0 & 1 \end{bmatrix} \begin{bmatrix} \nu_{1,k} \\ \nu_{2,k} \end{bmatrix},$$

where $\delta_2(x_k) = \frac{\sin(x_{2,k})}{x_{2,k}}$. Due to the delay, the received measurement is $y(k) = \tilde{y}_{k-d_k}$, where d_k is the random time delay governed by a Markov chain. The state d_k belongs to $\{0, 1, 2\}$ and its transition probability matrix is given by $\Pi = [\text{col}\{0.8, 0.5, 0.4\}, \text{col}\{0.2, 0.4, 0.4\}, \text{col}\{0, 0.1, 0.2\}]$. Furthermore, the regulated output can be discretized as $z_k = 0.1x_{1,k} + 0.1x_{2,k}$. The system parameters are $m = 0.5$ kg, $l = 0.5$m, $\varsigma = 0.25$, $k_1 = -49.5$, $k_2 = -167.5$, sampling period $T = 0.01$ s, and $\kappa = 0.5$ N/m. The prescribed disturbance attenuation level is set to be $\gamma = 0.707$. Furthermore, to avoid obtaining the trivial solution, we require $Y(r)R_0 > 0$, where $R_0 = [\ I \quad I \quad I\ ]^{\mathrm{T}}$. Using Algorithm 1 with $\alpha = 0.1$ and $\beta = 0.1$, the feasible solutions can be obtained:

$$Y(0) = \begin{bmatrix} 4.0058 & 2.3282 & -2.7031 & 1.2642 & 0.1225 & -0.0499 \\ 1.1747 & 7.0816 & 2.3124 & 4.9400 & 0.0555 & 0.1779 \end{bmatrix}^{\mathrm{T}},$$

$$Y(1) = \begin{bmatrix} 3.3485 & 2.3816 & -1.9732 & 1.3315 & 0.2693 & -0.0946 \\ 1.5605 & 7.3215 & 2.0400 & 5.0762 & 0.0181 & 0.2385 \end{bmatrix}^{\mathrm{T}},$$

$$Y(2) = \begin{bmatrix} 2.5211 & 2.3970 & -0.7846 & 1.3116 & 0.6977 & -0.2191 \\ 1.9231 & 7.4516 & 1.6530 & 5.1220 & -0.0865 & 0.3900 \end{bmatrix}^{\mathrm{T}}.$$

The mode-dependent filtering parameters can be designed as follows:

$$G(0) = \begin{bmatrix} 0.0003 & 0.0009 & -0.0024 & 0.0011 & -0.0010 & 0.0001 \\ -0.0001 & 0.0022 & 0.0007 & 0.0027 & -0.0004 & 0.0000 \end{bmatrix},$$

$$G(1) = \begin{bmatrix} 0.0004 & 0.0008 & -0.0015 & 0.0008 & -0.0003 & -0.0000 \\ -0.0001 & 0.0022 & 0.0005 & 0.0025 & -0.0005 & 0.0002 \end{bmatrix},$$

$$G(2) = \begin{bmatrix} 0.0006 & 0.0006 & -0.0001 & 0.0005 & 0.0010 & -0.0004 \\ -0.0001 & 0.0023 & 0.0001 & 0.0025 & -0.0008 & 0.0004 \end{bmatrix}.$$

For the purpose of comparison, using the same parameters, we can also derive the mode-independent filter. The matrix Y can be calculated as

$$Y = \begin{bmatrix} 2.2055 & 1.5912 & -1.2948 & 0.8993 & 0.1431 & -0.0495 \\ 1.0628 & 4.9386 & 1.3665 & 3.4065 & 0.0117 & 0.1241 \end{bmatrix}^{\mathrm{T}},$$

and the corresponding mode-independent filtering parameter G can be derived as

$$G = \begin{bmatrix} 0.0002 & 0.0005 & -0.0010 & 0.0006 & -0.0003 & -0.0000 \\ -0.0000 & 0.0015 & 0.0002 & 0.0018 & -0.0004 & 0.0001 \end{bmatrix}.$$

To illustrate the filtering performances by using the mode-dependent filter as well as the mode-independent filters, we illustrate the filtering results in Figure 2.1 and Figure 2.2, respectively. It is observed that:

- Both the mode-dependent and mode-independent filtering systems exhibit acceptable estimation performance, as shown in Figure 2.1. Both the estimate errors of the mode-dependent filter and the mode-independent filter converge to zero gradually, as shown in Figure 2.2.
- The mode-dependent filter results in smaller estimation error compared to the mode-independent filter.
- The disturbance attenuation levels for the mode-dependent filter and the mode-independent filter can be accordingly calculated as $\gamma_d = 0.1005$ and $\gamma_i = 0.1025$, respectively, which are less than the prescribed attenuation level $\gamma = 0.707$.

Remark 2.8. *It is worth pointing out that the calculated disturbance attenuation levels are reasonable as they both fall within the prescribed one. The prescribed attenuation level is an upper bound of the induced norm for any input vector in the input vector space with all possible directions. Only when the input vector would be a certain (unique) direction, the upper bound can be achieved; otherwise, the calculated disturbance attenuation level will be less than the prescribed one. In the inverted pendulum system example, the input vector is chosen from the input vector space almost arbitrarily, therefore, the resulting disturbance attenuation level can be any value between* 0 *and the prescribed* γ.

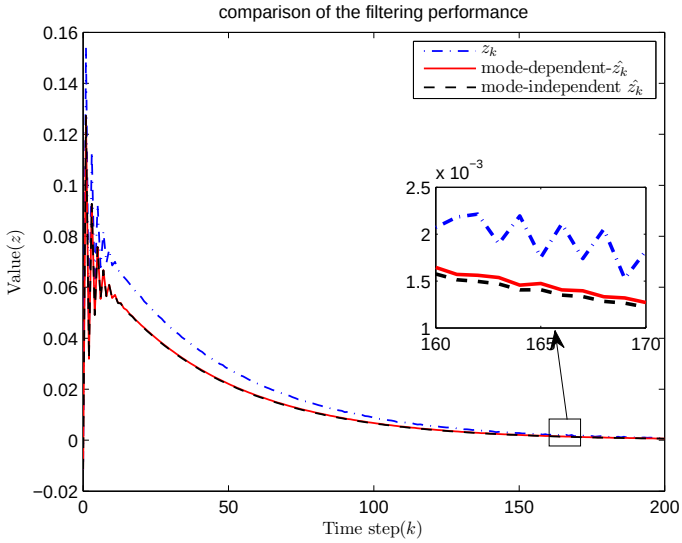

Figure 2.1: Filtering performance comparison.

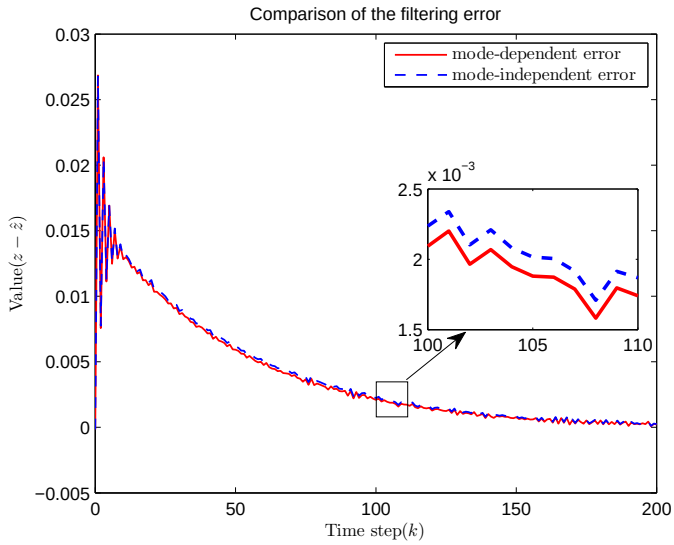

Figure 2.2: Filtering error.

2.6 Conclusion

In this chapter, the robust $\mathcal{H}_\infty$ filtering problem for a class of nonlinear stochastic systems considering both model uncertainties and random delays modeled by the Markov chains, has been investigated. The main features of this work are three-fold:

- The general algebraic HJI has been established to facilitate the filter design for general nonlinear stochastic systems with both model uncertainties and Markov

delays.

- Sufficient conditions have been derived for the filtering system to achieve stochastic stability in the sense of mean square and satisfy the prescribed disturbance attenuation level.
- The developed results have also been specialized for a special class of nonlinear stochastic systems.

Simulation studies and comparisons have been provided to demonstrate the effectiveness of the proposed approach. The results in this chapter add to the growing literature on the robust filter design for nonlinear stochastic systems with uncertainties and random delays. The main result of this chapter has been published in [71].

Chapter 3

State Feedback Predictive Control of Nonlinear NCSs with Two-Channel Packet Dropouts

3.1 Introduction

Chapter 2 studies the robust filtering problem of nonlinear NCSs. This chapter focuses the control problem of nonlinear NCSs. So far, most of the available results on NCSs are focused on systems with linear models (i.e., linear NCSs). Very limited efforts have been devoted to studying systems of nonlinear dynamics in network environments (i.e., nonlinear NCSs), although nonlinearity is an inherent attribute of many practical systems. In the literature on nonlinear NCSs, one way of dealing with nonlinear NCSs is the so-called emulation approach [147]. Based on the assumption that the pre-designed nonlinear system without networks is stable, this method allows one first to design the control protocol, and then to use the maximally allowable transmission interval and the maximally allowable delay to guarantee stability and system performance [44]. The exploitation of the emulation approach results in a few exciting consequences for nonlinear NCSs, such as [151, 103, 104, 44].

Another practical and effective method of tackling nonlinear NCSs is the MPC-based scheme [95]. On the one hand, the development and implementation of the Ethernet-like networks provide the capability of packing and transmitting data in the form of large packets [9], which lays a physical foundation for implementing the MPC-based scheme. On the other hand, the MPC-based scheme is able to pre-

dict the future control sequences by optimizing a prescribed objective function. By appropriately picking up the corresponding control input from the future control sequences, the communication imperfections such as time delays and data losses can be well compensated for or significantly mitigated. Motivated by the distinct advantages of MPC, increasing efforts have been devoted to investigating NCSs using the MPC-based scheme. The interesting results on linear NCSs can be referred to [148, 9, 80, 155, 171, 55, 132]. The typical results on nonlinear NCSs are briefly reviewed here. In [113], the MPC strategy is used to design the control packets and further to explicitly compensate for time delays for a class of constrained nonlinear systems; the feasibility and the regional ISS have been established. In [101], by considering the sensor-to-controller (S-C) and the controller-to-actuator (C-A) packet dropouts for a class of nonlinear NCSs, the MPC strategy has been utilized to guarantee the prescribed control performance and the robust stability. But the state constraint and input constraint are not considered in [101]. To further exploit the disturbance features, the ISS of the nonlinear NCSs with packet dropouts has been established using the MPC strategy in [120], yet only considering the C-A packet dropouts. Most recently, to make use of the stochastic properties of the network constraints, the nonlinear NCSs with packet dropouts modeled by Bernoulli processes are studied in [118, 122, 128]; the robust nonlinear MPC problem for nonlinear NCSs with Markovian packet dropouts is investigated in [121].

In this chapter, the predictive control problem of the *constrained* nonlinear system subject to both the C-A and S-C packet dropouts is considered in an Ethernet-like network environment. The MPC strategy is employed to design the control packets, and a novel packet transmission and compensation strategy is designed to alleviate the data-loss effects over the two channels based on the TCP-like protocol. Compared to the existing results in [120, 118, 122, 128, 121], the presented framework facilitates the incorporation of both the C-A and S-C packet dropouts explicitly into the controller design.

In this chapter, an efficient framework for designing, and implementing the MPC is proposed for the nonlinear constrained system subject to both S-C and C-A packet dropouts. The main contributions of this chapter are two-fold.

- An efficient control packet design and transmission mechanism that can reduce transmission load is developed. The optimization is carried out only when new information provided by the S-C packet dropouts and the acknowledgment packets, is available. Thus, the optimization is not needed for all the time

instants and the computational load from solving the optimization problem can be reduced. Furthermore, a transmission mechanism over the C-A channel is designed such that only necessary control packets are transmitted from the controller node to the actuator node (and the control packet is not needed to be transmitted for all the time instants). Such a mechanism can reduce transmission load for the C-A channel.

- The conditions for guaranteeing the regional ISpS of the resulting nonlinear NCSs are established. Due to the simultaneous existence of packet dropouts on the C-A and S-C channels, the optimal objective function cannot be directly used as an ISpS-type Lyapunov function. We present an auxiliary optimization problem from which a novel ISpS-type Lyapunov function is constructed to establish system stability.

The remainder of this chapter is organized as follows. The preliminary results on characterizing the stability for constrained nonlinear systems and the network model are presented in Section 3.2. The MPC-based control packet design as well as the packet transmission and compensation strategy are elucidated in Section 3.3. In Section 3.4, the stability of the resulting nonlinear NCSs is investigated and the regional ISpS is established. Next, an application study is conducted and the simulation results are provided in Section 3.5. Finally, the conclusions are addressed in Section 3.6.

The following notations are adopted in this chapter. The superscripts "T" and "-1" stand for the matrix transposition and the matrix inverse, respectively. $\mathbb{Z}$ ($\mathbb{Z}_{\geqslant 0}$) denotes the set of integers (non-negative integers) and $\mathbb{R}$ ($\mathbb{R}_{\geqslant 0}$) represents the real space (non-negative real space). Let $\|x\|$ denote the Euclidean norm of a given vector x and $\mathrm{col}\{x_1, x_2, \cdots, x_n\}$ denote the column operation as $[x_1^{\mathrm{T}}, x_2^{\mathrm{T}}, \cdots, x_n^{\mathrm{T}}]^{\mathrm{T}}$ for column vectors $x_1, x_2, \cdots, x_n$. For any given N bounded discrete-time signals $\mathbf{v} = \{v_0, v_1, v_2, \cdots, v_N\}$, define the subsequence as $\mathbf{v}_{k_1,k_2} \triangleq \{v_{k_1}, v_{k_1+1}, \cdots, v_{k_2}\}$ with $k_1, k_2 \in \mathbb{Z}_{\geqslant 0}$; define the truncation as $\mathbf{v}_{[k-1]} \triangleq \{v_0, v_1, v_2, \cdots, v_{k-1}\}$ and the norm as $\|\mathbf{v}\|_\infty \triangleq \sup_{k\geqslant 0} \|v_k\|$. Given a vector $x \in \mathbb{R}^n$ and a compact set $\Omega \subset \mathbb{R}^n$, denote the point-to-set distance as $\mathrm{d}|x|_\Omega \triangleq \inf\{\|\xi - x\|, \xi \in \Omega\}$. Given two sets $A \subseteq B \subseteq \mathbb{R}^n$, the difference between the two set is defined as $A \setminus B \triangleq \{x | x \in A, x \notin B\}$. Given two sets $A \subseteq \mathbb{R}^n$, $B \subseteq \mathbb{R}^n$, the Pontryagin difference set C is denoted as $C = A \sim B \triangleq \{x \in \mathbb{R}^n | x + \xi \in A, \forall \xi \in B\}$. A closed ball centralized at a given point $x_0 \in \mathbb{R}^n$ with a radius of $r \geqslant 0$ is denoted as $\mathcal{B}^n(x_0, r) \triangleq \{\xi \in \mathbb{R}^n | \|\xi - x_0\| \leqslant r\}$ and the

shorthand is written as $\mathcal{B}^n(r)$ when $x_0 = 0$. A continuous function $\alpha : \mathbb{R}_{\geqslant 0} \to \mathbb{R}_{\geqslant 0}$ is said to be a $\mathcal{K}$-function, if it is strictly increasing and $\alpha(s) > 0$ for $s > 0$ with $\alpha(0) = 0$. A continuous function $\alpha(.)$ is said to be a $\mathcal{K}_\infty$-function, if it is a $\mathcal{K}$-function, and $\alpha(s) \to \infty$ as $s \to \infty$. A continuous function $\beta : \mathbb{R}_{\geqslant 0} \times \mathbb{Z}_{\geqslant 0} \to \mathbb{R}_{\geqslant 0}$ is said to be a $\mathcal{KL}$-function, if $\beta(s, k)$ is a $\mathcal{K}$-function in s for every given $k \in \mathbb{Z}_{\geqslant 0}$, and it is strictly decreasing in k with $\beta(s, k) \to 0$ as $k \to \infty$. Let Id denote the identity function, i.e., $\mathrm{Id}(x) = x$.

3.2 Preliminary Results and Modeling

Consider the following discrete-time nonlinear system

$$x_{k+1} = f(x_k, u_k, \omega_k), \quad k \in \mathbb{Z}_{\geqslant 0}, \quad x_0 = \bar{x}, \tag{3.1}$$

where $x_k \in \mathbb{R}^n$ is the system state, $u_k \in \mathbb{R}^m$ is the control input and $\omega_k \in \mathbb{R}^r$ is the external disturbance. The system state and the control input are constrained as

$$x_k \in \mathcal{X}, \quad u_k \in \mathcal{U}, \quad \forall k \in \mathbb{Z}_{\geqslant 0}, \tag{3.2}$$

where $\mathcal{X}$ and $\mathcal{U}$ are compact sets such that $\{0\} \subset \mathcal{X} \subseteq \mathbb{R}^n$ and $\{0\} \subset \mathcal{U} \subseteq \mathbb{R}^m$, respectively. The external disturbance belongs to a compact set Υ with $\{0\} \subset \Upsilon \subseteq \mathbb{R}^r$, and $\rho_\omega \triangleq \max_{\omega \in \Upsilon}\{\|\omega\|\}$. For the system in (3.1), denote the nominal system model as

$$\hat{x}_{k+1} = \hat{f}(x_k, u_k) \triangleq f(x_k, u_k, 0), \quad k \in \mathbb{Z}_{\geqslant 0},$$

where $\hat{f}(0, 0) = 0$. It is assumed that $f(x, u, \omega)$ is locally Lipschitz in x and u, such that

$$\|f(x_1, u_1, \omega) - f(x_2, u_2, 0)\| \leqslant L_{f_x}\|x_1 - x_2\| + L_{f_u}\Delta_u + \mu(\|\omega\|),$$

for all $x_1, x_2 \in \mathcal{X}$, $u_1, u_2 \in \mathcal{U}$ and $\omega \in \Upsilon$, where L_{f_x} and L_{f_u} are local Lipschitz constants, $\Delta_u \triangleq \max\{\|u_1 - u_2\|\}$ and μ is a $\mathcal{K}$ function. Note that the assumption of local Lipschitz continuity is to guarantee the existence of the unique solution to the system in (3.1).

In the sequel, the well established results on the invariant set used in this work are recalled [6, 77].

Definition 3.1. *For the nonlinear system $x_{k+1} = f(x_k, \omega_k)$ with the uncertainty*

$\omega_k \in \Upsilon$, if there exists a set $\Omega \subset \mathbb{R}^n$ such that $f(x_k, \omega_k) \in \Omega$ for all $x_k \in \Omega$ and $\omega_k \in \Upsilon$, then the set Ω is called a robust positively invariant (RPI) set.

Definition 3.2. *For the system in (3.1) subject to the constraints in (3.2) and a set Ω, if there exists an admissible control input $u_k \in \mathcal{U}$ such that $f(x_k, u_k, \omega_k) \in \Omega$ for all $x_k \in \Omega$ and all $\omega_k \in \Upsilon$, then the set Ω is called a robust control invariant (RCI) set.*

Definition 3.3. *Consider the system in (3.1) subject to the constraints in (3.2) and associated with an RPI set Ω. The i-th step robustly stabilizable set $X_i(\Omega)$ is denoted by all the admissible states which can be steered into the target set Ω not more than i steps by using an admissible control sequence $\boldsymbol{u}_{[i]}$ for all $\boldsymbol{\omega}_{[i]} \in \Upsilon^i$.*

3.2.1 Regional Input-to-State Practical Stability (ISpS)

In order to analyze the stability of the nonlinear NCS under study, the regional input-to-state practical stability for the discrete-time nonlinear system is first investigated. The system in (3.1) can be rewritten as

$$x_{k+1} = g(k, x_k, \omega_k) \triangleq f(x_k, u_k, \omega_k),\ x_0 = \bar{x}, \tag{3.3}$$

where $x_k \in \mathbb{R}^n$ is the same system state as in (3.1), $\omega_k \in \mathbb{R}^m$ is the same external disturbance and the argument k in function g represents the time-varying property of the argument u_k in function f. Denote $x(k, \bar{x}, \boldsymbol{\omega}_{0,k-1})$ as the solution to the system in (3.3) at time instant k. For the system in (3.3), the definition of the regional ISpS is recalled [123, 113].

Definition 3.4. *Given a compact set $\Omega \in \mathbb{R}^n$, if it is an RPI set for the system in (3.3) with $\omega_k \in \Upsilon$, and if there exist a $\mathcal{KL}$ function β, a $\mathcal{K}$ function γ and a constant $c \geqslant 0$ such that*

$$\|x(k, \bar{x}, \boldsymbol{\omega}_{0,k-1})\| \leqslant \max\{\beta(\|\bar{x}\|, k), \gamma(\|\boldsymbol{\omega}_{[k-1]}\|_\infty)\} + c, \tag{3.4}$$

$\forall k \in \mathbb{Z}_{\geqslant 0}, \bar{x} \in \Omega$, then the system in (3.3) is said to be regional ISpS in Ω.

An effective tool of establishing ISS and ISpS is the comparison function [144, 59]. For the constrained nonlinear systems with two-channel packet dropouts, we recall the following regional ISpS-type Lyapunov function (a type of comparison function) [123, 113].

Definition 3.5. *For the system in (3.3), given two compact sets $\mathcal{X}$ and Ω with $\{0\} \subset \mathcal{X} \subseteq \mathbb{R}^n$, $\{0\} \subset \Omega \subseteq \mathcal{X}$ and $\mathcal{X}$ being an RPI set,*

- *(C1) if there exists a positive definite function $V(.,.) : \mathbb{R}^n \times \mathbb{Z}_{\geqslant 0} \to \mathbb{R}_{\geqslant 0}$ such that the following conditions hold:*

$$V(x_k, k) \geqslant \alpha_1(\|x_k\|) \quad \forall x_k \in \mathcal{X}, \tag{3.5}$$
$$V(x_k, k) \leqslant \alpha_3(\|x_k\|) + c_3 \quad \forall x_k \in \Omega, \tag{3.6}$$
$$V(x_{k+1}, k+1) - V(x_k, k) - \alpha_2(\|x_k\|) + \gamma(\|\omega_k\|) + c_2 \ \forall x_k \in \mathcal{X}, \tag{3.7}$$

  for all $k \in \mathbb{Z}_{\geqslant 0}$ and with α_1, α_2 and α_3 being $\mathcal{K}_\infty$ function, γ being $\mathcal{K}$ functions, and c_2, $c_3 \geqslant 0$;

- *(C2) if there exist a $\mathcal{K}$ function α_c, a constant $c_0 \geqslant 0$ and a function $\tilde{\gamma}$ with $(\mathrm{Id} - \tilde{\gamma})$ being $\mathcal{K}$ function, and define a compact set*

$$\Omega_\omega \triangleq \{x_k | V(x_k, k) \leqslant \theta(\gamma(\rho_\omega) + c_4), \forall k \in \mathbb{Z}_{\geqslant 0}\}, \tag{3.8}$$

  such that $\Omega_\omega \subseteq \Omega \sim \mathcal{B}^n(c_0)$ with $\theta \triangleq \alpha_4^{-1} \circ \tilde{r}$, $\alpha_4 \triangleq \underline{\alpha}_2 \circ \bar{\alpha}_3^{-1}$, $\underline{\alpha}_2(s) \triangleq \min\{\alpha_2(\frac{s}{2}), \alpha_c(\frac{s}{2})\}$, $\bar{\alpha}_3 \triangleq \alpha_3 + \mathrm{Id}$ and $c_4 = c_2 + \alpha_c(c_3)$,

then the function $V(x_k, k)$ is a regional ISpS-type Lyapunov function for the system in (3.3) with $\omega_k \in \Upsilon$.

Similar as in [123, 113], the continuity of the trajectory for the system in (3.3) is needed for establishing the regional ISpS.

Assumption 3.1. *For the system in (3.3), the trajectory $x(k, \bar{x}, \boldsymbol{\omega}_{0,k-1})$ is continuous at $\bar{x} = 0$ and $\boldsymbol{\omega}_{0,k-1} = 0$ with respect to the initial state and the disturbances for all $k \in \mathbb{Z}_{\geqslant 0}$.*

Remark 3.1. *Assumption 3.1 is a prerequisite for analyzing the solution to the nonlinear system under investigation [64]. This assumption can be guaranteed as long as the nonlinear systems satisfy the local Lipschtiz conditions according to Theorem 3.5 in [64].*

Theorem 3.1. *[123] Suppose that Assumption 3.1 holds. Given a compact set Ω and an RPI set $\mathcal{X}$ with $\{0\} \subset \Omega \subseteq \mathcal{X} \subset \mathbb{R}^n$ for the system in (3.3), if it admits an ISpS-type Lyapunov function associated with sets $\mathcal{X}$ and Ω, then the trajectory of the*

system in (3.3) satisfies $\lim_{k\to\infty} \mathrm{d}|x(k,\bar{x},\boldsymbol{\omega}_{0,k-1})|_{\Omega_\omega} = 0$ *and the system in (3.3) is regional ISpS in* $\mathcal{X}$.

3.2.2 Network Model

We consider the Ethernet-like communication networks that are deployed among the sensor, the controller and the actuator. In this type of networks, the data is transmitted in the form of large time-stamped (TS) packets [148], and the packet dropouts are apt to occur due to the network traffic congestions and/or physical components failures. It is assumed that the controller operates at the same sampling rate as the plant; the perfect synchronization among the sensor, the controller and the actuator is available, which is used to realize the TS technique. The Transmission Control Protocol (TCP)-like protocol is adopted for the C-A communication network. Unlike the User Datagram Protocol (UDP)-like protocol, whenever the smart actuator receives the data packet, it will send an acknowledgement packet to the controller. In the detailed NCS configuration depicted in Figure 3.1, the acknowledgement is realized

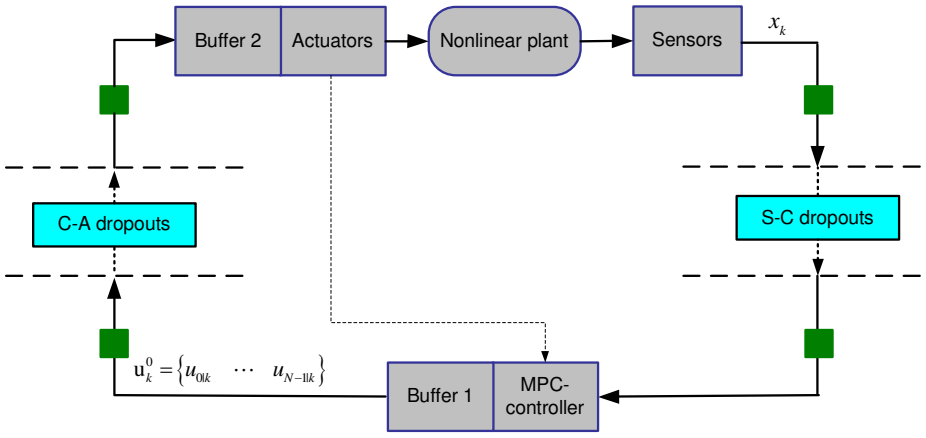

Figure 3.1: Nonlinear NCS configuration.

by the feedback link from the actuator to the controller. It is assumed that this feedback connection is reliable and without any packet dropouts and time delays. This is reasonable in practice. It is observed that 1) the transmission rate of this link is very low (only when the C-A packet is transmitted successfully, the acknowledgement packet will be sent); 2) the size of the acknowledge packet is very small (the content of the acknowledge packet is essentially the boolean variable 1). So the acknowledge packet is of very light transmission load and requires little bandwidth. In practice,

on the one hand, it is almost impossible that the packet dropouts occur in such an idle communication link without any network congestions; on the other hand, it is quite possible to guarantee the successful transmission of a one-bit boolean signal by using the hardware technology.

In the NCS configuration described in Figure 3.1, the plant evolves as the discrete-time dynamics in (3.1) subject to the constraints in (3.2); both the S-C packet dropout and the C-A packet dropout occur randomly. To describe the packet dropout effect, we denote the S-C packet dropout process as $\{\tau_{sc}(k)\}_{k\in\mathbb{Z}_{\geqslant 0}}$ and the C-A packet dropout process as $\{\tau_{ca}(k)\}_{k\in\mathbb{Z}_{\geqslant 0}}$, respectively. More specifically, the random process $\{\tau_{sc}(k)\}_{k\in\mathbb{Z}_{\geqslant 0}}$ is defined as: If the S-C packet dropout occurs at time instant k, $\tau_{sc}(k) = 0$, otherwise $\tau_{sc}(k) = 1$. Similarly, the C-A dropout process is defined as: If the C-A packet dropout occurs at time instant k, $\tau_{ca}(k) = 0$, otherwise, $\tau_{ca}(k) = 1$.

It is assumed that the maximum time durations of the consecutive S-C packet dropout and the consecutive C-A packet dropout are N_{sc} and N_{ca}, respectively. The maximum length of the consecutive packet dropouts is a measurement of the reliability of the communication networks, which will be used in the control packet design. The values of N_{sc} and N_{ca} are the network property parameters that can be determined by experiments.

3.2.3 Buffer Model

Two buffers are deployed in the configuration depicted in Figure 3.1; one is located in the control node denoted by Buffer 1 and the other is in the actuator node named Buffer 2. The buffer lengths for Buffer 1 and Buffer 2 are $2N_c+1$ and N_c, respectively, where $N_c \geqslant N_{ca} + N_{sc}$. Buffer 1 comprises three parts and their states are denoted as $\mathbf{B}_k^x$, $\mathbf{B}_k^u$ and $\mathbf{B}_k^c$, respectively. The part of state $\mathbf{B}_k^x$ is used to store the latest system state for estimating the future state in case of S-C packet dropouts. The part of state $\mathbf{B}_k^u$ is utilized to maintain the latest control sequence $\mathbf{u}_k^o$ generated from the MPC controller until the C-A packet dropout information is transmitted back from the acknowledgment link, i.e., $\mathbf{B}_k^u = \mathbf{u}_k^o$. (The acknowledgement information will determine whether the content of $\mathbf{B}_k^u$ is to update $\mathbf{B}_k^c$ or not). The part of state $\mathbf{B}_k^c$ is used to synchronize the control inputs as these in Buffer 2, for providing the actual control inputs of the plant to do state estimate if S-C packet dropout occurs (i.e., the system state is not available). The operating signal of $\mathbf{B}_k^c$ is governed by the acknowledgement link (i.e., the information of the C-A packet dropouts) and the

packet generation signal $r(k)$ which is defined by (3.10). Specifically, the operation of $\mathbf{B}_k^c$ can be modeled as: If $r(k) = 1 \&\& \tau_{ca}(k) = 1$, then $\mathbf{B}_k^c = \mathbf{B}_k^u$; otherwise, $\mathbf{B}_k^c = \text{col}\{\mathbf{B}_{k-1}^c(2), \cdots, \mathbf{B}_{k-1}^c(N_c), \mathbf{B}_{k-1}^c(1)\}$.

Buffer 2 is used to maintain the latest control input for the plant when there are packet dropouts occurring. Denote the state of Buffer 2 by $\mathbf{B}_k^a$. Assume that the input packet through C-A channel to Buffer 2 is $\mathbf{u}_k^a$ at time k when there is no packet dropout. Then the operation of Buffer 2 can be described as: If $\tau_{ca}(k) = 1$, then $\mathbf{B}_k^a = \mathbf{u}_k^a$; otherwise, $\mathbf{B}_k^a = \text{col}\{\mathbf{B}_{k-1}^a(2), \cdots, \mathbf{B}_{k-1}^a(N_c), \mathbf{B}_{k-1}^a(1)\}$.

3.3 Predictive Networked Controller Design

In this section, the realization of the networked control strategy is presented. Firstly, the control packet is designed by the constrained MPC-based algorithm, where both the state constraint and the input constraint are satisfied. Then an effective control transmission and compensation mechanism is presented. Finally, an explicit control law is derived.

3.3.1 Constrained Optimization Problem

In order to compensate for data losses due to the packet dropouts and simultaneously take into account the input and state constraints, the constrained MPC strategy is adopted here. For the nonlinear system in (3.1), the cost function at time k is defined as

$$J(\mathbf{u}_k, x_k) \triangleq \sum_{i=0}^{N_c-1} L(\hat{x}_{k+i|k}, u_{i|k}) + F(\hat{x}_{k+N_c|k}), \tag{3.9}$$

where $\mathbf{u}_k \triangleq \text{col}\{u_{0|k}, u_{1|k}, \cdots, u_{N_c-1|k}\}$, $\hat{x}_{k+i+1|k} = \hat{f}(\hat{x}_{k+i|k}, u_{i|k})$ and $\hat{x}_{k|k} = \hat{x}_k$. In the cost function (3.9), $L(\hat{x}_{i|k}, u_{i|k})$ is the stage cost and $F(\hat{x}_{N_c|k})$ is the terminal cost. The control packet is designed by solving the receding horizon optimization problem as follows.

Problem 3.1. $\boldsymbol{u}_k^o \triangleq \arg\min_{\boldsymbol{u}_k} J(\boldsymbol{u}_k, x_k)$ *subject to: (1) the state constraint and the input constraint* $\hat{x}_{k+i|k} \in \mathcal{X}$, $u_{i|k} \in \mathcal{U}$, *for all* $i = 0, 1, \cdots, N_c - 1$*; (2) the terminal state constraint* $\hat{x}_{N_c|k} \in \Omega_f$ *with* Ω_f *being a compact set satisfying* $\{0\} \subset \Omega_f \subset \mathbb{R}^n$*; (3) the nominal model* $\hat{x}_{k+i+1|k} = \hat{f}(\hat{x}_{k+i|k}, u_{i|k})$ *for all* $i = 0, 1, \cdots, N_c - 1$*, and* $\hat{x}_{k|k} = \hat{x}_k$.

Remark 3.2. *Although the constrained optimization Problem 3.1 shares the same form as these in nonlinear constrained MPC strategies without communication networks in [90, 123], two essential differences exist. 1) The initial state $\hat{x}_{k|k}$ of the optimization problem is different. The initial state for standard nonlinear MPC is always the actual system state x_k. But for the networked nonlinear MPC, the initial state $\hat{x}_{k|k}$ can be the actual system state x_k or the state estimate $\hat{x}_k$ due to the S-C packet dropouts. 2) The actual control input for the closed-loop system is different. At time k, the control input of MPC with network-free nonlinear systems takes only the first element $u^o_{0|k}$ of the optimal control sequence $\boldsymbol{u}^o_k$ as the actual control input for the closed-loop system. But for this study, at time k, any control sequences generated from time instant $k - N_{ca} + N_{sc}$ to k can be taken, then any element from the first to the $(N_{ca}+N_{sc})$-th of these control sequences may be chosen as the actual control input for the closed-loop nonlinear NCS, which can be seen in (3.11) in the next section. It is well known that $u^o_{0|k}$ is the best choice for the common MPC algorithms and it provides very nice results on feasibility and stability [95]. In this study, since the actual system state x_k and the best control input $u^o_{0|k}$ cannot be utilized, the resulting nonlinear system dynamics is more complicated. Therefore, we need establish new results on feasibility and stability.*

3.3.2 Control Packet Generation

In the control node, the control packet is generated by making the available information from the S-C packet dropouts and the information of the C-A packet dropouts provided by the acknowledgement packets. Meanwhile, a very efficient manner will be designed to produce the control packets, and the optimization Problem 3.1 will not be carried out for all the time instants. To describe this manner, we denote a variable $r(k)$ to indicate whether the optimization problem is needed or not. The

algorithm to determine the indicator $r(k)$ can be described by the following formula:

$$r(k)=\begin{cases}1 & \text{if } \tau_{sc}(k)=1,\\ 1 & \text{if } 1-\tau_{sc}(k)=1,\tau_{sc}(k-1)=1,1-\tau_{ca}(k-1)=1,\\ 1 & \text{if } \prod_{i=0}^{1}(1-\tau_{sc}(k-i))=1,\tau_{sc}(k-2)=1,\prod_{i=1}^{2}(1-\tau_{ca}(k-i))=1,\\ \vdots & \\ 1 & \text{if } \prod_{i=0}^{N_{sc}-2}(1-\tau_{sc}(k-i))=1,\tau_{sc}(k-N_{sc}+1)=1,\prod_{i=1}^{N_{sc}-1}(1-\tau_{ca}(k-i))=1,\\ 0 & \text{otherwise.}\end{cases} \tag{3.10}$$

In particular, whenever $r(k)=1$, the optimization problem is required to be solved; the control sequence will be generated and packaged, and the information $r(k)=1$ lets $\mathbf{B}_k^u$ in Buffer 1 be updated by $\mathbf{u}_k^o$; otherwise, the optimization is not conducted and the control packet is not generated, and the information $r(k)=0$ commands $\mathbf{B}_k^c$ in Buffer 1 to be updated from the previous stored control sequence.

It should be pointed out that, at time k, the optimization Problem 3.1 can only be directly solved if the system state x_k is received, i.e., $\tau_{sc}(k)=1$. But it also needs to conduct optimization in some situations (i.e., $r(k)=1$) while the current system state is not received. To handle this issue, it needs to estimate the system state based on the previous system state and control inputs. The latest (previous) system state has been stored in $\mathbf{B}_k^x$ in Buffer 1 according to buffer model, and the corresponding (previous) control input sequence can be found in $\mathbf{B}_k^c$ in Buffer 1. Thus, the current system state can be estimated using the prediction of the nominal system for several steps.

Remark 3.3. *It is worth noting that the above control packet generation approach is different from the existing results in [113, 120, 148], where the packets are generated for all the time instants. The principle under this approach is that it is not necessary to take any action if there is no further information provided (i.e., the measurement information is not accepted when the plant input has already been exploited by the predictions in solving the optimization problem, or simply, $r(k)=0$). The proposed control packet generation method offers two benefits: 1) since the constrained optimization dose not require being conducted for all the time instants, the computation load of the controller can be reduced; 2) the prediction action is not needed when $r(k)=0$, which can further increase the computational efficiency of the controller node.*

3.3.3 Packet Transmission and Compensation Strategy Design

In this subsection, we are going to design the mechanism for transmitting the designed packets and implementing the actual control input according to the data losses.

For the control node, an efficient packet transmission method is designed by making use of the acknowledgement information of C-A channel and the information of the S-C packet dropouts. Specifically, the packet transmission operation is carried out according to the packet generation indicator $r(k)$. Case 1): $r(k) = 1$. At the beginning, a newly-generated control packet will be pushed into $\mathbf{B}_k^u$ in Buffer 1 and simultaneously sent out through C-A channel to the actuator node; then once the successful transmission of the control packet over C-A channel is sent back by the acknowledgement link, i.e., $\tau_{ca}(k) = 1$, the content of $\mathbf{B}_k^u$ will be moved to replace $\mathbf{B}_k^c$. Case 2): $r(k) = 0$. No control packet is pushed into $\mathbf{B}_k^u$ or sent out through C-A channel. The buffer content $\mathbf{B}_k^c$ is shifted.

For the actuator node, if it receives the control packet, then control sequence will be updated by Buffer 2, and the acknowledgement packet will be sent back to the control node as $\tau_{ca}(k) = 1$. If the actuator node does not receive the packet, then no information will be sent, and the control sequence in Buffer 2 is shifted. After the updated operations, the first element of the control sequence in Buffer 2 will be used as the actual control input feeding the actuator.

Remark 3.4. *It is noted that the proposed control packet transmission mechanism is physically built on the TCP-like protocols which can provide the information of the C-A packet dropouts back to the controller node. The detailed control packet transmission algorithm indicated by $r(t)$ is designed by the principle of providing all the useful control information using only the necessary transmission load over the C-A channel. In the existing literature in [120, 101], the control packets are transmitted for all the time instants without taking into account the information of the C-A packet dropouts and the S-C packet dropouts simultaneously. These methods actually transmit a lot of redundant data through the C-A channel, which increases the burden and degrades the performance of the network. In contrast, the proposed control packet transmission mechanism only sends all the necessary (new) information to the actuator node. Thus, it can significantly reduce the transmission load of the C-A channel, and may further alleviate the packet dropouts or time delays.*

3.3.4 Explicit Control Law and Closed-loop Model

To explicitly describe the actual control input, some variables need to be defined first. Define $\{p(j), \forall j \in \mathbb{Z}_{\geqslant 0}\}$ as an ordered time instant sequence to describe the events that there are successful transmissions for the C-A channel; define the ordered time instant sequence $\{q(l), \forall l \in \mathbb{Z}_{\geqslant 0}\}$ to describe the events $\{r(k) = 1\}$; define $m_{q(l)} \triangleq \inf_j\{p(j)|q(l) \leqslant p(j) < q(l+1)\}$ with $\inf(\emptyset) = \infty$; denote the ordered time instant sequence $\{m_{q(l_i)}, \forall i \in \mathbb{Z}_{\geqslant 0}\}$ as a subsequence of $\{m_{q(l)}, \forall l \in \mathbb{Z}_{\geqslant 0}\}$ by deleting all the elements equal to ∞. By combining the buffer model, the packet transmission and compensation mechanism, the actual control input can be derived as

$$u_k = \mathbf{u}^o_{m_{q(l_i)}}(k - m_{q(l_i)}), \quad m_{q(l_i)} \leqslant k < m_{q(l_{i+1})}, \tag{3.11}$$

where $\mathbf{u}^o_{m_{q(l_i)}} \triangleq \text{col}\{u^o_{0|q(l_i)}, u^o_{1|q(l_i)}, \cdots, u^o_{N_c-1|q(l_i)}\}$. The resulting closed-loop system is given by

$$x_{k+1} = f(x_k, \mathbf{u}^o_{m_{q(l_i)}}(k - m_{q(l_i)}), \omega_k), \quad m_{q(l_i)} \leqslant k < m_{q(l_{i+1})}. \tag{3.12}$$

3.4 Stability Analysis

In this section, the regional ISpS of the nonlinear NCSs rendered by the proposed MPC strategy will be investigated. Before proving the regional ISpS of the resulting nonlinear NCSs, some notations and hypotheses are introduced.

Assumption 3.2. *The stage cost function $L(x, u)$ is locally Lipschitz in x and u, i.e., there exist constants $0 < L_x < \infty$ and $0 < L_u < \infty$ such that for all $x_1, x_2 \in \mathcal{X}$ and $u_1, u_2 \in \mathcal{U}$,*

$$\|L(x_1, u_1) - L(x_2, u_2)\| \leqslant L_x\|x_1 - x_2\| + L_u\Delta_u,$$

and $L(x, u)$ is lower bounded by

$$L(x, u) \geqslant \alpha_L(\|x\|) + \rho_L,$$

where $\rho_L \leqslant 0$ and α_L is a $\mathcal{K}_\infty$ function.

Assumption 3.3. *The terminal cost function $F(x)$ is locally Lipschitz as $\|F(x_1) - F(x_2)\| \leqslant L_F||x_1 - x_2\|$, $\forall x \in \mathcal{X}$ and $F(0) = 0$. Further, for all $x \in \Omega_f$, there exists*

an auxiliary control law $K_f(x) \in \mathcal{U}$ *such that*

$$F(\hat{f}(x, K_f(x))) - F(x) \leqslant -L(x, K_f(x)),$$

and $\hat{f}(x, K_f(x)) \in \Omega_f$.

Remark 3.5. *Assumption 3.2 and Assumption 3.3 are quite standard for the stage cost function and the terminal cost function, which have been adopted for the non-networked nonlinear systems [77, 90, 123] and the nonlinear NCSs [113, 120].*

To present Assumption 3.4, let us define a mapping as $f^j(x, \mathbf{u}^o_{m_{q(l_i)}}([0:j-1]), \boldsymbol{\omega}_{[0:j-1]}) \triangleq f(f^{j-1}(x, \mathbf{u}^o_{m_{q(l_i)}}([0:j-2]), \boldsymbol{\omega}_{[0:j-2]}), \mathbf{u}^o_{m_{q(l_i)}}(j-1), \omega), \forall j = 1, 2, \cdots, m_{q(l_{i+1})} - m_{q(l_i)}$ and $i \in \mathbb{Z}_{\geqslant 0}$, where $\boldsymbol{\omega}_{[0:j-1]} \in \Upsilon^j$ and $f^0(x, \mathbf{u}^o_{m_{q(l_i)}}([0:-1]), \omega) = x$.

Assumption 3.4. *There exists a compact set* $\mathcal{R}_X$ *with* $\{0\} \subset \mathcal{R}_X \subseteq \mathcal{X}$, *such that* $\mathcal{R}_X \subseteq X_{N_c}(\Omega_f) \sim \mathcal{B}^n(L_{f_x}^{N_c-1} L_\omega \rho_\omega)$ *and* $\mathcal{R}_X$ *is an RPI set for the mappings* $f^j(x, \boldsymbol{u}^o_{m_{q(l_i)}}([0:j-1]), \boldsymbol{\omega}_{[0:j-1]})$, *for all* $j = 1, 2, \cdots, m_{q(l_{i+1})} - m_{q(l_i)}$ *with* $i \in \mathbb{Z}_{\geqslant 0}$, *where* $X_{N_c}(\Omega_f)$ *is the* N_c*-step RCI set of the system in (3.1).*

Remark 3.6. *Assumption 3.4 is to guarantee the feasibility of the proposed constrained MPC algorithm in* $\mathcal{R}_X$*; see Proposition 3.1. The similar assumption is made for the nonlinear NCSs only with the C-A packet dropout in [120] and the nonlinear systems without networks in [90, 123]. The main difference is that Assumption 3.4 can address both the S-C packet dropout and the C-A packet dropout simultaneously using state estimation. In fact, if there is no S-C packet dropout which is the case in [120] and no state estimation, then* $q(l) = l$. *In particular, if at some time instant* l, *there is a C-A packet dropout* $p(j) = l$, *then the control packet* $\boldsymbol{u}^o_{m_{q(l_i)}}$ *becomes* $\boldsymbol{u}^o_l = \mathrm{col}\{u^o_{0|l}, u^o_{1|l}, \cdots, u^o_{N_c-1|l}\}$, *and the control input (3.11) is given by* $u_k = \boldsymbol{u}^o_l(k-l)$, *for* $l \leqslant k < p(j+1)$. *As a result, the mapping* $f^j(x, \boldsymbol{u}^o_{m_{q(l_i)}}([0:j-1]), \boldsymbol{\omega}_{[0:j-1]})$ *becomes exactly the corresponding mapping in [120], and the same assumption recovers from Assumption 3.4.*

Before proceeding, a constrained minimization problem needs to be stated, based on which the ISpS-type Lyapunov function candidate can be constructed.

Problem 3.2. *Minimize the following function* $\bar{J}(\hat{x}_{k|k}, \boldsymbol{u}_k)$ *as*

$$\bar{J}(\hat{x}_{k|k}, \boldsymbol{u}_k) \triangleq \sum_{i=0}^{N_c} L(\hat{x}_{k+i|k}, u_{i|k}) + F(\hat{x}_{N_c+1|k}), \quad \hat{x}_{k|k} = x_k,$$

subject to

$$\begin{cases} \hat{x}_{k+i|k} \in \mathcal{X}, & i = 0, 1, 2, \cdots, N_c - 1, \\ \hat{x}_{k+N_c|k} \in \Omega_f,\ \hat{x}_{k+N_c+1|k} \in \Omega_f, & \\ u_{i|k} \in \mathcal{U},\ \hat{x}_{k+i+1|k} = \hat{f}(\hat{x}_{k+i|k}, u_{i|k}), & i = 0, 1, 2, \cdots, N_c, \end{cases} \tag{3.13}$$

where $\boldsymbol{u}_k = \text{col}\{u_{0|k}, u_{1|k}, \cdots, u_{N_c|k}\}$.

Proposition 3.1. *Suppose Assumption 3.4 and Assumption 3.3 hold. Then Problem 3.1 is feasible for all* $x_0 \in \mathcal{R}_X$ *and Problem 3.2 is feasible in* $\mathcal{R}_X$.

Proof. According to the state estimation algorithm, it can be verified that the state estimate $\hat{x}_k$ belongs to $X_{N_c}(\Omega_f)$ whenever $x_k \in \mathcal{R}_X$ for all k. Thus, According to Assumption 3.4, Problem 3.1 is feasible for all $x_0 \in \mathcal{R}_X$. For Problem 3.2, for all state x_k in $X_{N_c}(\Omega_f)$, there exists a sequence of control action $\mathbf{u}_k^o$ steering the predicted state $\hat{x}_{k+N_c|k}$ into the terminal set Ω_f according to the definition of $X_{N_c}(\Omega_f)$. Define the control sequence $\bar{\mathbf{u}}_k^o \triangleq \text{col}\{\mathbf{u}_k^o, K_f(\hat{x}_{k+N_c|k})\}$ at time k. Then $\bar{\mathbf{u}}_k^o$ is a feasible control sequence for Problem 3.2 in terms of Assumption 3.3. Since $x_0 \in \mathcal{R}_X$ implies $x_k \in \mathcal{R}_X \subseteq X_{N_c}(\Omega_f)$, Problem 3.2 is feasible in $\mathcal{R}_X$. □

For the simplicity of presenting the stability conditions, the definitions of some parameters which will be used in the sequel, are given as follows. Define $b_1 \triangleq \sum_{i=1}^{N_c} L_x \frac{L_{f_x}^i - 1}{L_{f_x} - 1} L_{f_u}\Delta_u + (N_c+1)L_u\Delta_u + L_F \frac{L_{f_x}^{N_c+1} - 1}{L_{f_x} - 1} L_{f_u}\Delta_u - \rho_L$, $b_2 \triangleq (\frac{N_c L_x}{2} + L_F)(N_c + 1)L_{f_u}\Delta_u + (N_c+1)L_u\Delta_u - \rho_L$, $b_3 \triangleq (L_F \frac{1 - L_{f_x}^{N_c+2}}{1 - L_{f_x}} + L_x \sum_{i=1}^{N_c+1} \frac{1 - L_{f_x}^i}{1 - L_{f_x}}) L_{f_u}\Delta_u + (N_c+2)L_u\Delta_u$ and $b_4 = (L_F \frac{1 - L_{f_x}^{N_c+2}}{1 - L_{f_x}} + L_x \sum_{i=1}^{N_c+1} \frac{1 - L_{f_x}^i}{1 - L_{f_x}}) L_{f_u}\Delta_u + (N_c+2)L_u\Delta_u$. Furthermore, we define parameters

$$\rho_1 \triangleq \begin{cases} b_1 & \text{if } L_{f_x} \neq 1, \\ b_2 & \text{if } L_{f_x} = 1, \end{cases} \qquad \rho_2 \triangleq \begin{cases} b_3 & \text{if } L_{f_x} \neq 1, \\ b_4 & \text{if } L_{f_x} = 1. \end{cases}$$

Further, define the function

$$\gamma_{f_x}(s) \triangleq \begin{cases} (L_F L_{f_x}^{N_c+1} + \sum_{i=0}^{N_c} L_x L_{f_x}^i) \cdot \mu(s) & \text{if } L_{f_x} \neq 1, \\ (L_F + (N_c+1)L_x)s & \text{if } L_{f_x} = 1. \end{cases}$$

Assumption 3.5. *Suppose that the disturbance set* Υ *is such that the condition C2 in Definition 3.5 is satisfied with* $V(x_k, k) = L(x_k, u_k) + \bar{J}(\hat{x}_{k+1|k}, \boldsymbol{u}_k^*)$, $\Omega = \Omega_f$, $\alpha_2 = \alpha_L$,

$\alpha_3 = \alpha_F$, $\gamma = \gamma_{f_x}$, $c_2 = \rho_1$ *and* $c_3 = \rho_2$, *where* $\hat{x}_{k+1|k} = \hat{f}(x_k, u_k)$ *and* $\boldsymbol{u}_k^*$ *is the optimal solution to Problem 3.2.*

Remark 3.7. *This assumption is essentially to impose the condition on the bound of the disturbance set. That is, if one wants to achieve the regional ISpS, the external disturbance cannot be too "large". The similar assumptions have been made for the robust nonlinear MPC in [123, 113, 90]. In fact, one can always find a small enough disturbance set to meet this assumption [113, 123].*

The regional ISpS of the resulting nonlinear NCSs based on the proposed MPC control strategy is reported in the following Theorem 3.2.

Theorem 3.2. *Suppose that all the Assumptions hold with the compact sets* Ω_f *and* $\mathcal{X}$*, then the resulting NCSs in (3.12) is regional ISpS in* $\mathcal{R}_X$ *with respect to the disturbance* $\omega_k \in \Upsilon, \forall k \in \mathbb{Z}_{\geqslant 0}$*, and the system trajectory satisfies* $\lim_{k\to\infty} \mathrm{d}|x(k, \bar{x}, \boldsymbol{\omega}_{0,k-1})|_{\Omega_\omega} = 0$, $\forall \bar{x} \in \mathcal{R}_X$.

Proof. According to Proposition 3.1, for all $x_0 = \bar{x} \in \mathcal{R}_x$, we can define the optimal solution to Problem 3.2 as $\mathbf{u}_k^*$ with the initial state $\hat{x}_{k+1|k}$ at time k, namely,

$$\mathbf{u}_k^* \triangleq \arg\min_{\mathbf{u}_k} \{\bar{J}(\hat{x}_{k+1|k}, \mathbf{u}_k)\}, \quad \text{subject to (3.13)},$$

where $\hat{x}_{k+1|k} = \hat{f}(x_k, u_k)$ with u_k given by (3.11) and $\mathbf{u}_k^* = \mathrm{col}\{u_{0|k}^*, u_{1|k}^*, \cdots, u_{N_c|k}^*\}$. It follows that the optimal solution to Problem 3.2 with the initial state $\hat{x}_{k+2|k+1}$ is $\mathbf{u}_{k+1}^*$ at time $k+1$. Based on $\mathbf{u}_{k+1}^*$, we can construct a feasible control sequence $\bar{\mathbf{u}}_{k+1}^* = \mathrm{col}\{u_{0|k+1}^*, u_{1|k+1}^*, \cdots, u_{N_c-1|k+1}^*, K_f(\hat{x}_{k+N_c+2|k+1})\}$ for Problem 3.2 with the initial state $\hat{x}_{k+2|k+1}$ at time $k+1$. Choose $V(x_k, k) \triangleq L(x_k, u_k) + \bar{J}(\hat{x}_{k+1|k}, \mathbf{u}_k^*)$ as the ISpS-type Lyapunov function candidate at time k and define an auxiliary function $\bar{V}(x_{k+1}, k+1) \triangleq L(x_{k+1}, u_{k+1}) + \bar{J}(\hat{x}_{k+2|k+1}, \bar{\mathbf{u}}_{k+1}^*)$. The difference can be evaluated

as

$$\begin{aligned}
&\bar{V}(x_{k+1},k+1)-V(x_k,k)\\
=&L(x_{k+1},u_{k+1})+\bar{J}(\hat{x}_{k+2|k+1},\bar{\mathbf{u}}^*_{k+1})-L(x_k,u_k)-\bar{J}(\hat{x}_{k+1|k},\mathbf{u}^*_k)\\
=&-L(x_k,u_k)+L(x_{k+1},u_{k+1})-L(\hat{x}_{k+1|k},u^*_{0|k})\\
&+\sum_{i=2}^{N_c+1}L(\hat{x}_{k+i|k+1},u^*_{i-2|k+1})-L(\hat{x}_{k+i|k},u^*_{i-1|k})\\
&+L(\hat{x}_{N_c+k+2|k+1},K_f(\hat{x}_{k+N_c+2|k+1}))+F(\hat{x}_{N_c+k+3|k+1})\\
&-F(\hat{x}_{N_c+k+2|k+1})+F(\hat{x}_{N_c+k+2|k+1})-F(\hat{x}_{N_c+k+2|k}).
\end{aligned}\tag{3.14}$$

Since $\hat{x}_{k+N_c+2|k+1}\in\Omega_f$, it can be obtained that

$$L(\hat{x}_{N_c+k+2|k+1},K_f(\hat{x}_{k+N_c+2|k+1}))+F(\hat{x}_{N_c+k+3|k+1})-F(\hat{x}_{N_c+k+2|k+1})\leqslant 0.\tag{3.15}$$

By using the Lipschitz condition, we get

$$\begin{aligned}
&\sum_{i=2}^{N_c+1}L(\hat{x}_{k+i|k+1},u^*_{i-2|k+1})-L(\hat{x}_{k+i|k},u^*_{i-1|k})\\
\leqslant&\sum_{i=2}^{N_c+1}\left(L_xL_{f_x}^{i-1}\mu(\|\omega_k\|)+L_x\sum_{j=0}^{i-2}L_{f_x}^jL_u\Delta_u+L_u\Delta_u\right),\\
=&\sum_{i=1}^{N_c}\left(L_xL_{f_x}^i\mu(\|\omega_k\|)+L_xL_u\Delta_u\frac{L_{f_x}^i-1}{L_{f_x}-1}+L_u\Delta_u\right)\quad(L_{f_x}\neq 1).
\end{aligned}\tag{3.16}$$

Similarly, we have

$$L(x_{k+1},u_{k+1})-L(\hat{x}_{k+1|k},u^*_{0|k})\leqslant L_x\mu(\|\omega_k\|)+L_u\Delta_u.\tag{3.17}$$

The terminal cost can be bounded as

$$\begin{aligned}
&F(\hat{x}_{N_c+k+2|k+1})-F(\hat{x}_{N_c+k+2|k})\\
\leqslant&L_F\|\hat{x}_{N_c+k+2|k+1}-\hat{x}_{N_c+k+2|k}\|,\\
\leqslant&L_F(L_{f_x}^{N_c+1}\mu(\|\omega_k\|)+L_{f_u}\Delta_u\frac{L_{f_x}^{N_c+1}-1}{L_{f_x}-1})\quad(L_{f_x}\neq 1).
\end{aligned}\tag{3.18}$$

Substituting (3.15)-(3.18) into (3.14) and applying $L(x_k,u^o_{0|k})\geqslant\alpha_L(\|x_k\|)+\rho_L$ result

in

$$\begin{aligned}&\bar{V}(x_{k+1},k+1)-V(x_k,k)\\ \leqslant&-\alpha_L(\|x_k\|)+(L_FL_{f_x}^{N_c+1}+\sum_{i=0}^{N_c}L_xL_{f_x}^i)\cdot\mu(\|\omega_k\|)+b_1\quad(L_{f_x}\neq 1).\end{aligned}$$

Similarly, we can obtain

$$\bar{V}(x_{k+1},k+1)-V(x_k,k)\leqslant-\alpha_L(\|x_k\|)+(L_F+(N_c+1)L_x)\cdot(\mu(\|\omega_k\|))+b_2\quad(L_{f_x}=1).$$

By the optimality of Problem 3.2, $V(x_{k+1},k+1)\leqslant\bar{V}(x_{k+1},k+1)$. Consequently, we have

$$V(x_{k+1},k+1)-V(x_k,k)\leqslant-\alpha_L(\|x_k\|)+\gamma_{f_x}(\|\omega_k\|)+\rho_1,\tag{3.19}$$

for all x_k in the feasible set. Next, it is easy to derive that

$$V(x_k,k)=L(x_k,u_k)+\sum_{i=1}^{N_c+1}L(\hat{x}_{k+i|k},u_{i-1|k}^*)+F(\hat{x}_{k+N_c+2|k})\geqslant\alpha_L(\|x_k\|)+\rho_L.\tag{3.20}$$

Finally, we need to establish the upper bound of $V(x_k,k)$ for all $x_k\in\Omega$. To this end, given the initial state x_k at time k, we define an auxiliary control sequence for Problem 3.2 as

$$\mathbf{u}_k^{'}\triangleq\text{col}\{K_f(\hat{x}_{k+1|k}^{'}),K_f(\hat{x}_{k+2|k}^{'}),\cdots,K_f(\hat{x}_{k+N_c+1|k}^{'})\},$$

where $\hat{x}_{k+j|k}^{'}=\hat{f}(\hat{x}_{k+j-1|k}^{'},K_f(\hat{x}_{k+j-1|k}^{'}),\forall j\geqslant 2$, and $\hat{x}_{k+1|k}^{'}=\hat{f}(x_k,K_f(x_k))$. Then we have

$$\begin{aligned}V(x_k,k)=&L(x_k,u_k)-L(x_k,K_f(x_k))+\bar{J}(\hat{x}_{k+1|k},\mathbf{u}_k^*)\\&-\bar{J}(\hat{x}_{k+1|k},\mathbf{u}_k^{'})+\bar{J}(\hat{x}_{k+1|k},\mathbf{u}_k^{'})+L(x_k,K_f(x_k))\\&\leqslant L_u\Delta_u+\bar{J}(\hat{x}_{k+1|k},\mathbf{u}_k^*)-\bar{J}(\hat{x}_{k+1|k},\mathbf{u}_k^{'})+V_f(x_k),\end{aligned}\tag{3.21}$$

where $V_f(x_k)\triangleq\bar{J}(\hat{x}_{k+1|k},\mathbf{u}_k^{'})+L(x_k,K_f(x_k))$. By applying the Lipschitz condition

again, we have

$$\begin{aligned}
&\sum_{i=1}^{N_c+1} L(\hat{x}_{k+i|k}, u^*_{i|k}) - L(\hat{x}^{'}_{k+i|k}, K_f(\hat{x}^{'}_{k+i|k})) \\
\leqslant &\sum_{i=1}^{N_c} (L_x \|\hat{x}_{k+i|k} - \hat{x}^{'}_{k+i|k}\| + L_u \Delta_u) \\
\leqslant &\sum_{i=1}^{N_c} L_x \frac{1 - L^i_{f_x}}{1 - L_{f_x}} L_{f_u} \Delta_u + (N_c + 1) L_u \Delta_u \quad (L_{f_x} \neq 1),
\end{aligned}$$

and

$$\begin{aligned}
F(\hat{x}_{k+N_c+2|k}) - F(\hat{x}^{'}_{k+N_c+2|k}) \leqslant &L_F \|\hat{x}_{k+N_c+2|k} - \hat{x}^{'}_{k+N_c+2|k}\|, \\
\leqslant &L_F \frac{1 - L^{N_c+2}_{f_x}}{1 - L_{f_x}} L_{f_u} \Delta_u \quad (L_{f_x} \neq 1).
\end{aligned}$$

Therefore,

$$\begin{aligned}
&\bar{J}(\hat{x}_{k+1|k}, \mathbf{u}^*_k) - \bar{J}(\hat{x}_{k+1|k}, \mathbf{u}^{'}_k) \\
= &\sum_{i=1}^{N_c+1} L(\hat{x}_{k+i|k}, u^*_{i|k}) - L(\hat{x}^{'}_{k+i|k}, K_f(\hat{x}^{'}_{k+i|k})) + F(\hat{x}_{k+N_c+2|k}) - F(\hat{x}^{'}_{k+N_c+2|k}) \\
\leqslant &\sum_{i=1}^{N_c+1} L_x \frac{1 - L^i_{f_x}}{1 - L_{f_x}} L_{f_u} \Delta_u + (N_c + 1) L_u \Delta_u + L_F \frac{1 - L^{N_c+2}_{f_x}}{1 - L_{f_x}} L_{f_u} \Delta_u \quad (L_{f_x} \neq 1). \quad (3.22)
\end{aligned}$$

On the other hand, since $x_k \in \Omega_f$, then $\hat{x}^{'}_{k+i+1|k} \in \Omega_f$, for all $i = 0, 1, 2, \cdots, N_c + 1$. As a result,

$$F(\hat{x}^{'}_{k+i+1|k}) - F(\hat{x}^{'}_{k+i|k}) \leqslant -L(\hat{x}^{'}_{k+i|k}, K_f(\hat{x}^{'}_{k+i|k})), \quad (3.23)$$

for all $i = 0, 1, 2, \cdots, N_c$, where $\hat{x}^{'}_{k|k} = x_k$. Summing up both sides of (3.23) from 0 to N_c gives rise to

$$V_f(x_k) \leqslant F(x^{'}_{k|k}) \leqslant \alpha_F(\|x_k\|), \quad (3.24)$$

where $\alpha_F(s) = L_F s$. By plugging (3.22) and (3.24) into (3.21), we get

$$V(x_k, k) \leqslant \alpha_F(\|x_k\|) + (L_F \frac{1 - L^{N_c+2}_{f_x}}{1 - L_{f_x}} + L_x \sum_{i=1}^{N_c+1} \frac{1 - L^i_{f_x}}{1 - L_{f_x}}) L_{f_u} \Delta_u + (N_c + 2) L_u \Delta_u \quad (L_{f_x} \neq 1).$$

Analogously, we can obtain

$$V(x_k,k) \leqslant \alpha_F(\|x_k\|)+(L_F(N_c+2)+\frac{(N_c+2)(N_c+1)}{2}L_x)L_{f_u}\Delta_u+(N_c+2)L_u\Delta_u \quad (L_{f_x}=1).$$

By combining the cases of $(L_{f_x}=1)$ and $(L_{f_x}\neq 1)$, we have

$$V(x_k,k) \leqslant \alpha_F(\|x_k\|)+\rho_2.$$

Therefore, $V(x_k,k)$ is an ISpS-type Lyapunov function. According to Theorem 3.1, the resulting nonlinear NCS is ISpS in $\mathcal{R}_X$ and all the trajectories starting in $\mathcal{R}_X$ converge to set Ω_ω. The proof is completed. □

Remark 3.8. *Unlike the regional ISS established in [113, 120], the regional ISpS is proven for the resulting nonlinear NCSs. The insight that we resort to the regional ISpS can be seen from the proof procedure: the joint effects of the C-A packet dropouts and the S-C packet dropouts make the actual control input u_k be not a function of the current system state x_k. Therefore, the deviation or bias exists for the lower bound of the stage cost function $L(x_k,u_k)$, which finally results in the regional ISpS.*

Remark 3.9. *It is worth noting that a novel approach has been proposed to prove the regional ISpS for the resulting nonlinear NCSs by accommodating the joint effects of the C-A packet dropouts and the S-C packet dropouts as well as the compensation strategy. In the existing results in [120, 113, 77, 90, 123], the regional ISpS or ISS is generally established by proving that the optimal index performance $J(\boldsymbol{u}_k^*,x_k)$ is the ISpS-type or ISS-type Lyapunov function; see the detailed techniques in the stability of the MPC approach [95]. However, the communication constraints and the compensation strategy prevent us from using the optimal index performance $J(\boldsymbol{u}_k^*,x_k)$ as the ISpS-type Lyapunov function directly. To circumvent this issue, we first construct the auxiliary Problem 3.2, based on which a novel ISpS-type Lyapunov function $L(x_k,u_k)+\bar{J}(\hat{x}_{k+1|k},\boldsymbol{u}_k^*)$ is proposed and verified. It is worthwhile to point out that Problem 3.2 is only an auxiliary vehicle for the proof of the regional ISpS, and it does not require being solved when applying the designed network-based MPC strategy.*

3.5 Simulation

In this section, an example is given to verify the proposed MPC compensation strategy for a network-based control system. We consider the control problem for a cart-and-

spring system deployed in an Ethernet-like environment, where packet dropouts are apt to occur. The cart-and-spring system is shown in Figure 3.2, which has been studied in [123, 89] in the non-network environment. In the cart-and-spring system,

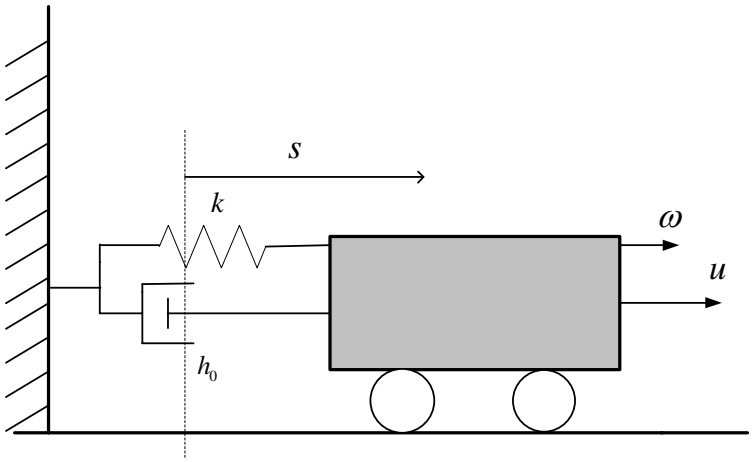

Figure 3.2: Cart and spring system.

s is the displacement of the carriage from the equilibrium point, where $u = 0$ and the external disturbance $\omega = 0$. The spring factor is nonlinear, and it is modeled as $k = k_0 e^{-s}$, and the damper factor is h_d. By setting $x_1 = s$ and $x_2 = \dot{s}$, the dynamic model of the cart-and-spring system can be derived as [123, 89]

$$\begin{cases} \dot{x}_1(t) = x_2(t), \\ \dot{x}_2(t) = -\frac{k_0}{M} e^{-x_1(t)} x_1(t) - \frac{h_d}{M} x_2(t) + \frac{u(t)}{M} + \frac{\omega(t)}{M}. \end{cases}$$

Further, the nonlinear model with a sampling period T_c can be discretized as

$$\begin{cases} x_1(k+1) = x_1(k) + T_c x_2(k), \\ x_2(k+1) = x_2(k) - T_c \frac{k_0}{M} e^{-x_1(k)} x_1(k) - T_c \frac{h_d}{M} x_2(k) + T_c \frac{u(k)}{M} + T_c \frac{\omega(k)}{M}. \end{cases}$$

The system parameters are given as follows: The spring linear factor is $k_0 = 0.10$ N/m; the mass of the carriage is $M = 4.5$ kg; the damper factor is $h_d = 1.1$ N·s/m and the sampling period is $T_c = 0.4$ s. The control input is constrained as $|u| \leqslant 4.5$ N and the states are constrained as $|x_1(k)| \leqslant 2.65$ m and $|x_2(k)| \leqslant 10.0$m/s. Like the objective function in [123], we choose stage cost function $L(x, u) = 0.01x^{\mathrm{T}}x + 0.01u^{\mathrm{T}}u$. The terminal cost function is chosen as the quadratic form $F(x) = x^{\mathrm{T}}Px$. By using the proposed method in [11], the terminal cost function is determined as

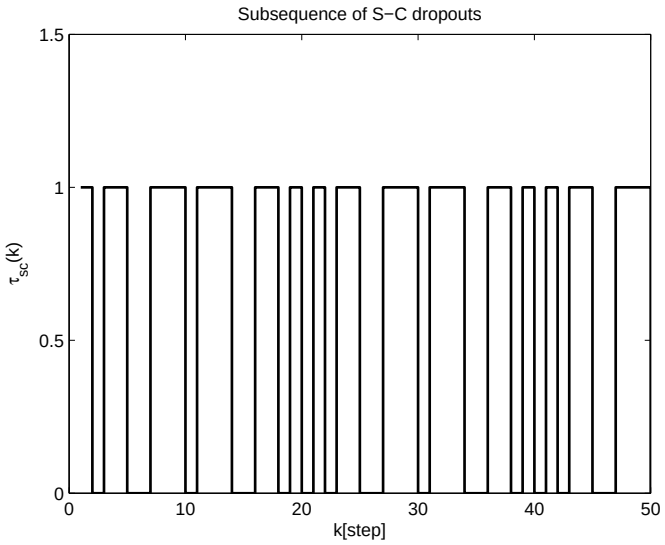

Figure 3.3: Subsequence of the S-C dropouts.

$P = 10^{-2} \times [4.83, 2.19; 2.19, 2.34]$; the terminal set can be chosen as $\Omega_f = \{x | x^{\mathrm{T}} P_\omega x < 1\}$, where $P_\omega = [0.6032, 0.2739; 0.2739, 0.2927]$ and an auxiliary control law can be designed as $K_f(x) = -Kx$ with $K = [0.9050, 2.1179]$ for the nonlinear NCS. For the system model, the Lipschitz constants can be determined as: $L_{f_x} = 1.9158$ and $L_{f_u} = 0.2444$ and the bound function is $\mu(s) = 0.2222s$. For the cost functions, the corresponding Lipschitz constants are determined as: $L_x = 0.2069$, $L_u = 0.09$, $\rho_L = 0$ and $L_F = 1.7265$, and the bound functions are: $\alpha_L(s) = 0.01s^2$ and $\alpha_F(s) = 1.7265s$. The disturbance bound is estimated to be $\rho_\omega = 0.008$.

The stationary operation conditions of the system are $x_1^o = 0.2$ m, $x_2^o = 0$ s/m and $u^o = 0.0540$ N. In the simulation, both the S-C channel and the C-A channel are subject to random packet dropouts. Both the packet dropouts are generated quite arbitrarily and may not follow any known statistic distribution or stochastic model. A sample subsequence of the S-C packet dropout is depicted in Figure 3.3, and the one for the C-A channel is demonstrated in Figure 3.4.

To verify the effectiveness of proposed MPC strategy, we conduct four sets of comparison simulations. Firstly, for the network-based cart-and-spring system subject to the two-channel packet dropouts described by Figure 3.4 and Figure 3.3, the simulations are carried out by implementing the proposed MPC compensation strategy. Then, for the same network-based system, the simulations are conducted using the MPC strategy proposed in [120], where only the C-A packet dropouts are taken into

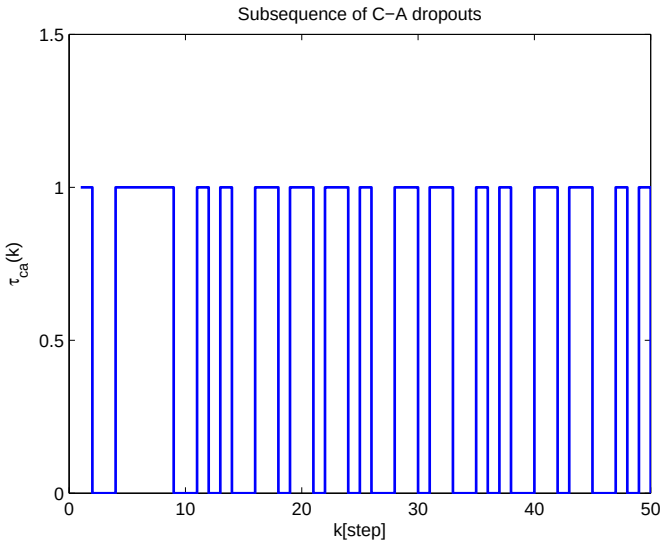

Figure 3.4: Subsequence of the C-A dropouts.

account, and the S-C packet dropout is ignored; the control input is applied as u_o when the S-C packet dropout occurs. Next, under the situation that both the C-A packet dropout and the S-C packet dropout are not considered, we run the simulations by the standard MPC for the same systems; the control input is also given as u_o in case of the packet dropouts. Finally, for the same cart-and-spring system, we assume that the system have perfect networks (no packet dropouts and delays for both two channels). In that situation, the simulations are also conducted using the standard MPC strategy.

All the simulation results are depicted in Figure 3.5 – Figure 3.7. Specifically, the controlled displacements of the four cases are shown in Figure 3.5; the velocities are depicted in Figure 3.6 and the control inputs are presented in Figure 3.7. It can be seen that: 1) The states controlled by the proposed MPC strategy are stable, and the constraints of the state and the control input are satisfied; 2) although the system is subject to the two-channel packet dropouts, the system performance using the proposed MPC strategy is comparable to the results of the perfect networks; 3) the system performance of the proposed MPC strategy outperforms the results of the strategy that only compensates for the C-A channel dropout proposed in [120], and is much better than the results in which the two-channel packet dropouts are ignored. These above observations imply that the proposed MPC strategy is valid and effective.

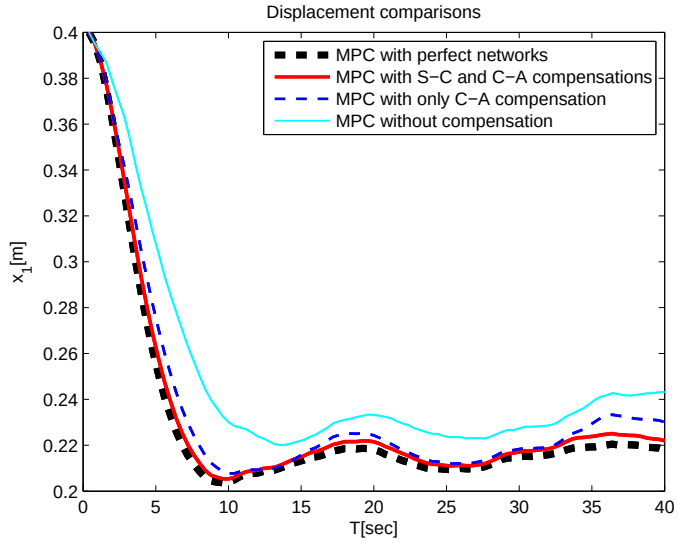

Figure 3.5: Comparisons of displacements.

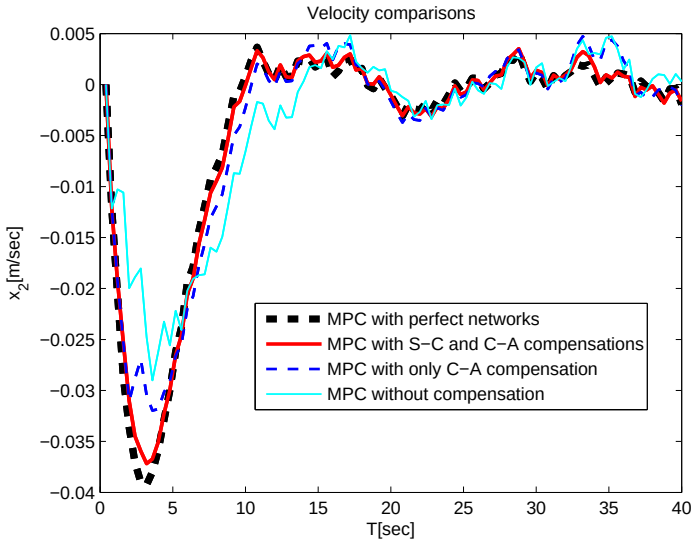

Figure 3.6: Comparisons of velocities.

3.6 Conclusion

We have investigated the networked control problem for the constrained nonlinear systems subject to disturbances and two-channel packet dropouts. The MPC-based control strategy has been used to design the control packet, and an efficient transmission and compensation mechanism has been designed such that all the necessary information can be transmitted but with reduced transmission load. To analyze the

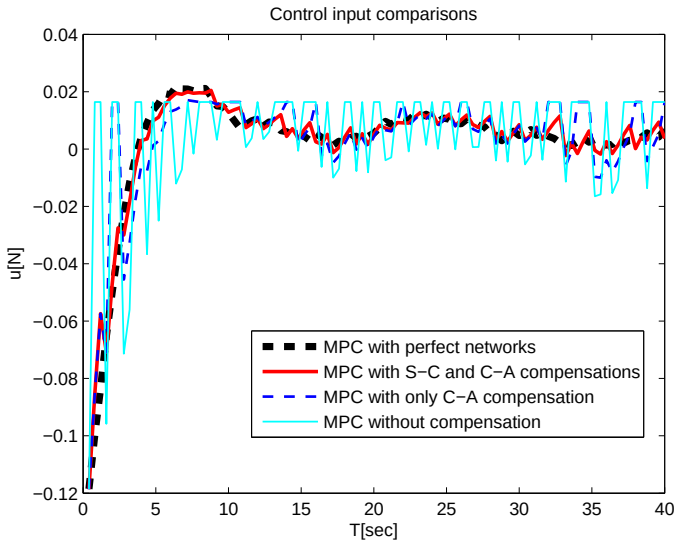

Figure 3.7: Comparisons of control input.

stability of the proposed control method, a generalized characterization of the regional ISpS has been established. Further, a novel approach has been developed to guarantee the regional ISpS of the resulting nonlinear systems. Finally, the effectiveness of the proposed control strategy has been verified by a network-based spring-and-cart system.

Chapter 4

Min-Max Model Predictive Control of NCSs with Delays and Packet Dropouts

4.1 Introduction

In **Chapter 3**, an MPC-based control strategy is proposed for a class of nonlinear NCSs to reduce the transmission load of communication networks. The result in **Chapter 3** can only deal with packet dropouts but the communication delays cannot be accommodated. In addition, the information of disturbances is not fully utilized. This chapter will design an MPC-based control strategy to handle the communication delays, packet dropouts and the disturbances. It is well known that the min-max MPC [133, 95] features the following: (1) It is capable of incorporating the external disturbance into the optimization problem, and (2) the designed optimal control law is robust against the worst disturbance. Therefore, the min-max MPC can be employed to improve the system performance compared to the standard MPC, i.e., receding horizon open-loop MPC (RHOMPC). In this chapter, the *min-max MPC scheme* for the constrained nonlinear NCSs with two-channel packet dropouts and time delays based on the UDP-like protocol is studied. The main contributions of this work are two-fold:

- A framework of synthesizing the constrained nonlinear NCSs using the min-max MPC strategy is proposed. The min-max MPC algorithm is utilized to design the control packets by incorporating the disturbance into the optimization prob-

lem. Thus, the system performance can be improved.

- A novel approach is proposed to prove ISpS of the resulting nonlinear NCS. Due to the joint effects of the packet dropouts and the time delays, as well as the min-max strategy, the ISS used in [120, 113] cannot be directly applied to this study, and the optimal value of the performance index for designing the control packet cannot be used as a Lyapunov function. In this study, we analyze the ISpS for the resulting nonlinear NCS. By constructing an auxiliary constrained optimization problem, a novel ISpS-type Lyapunov function is proposed, and then the corresponding ISpS conditions are established.

The remainder of this chapter is organized as follows. The design objective for the nonlinear NCSs and the preliminary results for the constrained nonlinear systems are presented in Section 4.2. In Section 4.3, the min-max MPC-based control packets are designed and the control compensation strategy is presented. In Section 4.4, the stability (ISpS) of the resulting nonlinear NCS is analyzed. The simulation results and the comparison studies are illustrated in Section 4.5. Finally, the conclusions are made in Section 4.6.

Nomenclature: The superscripts "T" and "-1" stand for the matrix transpose and the matrix inverse, respectively. The notation $\mathbb{Z}$ ($\mathbb{Z}_{\geqslant 0}$) denotes the set of integers (non-negative integers) and the symbol $\mathbb{R}$ ($\mathbb{R}_{\geqslant 0}$) represents the real space (non-negative real space). The Euclidean norm of a given vector x is denoted by $\|x\|$ and the column operation $\mathrm{col}\{x_1, x_2, \cdots, x_n\}$ is denoted as $[x_1^{\mathrm{T}}, x_2^{\mathrm{T}}, \cdots, x_n^{\mathrm{T}}]^{\mathrm{T}}$ for column vectors $x_1, x_2, \cdots, x_n$. For any given $N+1$ bounded discrete-time signals $\mathbf{v} = \{v_0, v_1, v_2, \cdots, v_N\}$, define the subsequence as $\mathbf{v}_{k_1,k_2} \triangleq \{v_{k_1}, v_{k_1+1}, \cdots, v_{k_2}\}$ with $k_1, k_2 \in \mathbb{Z}_{\geqslant 0}$; define the truncation as $\mathbf{v}_{[k-1]} \triangleq \{v_0, v_1, v_2, \cdots, v_{k-1}\}$ and the norm as $\|\mathbf{v}\|_\infty \triangleq \sup_{k\geqslant 0} \|v_k\|$. A continuous function $\alpha : \mathbb{R}_{\geqslant 0} \to \mathbb{R}_{\geqslant 0}$ is said to be a $\mathcal{K}$-function, if it is strictly increasing and $\alpha(s) > 0$ for $s > 0$ with $\alpha(0) = 0$. A continuous function $\alpha(.)$ is said to be a $\mathcal{K}_\infty$-function, if it is a $\mathcal{K}$-function, and $\alpha(s) \to \infty$ as $s \to \infty$. A continuous function $\beta : \mathbb{R}_{\geqslant 0} \times \mathbb{Z}_{\geqslant 0} \to \mathbb{R}_{\geqslant 0}$ is said to be a $\mathcal{KL}$-function, if $\beta(s, k)$ is a $\mathcal{K}$-function in s for every given $k \in \mathbb{Z}_{\geqslant 0}$, and it is strictly decreasing in k with $\beta(s, k) \to 0$ as $k \to \infty$. For two given sets $A \subseteq \mathbb{R}^n$, $B \subseteq \mathbb{R}^n$, the Pontryagin difference set C is denoted as $C = A \sim B$, which is defined by the set $\{x \in \mathbb{R}^n | x + y \in A, \forall y \in B\}$. A closed ball in n-dimensional space with radius of $r \geqslant 0$, centered at the origin, is denoted as $\mathcal{B}^n(r)$.

4.2 Problem Formulation and Preliminaries

4.2.1 Problem Formulation

Consider the NCS shown in Fig. 4.1, where both the S-C channel and the C-A channel are connected via Ethernet-like communication networks. On this type of communication links, the information can be transmitted in the form of large time-stamped (TS) packets [148]. The time delays and packet dropouts may occur simultaneously over both the S-C channel and C-A channel due to networked traffic congestions and/or physical components failures especially in unreliable wireless communication networks. At every time instant, there is only one packet sent from the sensor node to the controller node and only one sent from the controller node to the actuator node. The maximum number of consecutive packet dropouts is defined by the maximum number of time instants when packets are consecutively missing. The maximum time delay is defined as the maximum number of time instants between the time instant when the packet is sent and that when received. The maximum number of consecutive packet dropouts and the maximum time delay are bounded and independent of time instants, which are the network parameters. Specifically, the maximum numbers of consecutive packet dropouts for the S-C channel and the C-A channel are N_{sc} and N_{ca}, respectively. The maximum time delays for the S-C channel and the C-A channel are T_{sc} and T_{ca}, respectively. The controller operates with the same sampling rate as the system plant; the perfect synchronization among the sensor, the controller and the actuator is assumed to be held; the system state is measurable by the sensor node. The system dynamics is modeled as the following

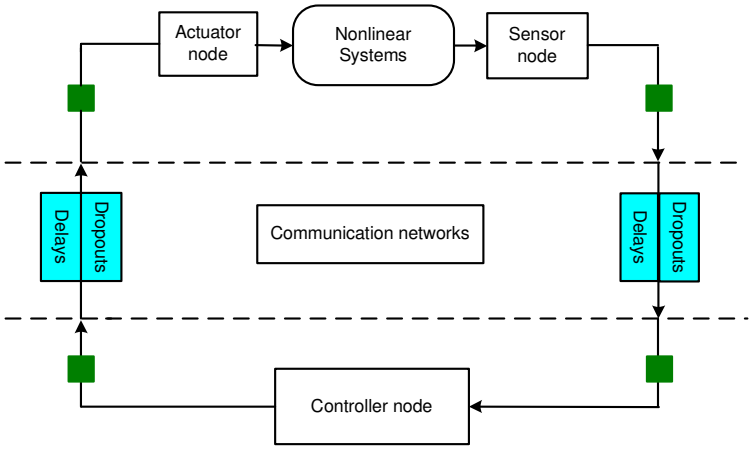

Figure 4.1: The setup of the NCS

nonlinear difference equation:

$$x_{k+1} = f(x_k, u_k, \omega_k), \quad k \in \mathbb{Z}_{\geqslant 0}, \quad x_0 = \bar{x}, \tag{4.1}$$

where $x_k \in \mathbb{R}^n$ is the system state, $u_k \in \mathbb{R}^m$ is the control input and $\omega_k \in \mathbb{R}^r$ is the external disturbance. The system state and the control input are constrained as

$$x_k \in \mathcal{X}, \quad u_k \in \mathcal{U}, \quad \forall k \in \mathbb{Z}_{\geqslant 0}, \tag{4.2}$$

where $\mathcal{X}$ and $\mathcal{U}$ are compact sets such that $\{0\} \subset \mathcal{X} \subseteq \mathbb{R}^n$ and $\{0\} \subset \mathcal{U} \subseteq \mathbb{R}^m$, respectively. The external disturbance belongs to a compact set Υ satisfying $\{0\} \subset \Upsilon \subseteq \mathbb{R}^r$ with $d_\omega \triangleq \max_{\omega_k \in \Upsilon} \|\omega_k\|$. It is assumed that $f(.,.,.)$ is locally Lipschitz such that

$$\|f(x_1, u_1, \omega) - f(x_2, u_2, 0)\| \leqslant L_{f_x}\|x_1 - x_2\| + L_{f_u}\triangle_u + L_{f_\omega}\|\omega\|, \tag{4.3}$$

for all $x_1, x_2 \in \mathcal{X}$, $u_1, u_2 \in \mathcal{U}$ and $\omega \in \Upsilon$, where L_{f_x}, L_{f_u} and L_{f_ω} are local Lipschitz constants, $\triangle_u \triangleq \max\{\|u_1 - u_2\|\}$.

The main objectives of this study are summarized as follows.

- To design the controller using the min-max MPC for the system in (4.1) that is simultaneously subject to the input and state constraints, the two-channel time delays and packet dropouts, and the external disturbance.
- To establish the ISpS of the resulting constrained nonlinear NCS.

4.2.2 Preliminary Results

To study the stability of the constrained nonlinear system in sequel, we first recall three well-developed definitions on the robust invariant set which have been reported in [6, 77].

Definition 4.1. *If there exists a compact set $\Omega \subset \mathbb{R}^n$ such that $f(x_k, \omega_k) \in \Omega$ whenever $x_k \in \Omega$ for all $\omega_k \in \Upsilon$ and $k \in \mathbb{Z}_{\geqslant 0}$, then the set Ω is said to be a robustly positive invariant (RPI) set for the system $x_{k+1} = f(x_k, \omega_k)$.*

Definition 4.2. *For the system in (4.1) subject to the constraints in (4.2) with a given compact set Ω, if there exists an admissible control input $u_k \in \mathcal{U}$ such that $f(x_k, u_k, \omega_k) \in \Omega$ for all $x_k \in \Omega$ and all $\omega_k \in \Upsilon$, then the set Ω is said to be a robust control invariant (RCI) set.*

Definition 4.3. *Consider the system in (4.1) subject to the constraints in (4.2) associated with an RPI set Ω. The i-th step robustly stabilizable set in $X_i(\Omega)$ is denoted by all the admissible states which can be steered into the target set Ω no more than i steps by using an admissible control sequence $\boldsymbol{u}_{[i]}(x)$ for all $\boldsymbol{\omega}_{[i]} \in \Upsilon^i$.*

For the sake of analyzing the stability of the nonlinear NCS, the results on ISpS for the discrete-time nonlinear system are revisited in the sequel. The system in (4.1) can be rewritten as

$$x_{k+1} = g_u(x_k, \omega_k), \quad x_0 = \bar{x}, \quad k \in \mathbb{Z}_{\geqslant 0}, \tag{4.4}$$

where $x_k \in \mathbb{R}^n$ is the same system state, $\omega_k \in \mathbb{R}^m$ is the same external disturbance and the subscript u represents the time-varying property of the function g_u. Denote $x(k, \bar{x}, \boldsymbol{\omega}_{0,k-1})$ as the solution to the system in (4.4) at time instant k. For the system in (4.4), the definition of ISpS is stated as follows.

Definition 4.4. *[144] Given a compact set $\Omega \in \mathbb{R}^n$, if it is an RPI set for the system in (4.4) with $\omega_k \in \Upsilon$, and if there exist a $\mathcal{KL}$-function β, a $\mathcal{K}$-function γ and a constant $c \geqslant 0$ such that*

$$\|x(k, \bar{x}, \boldsymbol{\omega}_{0,k-1})\| \leqslant \beta(\|\bar{x}\|, k) + \gamma(\|\boldsymbol{\omega}_{[k-1]}\|_\infty) + c, \tag{4.5}$$

$\forall k \in \mathbb{Z}_{\geqslant 0}, \bar{x} \in \Omega$, then the system in (4.4) is said to be ISpS in Ω.

The definition of ISpS in a set in Definition 4.4 is a modification from that in [144] originally proposed for time-invariant nonlinear systems. The notation of ISpS is a generalization of the well known ISS [59, 144]. In fact, ISpS will be reduced to ISS when the constant $c = 0$. Recently, ISS has been employed to study the stability of constrained nonlinear systems with network-induced delays in [113] and with packet dropouts in [120]. The ISpS property will be exploited in this study.

Similar to ISS, an effective tool for studying ISpS is the ISpS-type Lyapunov function [59, 144]. For the networked constrained nonlinear systems, the following ISpS-type Lyapunov function will be used.

Definition 4.5. *[59, 144] For the system in (4.4) with an RPI set $\mathcal{X}$ including the origin as an interior point, if there exists a positive definite function $V(.,.) : \mathbb{R}^n \times$*

$\mathbb{Z}_{\geqslant 0} \to \mathbb{R}_{\geqslant 0}$, *for all* $x_k \in \mathcal{X}$, *such that the following conditions hold:*

$$V(x_k, k) \geqslant \alpha_1(\|x_k\|), \tag{4.6}$$

$$V(x_k, k) \leqslant \alpha_3(\|x_k\|) + c_3, \tag{4.7}$$

$$V(x_{k+1}, k+1) - V(x_k, k) \leqslant -\alpha_2(\|x_k\|) + \gamma(\|\omega_k\|) + c_2, \tag{4.8}$$

with α_1, α_2 *and* α_3 *being* $\mathcal{K}_\infty$*-functions,* γ *being a* $\mathcal{K}$*-function, and* c_2, $c_3 \geqslant 0$, *then the function* $V(x_k, k)$ *is the ISpS-type Lyapunov function in* $\mathcal{X}$ *for the system in (4.4) with* $\omega_k \in \Upsilon$.

With the aid of the ISpS-type Lyapunov function, a sufficient condition guaranteeing ISpS can be established in the following lemma.

Lemma 4.1. *[77] Given an RPI set* $\mathcal{X}$ *with* $\{0\} \subset \mathcal{X} \subseteq \mathbb{R}^n$ *for the system in (4.4), if it admits an ISpS-type Lyapunov function associated with the set* $\mathcal{X}$, *then the system in (4.4) is ISpS in* $\mathcal{X}$.

4.3 Networked Controller Design

4.3.1 Control System Structure

In this subsection, the physical structure with the embedded MPC-based control scheme for the nonlinear NCS is depicted in Fig. 4.2. In this diagram, the actuator

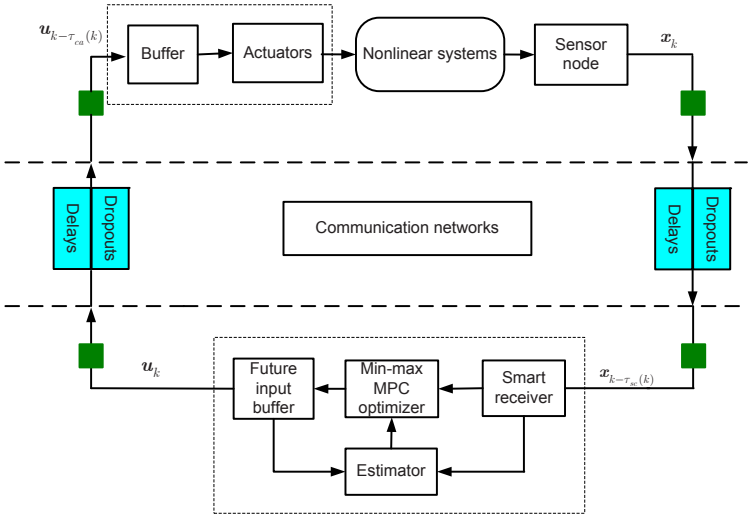

Figure 4.2: MPC based nonlinear NCS structure

node consists of the actuators and the actuator buffer. The buffer is used to store the available newest control command packets. The controller node includes the smart receiver, the MPC-based controller, the state estimator and the future input buffer. The smart receiver has a buffer which stores the previously received data. It performs two simple functions: One is to compare the latest received data with the stored data and to record the newest state of the system, and the other is to determine that the newest state is sent either to the controller or to the state estimator (see Fig. 4.3). The MPC-based controller is to generate the control sequence using the appropriate min-max MPC algorithm. The state estimator is used for reconstructing the current state for the MPC-based controller when the current system state is not available. The future input buffer is introduced to store a number of control sequences that will be sent to the actuator node over the C-A channel; meanwhile, a series of appropriate control signals will be sent to the estimator to reconstruct the current state.

Remark 4.1. *In [148], a similar control system structure has been adopted for linear NCSs using the generalized predictive control strategy, and the hardware-based experiment has been successfully conducted. So such a structure is physically realizable and the further development for nonlinear NCSs [113] is of practical merit. The theoretical analysis of the presented control system structure using the min-max MPC for nonlinear NCSs subject to the above mentioned constraints has not been reported in the literature, which motivates this study.*

Remark 4.2. *It is worth noting that the communication constraints (i.e., time delays and packet dropouts) in the S-C channel and the C-A channel have different effects for the control performance and the min-max MPC design. The communication constraints in the S-C channel mainly affect the accuracy of initial system state for the min-max optimization problem, but the imperfections in the C-A channel disturb the use of the optimal control signal. The communication constraints in the S-C channel are relatively easier to handle compared to these in the C-A channel. This is because the communication constraints in the S-C channel are known to the controller node, and the measure (state estimation) can be taken to mitigate the effects; but the communication constraints in the C-A channel occur after the generation of the control signal, and no action can be taken (except the prediction before the occurrence of the communication constraints). In the present study, we only consider one control unit among the large-scale NCSs. In general, the communication constraints are also affected by the communication topologies (e.g., the star topology, the line topology) in*

the large-scale NCSs. As a result, the design of the min-max MPC strategy for large-scale NCSs will be more complicated. For example, the distributed min-max MPC may need to be designed for each control unit; the prediction horizon of the min-max MPC of each control unit may be different due to the different maximum time delays and maximum number of consecutive packet dropouts in communication links. The controller structure design and min-max MPC strategy for large-scale NCSs need further study in the future.

4.3.2 Min-Max MPC Based Control Packet Design

In the literature, the RHOMPC strategy has been applied to tackle nonlinear NCSs in [113, 120, 101]. However, the RHOMPC strategy does not consider the external disturbances when performing optimization, and thus it may not be robust against the external disturbances, and suffer from conservativeness [95, 133]. Alternatively, the min-max MPC is able to consider the effect of external disturbances (by calculating the maximum disturbance at every time instant). In light of this promising feature, we employ the min-max MPC method to design the control packets. For the nonlinear system in (4.1) with time delays and packet dropouts, the cost function at time k is defined as

$$J_{N_c}(\mathbf{u}_k, \hat{x}_k, \boldsymbol{\omega}_k) \triangleq \sum_{i=0}^{N_c-1} L(\hat{x}_{k+i|k}, u_{i|k}) + F(\hat{x}_{k+N_c|k}), \tag{4.9}$$

where $\mathbf{u}_k \triangleq \text{col}\{u_{0|k}, u_{1|k}, \cdots, u_{N_c-1|k}\}$, $\boldsymbol{\omega}_k \triangleq \text{col}\{\omega_{0|k}, \omega_{1|k}, \cdots, \omega_{N_c-1|k}\} \in \Upsilon^{N_c}$, $\hat{x}_{k+i+1|k} = f(\hat{x}_{k+i|k}, u_{i|k}, \omega_{i|k})$ with $\hat{x}_{k|k} = \hat{x}_k$ and $\hat{x}_k$ being the state estimate (see Fig. 4.3 for more details), and N_c is a fixed integer satisfying $N_c > T_{ca} + N_{ca}$. In the cost function (4.9), $L(\hat{x}_{i|k}, u_{i|k})$ is the stage cost and $F(\hat{x}_{N_c|k})$ is the terminal cost. In this study, the control sequence is derived by solving the receding horizon min-max optimization problem as summarized below.

Problem 4.1. *Find a pair of optimal control sequence and admissible disturbance* $(\boldsymbol{u}_k^o, \boldsymbol{\omega}_k^o)$*, such that*

$$J_{N_c}^*(\hat{x}_k) = \min_{\boldsymbol{u}_k} \max_{\boldsymbol{\omega}_k} J_{N_c}(\boldsymbol{u}_k, \hat{x}_k, \boldsymbol{\omega}_k),$$

subject to: (1) the system model $\hat{x}_{k+i+1|k} = f(\hat{x}_{k+i|k}, u_{i|k}, \omega_{i|k})$ *for all* $i = 0, 1, \cdots, N_c - 1$*, and* $\hat{x}_{k|k} = \hat{x}_k$*; (2) the state prediction and input constraints* $\hat{x}_{k+i|k} \in \mathcal{X}$*,* $u_{i|k} \in \mathcal{U}$*, for all* $\omega_{i|k} \in \Upsilon$ *with* $i = 0, 1, \cdots, N_c - 1$*; (3) the terminal state constraint* $\hat{x}_{N_c|k} \in \Omega_o$ *for all* $\omega_{i|k} \in \Upsilon$ *with* Ω_o *(a known compact set) satisfying* $\{0\} \subset \Omega_o \subseteq \mathbb{R}^n$*. Here,*

$\boldsymbol{u}_k^o \triangleq \text{col}\{u_{0|k}^o, u_{1|k}^o, \cdots, u_{N_c-1|k}^o\}$ *and* $\boldsymbol{\omega}_k^o \triangleq \text{col}\{\omega_{0|k}^o, \omega_{1|k}^o, \cdots, \omega_{N_c-1|k}^o\}$.

Remark 4.3. *The length of the prediction horizon for a non-networked nonlinear system can be set as $N_c > 0$ such that the system performance is satisfactory. But for the nonlinear NCS in this study, it is required that the length of the prediction horizon is greater than $N_{ca} + T_{ca}$ in order for guaranteeing the capability of compensating for the worst situation when both the worst time delay and the largest consecutive packet dropout occur simultaneously.*

Remark 4.4. *It is worth noting that although the procedure of solving the constrained min-max optimal Problem 4.1 is inspired by the work for non-networked nonlinear systems in [3, 77], two essential differences exist. Firstly, the initial state in the Problem 4.1 is $\hat{x}_k$ which may be the actual system state x_k or the reconstructed state; see Figure 4.3. But for non-networked nonlinear systems, the initial state is always actual system state x_k. Secondly, the strategies on how to apply the control inputs are different. Specifically, the min-max MPC strategy for non-networked nonlinear systems takes the first element of the optimal control sequence $\boldsymbol{u}_k^o$ as the control input. For nonlinear NCSs, any element of the optimal control sequence $\boldsymbol{u}_k^o$ may be chosen as the control input due to the packet dropouts and/or time delays. This makes the stability analysis of the constrained nonlinear NCS very necessary yet challenging.*

4.3.3 Compensation Strategy

In this study, the UDP-like protocol is adopted for the Ethernet-like networks for both the S-C channel and the C-A channel. Unlike the TCP-like protocol, the UDP-like protocol does not send the acknowledgement packet when receiving a packet. For the nonlinear NCS in Figure 4.2, at time instant k, denote the time delay for the S-C channel as $\tau_{sc}(k)$, i.e., the state $x_{k-\tau_{sc}(k)}$ is received by the smart receiver at time instant k. When there is a packet dropout, $\tau_{sc}(k) = \infty$. Since the smart receiver is able to record the newest available state by comparing the current received state with the previous stored one, the time delay $\tau_{sc}(k)$ may not be directly used for describing the actual effect of time delays after the operations of the smart receiver. For example, at the time instant k, the time delay of the S-C channel is $\tau_{sc}(k)$ and the state $x_{k-\tau_{sc}(k)}$ is received. Assume that in the smart receiver, the state $x_{k-\tau_{sc}(k)+1}$ has already been received in the time instant $k-1$ and stored. In that situation, the smart receiver will use the state $x_{k-\tau_{sc}(k)+1}$ instead of the state $x_{k-\tau_{sc}(k)}$. Therefore,

the time delay evaluated by the smart receiver at time k is $\tau_{sc}(k) - 1$ rather than $\tau_{sc}(k)$. In order to describe the time delay evaluated by the smart receiver, we adopt the notation of the evaluated time delays used in [148, 113]. Specifically, denote τ_k as the evaluated time delay reported by the smart receiver for the S-C channel at the time instant k, which can be determined as:

$$\tau_k = \begin{cases} \tau_{sc}(k), & \text{If } k-1-\tau_{k-1} < k-\tau_{sc}(k), \\ \tau_{k-1}+1, & \text{If } k-1-\tau_{k-1} \geqslant k-\tau_{sc}(k), \end{cases}$$

and $\tau_0 = 0$. Similarly, we denote the time delay for the C-A channel as $d_{ca}(k)$ ($d_{ca}(k) = \infty$ when a packet dropout occurs) and d_k as the evaluated time delay for the received control sequence of the actuator node. The evaluated time delays τ_k and d_k satisfy the following properties: $\tau_k \leqslant T_{sc} + N_{sc}$ and $d_k \leqslant T_{ca} + N_{ca}$.

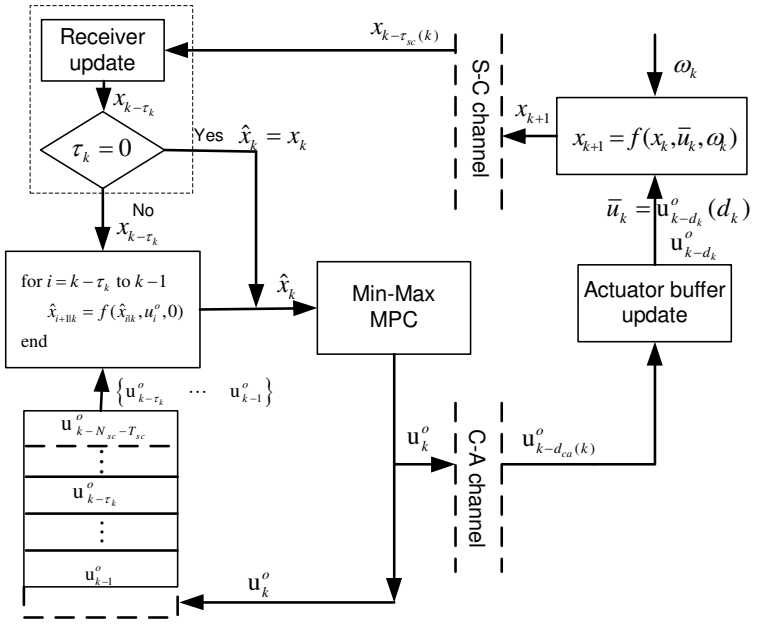

Figure 4.3: The control strategy

In this chapter, we use the same compensation mechanism as [114, 113, 148] for the nonlinear NCS except that the min-max MPC is designed to generate the control packet. The min-max MPC based compensation strategy is illustrated in Figure 4.3. For the sake of completeness, we briefly describe the min-max MPC based compensation strategy here. The reader may refer to [113, 114] for more details on the RHOMPC based compensation strategy. At time instant k, the state $x_{k-\tau_{sc}(k)}$ is

received by the smart sensor, based on which the latest state $x_{k-\tau_k}$ can be generated. On the one hand, if $\tau_k = 0$, then the latest state is directly sent to the MPC-based controller with $\hat{x}_k = x_k$. On the other hand, if $\tau_k \neq 0$, then the latest state $x_{k-\tau_k}$ will be sent to the estimator, which is used to recover the delayed or lost states. By the nominal model $\hat{x}_{i+1|k} = f(x_{i|k}, u_i^o(\hat{x}_i), 0)$ with the initial state $\hat{x}_{k-\tau_k|k} = x_{k-\tau_k}$, the estimator reconstructs the current state $\hat{x}_{k|k}$ by retrieving the previous control input sequences $\{\mathbf{u}^o_{k-\tau_k}, \cdots, \mathbf{u}^o_{k-1}\}$ (These control sequences are subsets of the sequences stored in the "future input buffer", where the previous control sequences $\{\mathbf{u}^o_{k-T_{sc}-N_{sc}}, \cdots, \mathbf{u}^o_{k-1}\}$ have been stored). Note that the prediction consistency is assumed to be satisfied, and the readers may refer to [41, 30] for more details. The reconstructed state $\hat{x}_k$ will be sent to the MPC-based controller. With the initial state $\hat{x}_k$, the min-max MPC controller will generate the optimal control sequence $\mathbf{u}^o_k$ by solving Problem 4.1. Once the control packet $\mathbf{u}^o_k$ is generated, it will be sent to the actuator node through the C-A channel; at the same time, the control packet will be pushed into the top of "future input buffer" to discard the last element $\mathbf{u}^o_{k-T_{sc}-N_{sc}}$.

At time instant k, the actuator node receives the control packet $\mathbf{u}^o_{k-d_{ca}(k)}$. Using the buffering technique, the newest control packet $\mathbf{u}^o_{k-d_k}$ will be generated and stored. For the actuators, the actual control input will be decided and chosen as $\bar{u}_k = \mathbf{u}^o_{k-d_k}(d_k)$ from the available newest control packet $\mathbf{u}^o_{k-d_k}$.

4.4 Stability Analysis

In this section, the stability of the proposed MPC-based nonlinear NCS is investigated by constructing a novel ISpS-type Lyapunov function. Due to the communication constraints, the actual control input $\bar{u}_k$ is different from that of the non-networked nonlinear systems, which makes the stability analysis more challenging. To start, we assume that the proposed networked min-max MPC algorithm is feasible as follows.

Assumption 4.1. *There exists a compact set $\mathcal{R}_X$ with $\{0\} \subseteq \mathcal{R}_X \subseteq X_{N_c}(\Omega_o) \sim \mathcal{B}^n(r_\omega)$, such that it is a RCI set for the mapping $f(x_k, \bar{u}_k, \omega_k)$, for all $k \in \mathbb{Z}_{\geqslant 0}$ and all $\omega_k \in \Upsilon$, where $r_\omega = \sum_{i=0}^{N_{sc}+T_{sc}-1} L^i_{f_x} L_{f\omega} d_\omega$.*

Remark 4.5. *Assumption 4.1 is to guarantee the feasibility of the constrained min-max MPC algorithm in $\mathcal{R}_X$ for the nonlinear NCS. For the constrained min-max MPC of non-networked systems, the region of initial states in the N_c-step RCI set $X_{N_c}(\Omega_o)$ is the feasible set and the feasibility is guaranteed by assuming the existence of an*

auxiliary control law in the terminal set [77]. However, since the control input for the networked system is $\bar{u}_k = \boldsymbol{u}^o_{k-d_k}(d_k)$ *and the initial state to Problem 4.1 is* $\hat{x}_k$*, which are different from that of the non-networked systems with* $u_k = \boldsymbol{u}^o_k(0)$ *and initial state* x_k *[77], we use the conditions in Assumption 4.1 to guarantee the feasibility.*

Similar to the non-networked min-max nonlinear MPC, two assumptions on the cost functions in (4.9) are required here.

Assumption 4.2. *The stage cost function* $L(x, u)$ *is locally Lipschitz in* x *and* u*, i.e., there exist constants* $0 < L_x < \infty$ *and* $0 < L_u < \infty$ *such that for all* $x_1, x_2 \in \mathcal{X}$ *and* $u_1, u_2 \in \mathcal{U}$

$$L(x_1, u_1) - L(x_2, u_2) \leqslant L_x \|x_1 - x_2\| + L_u \triangle_u,$$

and $L(x, u)$ *is lower bounded by*

$$L(x, u) \geqslant \alpha_L(\|x\|),$$

where α_L *is a* $\mathcal{K}_\infty$ *function.*

Assumption 4.3. *The terminal cost function* $F(x)$ *with* $F(0) = 0$ *is locally Lipschitz with the constant* L_F*,* $\forall x \in \mathcal{X}$*. Further, for all* $x \in \Omega_o$*, there exists an auxiliary control law* $K_f(x) \in \mathcal{U}$ *such that*

$$F(f(x, K_f(x), 0)) - F(x) \leqslant -L(x, K_f(x)),$$

and $f(x, K_f(x), 0) \in \Omega_o$*.*

Remark 4.6. *Assumption 4.2 and Assumption 4.3 are fairly standard requirements on the stage cost function and the terminal cost function. These assumptions have been adopted for the receding horizon open-loop MPC of non-networked nonlinear systems [77, 90, 123] and nonlinear NCSs [113, 120].*

Based on Assumption 4.3, we have the following Lemma 4.2.

Lemma 4.2. *If Assumption 4.3 holds, then* $\forall x \in \Omega_o$*, with the same control law* $K_f(x)$*, the following relationship holds:*

$$F(f(x, K_f(x), \omega)) - F(x) \leqslant -L(x, K_f(x)) + \sigma_\omega, \tag{4.10}$$

where $\sigma_\omega \triangleq L_F L_{f_\omega} d_\omega$*.*

Proof. According to Assumption 4.3, we have

$$\begin{aligned}
&F(f(x,K_f(x),\omega))-F(x)\\
=&F(f(x,K_f(x),\omega))-F(f(x,K_f(x),0))+F(f(x,K_f(x),0))-F(x)\\
\leqslant&F(f(x,K_f(x),\omega))-F(f(x,K_f(x),0))-L(x,K_f(x)).
\end{aligned}$$

Since $F(x)$ is Lipschitz with respect to the constant L_F, it has

$$\begin{aligned}
\|F(f(x,K_f(x),\omega))-F(f(x,K_f(x),0))\| \leqslant& L_F\|f(x,K_f(x),\omega)-f(x,K_f(x),0)\|\\
\leqslant& L_F L_{f_\omega} d_\omega=\sigma_\omega,
\end{aligned}$$

where the inequality in (4.3) has been utilized. The result in Lemma 4.2 is readily obtained. □

Before proceeding to construct the ISpS-type Lyapunov function candidate, another min-max optimization problem is presented.

Problem 4.2. *Find the optimal argument* $(\boldsymbol{u}_k^*,\boldsymbol{\omega}_k^*)$ *of the following min-max optimization problem as*

$$\bar{J}_{N_c+1}^*(\hat{x}_{k|k})\triangleq\min_{\boldsymbol{u}_k}\max_{\boldsymbol{\omega}_k}\sum_{i=0}^{N_c}L(\hat{x}_{k+i|k},u_{i|k})+F(\hat{x}_{k+N_c+1|k}),\quad \hat{x}_{k|k}=x_k,$$

subject to

$$\begin{cases}
\hat{x}_{k+i|k}\in\mathcal{X},\ \omega_{i|k}\in\Upsilon,\ \omega_{N_c|k}\in\Upsilon, & i=0,1,2,\cdots,N_c-1,\\
\hat{x}_{k+N_c|k}\in\Omega_o,\ \hat{x}_{k+N_c+1|k}\in\Omega_o, & \\
u_{i|k}\in\mathcal{U},\ \hat{x}_{k+i+1|k}=f(\hat{x}_{k+i|k},u_{i|k},\omega_{i|k}), & i=0,1,2,\cdots,N_c,
\end{cases}\tag{4.11}$$

where $\boldsymbol{u}_k=\mathrm{col}\{u_{0|k},u_{1|k},\cdots,u_{N_c|k}\}$, $\boldsymbol{\omega}_k=\mathrm{col}\{\omega_{0|k},\omega_{1|k},\cdots,\omega_{N_c|k}\}$.

Proposition 4.1. *Suppose Assumption 4.1 and Assumption 4.3 hold. Then Problem 4.2 and Problem 4.1 are feasible for all* $x_0\in\mathcal{R}_X$.

Proof. Firstly, we prove Problem 4.1 is feasible for all $x_0\in\mathcal{R}_X$. According to Assumption 4.1, for all $x_0\in\mathcal{R}_X$, one has $x_k\in\mathcal{R}_X$ for all $k\geqslant 0$. Furthermore, we are going to show that $\|x_k-\hat{x}_k\|\leqslant r_\omega$. In terms of the state estimation strategy

described in Figure 4.3, it has

$$\begin{aligned}\|x_k-\hat{x}_k\| =&\|x_k-\hat{x}_{k|k}\|\\ =&\|f(x_{k-1},\bar{u}_k,\omega_k)-f(\hat{x}_{k-1|k},\bar{u}_k,0)\|\\ \leqslant& L_{f_x}\|x_{k-1}-\hat{x}_{k-1|k}\|+L_{f_\omega}d_\omega\\ =&L_{f_x}^2\|x_{k-2}-\hat{x}_{k-2|k}\|+L_{f_x}L_{f_\omega}d_\omega+L_{f_\omega}d_\omega\\ =&L_{f_x}^{\tau_k}\|x_{k-\tau_k}-\hat{x}_{k-\tau_k|k}\|+\sum_{i=0}^{\tau_k-1}L_{f_x}^i L_{f_\omega}d_\omega\end{aligned}$$

Since $x_{k-\tau_k}=\hat{x}_{k-\tau_k|k}$ and $\tau_k\leqslant T_{sc}+N_{sc}$, it has $\|x_k-\hat{x}_k\|\leqslant r_\omega$. As a result, for all $x_k\in\mathcal{R}_X$, one has $\hat{x}_k\in X_{N_c}(\Omega_o)$. That is, Problem 4.1 is feasible. Secondly, we show that Problem 4.2 is feasible in $\mathcal{R}_X$ as follows. For all $x_0\in\mathcal{R}_X$, one has $x_k\in\mathcal{R}_X\subseteq X_{N_c}(\Omega_o)$ because of Assumption 4.1. Thus, for all initial state x_k, there exists a pair $(\mathbf{u}_k^o,\boldsymbol{\omega}_k^o)$ driving the state $x_{k+N_c|k}$ into the terminal set Ω_o by N_c steps. Further, by using Assumption 4.3, one can verify that $\bar{\boldsymbol{\omega}}_k=\mathrm{col}\{\boldsymbol{\omega}_k^o,0\}$ and $\bar{\mathbf{u}}_k=\mathrm{col}\{\mathbf{u}_k^o,K_f(x_{k+N_c|k})\}$ are a possible solution to Problem 4.2. This completes the proof. □

Remark 4.7. *It is noted that Problem 4.2 and Problem 4.1 are different. Problem 4.1 is used to design the control packet while Problem 4.2 is used for stability analysis. It is very important to establish the feasibility of Problem 4.2, since the ISpS-type Lyapunov function will be built on the optimal solution to Problem 4.2, which can be seen in the sequel.*

Now we are in a position to construct an ISpS-type Lyapunov function candidate as:

$$V(x_k,k)\triangleq L(x_k,\bar{u}_k)+\bar{J}_{N_c+1}^*(\hat{x}_{k+1|k}),$$

where $\hat{x}_{k+1|k}=f(x_k,\bar{u}_k,0)$. Specifically, $V(x_k,k)$ can be written as

$$V(x_k,k)=L(x_k,\bar{u}_k)+\min_{\mathbf{u}_k}\max_{\boldsymbol{\omega}_k}\sum_{i=1}^{N_c+1}L(\hat{x}_{k+i|k},u_{i|k})+F(\hat{x}_{k+N_c+2|k}),\quad \hat{x}_{k+1|k}=f(x_k,\bar{u}_k,0),$$

subject to

$$\begin{cases} \hat{x}_{k+i|k} \in \mathcal{X},\ \omega_{i|k} \in \Upsilon,\ \omega_{N_c+1|k} \in \Upsilon & i = 1, 2, \cdots, N_c, \\ \hat{x}_{k+N_c+1|k} \in \Omega_o,\ \hat{x}_{k+N_c+2|k} \in \Omega_o, & \\ u_{i|k} \in \mathcal{U},\ \hat{x}_{k+i+1|k} = f(\hat{x}_{k+i|k}, u_{i|k}, \omega_{i|k}), & i = 1, 2, \cdots, N_c + 1, \end{cases}$$

where $\mathbf{u}_k = \text{col}\{u_{1|k}, \cdots, u_{N_c+1|k}\}$, $\boldsymbol{\omega}_k = \text{col}\{\omega_{1|k}, \cdots, \omega_{N_c+1|k}\}$, and the optimal solution is denoted as $\mathbf{u}_k^* \triangleq \text{col}\{u_{1|k}^*, \cdots, u_{N_c+1|k}^*\}$ and $\boldsymbol{\omega}_k^* \triangleq \text{col}\{\omega_{1|k}^*, \cdots, \omega_{N_c+1|k}^*\}$. Firstly, we have the following Lemma 4.3 which gives the lower and upper bounds of $V(x_k, k)$ for all $x_k \in \mathcal{R}_X$.

Lemma 4.3. *Under Assumption 4.1-4.3, the ISpS-type Lyapunov function candidate is bounded as*

$$\alpha_L(\|x_k\|) \leqslant V(x_k, k) \leqslant \sigma \cdot \alpha_F(\|x_k\|) + c_u,\ \forall x_k \in \mathcal{R}_X, \tag{4.12}$$

where $\sigma = \max\{\frac{J_m}{\alpha_F(r_m)}, 1\}$, $\alpha_F(s) = L_F s$, $J_m = \max_{x_k \in \mathcal{X}, k \in \mathcal{Z}_{\geqslant 0}} V(x_k, k)$, $r_m = \max_r\{\mathcal{B}^n(r) \subseteq \Omega_o\}$ *and* $c_u = (L_x \sum_{i=2}^{N_c+1} \sum_{j=0}^{i-2} L_{f_x}^j + L_F \sum_{j=0}^{N_c} L_{f_x}^j) L_{f_\omega} d_\omega + (N_c + 2) L_u \triangle_u + L_F L_{f_u} \triangle_u \sum_{j=0}^{N_c+1} L_{f_x}^j + L_x L_{f_u} \triangle_u \sum_{i=1}^{N_c+1} \sum_{j=0}^{i-1} L_{f_x}^j$.

Proof. According to Assumption 4.2, we can readily establish the left-hand side inequality of (4.12). To derive the upper bound of $V(x_k, k)$, we consider the following two cases.

Case 1: $x_k \in \Omega_o$. In this case, if the control law is chosen as $K_f(x_k)$, then $\bar{x}_{k+1|k} = f(x_k, K_f(x_k), 0)$ belonging to Ω_o according to Assumption 4.3. By induction, we have $\bar{x}_{k+i+1|k} \in \Omega_o$ when the control law $K_f(\bar{x}_{k+i|k})$ is applied for all $i = 0, 1, \cdots, N_c + 1$. Therefore, for all $x_k \in \Omega_o$, we have

$$F(\bar{x}_{k+i+1|k}) - F(\bar{x}_{k+i|k}) \leqslant -L(\bar{x}_{k+i|k}, K_f(\bar{x}_{k+i|k})), \tag{4.13}$$

where $\bar{x}_{k|k} = x_k$ and $\bar{x}_{k+i+1|k} = f(\bar{x}_{k+i|k}, K_f(\bar{x}_{k+i|k}), 0)$, $\forall i = 0, 1, \cdots, N_c + 1$. By summing up (4.13) from $i = 0$ to $N_c + 1$, we get

$$F(\bar{x}_{k+N_c+2|k}) + \sum_{i=0}^{N_c+1} L(\bar{x}_{k+i|k}, K_f(\bar{x}_{k+i|k})) \leqslant F(x_k).$$

Thus, we further have

$$\begin{aligned}
V(x_k,k) \leqslant & V(x_k,k) - F(\bar{x}_{k+N_c+2|k}) - \sum_{i=0}^{N_c+1} L(\bar{x}_{k+i|k}, K_f(\bar{x}_{k+i|k})) + F(x_k) \\
\leqslant & L(x_k,\bar{u}_k) - L(x_k, K_f(x_k)) + \max_{\boldsymbol{\omega}_k \in \Upsilon^{N_c+1}} \left(\sum_{i=1}^{N_c+1} L(\hat{x}_{k+i|k}, u^*_{i|k}) + F(\hat{x}_{k+N_c+2|k}) \right) \\
& - F(\bar{x}_{k+N_c+2|k}) - \sum_{i=1}^{N_c+1} L(\bar{x}_{k+i|k}, K_f(\bar{x}_{k+i|k})) + F(x_k) \\
\leqslant & \max_{\boldsymbol{\omega}_k \in \Upsilon^{N_c+1}} \left(\sum_{i=1}^{N_c+1} L(\hat{x}_{k+i|k}, u^*_{i|k}) - L(\bar{x}_{k+i|k}, K_f(\bar{x}_{k+i|k})) + F(\hat{x}_{k+N_c+2|k}) \right. \qquad (4.14) \\
& \left. - F(\bar{x}_{k+N_c+2|k}) \right) + L(x_k,\bar{u}_k) - L(x_k, K_f(x_k)) + F(x_k). \qquad (4.15)
\end{aligned}$$

To proceed, the following two results should be utilized. According to Assumption 4.2-4.3, the following can be obtained:

$$\begin{aligned}
F(\hat{x}_{k+N_c+2|k}) - F(\bar{x}_{k+N_c+2|k}) \leqslant & L_F \|\hat{x}_{k+N_c+2|k} - \bar{x}_{k+N_c+2|k}\| \\
\leqslant & L_F \left(L_{f_u} \triangle_u \sum_{j=0}^{N_c+1} L_{f_x}^j + L_{f_\omega} d_\omega \sum_{j=0}^{N_c} L_{f_x}^j \right), \qquad (4.16)
\end{aligned}$$

$$L(\hat{x}_{k+1|k}, u^*_{i|k}) - L(\bar{x}_{k+1|k}, K_f(\bar{x}_{k+1|k})) \leqslant L_x L_{f_u} \triangle_u, \qquad (4.17)$$

and

$$\begin{aligned}
& L(\hat{x}_{k+i|k}, u^*_{i|k}) - L(\bar{x}_{k+i|k}, K_f(\bar{x}_{k+i|k})) \\
\leqslant & L_x \left(L_{f_\omega} d_\omega \sum_{j=0}^{i-2} L_{f_x}^j + \sum_{j=0}^{i-1} L_{f_x}^j L_{f_u} \triangle_u \right) + L_u \triangle_u, i \geqslant 2. \qquad (4.18)
\end{aligned}$$

Substituting (4.16), (4.17) and (4.18) into (4.14) results in

$$V(x_k,k) \leqslant L_u\triangle_u + L_x\sum_{i=1}^{N_c+1}\sum_{j=0}^{i-1}L_{f_x}^j L_{f_u}\triangle_u + L_xL_{f_\omega}d_\omega\sum_{i=2}^{N_c+1}\sum_{j=0}^{i-2}L_{f_x}^j + \sum_{i=1}^{N_c+1}L_u\triangle_u + L_F\left(L_{f_u}\triangle_u\sum_{j=0}^{N_c+1}L_{f_x}^j + L_{f_\omega}d_\omega\sum_{j=0}^{N_c}L_{f_x}^j\right) + \alpha_F(\|x_k\|). \tag{4.19}$$

Case 2: $x_k \in \mathcal{R}_X \setminus \Omega_o$. In this situation, we use the same idea in [77]. Since $\mathcal{X}$ and $\mathcal{U}$ are compact sets, then there exists a upper bound of $V(x_k,k)$ such that $V(x_k,k) \leqslant J_M$ with $0 < J_M < \infty$. For the ball $\mathcal{B}^n(r)$, there exists the maximum r such that $r_m = \max\{\mathcal{B}^n(r) \subseteq \Omega_o\}$. Obviously, for all $x_k \in \mathcal{R}_X \setminus \Omega_o$, we have $\alpha_F(\|x_k\|) > \alpha_F(r_m)$. As a result, it has

$$V(x_k,k) \leqslant J_M = \frac{J_M}{\alpha_F(r_m)}\alpha_F(r_m) \leqslant \frac{J_M}{\alpha_F(r_m)}\alpha_F(\|x_k\|). \tag{4.20}$$

By jointly considering (4.19) for $x_k \in \Omega_o$ and (4.20) for $x_k \in \mathcal{R}_X \setminus \Omega_o$, the result in (4.12) can be derived. This completes the proof. □

In what follows, the stability result of the nonlinear NCS with the designed min-max MPC algorithm is presented in Theorem 4.1.

Theorem 4.1. *Suppose Assumption 4.1-4.3 hold. Then the function $V(x_k,k)$ is the ISpS-type function for the resulting nonlinear NCS, and further the closed-loop system is ISpS for all the initial state in $\mathcal{R}_X$.*

Proof. Firstly, Problem 4.2 can also be solved by the dynamic programming approach [40, 95], i.e., it can be solved recursively as:

$$\begin{aligned}\bar{J}_i^*(x_k) = &\min_{u\in\mathcal{U}}\max_{\omega\in\Upsilon}\left\{L(x_k,u) + \bar{J}_{i-1}^*(f(x_k,u,\omega)\right\}\\ &\text{subject to } f(x_k,u,\omega) \in X_{i-2}(\Omega_o),\end{aligned}$$

where $\bar{J}_0^*(x) = F(x)$ with $x \in \Omega_o$, $X_0(\Omega_o) = \Omega_o$, $X_{-1}(\Omega_o) = \Omega_o$ and i is from N_c+2 to 1. Then we begin with the calculation of $V(x_{k+1},k) - V(x_k,k)$ as

$$V(x_{k+1},k+1) - V(x_k,k) = V(x_{k+1},k+1) - \bar{J}_{N_c+2}^*(x_{k+1}) + \bar{J}_{N_c+2}^*(x_{k+1}) - V(x_k,k). \tag{4.21}$$

We first evaluate the bound of $V(x_{k+1}, k+1) - \bar{J}^*_{N_c+2}(x_{k+1})$ in (4.21) as

$$\begin{aligned}
&V(x_{k+1}, k+1) - \bar{J}^*_{N_c+2}(x_{k+1}) \\
=&L(x_{k+1|k+1}, \bar{u}_{k+1}) + \bar{J}^*_{N_c+1}(\hat{x}_{k+2|k+1}) - \min_{u\in\mathcal{U}} \max_{\omega\in\Upsilon} \left\{L(x_{k+1}, u) + \bar{J}^*_{N_c+1}(f(x_{k+1}, u, \omega))\right\} \\
=&L(x_{k+1|k+1}, \bar{u}_{k+1}) - L(x_{k+1}, u^*_{k+1}) + \bar{J}^*_{N_c+1}(\hat{x}_{k+2|k+1}) - \max_{\omega\in\Upsilon} \bar{J}^*_{N_c+1}(f(x_{k+1}, u^*_{k+1}, \omega)) \\
\leqslant&L_u \triangle_u + \bar{J}^*_{N_c+1}(\hat{x}_{k+2|k+1}) - \bar{J}^*_{N_c+1}(x^*_{k+2}),
\end{aligned}$$

where we denote $x^*_{k+2} = f(x_{k+1}, u^*_{k+1}, \omega^*_{k+1})$.

To proceed, we need to find the upper bound of $\bar{J}^*_{N_c+1}(\hat{x}_{k+2|k+1}) - \bar{J}^*_{N_c+1}(x^*_{k+2})$. Since

$$\begin{aligned}
&\bar{J}^*_1(\hat{x}_{k+N_c+2|k+1}) - \bar{J}^*_1(x^*_{k+N_c+2}) \\
=&\min_{u\in\mathcal{U}} \max_{\omega\in\Upsilon} \left\{L(\hat{x}_{k+N_c+2|k+1}, u) + F(\hat{x}_{k+N_c+3|k+1})\right\} \\
&- \min_{u\in\mathcal{U}} \max_{\omega\in\Upsilon} \left\{L(x^*_{k+N_c+2}, u) + F(x^*_{k+N_c+3})\right\} \\
\leqslant&\max_{\omega\in\Upsilon} \{L(\hat{x}_{k+N_c+2|k+1}, u^*_{N_c+2|k+1}) - L(x^*_{k+N_c+2}, u^*_{k+N_c+2}) \\
&+ F(\hat{x}_{k+N_c+3|k+1}) - F(x^*_{k+N_c+3})\} \\
=&L(\hat{x}_{k+N_c+2|k+1}, u^*_{N_c+2|k+1}) - L(x^*_{k+N_c+2}, u^*_{k+N_c+2}) \\
&+ \max_{\omega\in\Upsilon} \left\{F(\hat{x}_{k+N_c+3|k+1}) - F(x^*_{k+N_c+3})\right\} \\
\leqslant&L_x \left(L^{N_c}_{f_x} L_{f_\omega} d_\omega + \triangle_u L_{f_u} \sum_{i=0}^{N_c} L^i_{f_x} + 2L_{f_\omega} d_\omega \sum_{i=0}^{N_c-1} L^i_{f_x} \right) \\
&+ L_u \triangle_u + L_F L^{N_c+1}_{f_x} L_{f_\omega} d_\omega + L_F \triangle_u L_{f_u} \sum_{i=0}^{N_c+1} L^i_{f_x} + 2L_F L_{f_\omega} d_\omega \sum_{i=0}^{N_c} L^i_{f_x}.
\end{aligned}$$

Furthermore, we have

$$\begin{aligned}
&\bar{J}^*_{i+1}(\hat{x}_{k+N_c+2-i|k+1}) - \bar{J}^*_{i+1}(x^*_{k+N_c+2-i}) \\
=&\min_{u\in\mathcal{U}} \max_{\omega\in\Upsilon} \left\{L(\hat{x}_{k+N_c+2-i|k+1}, u) + \bar{J}^*_i(\hat{x}_{k+N_c+3-i|k+1})\right\} \\
&- \min_{u\in\mathcal{U}} \max_{\omega\in\Upsilon} \left\{L(x^*_{k+N_c+2-i}, u) + \bar{J}^*_i(x^*_{k+N_c+3-i})\right\} \\
\leqslant&\max_{\omega\in\Upsilon} \{\bar{J}^*_i(\hat{x}_{k+N_c+3-i|k+1}) - \bar{J}^*_i(x^*_{k+N_c+3-i})\} \\
&+ L(\hat{x}_{k+N_c+2-i|k+1}, u^*_{k+N_c+2-i|k+1}) - L(x^*_{k+N_c+2-i}, u^*_{k+N_c+2-i}).
\end{aligned}$$

Therefore, by induction, it can be obtained that

$$\begin{aligned}
&\bar{J}^*_{N_c+1}(\hat{x}_{k+2|k+1}) - \bar{J}^*_{N_c+1}(x^*_{k+2}) \\
\leqslant & L_x \sum_{j=0}^{N_c+1} \left(L^j_{f_x} L_{f_\omega} d_\omega + \triangle_u L_u \sum_{i=0}^{j} L^i_{f_x} \right) + 2L_x L_{f_\omega} d_\omega \sum_{j=1}^{N_c+1} \sum_{i=0}^{j-1} L^i_{f_x} \\
& + (N_c+2) L_u \triangle_u + L_F \left(L^{N_c+2}_{f_x} L_{f_\omega} d_\omega + \triangle_u L_{f_u} \sum_{i=0}^{N_c+2} L^i_{f_x} + 2L_{f_\omega} d_\omega \sum_{i=0}^{N_c+1} L^i_{f_x} \right).
\end{aligned}$$

As a result,

$$\begin{aligned}
&V(x_{k+1}, k+1) - \bar{J}^*_{N_c+2}(x_{k+1}) \\
\leqslant & \left(L_x \sum_{j=0}^{N_c+1} L^j_{f_x} + L_F L^{N_c+2}_{f_x} + 2L_x \sum_{j=1}^{N_c+1} \sum_{i=0}^{j-1} L^i_{f_x} + 2L_F \sum_{i=0}^{N_c+1} L^i_{f_x} \right) L_{f_\omega} d_\omega \\
& + \left(L_x \sum_{j=0}^{N_c+1} \sum_{i=0}^{j} L^i_{f_x} + L_F \sum_{i=0}^{N_c+2} L^i_{f_x} \right) L_{f_u} \triangle_u + (N_c+3) L_u \triangle_u. \qquad (4.22)
\end{aligned}$$

Next, we need to find the upper bound of $\bar{J}^*_{N_c+2}(x_{k+1}) - V(x_k, k)$ in (4.21). We have

$$\begin{aligned}
&\bar{J}^*_{N_c+2}(x_{k+1}) - V(x_k, k) \\
=& \bar{J}^*_{N_c+2}(x_{k+1}) - \bar{J}^*_{N_c+1}(\hat{x}_{k+1|k}) - L(x_k, \bar{u}_k) \\
=& \min_{u \in \mathcal{U}} \max_{\omega \in \Omega_o} \{ L(x_{k+1}, u) + \bar{J}^*_{N_c+1}(x^*_{k+2}) \} \\
& - \min_{u \in \mathcal{U}} \max_{\omega \in \Omega_o} \{ L(\hat{x}_{k+1|k}, u) + \bar{J}^*_{N_c}(\hat{x}_{k+2|k}) \} - L(x_k, \bar{u}_k) \\
\leqslant & L_x \| x_{k+1} - \hat{x}_{k+1|k} \| + L_u \triangle_u + \max_{\omega \in \Upsilon} \{ \bar{J}^*_{N_c+1}(x^*_{k+2}) - \bar{J}^*_{N_c}(\hat{x}_{k+2|k}) \} - L(x_k, \bar{u}_k).
\end{aligned}$$

For $i = 2$ to $N_c + 1$, we have

$$\begin{aligned}
&\bar{J}^*_{N_c-i+3}(x^*_{k+i}) - \bar{J}^*_{N_c-i+2}(\hat{x}_{k+i|k}) \\
\leqslant & L(x^*_{k+i}, u^*_{k+i}) - L(\hat{x}_{k+i|k}, u^*_{k+i|k}) + \max_{\omega \in \Upsilon} \left\{ \bar{J}^*_{N_c-i+2}(x^*_{k+i+1}) - \bar{J}^*_{N_c-i+1}(\hat{x}_{k+i+1|k}) \right\}.
\end{aligned}$$

And for $i = 1$, we get

$$
\begin{aligned}
&\bar{J}_1^*(x^*_{k+N_c+2}) - \bar{J}_0^*(\hat{x}_{k+N_c+2|k}) \\
=&\min_{u\in\mathcal{U}}\max_{\omega\in\Upsilon}\left\{L(x^*_{k+N_c+2},u)+F(f(x^*_{k+N_c+2},u,\omega))\right\} - F(\hat{x}_{k+N_c+2|k}) \\
\leqslant&\max_{\omega\in\Upsilon}\left\{L(x^*_{k+N_c+2},K_f(x^*_{k+N_c+2}))+F(f(x^*_{k+N_c+2},K_f(x^*_{k+N_c+2}),\omega))\right\} - F(\hat{x}_{k+N_c+2|k}) \\
=&\max_{\omega\in\Upsilon}\left\{L(x^*_{k+N_c+2},K_f(x^*_{k+N_c+2}))+F(f(x^*_{k+N_c+2},K_f(x^*_{k+N_c+2}),\omega)) - F(x^*_{k+N_c+2})\right\} \\
&+F(x^*_{k+N_c+2}) - F(\hat{x}_{k+N_c+2|k}) \\
\leqslant&\sigma_\omega + L_F\|x^*_{k+N_c+2} - \hat{x}_{k+N_c+2|k}\| \\
\leqslant&\sigma_\omega + L_F(L_{f_u}\triangle_u + 2L_{f_\omega}d_\omega)\sum_{i=0}^{N_c} L_{f_x}^i + L_F L_{f_x}^{N_c+1}\|\omega_k\|,
\end{aligned}
$$

where Lemma 4.2 has been used. By induction, we get

$$
\begin{aligned}
&\bar{J}^*_{N_c+1}(x^*_{k+2}) - \bar{J}^*_{N_c}(\hat{x}_{k+2|k}) \\
\leqslant&L_x\sum_{j=0}^{N_c-1}\left((L_{f_u}\triangle_u + 2L_{f_\omega}d_\omega)\sum_{i=0}^{j}L_{f_x}^i + L_{f_x}^{i+1}L_{f_\omega}\|\omega_k\|\right) \\
&+N_cL_u\triangle_u + \sigma_\omega + L_F\left((L_{f_u}\triangle_u + 2L_{f_\omega}d_\omega)\sum_{i=0}^{N_c}L_{f_x}^i + L_{f_x}^{N_c+1}\|\omega_k\|\right).
\end{aligned}
$$

Therefore, $\bar{J}^*_{N_c+2}(x_{k+1}) - V(x_k,k)$ is upper bounded as

$$
\begin{aligned}
&\bar{J}^*_{N_c+2}(x_{k+1}) - V(x_k,k) \\
\leqslant&-\alpha_F(\|x_k\|) + \sigma_\omega + (L_{f_u}\triangle_u + 2L_{f_\omega}d_\omega)\left(L_x\sum_{j=0}^{N_c-1}\sum_{i=0}^{j}L_{f_x}^i + L_F\sum_{i=0}^{N_c}L_{f_x}^i\right) \\
&+(N_c+1)L_u\triangle_u + \left(L_xL_{f_\omega} + L_x\sum_{j=0}^{N_c-1}L_{f_x}^{j+1}L_{f_\omega} + L_FL_{f_x}^{N_c+1}L_{f_\omega}\right)\|\omega_k\|. \qquad (4.23)
\end{aligned}
$$

Finally, by combining (4.22) and (4.23), we have

$$
V(x_{k+1},k+1) - V(x_k,k) \leqslant -\alpha_F(\|x_k\|) + \gamma_v(\|\omega_k\|) + c_v, \qquad (4.24)
$$

where $c_v \triangleq ((3L_x+4L_F)\sum_{j=0}^{N_c}L_{f_x}^j + (L_x + 2L_F + L_FL_{f_x})\ L_{f_x}^{N_c+1} + 4L_x\sum_{j=0}^{N_c-1}\sum_{i=0}^{j}$
$L_{f_x}^i)L_{f_\omega}d_\omega + (2N_c+4)L_u\triangle_u + \sigma_\omega + ((2L_x+2L_F)\sum_{i=0}^{N_c}L_{f_x}^i + (L_x + L_F + L_FL_{f_x})L_{f_x}^{N_c+1}$

$+2L_x\sum_{j=0}^{N_c-1}\sum_{i=0}^{j}L_{f_x}^{i})L_{f_u}\triangle_u$ and $\gamma_v(s_1)\triangleq(L_x\sum_{j=0}^{N_c}L_{f_x}^{j}+L_FL_{f_x}^{N_c+1})L_{f_\omega}\cdot(s_1)$.

According to Lemma 4.3 and (4.24), the function $V(x_k,k)$ is the ISpS-type Lyapunov function. Therefore, the resulting nonlinear NCS is ISpS by Lemma 4.1. The proof is completed. □

Remark 4.8. *It is worth noting that for the non-networked systems using the min-max MPC strategy, the stability can be established by proving that the optimal value of the performance index is the Lyapunov function; see, e.g. the asymptotical stability in [133, 95] for systems without disturbances and ISS for systems subject to disturbances in [123, 77]. However, for the nonlinear NCS with the proposed min-max MPC strategy, the optimal value of the performance index $J_{N_c}^*(x_k)$ can not be used as the Lyapunov function. This is because the actually implemented control input u_k may not be the optimal solution u_k^o to the constrained optimization Problem 4.1 due to the packet dropouts and time delays. In this proof, to tackle this problem for establishing ISpS, we propose a novel way to construct the Lyapunov function. That is, the auxiliary constrained optimization Problem 4.2 is first designed, and then the ISpS-type Lyapunov function is constructed based on the solution of Problem 2.*

4.5 Simulation Example

In this section, simulation studies are conducted by applying the proposed networked min-max MPC strategy to a networked cart-and-spring system. Furthermore, some comparisons are carried out to demonstrate the improved performance.

The diagram of the networked cart-and-spring system under investigation is demonstrated in Figure 4.4, which has been studied in [123, 89] by using MPC in a non-network environment. In the scenario described by Figure 4.4, there are Ethernet-like networks deployed on both the S-C channel and the C-A channel, where packet dropouts and time delays occur randomly; the networked min-max MPC-based controller is to be designed. In this networked cart-and-spring system, s is the displacement of the carriage from the equilibrium point. The spring factor is modeled as $k=k_0e^{-s}$, and the damping factor is h_d. By setting $x_1=s$ and $x_2=\dot{s}$, the dynamic model of the cart-and-spring system can be derived as [123, 89]

$$\begin{cases}x_1(k+1)=x_1(k)+T_cx_2(k),\\ x_2(k+1)=x_2(k)-T_c\frac{k_0}{M}e^{-x_1(k)}x_1(k)-T_c\frac{h_d}{M}x_2(k)+T_c\frac{u(k)}{M}+T_c\frac{\omega(k)}{M}.\end{cases}$$

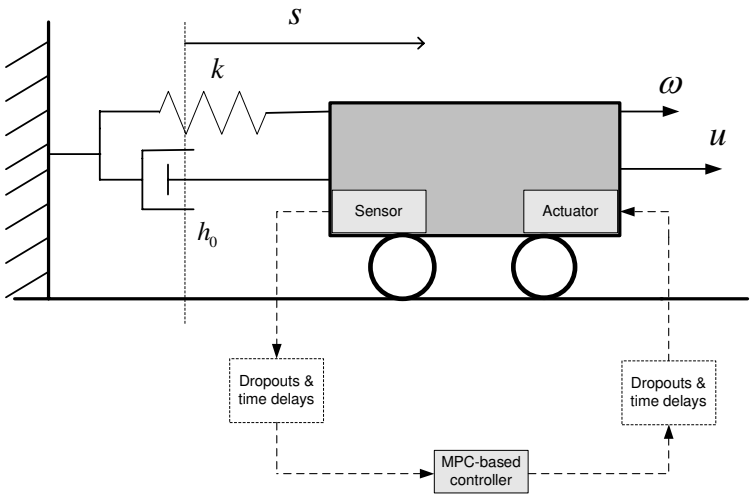

Figure 4.4: Networked cart-and-spring system.

In this study, the mass of the carriage is set to be $M = 1.0$ kg; the spring linear factor is $k_0 = 0.33$ N/m; the damper factor is $h_d = 1.1$ Ns/m and the sampling period is $T_c = 0.1$ s. The state and control input constraints are set as $|x_1(t)| \leqslant 2.65$ m and $|u| \leqslant 4.5$ N, respectively. The stage cost function is chosen as $L(x, u) = x^{\mathrm{T}}Qx + u^{\mathrm{T}}Q_u u$, where $Q = I$, $Q_u = I$. To determine the terminal cost, the approach in [11] is adopted. Firstly, the nonlinear function is linearized at the operation point $x_1^o = 0$ and $x_2^o = 0$. Then a local feedback control is designed as $K = [0.7230, 0.8121]$ using the LQR method. Finally, the terminal cost can be determined as $F(x) = x^{\mathrm{T}}Px$, with $P = [5.2500, -0.5306; -0.5306, 0.8515]$. The terminal set has been chosen as $\Omega_o = \{x | x^{\mathrm{T}}Px \leqslant 4\}$. The methods of computing the terminal set can be referred to [8, 97, 110].

In the simulation, the time delays and the packet dropouts of the S-C channel and the C-A channel are generated randomly. The maximum time delays of the S-C channel and the C-A channel are $T_{sc} = 4$ and $T_{ca} = 3$, respectively. The detailed delay sequences are depicted in Figure 4.5. The maximum numbers of consecutive packet dropouts of the two channels are $N_{sc} = 3$ and $N_{ca} = 2$, respectively. The packet dropout information is demonstrated in Figure 4.6, where $D_{sc} = 1$ and $D_{ca} = 1$ represent the packet dropout occurring on the S-C channel and the C-A channel, respectively.

For the purpose of comparison, four groups of simulations have been conducted.

- **Test 1:** The proposed networked min-max MPC strategy is applied to the networked cart-and-spring system (in Figure 4.3) subject to two-channel packet

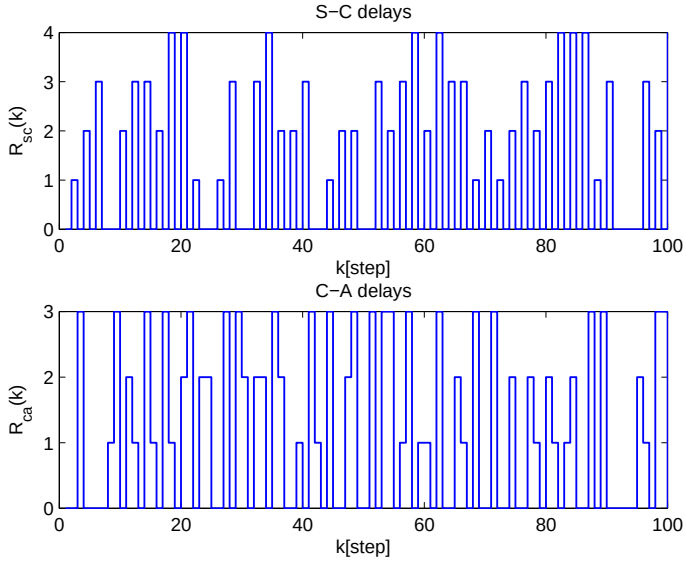

Figure 4.5: Delay sequences of the S-C and the C-A channels.

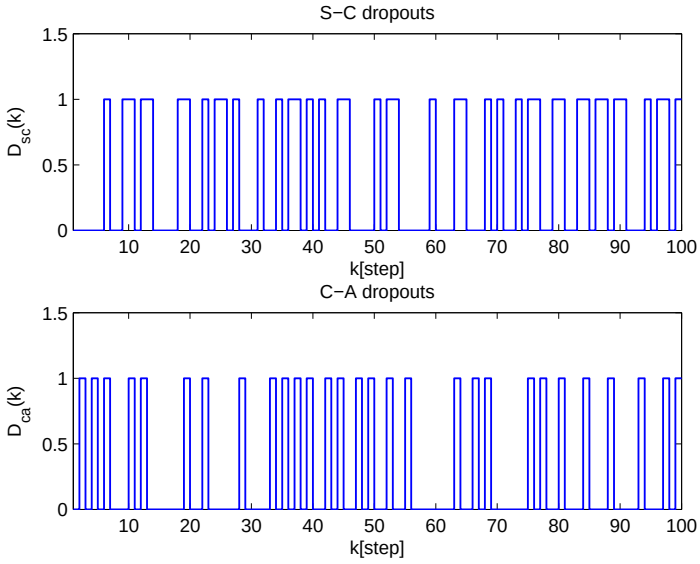

Figure 4.6: Packet dropout sequences of the S-C and the C-A channels.

dropouts and time delays as shown in Figure 4.6 and Figure 4.5. Both the two-channel packet dropouts and the time delays are well compensated.

- **Test 2:** The standard min-max MPC strategy is utilized for the same system setup with perfect networks (i.e., no packet dropouts and no time delays for the two-channel links).

- **Test 3:** The conventional MPC (i.e., RHOMPC) method but with the same control and compensation strategy proposed in this chapter is applied for the same system setup.

- **Test 4:** The standard min-max MPC strategy is directly implemented to the same system setup, but neither the time delays nor the packet dropouts are considered and no compensation strategy is taken.

After testing the above four groups of simulations, we summarize the results of Test 1, Test 2, and Test 3 as follows. The control inputs of three different tests are demonstrated in Figure 4.7, and the two states of the system are illustrated in Figure 4.8 and Figure 4.9, respectively. For Test 4, when applying the standard min-max MPC without any compensation, both of the system states are divergent.

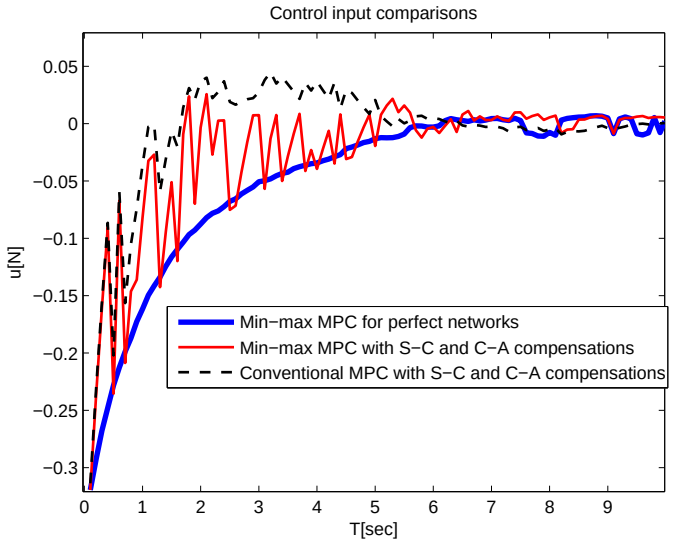

Figure 4.7: Comparisons of control inputs.

From the simulation results, it can be seen that:

- The nonlinear NCS controlled by the proposed min-max MPC strategy is stable and all the constraints are satisfied.

- The control performance of the nonlinear NCS using the proposed min-max MPC method and the compensation strategy is comparable to the performance of the control system with perfect networks, and it outperforms the results of the conventional MPC strategy.

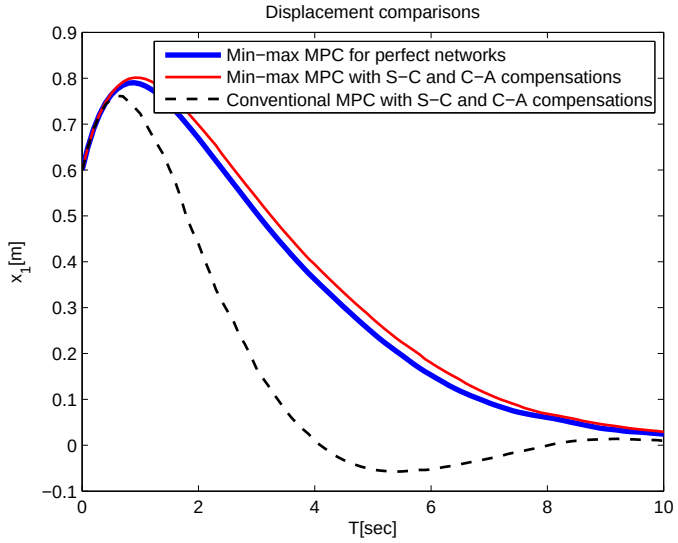

Figure 4.8: Comparisons of control performance: displacement.

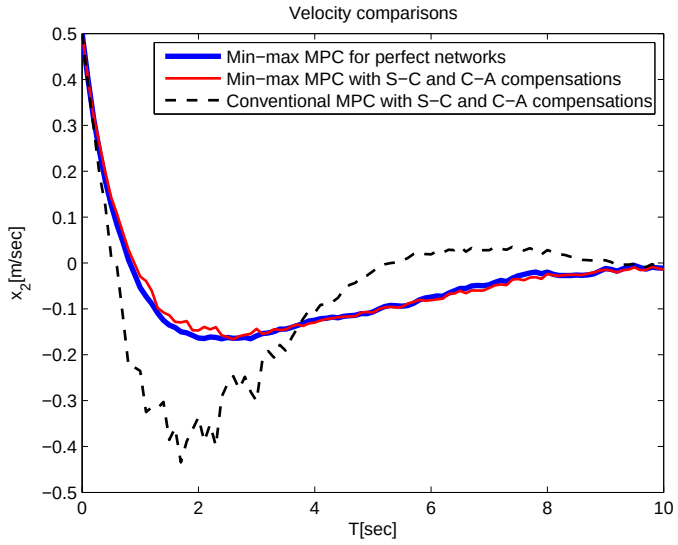

Figure 4.9: Comparisons of control performance: velocity.

- The proposed compensations strategy is necessary and effective; otherwise, the nonlinear NCS may diverge due to the packet dropouts and the time delays, as observed from Test 4.

4.6 Conclusion

In this chapter, the networked control problem has been investigated for a class of constrained nonlinear systems simultaneously subject to packet dropouts and time delays over both the S-C channel and the C-A channel. An effective networked control framework based on the min-max MPC method has been proposed, which is featuring the following: 1) It can effectively compensate for mixed networked time delays and packet dropouts occurring not only on the S-C channel but also on the C-A channel simultaneously; 2) it takes into account the effects of external disturbances to improve control performance; and 3) it well handles the state constraints and input constraints. It has further been proven that the closed-loop nonlinear networked system with the designed control strategy is ISpS by using a novel approach. In this approach, a novel ISpS-type Lyapunov function has been presented based on the construction of an auxiliary constrained min-max optimization problem. The effectiveness of the proposed control framework has been verified by simulation studies and comparisons.

Chapter 5

Output Feedback Predictive Control of NCSs with Intermittent Measurements

5.1 Introduction

Chapter 3 and **4** focus on the state feedback MPC problems for nonlinear NCSs, and it is assumed that the system state is measurable, which may not be satisfied in many practical applications. To remove this assumption, this chapter studies the *robust output feedback MPC design* problem for a class of *constrained linear systems* subject to periodical measurement packet dropouts and external disturbances. In the literature on the robust output feedback MPC for constrained linear systems, there are mainly three approaches, namely, the set-membership approach [4], the approach using partial fixed feedback control laws [15, 68, 24], and the direct approach [93, 94]. Through these approaches, it has been proven that the system state asymptotically converges to a compact set given bounded disturbances. However, these methods cannot be used to design the MPC for systems subject to intermittent measurements. Specifically, when it comes to designing the robust output feedback MPC for constrained systems subject to measurement losses, several questions shall naturally arise: How to design the robust output feedback MPC to fulfill the system constraints by addressing the measurement losses? How to guarantee convergence when measurement dropouts and (bounded) disturbances co-exist? And how the measurement dropouts would affect the control performance? These questions will be answered in this work

considering periodical measurement dropouts.

In this chapter, the framework based on the approach with partial fixed feedback control law is adopted to design the output feedback MPC algorithm. Instead of designing an ordinary Luenberger observer, a novel observer is first designed such that the error dynamic system is asymptotically stable for consecutive packet dropouts, and the error converges to certain compact set. By treating the error as a bounded disturbance, we decouple the dynamics of the state estimation system and the error system. Furthermore, using the augmentation and tightening techniques to handle constraints while incorporating the measurement losses, we design a novel output feedback MPC algorithm. These operations raise the feasibility and stability issues, which have been studied accordingly. The main contributions of this chapter are two-fold.

- A robust output feedback MPC framework is proposed for the constrained linear systems subject to periodical measurement dropouts. In particular, an observer is first designed by considering the measurement dropouts; the dynamic model of estimation error is then derived, and the error bounds are established; the tightened sets on input and state are proposed such that the system constraints can be fulfilled in spite of external disturbances and periodical measurement losses.

- The theoretical results of the control performance by using the proposed robust output feedback MPC algorithm are developed. Specifically, the iterative feasibility of the proposed algorithm is guaranteed; the exact convergence bounds of the system state are established by considering the effects of periodical measurement losses.

The remainder of this chapter is organized as follows. The design objective and the problem formulation are presented in Section 5.2. In Section 5.3, the networked observer is designed and the bounds of estimation error are established. In Section 5.4, the issue of tightening the constraints is discussed and the robust output feedback MPC algorithm is proposed. In Section 5.5, the feasibility of the proposed algorithm and convergence properties of the closed-loop system states are established. The simulation results and comparison studies are illustrated in Section 5.6. Finally, some concluding remarks are addressed in Section 5.7.

Nomenclature: The superscripts "T" and "-1" stand for the matrix transpose and the matrix inverse, respectively. The notation $\mathbb{Z}$ ($\mathbb{Z}_{\geqslant 0}$) denotes the set of inte-

gers (non-negative integers) and the symbol $\mathbb{R}$ ($\mathbb{R}_{\geqslant 0}$) represents the real space (non-negative real space). Given two sets $\mathcal{X} \subset \mathbb{R}^n$ and $\mathcal{Y} \subset \mathbb{R}^n$, the Minkowski set addition is denoted by $\mathcal{X} \oplus \mathcal{Y} \triangleq \{x+y|\ x \in \mathcal{X}, y \in \mathcal{Y}\}$, and the P-difference $\mathcal{X}$ minus $\mathcal{Y}$ is denoted by $\mathcal{X} \sim \mathcal{Y} \triangleq \{z \in \mathbb{R}^n|\ z+y \in \mathcal{X}, \forall\ y \in \mathcal{Y}\}$. Given a sequence of sets $\{\mathcal{X}_i \subset \mathbb{R}^n\}$ with $a \leqslant i \leqslant b, i \in \mathbb{Z}$, $a \leqslant b$ and $a \in \mathbb{Z}, b \in \mathbb{Z}$, we define $\bigoplus_{i=a}^{b} \mathcal{X}_i \triangleq \mathcal{X}_a \oplus \cdots \oplus \mathcal{X}_b$. Given a set $\mathcal{X} \subset \mathbb{R}$ and a real matrix M with compatible dimension, we denote $M\mathcal{X}$ by $M\mathcal{X} \triangleq \{Mx|\ x \in \mathcal{X}\}$. For n sets $\mathcal{X}_1$, $\mathcal{X}_2$, $\cdots$, $\mathcal{X}_n$, the Cartesian product $\mathcal{X}_1 \times \mathcal{X}_2 \times \cdots \times \mathcal{X}_n$ is denoted as $\text{col}\{\mathcal{X}_1, \mathcal{X}_2, \cdots, \mathcal{X}_n\}$ or written as $\begin{bmatrix} \mathcal{X}_1 \\ \mathcal{X}_2 \\ \vdots \\ \mathcal{X}_n \end{bmatrix}$. Given a vector $v \in \mathbb{R}^n$ and a set $\mathcal{X} \subset \mathbb{R}^n$, we write $\{v\} \oplus \mathcal{X}$ as $v \oplus \mathcal{X}$. Given two numbers $m \in \mathbb{Z}_{\geqslant 0}$ and $b \in \mathbb{Z}_{\geqslant 0} - 0$, we denote m modulo n by mod $(\frac{m}{n})$. For a sequence of column vectors $v_i \in \mathbb{R}^{n \times 1}$ with $i = 0, 1, \cdots, m$, we denote $\text{col}\{v_1, v_2, \cdots, v_m\} \triangleq [v_1^{\mathrm{T}}, v_2^{\mathrm{T}}, \cdots, v_m^{\mathrm{T}}]^{\mathrm{T}}$.

5.2 Problem Formulation

Consider the following dynamical system:

$$x_{k+1} = Ax_k + Bu_k + D\omega_k, \tag{5.1}$$

where $x_k \in \mathbb{R}^n$ is the state vector, $u_k \in \mathbb{R}^{n_u}$ is the control input and $\omega_k \in \mathbb{R}^{n_w}$ is the external disturbance. The system state and the control input are constrained as

$$x_k \in \mathcal{X} \subseteq \mathbb{R}^n, u_k \in \mathcal{U} \subseteq \mathbb{R}^{n_u}, \forall k \in \mathbb{Z}_{\geqslant 0}, \tag{5.2}$$

and the external disturbance ω_k belongs to a set $\mathcal{W} \subseteq \mathbb{R}^{n_w}$, where $\mathcal{X}, \mathcal{U}$ and $\mathcal{W}$ are compact sets including origin as an interior point. The output measurement is given by

$$y_k = Cx_k + Ev_k, \tag{5.3}$$

where $y_k \in \mathbb{R}^{n_y}$ is the sensor output and $v_k \in \mathbb{R}^{n_v}$ is the sensor noise, being bounded in a compact set $\mathcal{V} \subseteq \mathbb{R}^{n_v}$ with origin as an interior point. There is a communication network deployed between the controller and the sensor. The communication link is subject to periodically consecutive measurement dropouts. The length of

each dropout event is equal to one unit (time instant), and there are T_d consecutive dropouts occurring between any two adjoining successful transmissions, where T_d is a fixed integer with $0 < T_d < \infty$. That is, the measurement is only received at the time instant $k = n(T_d + 1)$, where $n = 0, 1, \cdots$. This configuration of the control system under investigation is depicted in Figure 5.1.

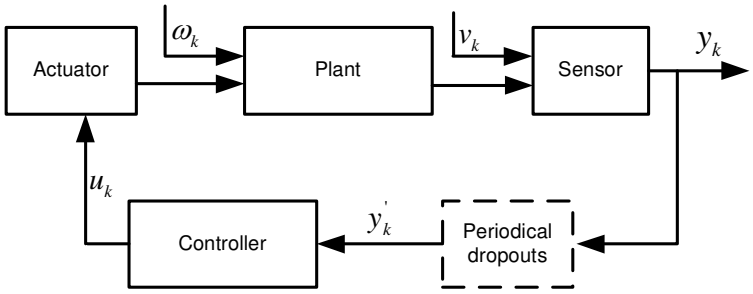

Figure 5.1: System setup.

For the dynamical systems in (5.1) and (5.3), we have the following standard assumption.

Assumption 5.1. *The triple (A, B, C) is stabilizable and observable.*

The objective of this study is to design a robust output feedback model predictive controller in the form of

$$\begin{cases} \hat{x}_{k+1} = g(\hat{x}_k, y_k'), \\ u_k = \kappa(\hat{x}_k), \end{cases}$$

such that 1) the input and state constraints in (5.2) are satisfied; 2) the system state in (5.1) approaches to a compact set (depending on T_d), for all disturbances $\omega_k \in \mathcal{W}$ and $v_k \in \mathcal{V}$. Here $\hat{x}_k$ is the state estimate and y_k' is the available measurement shown in Figure 5.1.

Remark 5.1. *Due to the presence of the persistent disturbances v_k and ω_k, it is not possible to design a controller to achieve the asymptotic regulation, i.e., $\lim_{k\to\infty} x_k = 0$ [93, 14], even though there is no measurement dropout. The achievable result of robust output feedback MPC for a non-networked system is to regulate the system state towards a compact set which contains zero as an interior point, and further to make the compact set as small as possible; see, e.g., [93, 15]. In this study, considering the measurement losses and persistent disturbances, we aim to drive the system state towards some compact sets, which contain zero and are as small as possible, by designing a novel robust output feedback model predictive controller.*

Before proceeding, we recall some standard definitions of system with disturbance bounded by compact set [6, 66, 93], which will be used in the sequel.

Definition 5.1. *A set $\mathcal{P}$ is said to be a* positively invariant set *for the system $x_{k+1} = f(x_k)$ with the constraint $\mathcal{X}$, if $\mathcal{P} \subseteq \mathcal{X}$ and $f(x_k) \in \mathcal{P}$, for all $x_k \in \mathcal{P}$. A set $\mathcal{P}$ is said to be a* robust positively invariant set *for the system $x_{k+1} = f(x_k, \omega_k)$ with the constraints $\mathcal{X}$ and $\mathcal{W}$, if $\mathcal{P} \subseteq \mathcal{X}$ and $f(x_k, \omega_k) \in \mathcal{X}$, for all $x_k \in \mathcal{X}$ and $\omega_k \in \mathcal{W}$.*

Definition 5.2. *For the system $x_{k+1} = f(x_k, \omega_k)$ and $y_k = g(x_k, v_k)$ with constraints $\mathcal{W}$, $\mathcal{V}$ and $\mathcal{Y}$, the* maximal output admissible set *is defined as all the initial states which assure all the constraints to be met, i.e., the set $\{x_0 \in \mathbb{R}^n |\ y_k \in \mathcal{Y}, \forall\ \omega_k \in \mathcal{W}, v_k \in \mathcal{V}, k \in \mathbb{Z}_{\geqslant 0}\}$.*

5.3 Observer Design and Estimation Error Analysis

To design the output feedback model predictive controller, the system state should be estimated. In this section, the observer for the system in (5.1) with the unreliable measurement y'_k is first designed, and then the error dynamics between the system in (5.1) and the designed observer is analyzed.

5.3.1 Observer Design

In order to describe the networked observer, we denote the time instants when the network transmission is successful as τ_i, $i = 0, 1, \cdots$. It is observed that $\tau_{i+1} - \tau_i = T_d + 1$. The observer of the control system in Figure 5.1 is designed as follows.

$$\begin{cases} \begin{cases} \hat{x}_{k+1} = A\hat{x}_k + Bu_k + L(\hat{y}_k - y'_k), \\ \hat{y}_k = C\hat{x}_k, \end{cases} & \text{if} \quad k = \tau_i, i = 0, 1, \cdots, \\ \hat{x}_{k+1} = A\hat{x}_k + Bu_k, & \text{if} \quad \tau_i < k < \tau_{i+1}, i = 0, 1, \cdots. \end{cases} \tag{5.4}$$

Define $e_k \triangleq x_k - \hat{x}_k$, and the error dynamics can be derived as

$$e_{\tau_i+l} = A^{l-1} e_{\tau_i+1} + \sum_{j=0}^{l-2} A^j D\omega_{\tau_i+l-1-j}, \quad 2 \leqslant l \leqslant T_d + 1, \tag{5.5}$$

$$\begin{aligned} e_{\tau_{i+1}+1} &= \Phi_L e_{\tau_{i+1}} + LEv_{\tau_{i+1}} + D\omega_{\tau_{i+1}} \\ &= \Phi_L A^{T_d} e_{\tau_i+1} + \Phi_L \sum_{j=0}^{T_d-1} A^j D\omega_{\tau_i+T_d-j} + LEv_{\tau_i+1} + D\omega_{\tau_i+1}, \end{aligned} \tag{5.6}$$

where $\Phi_L \triangleq A + LC$. To regulate the system error towards some compact sets, we need to design the observer gain L such that the error dynamics is stable under zero disturbances. The existence of the observer gain L is guaranteed by the following Proposition 5.1.

Proposition 5.1. *There exists an observer gain L such that the matrix $\Phi_L A^{T_d}$ is stable.*

Remark 5.2. *The design of the observer gain L in this work is different from that of the Luenberger observer. The gain L of the Luenberger observer is normally designed such that $A + LC$ is stable. Since the measurement output is subject to data losses in a network environment, a more stringent condition should be imposed on the gain L. Therefore, it requires designing the gain L such that $\Phi_L A^{T_d}$ is stable.*

5.3.2 Bounds of Estimation Error

By defining $\bar{\mathcal{W}}_k \triangleq \bigoplus_{i=0}^{k-1} A^i D\mathcal{W}$ and $\mathcal{W}_e = \Phi_L \bar{\mathcal{W}}_{T_d+1} \oplus LE\mathcal{V} \oplus D\mathcal{W}$, we can write the error dynamics in (5.5) and (5.6) as

$$e_{\tau_i+l} = A^{l-1} e_{\tau_i+1} + \bar{\omega}_{\tau_i+l-1}, \quad \bar{\omega}_{\tau_i+l-1} \in \bar{\mathcal{W}}_l, \quad 2 \leqslant l \leqslant T_d + 1, \tag{5.7}$$

$$e_{\tau_{i+1}+1} = \Phi_L A^{T_d} e_{\tau_i+1} + \bar{\omega}_{\tau_i+T_d+1}, \quad \bar{\omega}_{\tau_i+T_d+1} \in \mathcal{W}_e. \tag{5.8}$$

For the error system in (5.7) and (5.8), the system state will not necessarily converge to zero due to the persistent external disturbance $\{\bar{\omega}_{\tau_i+l}\}$. In fact, we have the following lemma to characterize the convergence bounds of the error dynamics.

Lemma 5.1. *For the error system in (5.7) and (5.8), there exists a robust positively invariant set $\mathcal{E}$ such that if $e_{\tau_0+1} \in \mathcal{E}$, then $e_{\tau_i+1} \in \mathcal{E}$ and $e_{\tau_i+l} \in A^{l-1}\mathcal{E} \oplus \bar{\mathcal{W}}_{l-1}$, $2 \leqslant l \leqslant T_d + 1$, $\forall i = 0, 1, \cdots$.*

Proof. Since $\Phi_L A^{T_d}$ is stable, and $\mathcal{W}_e$ is a compact set, there exists a robust positively invariant set $\mathcal{E}$ for the error system in (5.8) such that $e_{\tau_i+1} \in \mathcal{E}$ whenever $e_{\tau_0+1} \in \mathcal{E}$ according to [6, 66, 93]. Further, $e_{\tau_i+l} \in A^{l-1}\mathcal{E} \oplus \bar{\mathcal{W}}_{l-1}$, $2 \leqslant l \leqslant T_d + 1$ can be derived from (5.7). □

Remark 5.3. *The robust positively invariant set $\mathcal{E}$ serves as the nominal equilibrium point for the error dynamics in (5.8). Therefore, it is desirable that the set $\mathcal{E}$ can be determined as small as possible. The numerical methods to calculate the minimal robust positively invariant set $\mathcal{E}$ can be referred to [109, 125, 126]. For simplicity, we assume that the initial error is in the invariant set in Lemma 5.1. In fact, even though the initial state e_{τ_0+1} is given arbitrarily (not in the invariant set), the state e_{τ_i+1} will converge to the compact set $\bigoplus_{i=0}^{\infty}(\Phi_L A^{T_d})^i \mathcal{W}_e$ as $i \to \infty$ [126, 94], and the similar results can be developed readily.*

Remark 5.4. *It is worth noting that Lemma 5.1 also provides the state bounds of the designed observer in (5.4). That is, whenever the initial state of the observer is given as $\hat{x}_0 \in x_0 \oplus \mathcal{E}$, the observer state is bounded as $\hat{x}_{\tau_i+1} \in x_{\tau_i+1} \oplus \mathcal{E}$ at time instant τ_i, and $\hat{x}_{\tau_i+l} \in x_{\tau_i+1} \oplus (A^{l-1}\mathcal{E} \oplus \bar{\mathcal{W}}_{l-1})$ at time instants $\tau_i + l$ for $2 \leqslant l \leqslant T_d + 1$.*

5.4 Robust Output Feedback MPC Design

In this section, the state feedback MPC algorithm is first revisited for a nominal system without disturbances and data losses. Then based on the state feedback MPC, the tightened constraints are proposed to fulfill the required constraints by accommodating the effects of disturbances and measurement losses. Finally, a new robust output feedback MPC algorithm is designed.

5.4.1 Nominal State Feedback MPC

Before designing the robust model predictive control algorithm for the system in (5.1) with constraints (5.2) and the measurement y'_k, let us first recall the state feedback MPC algorithm for the corresponding nominal system with measurable system state:

$$\bar{x}_{k+1} = A\bar{x}_k + B\bar{u}_k, \tag{5.9}$$

where the state and input are constrained as $\bar{x}_k \in \mathcal{X}$ and $\bar{u}_k \in \mathcal{U}$, respectively. For the system in (5.9), we assume that F is a gain of the state feedback control such

that $A + BF$ is stable (such a gain F can always be designed because (A, B) is stabilizable). We further define $\Phi_F = A + BF$ and $\bar{C}_k = [\bar{c}_{k|k}^{\mathrm{T}}, \bar{c}_{k+1|k}^{\mathrm{T}}, \cdots, \bar{c}_{k+N-1|k}^{\mathrm{T}}]^{\mathrm{T}}$. Given a positive-definite matrix Ψ, a constrained minimization problem associated with the system in (5.9) can be defined as follows.

Problem 5.1. $\min J(\bar{C}_k) = \bar{C}_k^{\mathrm{T}} \Psi \bar{C}_k$, *subject to: (1)* $\bar{x}_{k+i|k} = \Phi_F \bar{x}_{k+i-1|k} + B\bar{c}_{k+i-1|k}$, $i \geqslant 1$, $\bar{x}_{k|k} = \bar{x}_k$; *(2)* $\bar{u}_{k+i|k} = F\bar{x}_{k+i|k} + \bar{c}_{k+i|k}$, $i \geqslant 0$; *(3)* $\bar{x}_{k+i|k} \in \mathcal{X}$, $i \geqslant 0$; *(4)* $\bar{u}_{k+i|k} \in \mathcal{U}$, $i \geqslant 0$; *(5)* $\bar{c}_{k+i|k} = 0, i \geqslant N$.

For Problem 5.1, we denote the optimal solution as $\bar{C}_k^*$. Now the state feedback MPC algorithm for the system in (5.9) can be readily described in Algorithm 2.

Algorithm 2 State feedback MPC algorithm

1: **procedure** GET-CONTROL($\bar{x}_k$)
2: Calculate $\bar{C}_k^*$ by solving Problem 5.1,
3: $\bar{u}_k = F\bar{x}_k + \bar{c}_{k|k}^*$,
4: **end procedure**

It is noted that the state feedback MPC algorithm described in Algorithm 2 has been employed in [67, 14]. Different from the direct MPC approach [95, 96], in Algorithm 2, the state feedback $F\bar{x}_k$ is partly incorporated into the control input for the optimization, and an extra term $\bar{c}_k$ is added to increase the degree of freedom of the constrained optimization problem. Algorithm 2 is reported to be more computationally efficient but without compromising the control performance in comparison with the standard one, thus we will adopt the framework in Algorithm 2 to develop the robust output feedback MPC algorithm. The results of the same framework on output feedback MPC for systems without dropouts can be referred to [68, 86, 15].

5.4.2 Constraints Tightening

Due to the joint effects of the estimation error, the disturbances and the data losses, the state and input constraints of the system in (5.1) cannot be fulfilled even though the state and input constraints of the nominal system are satisfied. Thus, in what follows, we are going to tighten the state and input constraints of the nominal system by incorporating the bounds of the estimation error and disturbances, and the features of data losses, such that the corresponding constraints of the system in (5.1) can be satisfied. This tightening procedure of the constraints will be carried out by two parts.

Firstly, we will adjust the constraints from prediction horizon $i = 0$ to $N-1$. We start by tightening the state and input constraints of the nominal system of the observer in (5.4). By regarding the estimation error as a disturbance, the nominal system for the observer in (5.4) can be derived, which has the same form as (5.9). In order to describe the effects of the disturbance v_k and the estimation error e_k, we define a new disturbance sequence as

$$d_k = \begin{cases} -LCe_k - LEv_k & \text{if} \quad k = \tau_i, i = 0, 1, \cdots, \\ 0, & \text{if} \quad \tau_i < k < \tau_{i+1}, i = 0, 1, \cdots. \end{cases} \tag{5.10}$$

Two associated compact sets are also defined as $\mathcal{D} = -LC\mathcal{E} \oplus (-LE)\mathcal{V}$ and $\mathcal{D}_k = \delta(k-\tau_i)(-LC\mathcal{E}) \oplus (-LE)\mathcal{V}$, where $\delta(t)$ is the indicator function, i.e., $\delta(t) = 1$ if $t = 0$; $\delta(t) = 0$ if $t \neq 0$. It can be seen that $d_k \in \mathcal{D}_k \subseteq \mathcal{D}$. By considering the new disturbance for the nominal system of the observer, we have

$$\hat{x}_{k+i|k} = \bar{x}_{k+i|k} + \sum_{j=0}^{i-1} \Phi_F^j d_{k+i-1-j}, \quad i = 0, 1, \cdots, N-1, \tag{5.11}$$

$$\hat{u}_{k+i|k} = \bar{u}_{k+i|k} + F\sum_{j=0}^{i-1} \Phi_F^j d_{k+i-1-j}, \quad i = 0, 1, \cdots, N-1. \tag{5.12}$$

The state and input constraints from horizon $i = 0$ to $N-1$ can be tightened in the following lemma.

Lemma 5.2. *Suppose that $e_0 \in \mathcal{E}$ and that the measurement data is transmitted successfully at the time instant $k = 0$. If the following constraints are fulfilled as*

$$\bar{x}_{k+i|k} \in \mathcal{X}_k^i, \quad i = 0, 1, \cdots, N-1,$$
$$\bar{u}_{k+i|k} \in \mathcal{U}_k^i, \quad i = 0, 1, \cdots, N-1,$$

then $x_{k+i|k} \in \mathcal{X}$ and $u_{k+i|k} \in \mathcal{U}$, for all $i = 0, 1, \cdots, N-1$, where $\mathcal{X}_k^i \triangleq \mathcal{X} \sim \mathcal{E}_k^i \sim \mathcal{R}_k^i$, $\mathcal{E}_k^i = \bar{\mathcal{E}}(f(k+i))$, $\mathcal{U}_k^i \triangleq \mathcal{U} \sim F\mathcal{R}_k^i$, $\mathcal{R}_k^i \triangleq \bigoplus_{j=0}^{i-1} \Phi_F^j \mathcal{D}_{k+i-1-j}$, the compact set $\bar{\mathcal{E}}$ is defined as

$$\bar{\mathcal{E}} \triangleq \operatorname{col}\left\{ \begin{array}{cccc} \mathcal{E} & A\mathcal{E} \oplus \bar{\mathcal{W}}_1 & \cdots & A^{T_d}\mathcal{E} \oplus \bar{\mathcal{W}}_{T_d} \end{array} \right\},$$

and $f(n)$ is defined as

$$f(n) = \begin{cases} \mod\left(\frac{n}{T_d+1}\right), & \text{if} \quad \mod\left(\frac{n}{T_d+1}\right) \neq 0, \\ T_d + 1, & \text{if} \quad \mod\left(\frac{n}{T_d+1}\right) = 0, \end{cases}$$

where n is a positive integer.

Proof. According to (5.11) and (5.12), it can be obtained that:

$$x_{k+i|k} = \bar{x}_{k+i|k} + e_{k+i} + \sum_{j=0}^{i-1} \Phi_F^j d_{k+i-1-j}, \tag{5.13}$$

$$u_{k+i|k} = \bar{u}_{k+i|k} + F \sum_{j=0}^{i-1} \Phi_F^j d_{k+i-1-j}. \tag{5.14}$$

Since $e_0 \in \mathcal{E}$ and there is no dropout at the time instant 0, we have $e_{k+i} \in \mathcal{E}_k^i$ according to Lemma 5.1. By assumption, it has $\bar{x}_{k+i|k} \in \mathcal{X}_k^i$. Therefore, according to (5.13), we have

$$\begin{aligned} x_{k+i|k} \in & \mathcal{X}_k^i \oplus \mathcal{E}_k^i \oplus \mathcal{R}_k^i \\ = & (\mathcal{X} \sim \mathcal{E}_k^i \sim \mathcal{R}_k^i) \oplus \mathcal{E}_k^i \oplus \mathcal{R}_k^i \subseteq \mathcal{X}. \end{aligned}$$

Similarly, by applying $\bar{u}_{k+i|k} \in \mathcal{U}_k^i$ to (5.14) we can obtain

$$u_{k+i|k} \in \mathcal{U}_k^i \oplus F\mathcal{R}_k^i = (\mathcal{U} \sim F\mathcal{R}_k^i) \oplus F\mathcal{R}_k^i \subseteq \mathcal{U}.$$

The proof is completed. □

Secondly, we are going to tighten the terminal constraints (i.e., constraints for $i \geqslant N$). In order to make use of the periodical characteristics of the newly constructed disturbance d_k, we augment the system state when $i \geqslant N$ as follows. Define

$$\hat{X}_{k,n} = \begin{bmatrix} \hat{x}_{k+N+(n-1)T_d|k} \\ \hat{x}_{k+N+(n-1)T_d+1|k} \\ \vdots \\ \hat{x}_{k+N+(n-1)T_d+T_d|k} \end{bmatrix}, \quad \hat{U}_{k,n} = \begin{bmatrix} \hat{u}_{k+N+(n-1)T_d|k} \\ \hat{u}_{k+N+(n-1)T_d+1|k} \\ \vdots \\ \hat{u}_{k+N+(n-1)T_d+T_d|k} \end{bmatrix},$$

$$\bar{F}=\begin{bmatrix} F & 0 & 0 & 0 \\ 0 & F & 0 & 0 \\ 0 & 0 & \ddots & 0 \\ 0 & 0 & 0 & F \end{bmatrix}, \bar{d}_{k,n}=\begin{bmatrix} \sum_{j=0}^{T_d}\Phi_F^j d_{k+N+(n-1)T_d+T_d-j} \\ \sum_{j=0}^{T_d}\Phi_F^j d_{k+N+(n-1)T_d+T_d+1-j} \\ \vdots \\ \sum_{j=0}^{T_d}\Phi_F^j d_{k+N+(n-1)T_d+2T_d-j} \end{bmatrix},$$

$$\bar{\Phi}_F=\begin{bmatrix} \Phi_F^{T_d+1} & 0 & 0 & 0 \\ 0 & \Phi_F^{T_d+1} & 0 & 0 \\ 0 & 0 & \ddots & 0 \\ 0 & 0 & 0 & \Phi_F^{T_d+1} \end{bmatrix}.$$

Then the state prediction and the control input for $i \geqslant N$ can be rewritten as:

$$\hat{X}_{k,n+1}=\bar{\Phi}_F\hat{X}_{k,n}+\bar{d}_{k,n}, n \geqslant 1, \tag{5.15}$$

$$\hat{U}_{k,n}=\bar{F}\hat{X}_{k,n}, n \geqslant 1, \tag{5.16}$$

where $\bar{d}_{k,n} \in \bar{\mathcal{D}}_{k,n}$ with

$$\bar{\mathcal{D}}_{k,n}=\begin{bmatrix} \bigoplus_{j=0}^{T_d}\Phi_F^j\mathcal{D}_{k+N+(n-1)T_d+T_d-j} \\ \bigoplus_{j=0}^{T_d}\Phi_F^j\mathcal{D}_{k+N+(n-1)T_d+T_d+1-j} \\ \vdots \\ \bigoplus_{j=0}^{T_d}\Phi_F^j\mathcal{D}_{k+N+(n-1)T_d+2T_d-j} \end{bmatrix}.$$

Since the new disturbance d_k occurs with the period of T_d+1 according to the definition of $\mathcal{D}_k$, it can be obtained that $\bar{\mathcal{D}}_{k,1}=\cdots=\bar{\mathcal{D}}_{k,n}=\bar{\mathcal{D}}_{k,n+1}=\cdots, n \geqslant 1$ and $\bar{\mathcal{D}}_{k,1}$ is a compact set. As a result, $\bar{d}_{k,n} \in \bar{\mathcal{D}}_{k,1}, \forall n \geqslant 1$. To this end, we are in the position to tighten the terminal set in the following lemma.

Lemma 5.3. *There exists a sequence of compact sets $\mathcal{O}_k$ such that, if $\bar{X}_{k+N|k} \in \mathcal{O}_k \sim \bar{\mathcal{R}}_k$, then $x_{k+i|k} \in \mathcal{X}$ and $u_{k+i|k} \in \mathcal{U}$, for all $i \geqslant N$, where*

$$\mathcal{O}_k \triangleq \left\{ \hat{X}_{k,1}: \begin{array}{c} \bar{\Phi}^n\hat{X}_{k,1} \in \bar{\mathcal{X}} \sim \bar{\mathcal{D}}_{k,1} \sim \bar{\mathcal{E}} \\ \bar{F}\bar{\Phi}^n\hat{X}_{k,1} \in \bar{\mathcal{U}} \sim \bar{F}\bar{\mathcal{D}}_{k,1} \end{array}, \forall n=0,1,\cdots,n_k^*, \right\},$$

$$\bar{\mathcal{X}} \triangleq \begin{bmatrix} \mathcal{X} \\ \mathcal{X} \\ \vdots \\ \mathcal{X} \end{bmatrix}, \bar{\mathcal{U}} \triangleq \begin{bmatrix} \mathcal{U} \\ \mathcal{U} \\ \vdots \\ \mathcal{U} \end{bmatrix}, \bar{X}_{k+N|k}=\begin{bmatrix} \bar{x}_{k+N|k} \\ \bar{x}_{k+N+1|k} \\ \vdots \\ \bar{x}_{k+N+T_d|k} \end{bmatrix}, \bar{\mathcal{R}}_k \triangleq \begin{bmatrix} \mathcal{R}_k^N \\ \mathcal{R}_k^{N+1} \\ \vdots \\ \mathcal{R}_k^{N+T_d} \end{bmatrix},$$

and n_k^* is a finite integer.

Proof. The terminal constraints $x_{k+i|k} \in \mathcal{X}$ and $u_{k+i|k} \in \mathcal{U}$ from $i \geqslant N$ are amount to imposing the constraints for the equations in (5.15) and (5.16) subject to the following constraints:

$$\hat{X}_{k,n} \in \bar{\mathcal{X}} \sim \bar{\mathcal{E}},\ \hat{U}_{k,n} \in \bar{\mathcal{U}},\ n \geqslant 1. \tag{5.17}$$

Since $\bar{\Phi}_F$ is stable and $(\bar{\Phi}_F, \bar{F})$ is observable, then according to [66, 6], there exists a finitely determined integer n_k^* such that the terminal set $\{\hat{X}_{k,n} : \hat{X}_{k,n} \in \bar{\mathcal{X}} \sim \bar{\mathcal{E}}, \hat{U}_{k,n} \in \bar{\mathcal{U}}, \forall n \geqslant 0\}$ can be equivalently computed by the maximum output admissible set $\mathcal{O}_k$. On the other hand, it can be derived that

$$\hat{x}_{k+N+i|k} = \bar{x}_{k+N+i|k} + \sum_{j=0}^{N+i-1} \Phi_F^j d_{k+N+i-1-j},\ i = 0, 1, \cdots, T_d, \tag{5.18}$$

$$\hat{u}_{k+N+i|k} = \bar{u}_{k+N+i|k} + F \sum_{j=0}^{N+i-1} \Phi_F^j d_{k+N+i-1-j},\ i = 0, 1, \cdots, T_d. \tag{5.19}$$

Since $\bar{X}_{k+N|k} \in \mathcal{O}_k \sim \bar{\mathcal{R}}_k$, we have $\hat{X}_{k,1} \in (\mathcal{O}_k \sim \bar{\mathcal{R}}_k) \oplus \bar{\mathcal{R}}_k \subseteq \mathcal{O}_k$ in terms of (5.18) and (5.19). Finally, because the maximum output admissible set $\mathcal{O}_k$ is a robust positively invariant set for the system in (5.16)-(5.15) subject to the constraints (5.17), $\hat{X}_{k,1} \in \mathcal{O}_k$ implies that the terminal constraints $x_{k+i|k} \in \mathcal{X}$ and $u_{k+i|k} \in \mathcal{U}$ are fulfilled, for all $i \geqslant N$. □

Remark 5.5. *It is worth noting that the tightened results in Lemma 5.2 and 5.3 generalize the results in [14, 15] by specifically taking into account periodical packet dropouts, and can capture these results as special cases. In fact, the results in Lemma 5.2 and 5.3 reduce to these in [14, 15] in case of $T_d = 0$, i.e., no measurement loss occurs.*

5.4.3 Robust Output Feedback MPC Algorithm

Based on the tightened constraints derived in Lemma 5.2 and Lemma 5.3, a new constrained minimization problem can be designed as follows.

Problem 5.2. $\min J(C_k) = C_k^{\mathrm{T}} \Psi C_k$, *subject to: (1)* $\bar{x}_{k+i|k} = \Phi_F \bar{x}_{k+i-1|k} + B c_{k+i-1|k}$, $i = 0, 1, \cdots, N-1$, $\bar{x}_{k|k} = \hat{x}_k$; *(2)* $\bar{u}_{k+i|k} = F \bar{x}_{k+i|k} + c_{k+i|k}$, $i = 0, 1, \cdots, N-1$; *(3)* $\bar{x}_{k+i|k} \in \mathcal{X}_k^i$, $i = 0, 1, \cdots, N-1$; *(4)* $\bar{u}_{k+i|k} \in \mathcal{U}_k^i$, $i = 0, 1, \cdots, N-1$; *(5)* $\bar{X}_{k+N|k} \in \mathcal{O}_k \sim \bar{\mathcal{R}}_k$.

By Defining the optimal solution to Problem 5.2 as $C_k^* = [c_{k|k}^*, \cdots, c_{k+N-1|k}^*]^{\mathrm{T}}$, we have the following new robust output feedback MPC Algorithm 3 for the system in (5.1).

Algorithm 3 Robust output feedback MPC algorithm

procedure GET-OUTPUT-CONTROL(y_k',$\hat{x}_{k-1}$)
  Derive $\hat{x}_k$ from the observer in (5.4),
  Assign $\bar{x}_k = \hat{x}_k$,
  for $i = 0$ to $N-1$ **do**
    Calculate $\mathcal{X}_k^i$, $\mathcal{U}_k^i$,
  end for
  Calculate $\mathcal{O}_k$, $\bar{\mathcal{R}}_k$,
  Obtain C_k^* by solving Problem 5.2,
  Assign $u_k = F\hat{x}_k + c_{k|k}^*$.
end procedure

5.5 Feasibility and Stability Analysis

In this section, the feasibility of the proposed algorithm is first studied; then the stability of the resulting closed-loop system is investigated and the convergence bounds of the system state are established.

5.5.1 Feasibility Analysis

Feasibility of the proposed control algorithm is an important issue to facilitate its practical application. The essential idea of the iterative feasibility lies in that, if an algorithm is feasible for the first step, it will be feasible for the following steps. For the feasibility of Algorithm 3, we essentially require the feasibility of Problem 5.2, which is provided in Theorem 5.1.

Theorem 5.1. *Assume that the constrained optimization Problem 5.2 is feasible at $k = 0$. Then it is feasible for all $k \geqslant 0$.*

Proof. The proof is derived by mathematical induction. First, the optimization Problem 5.2 is feasible at time $k = 0$ according to the assumption. Second, without loss of generality, we assume that Problem 5.2 is feasible at time $k \geqslant 0$, and the optimal solution to Problem 5.2 is C_k^o, where $C_k^o \triangleq [c_{k|k}^o, c_{k+1|k}^o, \cdots, c_{N-1|k}^o]^{\mathrm{T}}$. Define

$\tilde{C}_{k+1} \triangleq [c^o_{k+1|k}, c^o_{k+2|k}, \cdots, c^o_{N-1|k}, 0]^{\mathrm{T}}$. It can be verified that $\tilde{C}_{k+1}$ is a possible solution to Problem 5.2 at time $k+1$ such that the input constraint and the state constraint can be fulfilled. By plugging $\tilde{C}_{k+1}$ into Problem 5.2, we can obtain

$$\bar{x}_{k+i|k+1} = \bar{x}_{k+i|k} + \Phi_F^{i-1} d_k, \tag{5.20}$$

$$\bar{u}_{k+i|k+1} = \bar{u}_{k+i|k} + F\Phi_F^{i-1} d_k. \tag{5.21}$$

Since $\bar{x}_{k+i|k} \in \mathcal{X}_k^i = \mathcal{X} \sim \mathcal{E}_k^i \sim \mathcal{R}_k^i$, according to the relationship in (5.20), the following can be derived

$$\begin{aligned}
\bar{x}_{k+i|k+1} \in & \mathcal{X}_k^i \oplus \Phi_F^{i-1}\mathcal{D}_k \\
= & (\mathcal{X} \sim \mathcal{E}_k^i \sim \mathcal{R}_k^i) \oplus \Phi_F^{i-1}\mathcal{D}_k \\
= & \left[\mathcal{X} \sim \mathcal{E}_k^i \sim \left(\bigoplus_{j=0}^{i-1} \Phi_F^j \mathcal{D}_{k+i-1-j}\right)\right] \oplus \Phi_F^{i-1}\mathcal{D}_k \\
\subseteq & \mathcal{X} \sim \mathcal{E}_{k+1}^{i-1} \sim \left(\bigoplus_{j=0}^{i-2} \Phi_F^j \mathcal{D}_{k+i-1-j}\right) = \mathcal{X}_{k+1}^{i-1}.
\end{aligned}$$

For the input constraint, from (5.21), we have

$$\begin{aligned}
\bar{u}_{k+i|k+1} \in & \mathcal{U}_k^i \oplus F\Phi_F^{i-1}\mathcal{D}_k \\
= & (\mathcal{U} \sim F\mathcal{R}_k^i) \oplus F\Phi_F^{i-1}\mathcal{D}_k \\
= & \left[\mathcal{U} \sim \left(F\bigoplus_{j=0}^{i-1} \Phi_F^j \mathcal{D}_{k+i-1-j}\right)\right] \oplus F\Phi_F^{i-1}\mathcal{D}_k \\
\subseteq & \mathcal{U} \sim F\mathcal{R}_{k+1}^{i-1} = \mathcal{U}_{k+1}^{i-1}.
\end{aligned}$$

Therefore, the input constraint and the state constraint can be satisfied if $\tilde{C}_{k+1}$ is applied to Problem 5.2 at time $k+1$, i.e., Problem 5.2 is feasible at time $k+1$. By induction, the algorithm in Problem 5.2 is iteratively feasible. □

5.5.2 Stability Analysis

In this subsection, the stability of the closed-loop system rendered by the designed robust model predictive controller is studied by the Lyapunov stability theory, and the convergence property of the system state is investigated. The theoretical results are summarized in the following theorem.

Theorem 5.2. *For the system in (5.1) with the constraints in (5.2), if the control input is given as* $u_k = F\hat{x}_k + c^o_{k|k}$*, where* $\hat{x}_k$ *is the observer state in (5.4) and* $c^o_{k|k}$ *is the optimal solution to Problem 5.2, then the system state asymptotically and periodically converges to* $T_d + 1$ *compact sets, i.e., the state sequences* $\{x_{(k-1)(T_d+1)+1}\}$, $\{x_{(k-1)(T_d+1)+2}\}$, $\cdots$, $\{x_{k(T_d+1)}\}$ *will converge to* $T_d + 1$ *different compact sets, respectively, where* $k = 1, 2, \cdots$.

Proof. Take the Lyapunov function candidate as $V(\hat{x}_k) = C^{o\mathrm{T}}_k \Theta C^o_k$, and an auxiliary function $\bar{V}(\hat{x}_{k+1}) = \tilde{C}^{\mathrm{T}}_{k+1}\Theta\tilde{C}_{k+1}$, where Θ is a positive definite matrix with appropriate dimension. According to the definitions of C^o_k and $\tilde{C}_{k+1}$, it can be derived that

$$\bar{V}(\hat{x}_{k+1}) - V(\hat{x}_k) = -c^{o\mathrm{T}}_{k|k}\Theta c^o_{k|k} < 0.$$

Because of the optimality, we have $\bar{V}(\hat{x}_{k+1}) \geqslant V(\hat{x}_{k+1})$. Consequently, it has

$$V(\hat{x}_{k+1}) - V(\hat{x}_k) < -c^{o\mathrm{T}}_{k|k}\Theta c^o_{k|k}.$$

Since $V(\hat{x}_k)$ is bounded, we further have

$$-\infty < V(\infty) - V(\hat{x}_k) = -\sum_{j=k}^{\infty} c^{o\mathrm{T}}_{j|j}\Theta c^o_{j|j} < 0. \tag{5.22}$$

By applying the property of the convergent sequence for (5.22), we have $\lim_{k\to\infty} c^{o\mathrm{T}}_{k|k}$ $\Theta c^o_{k|k} = 0$, i.e., $\lim_{k\to\infty} c^o_{k|k} = 0$.

In what follows, we will analyze the convergence property of the system state by analyzing the observer system and applying this result. To this end, we first define the following symbols to augment the dynamics of the predicted state as follows:

$$X_k = \begin{bmatrix} x_{(k-1)(T_d+1)+1} \\ x_{(k-1)(T_d+1)+2} \\ \vdots \\ x_{k(T_d+1)} \end{bmatrix}, Y_k = \begin{bmatrix} \hat{x}_{(k-1)(T_d+1)+1} \\ \hat{x}_{(k-1)(T_d+1)+2} \\ \vdots \\ \hat{x}_{k(T_d+1)} \end{bmatrix},$$

$$\bar{C}_k = \begin{bmatrix} \sum_{j=0}^{T_d} c^o_{(k-1)(T_d+1)+1-j|(k-1)(T_d+1)+1-j} \\ \sum_{j=0}^{T_d} c^o_{(k-1)(T_d+1)+2-j|(k-1)(T_d+1)+2-j} \\ \vdots \\ \sum_{j=0}^{T_d} c^o_{k(T_d+1)-j|k(T_d+1)-j} \end{bmatrix},$$

$$\bar{V}_k = \begin{bmatrix} -LCe_{k(T_d+1)+1} - LEv_{k(T_d+1)+1} \\ \Phi_F(-LCe_{k(T_d+1)+1} - LEv_{k(T_d+1)+1}) \\ \vdots \\ \Phi_F^{T_d-1}(-LCe_{k(T_d+1)+1} - LEv_{k(T_d+1)+1}) \\ \Phi_F^{T_d}(-LCe_{(k-1)(T_d+1)+1} - LEv_{(k-1)(T_d+1)+1}) \end{bmatrix}, \bar{\mathcal{V}} = \begin{bmatrix} \mathcal{D} \\ \Phi_F\mathcal{D} \\ \vdots \\ \Phi_F^{T_d-1}\mathcal{D} \\ \Phi_F^{T_d}\mathcal{D} \end{bmatrix}.$$

By applying the optimal control input $u_k = F\hat{x}_k + c^o_{k|k}$ to the observer in (5.4) and rearranging the equations, we have

$$Y_{k+1} = \bar{\Phi}_F Y_k + \bar{C}_k + \bar{V}_k, \quad k \geqslant 1, \tag{5.23}$$

where $\bar{V}_k \in \bar{\mathcal{V}}$. Since $\bar{\Phi}_F$ is stable and $\lim_{k\to\infty} \bar{C}_k = 0$, the closed-loop system is asymptotically stable without disturbances. Further, according to (5.23), it can be obtained that

$$Y_k = (\bar{\Phi}_F)^{k-1} Y_1 + \sum_{j=0}^{k-2} \bar{\Phi}_F^j \bar{C}_{k-1-j} + \sum_{j=0}^{k-2} \bar{\Phi}_F^j \bar{V}_{k-1-j}.$$

Since $\bar{\Phi}_F$ is stable, it can be derived that the compact set $\lim_{n\to\infty} \bigoplus_{j=0}^{n-2} \bar{\Phi}_F^j \bar{\mathcal{V}}$ can be uniquely determined according to [14, 15]. Without loss of generality, we define

$$\lim_{k\to\infty} \bigoplus_{j=0}^{k-2} \bar{\Phi}_F^j \bar{\mathcal{V}} \triangleq \mathcal{E}_d.$$

Further, we have $\lim_{n\to\infty} \sum_{j=0}^{k-2} \bar{\Phi}_F^j \bar{C}_{k-1-j} = 0$ because of $\lim_{k\to\infty} c^o_{k|k} = 0$. Therefore,

$$\lim_{k\to\infty} Y_k = \mathcal{E}_d.$$

As a result, the system state will converge as $\lim_{k\to\infty} X_k = \lim_{k\to\infty} Y_k \oplus \bar{\mathcal{E}} = \mathcal{E}_d \oplus \bar{\mathcal{E}}$. Since $\bar{\Phi}_F^j$ is a diagonal matrix and the set $\bar{\mathcal{V}}$ is the Cartesian product of T_d+1 compact sets, the set $\mathcal{E}_d$ is also the Cartesian product of T_d+1 compacts. In addition, we know that the set $\bar{\mathcal{E}}$ is the Cartesian product of T_d+1 compacts. Thus, the convergence set

$\mathcal{E}_d \oplus \bar{\mathcal{E}}$ is also the Cartesian product of $T_d + 1$ compact sets. As a result, the system state converges to (disjoint) $T_d + 1$ compact sets periodically. □

Remark 5.6. *Note that the set* $\lim_{n\to\infty} \bigoplus_{j=0}^{k-2} \bar{\Phi}_F^j \bar{\mathcal{V}}$ *can be approximately calculated by using some finitely determined integer and some constant according to [125, 126]. In fact, if we assume that the finitely determined integer is* n_o *and the constant is* $0 < \beta \leqslant 1$*, then the system state will periodically converge to* T_d+1 *compact sets. That is,* $\{x_{(k-1)(T_d+1)+1}\}$ *converges to* $\beta[\bigoplus_{j=0}^{n_o}(\Phi_F^{T_d+1})^j\mathcal{D}] \oplus \bar{\mathcal{E}}(1)$*,* $\{x_{(k-1)(T_d+2)+1}\}$ *converges to* $\beta[\bigoplus_{j=0}^{n_o}(\Phi_F^{T_d+1})^j\Phi_F\mathcal{D}]\oplus\bar{\mathcal{E}}(2), \cdots$*, and* $\{x_{(T_d+1)}\}$ *converges to* $\beta[\bigoplus_{j=0}^{n_o}(\Phi_F^{T_d+1})^j\Phi_F^{T_d}\mathcal{D}]\oplus \bar{\mathcal{E}}(T_d+1)$*, for* $k = 1, 2, \cdots$.

5.6 Simulations and Comparison Studies

In this section, the simulation studies of the proposed robust output feedback MPC strategy are carried out to verify the developed theoretical results. The proposed algorithm is first tested for a 1-D system and 2-D system, respectively. Then the simulation results are demonstrated and discussed.

5.6.1 Example 1

The dynamical system is described as:

$$x_{k+1} = 1.5x_k + u_k + w_k,$$

where $x_k \in \mathbb{R}$ is the system state, $u_k \in \mathbb{R}$ is the control input and the process disturbance $w_k \in \mathbb{R}$ is bounded as $-0.01 \leqslant w_k \leqslant 0.01$. The sensor measurement is expressed as:

$$y_k = 2x_k + 0.8v_k,$$

where the measurement disturbance is bounded as $-0.01 \leqslant v_k \leqslant 0.01$. Suppose that a wireless communication link is deployed between the controller and the sensor, and the communication link is subject to data losses with a dropout period $T_d = 3$. For this control system, the state is required to be constrained as $-1 \leqslant x_k \leqslant 1$ and the control input is constrained as $-1 \leqslant u_k \leqslant 1$. In order to implement the proposed output feedback MPC algorithm, the observer in (5.4) is first designed. Here, the observer gain is designed as $L = -0.8$. As a result, $\Phi_L = -0.1$. It can be verified that $\Phi_L A^{T_d} = -0.3375$ which is stable. Thus, $L = -0.8$ fulfills the requirement of

the observer with packet dropouts. In the simulation, the process disturbance w_k is realized by a uniformly distributed process bounded in $[-0.01, 0.01]$; the measurement noise v_k is also generated by a uniform distributed process bounded in $[-0.01, 0.01]$; the initial value of the state is chosen as $x_0 = 1.0$ and the value of the observer state is $\hat{x}_0 = 1.1$. For the MPC, the prediction horizon is determined as $N = 5$ and the auxiliary feedback gain is set to be $F = -1$.

Results Analysis

After applying the proposed output feedback MPC Algorithm 2 using the simulation setup as described above, simulation results are demonstrated below. The error dynamics described in (5.8) and (5.7), and its bounds calculated by the compact sets in Lemma 5.1 are demonstrated in Figure 5.2.

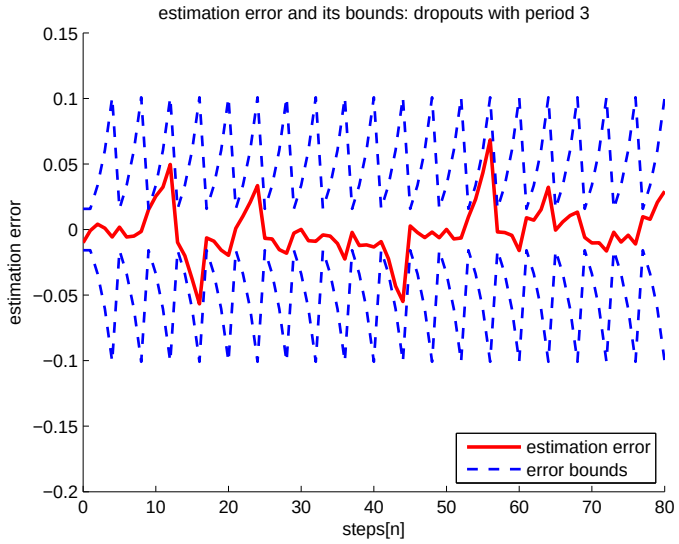

Figure 5.2: Observer error and its bounds.

The control input rendered by $u_k = F\hat{x}_k + c^o_{k|k}$ is shown in Figure 5.3, and the system state as well as the estimated state (by the observer) are illustrated in Figure 5.4.

- From Figure 5.2, it can be seen that the error has been well bounded by an upper bound and a lower bound. These bounds are periodically calculated by the compact-set sequence $\{\mathcal{E}, A\mathcal{E} \oplus \bar{\mathcal{W}}_1, A^2\mathcal{E} \oplus \bar{\mathcal{W}}_2, A^3\mathcal{E} \oplus \bar{\mathcal{W}}_3\}$ according to Lemma 5.1. This observation verifies the results in Lemma 5.1.

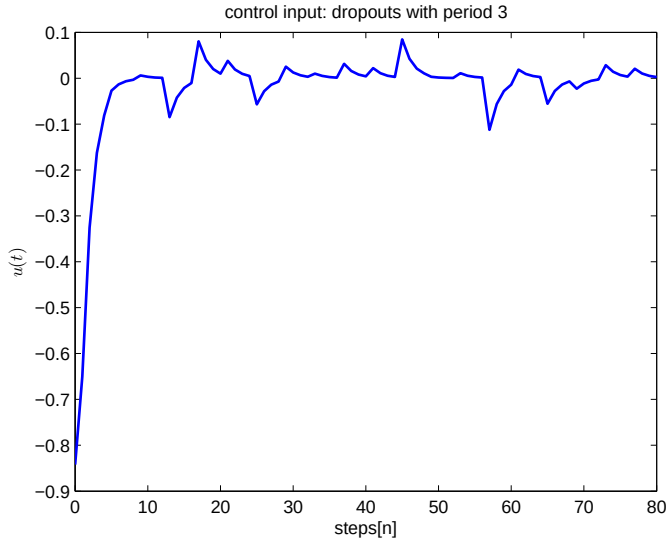

Figure 5.3: Control input.

- From the derived control input in Figure 5.3, it can be observed that the control input satisfies the control constraints.

- In Figure 5.4, the state bounds are calculated based on Theorem 5.2. From this figure, it can be seen that: 1) the system state fulfills the pre-specified state constraints; 2) the observer designed in (5.4) can effectively estimate the system state in spite of the lost measurement and disturbances; 3) the system state converges towards the theoretical compact sets which can be determined by Theorem 5.2.

In summary, the proposed robust output feedback MPC is feasible and the closed-loop system is stable with the system state periodically converging to the compact sets.

Comparison Study

In order to analyze the effects of packet dropouts to the closed-loop system, the comparison studies have been conducted on evaluating control performance of two groups of simulations, i.e., Group A and Group B.

- **Group A:** The proposed robust output feedback Algorithm 2 is implemented for the above described system setup.

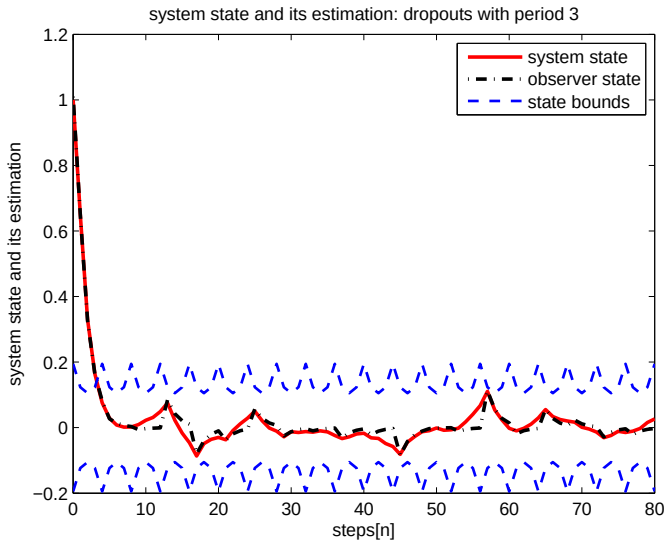

Figure 5.4: Systems state and its bounds.

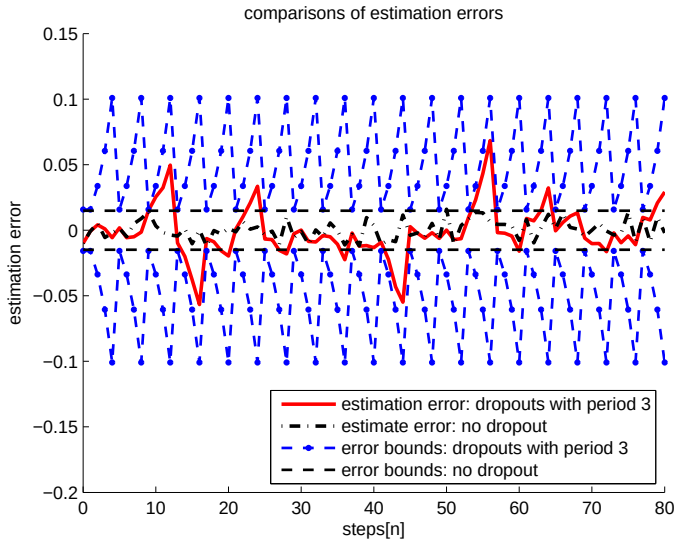

Figure 5.5: Estimation errors and their bounds.

- **Group B:** The standard output feedback MPC algorithm (i.e., the proposed Algorithm 2 with $T_d = 0$) is applied for the same system setup but without measurement dropouts (i.e., perfect network is assumed here).

The estimation errors and their bounds are illustrated in Figure 5.5. The control inputs and system states of both cases are shown in Figure 5.6 and 5.7, respectively.

By inspecting the simulation results, we have the following observations.

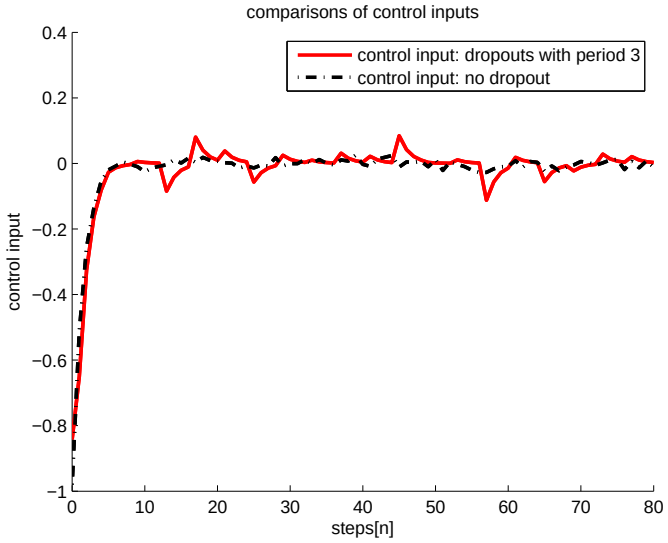

Figure 5.6: Comparisons of control inputs.

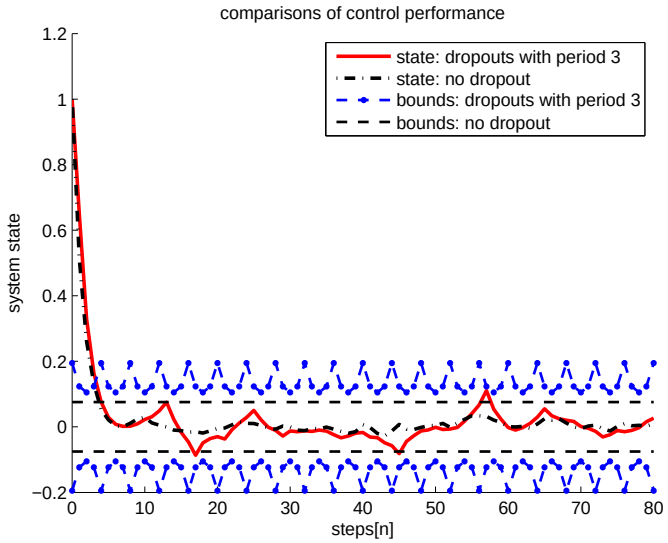

Figure 5.7: Comparisons of state bounds.

- From Figure 5.5, it can be seen that: 1) both the estimation errors in Group A and Group B are bounded by their corresponding error bounds; 2) both the lower error bound and the upper one in Group B are determined by a fixed value, while the corresponding error bounds in Group A vary according to the results of Lemma 5.1 (i.e., the values of bounds change with the period 4). This is caused by the occurrences of the periodical consistent packet dropouts with

$T_d = 3$; 3) the error bounds in Group B are more stringent than those in Group A, and the estimation error in Group A violates the error bounds in Group B. This implies that the packet dropouts increase the estimation errors due to the incomplete measurement information.

- From Figure 5.6, it can be observed that both the control inputs for both simulations satisfy the input constraints, but the control input in Group A shows more fluctuation than that in Group B, which is also contributed by packet dropouts.

- Similarly, by inspecting Figure 5.7, we can see that: 1) the error bounds of the system state in Group B are fixed for all the time. On the contrary, in Group A they vary according to the results described in Theorem 5.2; 2) the system state in Group A goes beyond the convergence region determined in Group B; 3) the convergence bounds of the system state in Group A are larger compared to those in Group B. These three different aspects also are caused by the packet dropouts which degrade the system performance.

To summarize, the packet dropouts enlarge the estimation error, make greater uncertainties of the convergence region for the system state, and require more control efforts for achieving the same system performance.

5.6.2 Example 2

To further verify the proposed results, we consider a 2-D system and its parameters are given as follows: $A = \begin{bmatrix} 1 & 1 \\ 0 & 1 \end{bmatrix}$, $B = \begin{bmatrix} 1 \\ 1 \end{bmatrix}$, $D = \begin{bmatrix} 1 & 0 \\ 0 & 1 \end{bmatrix}$, $C = \begin{bmatrix} 1 & 1 \end{bmatrix}$, and $E = 1$. The disturbances are bounded as $\|\omega_k\|_\infty \leqslant 0.1$, and $\|v_k\|_\infty \leqslant 0.05$. The system state is bounded as $-50 \leqslant x_{k,1} \leqslant 3$ and $-50 \leqslant x_{k,2} \leqslant 3$, and the control input is bounded as $-3 \leqslant u_k \leqslant 3$. Note that the similar example has been used in [93, 125] for system without packet dropouts. The consecutive dropout length is $T_d = 2$. The observer gain L is designed as $L = \text{col}\{-1.08, -0.22\}$ according to Proposition 5.1, and the feedback control gain is $F = [-1, -1]$. The prediction horizon for the MPC is chosen as $N = 4$.

By executing Algorithm 2 using the MATLAB program, the simulation results are reported as follows. The control input is demonstrated in Figure 5.8; the estimate error trajectory and its convergence sets are depicted in Figure 5.9 and the state

trajectory and its convergence sets are shown in Figure 5.10. Figure 5.8 implies the designed algorithm is feasible. From Figure 5.9, we can see that the error trajectory periodically converges to three sets, which verifies the results in Lemma 5.1. Through Figure 5.10, it can be seen that the state trajectory also periodically converges to three sets as stated in Theorem 5.2. However, by inspecting Figure 5.9[1] and 5.10 [2], we observe that the error and state trajectories actually converges to smaller sets than the theoretical calculated sets, which means that the calculation of the theoretical sets may be a little conservative. Hence it deserves further research to calculate less conservative convergence sets.

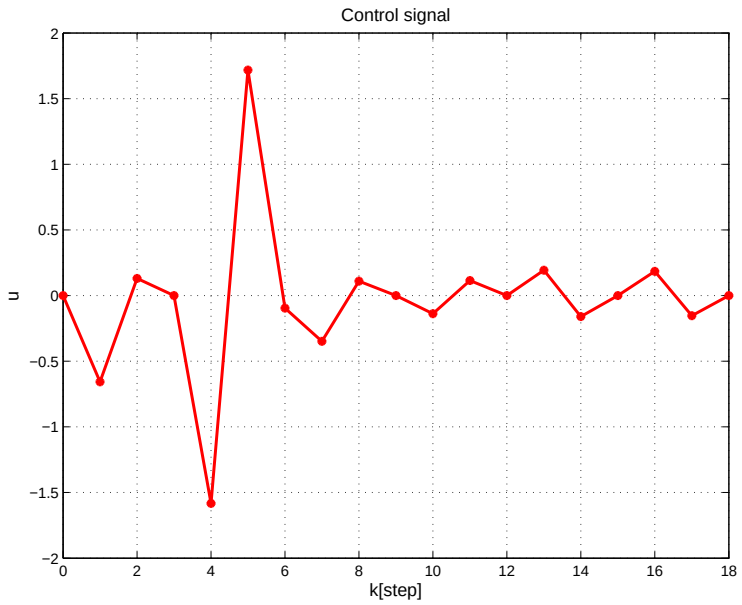

Figure 5.8: Control signal.

5.7 Conclusion

In this chapter, the robust output feedback MPC problem has been investigated for a class of networked constrained linear systems subject to periodical measurement packet dropouts and disturbances. A new design of the robust output feedback MPC

[1]The error trajectory sequence at $k = 3(n-1)+1$ converges to the set $E(1)$; the error trajectory sequence at $k = 3(n-1)+2$ converges to the set $E(2)$; the error trajectory sequence at $k = 3(n-1)+3$ converges to the set $E(3)$, $n = 1, 2, \cdots$.

[2]The state trajectory sequence at k = 3(n-1)+1 converges to the set $X(1)$; the state trajectory sequence at $k = 3(n-1)+2$ converges to the set $X(2)$; the state trajectory sequence at $k = 3(n-1)+3$ converges to the set $X(3)$, $n = 1, 2, \cdots$.

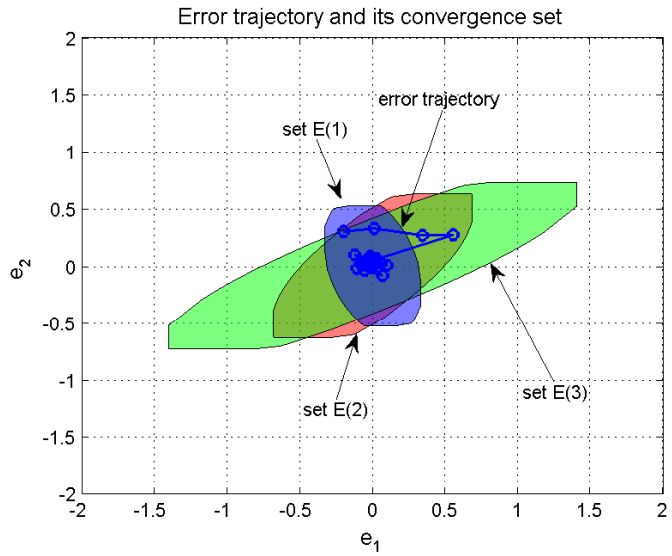

Figure 5.9: Error trajectory and its convergence sets.

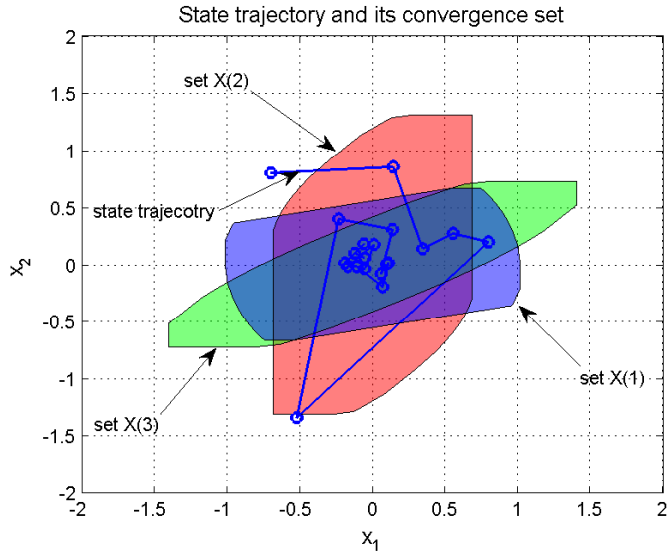

Figure 5.10: State trajectory and its convergence sets.

that simultaneously considers the following aspects has been designed: 1) the state and input constraints, 2) the bounded external disturbances, and 3) the periodical packet dropouts. In particular, the networked observer subject to the packet dropouts has first been designed and the bounds of estimation errors have been established; the networked robust output feedback MPC algorithm has been proposed by using the tightened technique. It has been shown that the proposed robust output feedback

MPC algorithm is feasible and that the closed-loop system state asymptotically and periodically converges to some compact sets.

Chapter 6

Robust Distributed MPC of Large-scale Nonlinear Systems

6.1 Introduction

6.1.1 Background and Motivation

In **Chapter3, 4 and 5**, the MPC problems are studied for single nonlinear systems with communication networks. With the development of the network technologies and the advancement of modern industrial systems, the control of large-scale and complex systems is an urgent demand. As one emerging research direction of MPC, the MPC-based control problem of large-scale systems or multi-agent systems has been spurring increasing interest recently. There are two traditional schemes of the MPC design of large-scale systems. One approach is the centralized MPC scheme[156, 50]. It aims to control the entire large-scale system by using only one central controller. The centralized design is capable of achieving desired control performance provided that the controller has enough computing power as theoretically desired. However, such a computational requirement cannot be met in most of practical applications, especially when the number of subsystems is very large.

On the contrary, there is another approach called the decentralized MPC scheme [127, 124] that features the computational efficiency. It decouples the large-scale system into subsystems (agents) by ignoring interactions, and then assigns an independent controller to each subsystem. The ignorance of coupled effects among subsystems may result in unsatisfactory control performance or even destroy the stability.

To overcome the drawbacks of the centralized MPC and the decentralized MPC,

increasing attention has been devoted to investigating the distributed MPC. With the similar controller structure as the decentralized MPC, the distributed MPC assigns each subsystem a controller, but the interactions among coupled subsystems are incorporated into each controller design based on the communication links among these subsystems. As a result, the distributed MPC could achieve comparable control performance as the centralized scheme, yet with less computational complexity, thanks to the decentralized structure.

In the literature on distributed MPC, some promising results have been reported for large-scale linear systems, nonlinear systems, and their applications.

- **Distributed MPC for large-scale linear systems.** In [57, 7, 99], the distributed MPC problem is studied for unconstrained coupled linear subsystems, where the coupled terms are treated as bounded disturbances. In [145], a nonconvex optimizer is proposed to design the distributed MPC for unconstrained linear dynamics. The authors in [88] tackle the distributed MPC problem for constrained linear subsystems based on the cooperative game theory.

- **Distributed MPC for large-scale nonlinear systems.** The researchers develop a distributed MPC strategy to handle continuous-time decoupled nonlinear subsystems with coupled objective functions in [23]. Further, the discrete-time case is discussed in [61]. Furthermore, the author in [21] extends the results in [23] for coupled nonlinear subsystems using the consistency constraint. By considering the coupled term as a bounded disturbance, the authors in [31] study the distributed MPC problem for discrete-time decoupled nonlinear agent systems with delayed information exchange. The work in [146] generalizes the result in [145] for the nonlinear counterpart. In addition, some practical designs are also researched. For instance, a terminal penalty distributed MPC [150] is designed for the power system automatic generation control. In [22], the distributed MPC problem is investigated for a vehicle platoon. Note that these aforementioned results are developed under the assumption that the exact system models are available.

In practice, however, the system model is inevitably subject to disturbances. Therefore, it is of paramount importance to investigate the robust MPC design considering external disturbances. Yet, few results have been reported for robust distributed MPC. In [130], the robust distributed MPC problem is investigated for decoupled linear subsystems subject to external disturbances and coupled input constraints. In

[83], the robust distributed MPC is designed for a class of nonlinear systems with two coupled inputs and disturbances, based on the existence of the control Lyapunov function. Furthermore, the authors in [81] propose a sequential distributed MPC to extend the result in [83], and they further develop an iterative distributed MPC framework for affine nonlinear systems subject to communication constraints in [82].

6.1.2 Main Contribution

To explicitly deal with external disturbances, this chapter focuses on the robust distributed MPC design for *general continuous-time decoupled nonlinear subsystems* subject to external disturbances and control input constraints. The coupling among subsystems is raised by the collective control objective.

It has been pointed out in [39] that, the conventional MPC may not be robust against external disturbances, and the closed-loop system might be destabilized even for small perturbations. In order to design a distributed MPC framework which will be robust against the external disturbances, a novel strategy called *robustness constraint* has been proposed in this study. The main contributions of this chapter are mainly three-fold.

(1) A novel robust distributed MPC algorithm has been developed for the decoupled nonlinear subsystems subject to external disturbances and control input constraints. The novelty lies in that the robustness constraint which contains the conventional terminal constraint is designed in the robust distributed MPC. Due to the robustness constraint, the robust distributed MPC algorithm is capable of handling the bounded external disturbances and stabilizing the overall large-scale system.

(2) The feasibility of the robust distributed MPC algorithm has been rigorously analyzed. By iteratively ensuring the control input constraint and the robustness constraint in the each optimization problem for the corresponding subsystem, the feasibility of the robust distributed MPC algorithm is proven. It is shown that, the conditions of ensuring the feasibility explicitly depend on the bound of external disturbances and the sampling period.

(3) The robust stability conditions have been established for the overall large-scale system. Based on Lyapunov theory, it is shown that, the stability conditions of the overall large-scale system is related to the bound of external disturbances,

the sampling period and the cooperation weights. The bounds of these three factors for guaranteeing the robust stability are developed. The overall large-scale system is proven to converge to an invariant set under the established conditions.

6.1.3 Organization and Notations

The rest of this chapter is organized as follows: The formulation of the robust distributed MPC scheme is presented in Section 6.2. The constrained optimization problem and the robust distributed MPC are proposed in Section 6.3. In Section 6.4, the feasibility of the robust distributed MPC is analyzed and the conditions for guaranteeing the feasibility are established. The stability analysis is reported in Section 6.5. The simulation studies are provided in Section 6.6. Finally, the conclusions are summarized in Section 6.7.

The notations used in this chapter are fairly standard. The superscripts "T" and "-1" represent the matrix transposition and the matrix inverse, respectively. The symbol $\mathbb{R}$ represents the real space. Given a column vector x and a matrix P with appropriate dimensions, denote $\|x\|$ as the Euclidean norm of x and $\|x\|_P \triangleq \sqrt{x^{\mathrm{T}}Px}$ as the P-weighted norm of x, respectively. For a given matrix Q, $Q > 0$ ($Q \geqslant 0$) means that the matrix Q is positive definite (semi-positive definite); the eigenvalue of matrix Q is denoted as $\lambda(Q)$; the maximum eigenvalue of matrix Q is denoted as $\bar{\lambda}(Q)$ and the minimum one is denoted as $\underline{\lambda}(Q)$. The notation $\mathrm{col}\{x_1, x_2, \cdots, x_n\}$ stands for the column operation as $[x_1^{\mathrm{T}}, x_2^{\mathrm{T}}, \cdots, x_n^{\mathrm{T}}]^{\mathrm{T}}$ for column vectors $x_1, x_2, \cdots, x_n$. Given two sets $A \subseteq B \subseteq \mathbb{R}^n$, the difference between the two sets is defined as $A \setminus B \triangleq \{x | x \in A, x \notin B\}$.

6.2 Problem Formulation

Consider a large-scale dynamical nonlinear system consisting of M agents denoted as $\{\mathcal{A}_i, i = 1, 2, \cdots, M\}$. The model of each agent $\mathcal{A}_i$ is described as:

$$\dot{x}_i(t) = f_i(x_i(t), u_i(t)) + \omega_i(t), \quad t \geqslant 0, x_i(0) = x_i^0,$$

where $x_i(t) \in \mathbb{R}^n$ is the system state of agent $\mathcal{A}_i$, $u_i(t) \in \mathbb{R}^m$ is the control input and $\omega_i(t) \in \mathbb{R}^n$ is the external disturbance. Here, the control input $u_i(t)$ is constrained by

the following compact set

$$u_i(t) \in \mathcal{U}_i \subseteq \mathbb{R}^m, \quad t \geqslant 0$$

with $\{0\} \in \mathcal{U}_i$. The external disturbance is assumed to be bounded in a compact set $\mathcal{W}_i \subset \mathcal{R}^n$ and the bound is defined as $\rho_i \triangleq \sup_{\omega_i(t)\in\mathcal{W}_i} \|\omega_i(t)\|$.

The communication topology of the multi-agent system is characterized as a weighted directed graph $\mathcal{G} \triangleq \{\mathcal{A}, \mathcal{E}, \mathcal{R}\}$, where $\mathcal{A} = \{\mathcal{A}_i, i = 1, 2, \cdots, M\}$ represents all the nodes (agents), $\mathcal{E} \subset \mathcal{A} \times \mathcal{A}$ is the collection of all directed edges between two connected agents, and $\mathcal{R} = \{r_{ij}\}$ is the weighted matrix characterizing the cooperation weights between two connections, where $i = 1, \cdots, M$ and $j = 1, \cdots, M$. For each agent $\mathcal{A}_i$, its neighbors are defined as the agents from which it can receive information, and the indices of its neighbors are denoted as $\mathcal{N}_i$. In $\mathcal{R}$, $r_{ij} > 0$ if $j \in \mathcal{N}_i$; otherwise $r_{ij} = 0$. To focus on the design of robust distributed MPC strategy, it is assumed that the graph $\mathcal{G}$ is fixed and connected, and hence, each agent has at least one neighbor; a similar assumption has also been made in [23, 21, 31].

For the M-agent system, the state vector of the overall system is denoted by $x(t) = \text{col}\{x_1(t),\, x_2(t), \cdots, x_M(t)\}$ and the state vector of all the neighbors of agent $\mathcal{A}_i$ is denoted by $x_{-i}(t) = \text{col}\{x_{j_1}(t), x_{j_2}(t), \cdots\}$, for all $j_k \in \mathcal{N}_i$. Similarly, the overall control input is characterized as $u(t) = \text{col}\{u_1(t),\, u_2(t), \cdots, u_M(t)\}$ and the control input constraint $\mathcal{U}$ is the Cartesian product $\mathcal{U}_1 \times \cdots \times \mathcal{U}_M$. The disturbance of the overall system is denoted by $\omega(t) = \text{col}\{\omega_1(t), \omega_2(t), \cdots, \omega_M(t)\}$ and the bound of the disturbance set $\mathcal{W}$ is the Cartesian product $\mathcal{W}_1 \times \cdots \times \mathcal{W}_M$. Based on the notations above, the overall nonlinear system can be described as

$$\dot{x}(t) = f(x(t), u(t)) + \omega(t), x(0) = x_0, \quad t \geqslant 0, \tag{6.1}$$

where $f(x(t), u(t)) = \text{col}\{\ f_1(x_1(t), u_1(t)),\ \cdots,\ f_M(x_M(t), u_M(t))\}$ and $x_0 = \text{col}\{\ x_1^0,\ \cdots,\ x_M^0\}$. The nominal system can be represented as

$$\dot{\bar{x}}(t) = f(\bar{x}(t), u(t)), \quad t \geqslant 0.$$

For the system in (6.1), the following standard assumption is made [11, 23, 21]:

Assumption 6.1. *(a) The function $f : \mathbb{R}^{nM} \times \mathbb{R}^{mM} \to \mathbb{R}^{nM}$ has continuous second derivative and satisfies $f(0, 0) = 0$; (b) the system has a unique, absolutely continuous solution for any initial condition x_0, any piecewise right-continuous control $u : [0, \infty) \to \mathcal{U}$, and any disturbance realization $\omega : [0, \infty] \to \mathcal{W}$.*

The described multi-agent nonlinear system model under study (with the corresponding communication topology) can be used to characterize many practical systems such as team-vehicle systems [31], a group of robots [23, 62], and large-scale chemical processes[127]. For these systems, based on the communication topology, it is of great practical interest to investigate how to design the control and fulfill prescribed cooperative tasks while preserving the optimal performance. The following control objective function has been widely adopted [31, 23, 130]

$$\begin{aligned} J(\hat{x}(s;t_k),\hat{u}(s;t_k)) = &\int_{t_k}^{t_k+T} \|\hat{x}(s;t_k)\|_Q^2 + \|\hat{u}(s;t_k)\|_R^2 \\ &+ \sum_{i=0}^{M}\sum_{j\in\mathcal{N}_i} r_{ij}\|\hat{x}_i(s;t_k)-\hat{x}_j(s;t_k)\|_{Q_{ij}}^2 ds + \|\hat{x}(t_k+T;t_k)\|_P^2, \end{aligned}$$

where $\hat{x}(t_k;t_k) = x(t_k)$, t_k with $k = 0, 1, \cdots$, is the sampling time instant, T is the prediction horizon, $\hat{x}(s;t_k)$, $t_k \leqslant s \leqslant t_k + T$, stands for the predicted nominal system trajectory from time t_k to $t_k + T$, $\hat{u}(s;t_k)$, $t_k \leqslant s \leqslant t_k + T$, represents the predicted control trajectory from t_k to $t_k + T$, $Q = \text{diag}(Q_1, \cdots, Q_M)$ with $Q_i > 0$, $R = \text{diag}(R_1, \cdots, R_M)$ with $R_i > 0$ and $P = \text{diag}(P_1, \cdots, P_M)$ with $P_i > 0$, $i = 1, 2, \cdots, M$.

The robust centralized cooperative MPC strategy at every sampling time t_k can be designed by solving the following constrained optimization problem:

Problem 6.1.

$$\begin{aligned} \hat{u}^*(s;t_k) = &\arg\min_{\hat{u}(s;t_k)} J(\hat{x}(s;t_k),\hat{u}(s;t_k)), \textit{ subject to:} \\ &\hat{u}(s;t_k) \in \mathcal{U}, t_k \leqslant s \leqslant t_k + T, \\ &\dot{\hat{x}}(s;t_k) = f(\hat{x}(s;t_k),\hat{u}(s;t_k)), t_k \leqslant s \leqslant t_k + T \\ &\hat{x}(t_k+T;t_k) \in \Omega, \end{aligned}$$

where Ω is the terminal set and $\hat{x}(t_k;t_k) = x(t_k)$.

The centralized cooperative MPC strategy suffers the computational complexity, whereas the decentralized MPC may result in poor control performance. The distributed MPC strategy, capable of improving both issues as mention above, is adopted in this study. Some promising distributed MPC methods have been proposed in [23, 21, 61, 31] for nonlinear systems; however, they do not consider the

external disturbances. Motivated by this fact, in this work, we aim to design a new *robust distributed MPC* strategy to stabilize the M-agent system with subsystems being subject to bounded external disturbances.

In general, the design of conventional or distributed MPC schemes needs a local state feedback law within the terminal set [95, 21]. To describe such a state feedback law, consider the linearized system of each agent $\mathcal{A}_i$ at origin, which can be derived as $\dot{x}_i(t) = A_i x(t) + B_i u_i(t) + \omega_i(t)$, where $A_i = \partial f_i/\partial x(0,0)$, $B = \partial f_i/\partial u(0,0)$. The nominal linearized system is

$$\dot{\bar{x}}_i(t) = A_i \bar{x}(t) + B_i u_i(t). \tag{6.2}$$

Like the conventional MPC [95, 11] and the nominal distributed MPC in [23, 61], this study uses the similar assumption for the nominal linearized systems.

Assumption 6.2. *For the linearized system in (6.2) of every agent $\mathcal{A}_i$, there exists a state feedback control law $u_i(t) = K_i x_i(t)$, such that the closed-loop system is stable, i.e., $A_i^c \triangleq A_i + B_i K_i$ is stable.*

6.3 Robust Distributed MPC

In this section, we first present the setup of the robust distributed MPC. Further, a new constrained optimization problem associated with each agent is formulated, and a novel robust distributed MPC algorithm is proposed.

6.3.1 Setup of Robust Distributed MPC

For the overall system, it is assumed that each agent has the same sampling period δ, and the synchronization is ensured, i.e., every agent is able to measure the system state of itself, receive information from its neighbors and apply the control signal at the same time instants t_k, $k = 0, 1, \cdots$, where $t_{k+1} = t_k + \delta$. Furthermore, every agent communicates with its neighbors and exchanges necessary information according to the communication topology through reliable communication links (i.e., no data losses or delays).

To calculate the centralized control objective function $J(\hat{x}(s;t_k), \hat{u}(s;t_k))$ by using a distributed manner, we consider the following control objective function of each

agent $\mathcal{A}_i$, $i = 1, \cdots, M$:

$$J_i^c(\hat{x}_i(s;t_k), \hat{u}_i(s;t_k), \hat{x}_{-i}(s;t_k)) = \int_{t_k}^{t_k+T} \|\hat{x}_i(s;t_k)\|_{Q_i}^2 + \|\hat{u}_i(s;t_k)\|_{R_i}^2 + \sum_{j\in\mathcal{N}_i} r_{ij}\|\hat{x}_i(s;t_k) - \hat{x}_j(s;t_k)\|_{Q_{ij}}^2 ds + \|\hat{x}_i(t_k+T;t_k)\|_{P_i}^2,$$

where T is the control horizon with $T \geqslant \delta$, $\hat{u}_i(s;t_k)$ is the control trajectory to be optimized; $\hat{x}_i(s;t_k)$ is the predicted nominal state trajectory of agent $\mathcal{A}_i$, and can be generated by the nominal model

$$\dot{\hat{x}}_i(s;t_k) = f_i(\hat{x}_i(s;t_k), \hat{u}_i(s;t_k)), \quad \hat{x}_i(t_k;t_k) = x_i(t_k),$$

and $\hat{x}_i(t_k+T;t_k)$ is the terminal nominal state of agent $\mathcal{A}_i$. However, in practice, the predicted nominal state trajectories of the neighbors, i.e., $\hat{x}_j(s;t_k)$, $s \in [t_k, t_k+T]$ are not available for the agent $\mathcal{A}_i$ at time t_k. To circumvent this problem, an alternative control objective function is proposed for each agent $\mathcal{A}_i$ as:

$$J_i(\hat{x}_i(s;t_k), \hat{u}_i(s;t_k), \hat{x}_{-i}^a(s;t_k)) = \int_{t_k}^{t_k+T} \|\hat{x}_i(s;t_k)\|_{Q_i}^2 + \|\hat{u}_i(s;t_k)\|_{R_i}^2 + \sum_{j\in\mathcal{N}_i} r_{ij}\|\hat{x}_i(s;t_k) - \hat{x}_j^a(s;t_k)\|_{Q_{ij}}^2 ds + \|\hat{x}_i(t_k+T;t_k)\|_{P_i}^2,$$

where $\hat{x}_j^a(s;t_k)$, $j \in \mathcal{N}_i$ is the assumed state trajectory for the neighbor j of agent $\mathcal{A}_i$ which evolves according to the following differential equation:

$$\dot{\hat{x}}_j^a(s;t_k) = f_j(\hat{x}_j^a(s;t_k), \hat{u}_j^a(s;t_k)), \hat{x}_j^a(t_k;t_k) = \hat{x}_j^*(t_k;t_{k-1}).$$

Here, $\hat{x}_j^*(s;t_k)$ denotes the optimal predicted nominal state trajectory and $\hat{u}_j^a(s;t_k)$ is the assumed control trajectory, which will be elaborated in **Problem 6.2** in this section. The similar control objective function has been adopted in [31, 23, 21, 61] for nonlinear multi-agent systems *without* incorporating the effect from external disturbances.

Before proceeding to the design of the constrained optimization problem, we need to design the terminal set which will play an instrumental role in analyzing the feasibility, stability and robustness of the MPC algorithm. The main idea of determining the terminal set has been reported in [97, 11]. By considering the nominal system of

each agent $\mathcal{A}_i$, $i = 1, \cdots, M$:

$$\dot{\bar{x}}_i(t) = f_i(\bar{x}_i(t), u_i(t)), \quad \text{subject to:} \quad u_i(t) \in \mathcal{U}_i, t \geqslant 0, \tag{6.3}$$

we have the following Lemma 6.1.

Lemma 6.1. *Suppose that Assumption 6.2 holds for each agent $\mathcal{A}_i$. For the system in (6.3), there exist a constant $\varepsilon_i > 0$ and a matrix $P_i > 0$, such that: (1) The set $\Omega_i(\varepsilon_i) \triangleq \{\bar{x}_i(t) : V_i(\bar{x}_i(t)) \leqslant \varepsilon_i^2\}$ is a control invariant set with the control law $u_i(t) = K_i\bar{x}_i(t)$, i.e., any initial state $\bar{x}_i(0) \in \Omega_i(\varepsilon_i)$ implies $\bar{x}_i(t) \in \Omega_i(\varepsilon_i)$, and $u_i(t) = K_i\bar{x}_i(t) \in \mathcal{U}_i$, $\forall t \geqslant 0$; (2) for any $\bar{x}_i(t) \in \Omega_i(\varepsilon_i)$, the inequality $\dot{V}_i(\bar{x}_i(t)) \leqslant -\|\bar{x}_i(t)\|^2_{Q_i^*}$ holds, where $V_i(\bar{x}_i(t)) = \|\bar{x}_i(t)\|^2_{P_i}$, K_i is a state feedback control gain satisfying Assumption 6.2 and $Q_i^* = Q_i + K_i^{\mathrm{T}} R_i K_i$.*

Proof. The proof can be derived by following the similar lines as in [97, 11, 21]. Thus, it is omitted here. □

6.3.2 Robust Distributed MPC Algorithm

For the distributed setup, a new constrained optimization problem associated with each agent $\mathcal{A}_i$ is designed as follows.

Problem 6.2.

$$\begin{aligned}
\hat{u}_i^*(s; t_k) = &\arg \min_{\hat{u}_i(t;t_k)} J_i(\hat{x}_i(s; t_k), \hat{u}_i(s; t_k), \hat{x}^a_{-i}(s; t_k)), \textit{subject to:} \\
&\dot{\hat{x}}_i(s; t_k) = f_i(\hat{x}_i(s; t_k), \hat{u}_i(s; t_k)), s \in [t_k, t_k + T] \\
&\dot{\hat{x}}^a_j(s; t_k) = f_j(\hat{x}^a_j(s; t_k), \hat{u}^a_j(s; t_k)), s \in [t_k, t_k + T] \\
&\hat{u}_i(s; t_k) \in \mathcal{U}_i, s \in [t_k, t_k + T] \\
&\|\hat{x}_i(s; t_k)\|_{P_i} \leqslant \frac{T\alpha_i}{s - t_k}\varepsilon_i, s \in [t_k + \delta, t_k + T],
\end{aligned} \tag{6.4}$$

where $j \in \mathcal{N}_i$, $\alpha_i \in (0, 1)$ is a design parameter, ε_i is the constant determined in Lemma 6.1, $\hat{x}_i(t_k; t_k) = x_i(t_k)$, and $\hat{x}^a_j(t_k; t_k) = \hat{x}^*_j(t_k; t_{k-1})$. The assumed state trajectory for the neighbor j of agent $\mathcal{A}_i$ is generated using the following mechanism:

$$\hat{u}^a_j(s; t_k) = \begin{cases} \hat{u}^*_j(s; t_{k-1}), & \textit{if} \quad s \in [t_k, t_{k-1} + T] \\ K_j\hat{x}^a_j(s; t_k), & \textit{if} \quad s \in [t_{k-1} + T, t_k + T]. \end{cases} \tag{6.5}$$

Remark 6.1. *The novelty of* **Problem 6.2** *lies in the* robustness constraint *in (6.4), compared to the optimization problems in the existing distributed MPC schemes [23, 21, 61]. The roles of the robustness constraint in (6.4) are two-fold: (1) It serves as the terminal constraint as in the conventional MPCs and the distributed MPCs when* $s = t_k + T$*, i.e.,* $\hat{x}_i(t_k + T; t_k) \in \Omega_i(\alpha_i \varepsilon_i)$*, which is central to analyze the stability of the overall system; (2) it provides a monotonically decreasing boundary to confine the predicted nominal state trajectory during* $[t_k + \delta, t_k + T]$*. This generates a control signal providing robustness for the distributed MPC.*

With the aid of **Problem 6.2**, the implementation of the distributed controller associated with each agent $\mathcal{A}_i$ can be briefly described as follows. At time t_k, the controller of each agent ($\mathcal{A}_i$) samples the state $x_i(t_k)$ and receives the assumed state trajectories from its neighbors via the communication links. Then the controller solves **Problem 6.2** to generate $\hat{u}^*(s; t_k)$ for $s \in [t_k, t_k + T]$. Also, it generates the assumed state trajectory $\hat{x}_i^a(s; t_{k+1})$ for next optimization horizon from t_{k+1} to $t_{k+1} + T$ and sends the result to its neighbors.

It is observed from Lemma 6.1 that, if the state of the agent $\mathcal{A}_i$ enters the terminal set $\Omega_i(\varepsilon_i)$, the state feedback control law $u_i(t) = K_i x_i(t)$ can stabilize the nominal system and guarantee robustness for the actual system. To make use of this property and to reduce the computational complexity, we propose to apply the switched control strategy, which is also called dual-mode MPC strategy [97, 95, 21]. That is, for each agent $\mathcal{A}_i$, when the system state is outside the terminal set $\Omega_i(\varepsilon_i)$, the control input signal is applied according to the solution of **Problem 6.2**; when the system state enters the terminal set $\Omega_i(\varepsilon_i)$, the stabilizing state feedback law $u_i(t) = K_i x_i(t)$ is then applied. When considering the existence of external disturbances, it is worthwhile to mention that the actual system state $x_i(s; t_k)$, $s \in (t_k, t_k + \delta)$ is not available during the sampling period. So we use $\hat{x}_i^*(s; t_k)$ to determine whether the actual system state is in the terminal set $\Omega_i(\varepsilon_i)$ or not. Before establishing the testing criterion, we make the following assumption.

Assumption 6.3. *[21] For each agent* $\mathcal{A}_i$*, the system dynamics satisfies the following condition:*

$$\|f_i(x_1, u) - f_i(x_2, u)\|_{P_i} \leqslant L_i \|x_1 - x_2\|_{P_i}, \tag{6.6}$$

where L_i *is a constant.*

By using Assumption 6.3, the following claim can be used as a criterion to test the actual system state.

Claim 6.1. *For each agent $\mathcal{A}_i$, suppose that Assumption 6.3 holds. For any $s \in [t_k, t_k + T]$, if*

$$\|\hat{x}_i^*(s;t_k)\|_{P_i} \leqslant \varepsilon_i - \underline{\lambda}(P_i^{\frac{1}{2}})\rho_i(s-t_k)e^{l_i(s-t_k)}, \tag{6.7}$$

then $x_i(s;t_k) \in \Omega_i(\varepsilon_i)$.

The proof of Claim 6.1 can be derived by applying Lemma 6.2 in the next section. According to Claim 6.1, the control input and assumed control trajectory for each agent $\mathcal{A}_i$ are determined as follows: If $\|\hat{x}_i^*(s;t_k)\|_{P_i} > \varepsilon_i - \underline{\lambda}(P_i^{\frac{1}{2}})\rho_i(s-t_k)e^{l_i(s-t_k)}$, for any $s \in [t_k, t_k + \delta]$, then take the control input as $u_i(s;t_k) = \hat{u}_i^*(s;t_k)$ and generate the assumed control trajectory $\hat{u}_j^a(s;t_{k+1})$ as in (6.5). Otherwise determine the first time instant $t_i^o \in [t_k, t_k + \delta]$ such that

$$\|\hat{x}_i^*(t_i^o;t_k)\|_{P_i} \leqslant \varepsilon_i - \underline{\lambda}(P_i^{\frac{1}{2}})\rho_i(t_i^o-t_k)e^{l_i(t_i^o-t_k)},$$

then take

$$u_i(s;t_k) = \begin{cases} \hat{u}_i^*(s;t_k), & \text{for} \quad s \in [t_k, t_i^o], \\ K_i\bar{x}_i^k(s;t_k), & \text{for} \quad s \in [t_i^o, t_k + \delta], \end{cases} \tag{6.8}$$

and design the assumed control trajectory as:

$$\hat{u}_i^a(s;t_{k+1}) = K_i\bar{x}_i^k(s;t_k), \quad s \in [t_{k+1}, t_{k+1} + T], \tag{6.9}$$

where $\bar{x}_i^k(s;t_k)$, $s \in [t_i^o, t_{k+1}+T]$, is determined by the differential equation $\dot{\bar{x}}_i^k(s;t_k) = f_i(\bar{x}_i^k(s;t_k), K_i\bar{x}_i^k(s;t_k))$, with initial state $\bar{x}_i^k(t_i^o;t_k) = \hat{x}_i^*(t_i^o;t_k)$. In this case, the assumed state trajectory will be $\hat{x}_i^a(s;t_{k+1}) = \bar{x}_i^k(s;t_k)$, $s \in [t_{k+1}, t_{k+1} + T]$.

By integrating **Problem 6.2** *with the dual-mode mechanism and the state testing criterion, we propose the robust distributed MPC algorithm. In this study, we refer the novel control strategy as* robust dual-mode distributed MPC *which is detailed in* **Algorithm 4**.

6.4 Feasibility Analysis

In this section, the feasibility of the robust dual-mode distributed MPC algorithm is analyzed and the conditions of ensuring the feasibility are established. The main tools employed to prove the feasibility are the triangle inequality and the Gronwall-Bellman inequality. The sketch of proving the feasibility is as follows: The iterative

Algorithm 4 Robust dual-mode distributed MPC

Require: Sampling period δ; control horizon T; initial state x_i^0; bound of disturbance ρ_i; assumed state trajectories of neighbors $x_j^0(t)$, $t \in [0, T]$, $j \in \mathcal{N}_i$; constant ε_i; parameter $\alpha_i \in (0, 1)$; index $k = 0$.

Ensure: $x_i(t_0) = x_i^0$ and $\hat{x}_j^a(s; t_0) = x_j^0$, $s \in [0, T]$.

1: **while** The accuracy is not satisfactory **do**
2: Sample system state $x(t_k)$;
3: Receive neighbors' assumed state trajectories $\hat{x}_j^a(s; t_k)$, $j \in \mathcal{N}_i$, $s \in [t_k, t_k + T]$
4: Solve Problem 6.2 to generate $\hat{u}_i^*(s; t_k)$ and $\hat{x}_i^*(s; t_k)$, $s \in [t_k, t_k + T]$,
5: **if** (6.7) holds **then**
6: Generate the control input $u(s; t_k)$, $s \in [t_k, t_k + \delta]$ as (6.8);
7: Design the assumed control input $\hat{u}_i^a(s; t_{k+1})$, $s \in [t_{k+1}, t_{k+1} + T]$ as (6.9);
8: **else**
9: Generate the control input as $u_i(s; t_k) = \hat{u}_i^*(s; t_k)$, $s \in [t_k, t_k + \delta]$;
10: Design the assumed control input $\hat{u}_i^a(s; t_{k+1})$, $s \in [t_{k+1}, t_{k+1}+T]$ as in (6.5);
11: **end if**
12: Generate the assumed state trajectory $\hat{x}_i^a(s; t_{k+1})$, $s \in [t_{k+1}, t_{k+1} + T]$.
13: Send the assumed state trajectory to its neighbors;
14: Apply the control input $u_i(s; t_k)$, $s \in [t_k, t_k + \delta]$;
15: $k = k + 1$.
16: **end while**

feasibility for the overall agent system will be proven by the iterative feasibility of **Problem 6.2** *for each agent, which will be achieved by following two steps. Firstly, the condition is established to guarantee the terminal constraint satisfaction (as a part of the robustness constraint). Secondly, the control input constraint and the robustness constraint are proven to be satisfied under appropriate conditions.*

6.4.1 Initial Feasibility and Feasible Control Candidate

In order to prove the iterative feasibility by the induction principle, **Problem 6.2** *needs to be feasible at the initial time instant t_0 (i.e., there exists a control trajectory driving the initial state into the terminal set while satisfying all the constraints). This requirement can be fulfilled by choosing an appropriate prediction horizon (T). Like the conventional MPC [97] and nominal distributed MPC [21], the following assumption is made with regard to the prediction horizon.*

Assumption 6.4. *For the overall agent system $\{\mathcal{A}_i,\ i = 1, \cdots, M\}$, at time $t_0 = 0$, with the initial state x_0, assume that there exists a prediction horizon $T > 0$ such that* **Problem 6.2** *associated with each agent $\mathcal{A}_i$ has a solution.*

Similar to the conventional MPC, for each agent $\mathcal{A}_i$ with a given prediction horizon T, all the initial state x_i^0 for which **Problem 6.2** *has a solution, is called the feasible set. For each agent $\mathcal{A}_i$, the feasible set is denoted as $\mathcal{Z}_i$.*

By following the line of the induction principle, for each agent $\mathcal{A}_i$, if **Problem 6.2** *is feasible at time t_k, then it is needed to find a feasible control trajectory at time t_{k+1}. This will be achieved by first constructing an appropriate control trajectory candidate which should be then proven a qualified feasible control trajectory. The feasible control trajectory candidate $\tilde{u}_i(s;t_{k+1})$ at time t_{k+1} is constructed as follows:*

$$\tilde{u}_i(s;t_{k+1}) = \begin{cases} \hat{u}_i^*(s;t_k), & \text{if} \quad s \in [t_{k+1}, t_k + T], \\ K_i\tilde{x}_i(s;t_{k+1}), & \text{if} \quad s \in [t_k + T, t_{k+1} + T]. \end{cases}$$

And the feasible state trajectory candidate will be generated as:

$$\dot{\tilde{x}}_i(s;t_{k+1}) = f_i(\tilde{x}_i(s;t_{k+1}), \tilde{u}_i(s;t_{k+1})), s \in [t_{k+1}, t_{k+1} + T],$$

where the initial state is given by $\tilde{x}_i(t_{k+1};t_{k+1}) = x_i(t_{k+1})$. The method of generating the feasible control trajectory candidate is similar as [97] for conventional MPC and as [23, 21] for nominal distributed MPC. However, when considering the effect of external disturbances, the generated state trajectory candidate will not be matched to the predicted system trajectory. And therefore, the feasibility analysis will be different and more challenging compared to [23, 61]. In the sequel, we shall develop conditions under which the feasible control trajectory candidate at time t_{k+1} is indeed a feasible solution to **Problem 6.2**.

6.4.2 Feasibility of the Terminal Constraint

In order to establish the feasibility of the terminal constraint, a lemma, characterizing the deviation between the actual state trajectory $x_i(s;t_k)$ and the predicted nominal state trajectory $\hat{x}_i(s;t_k)$, is first presented.

Lemma 6.2. *Suppose that Assumption 6.3 holds, then for each agent $\mathcal{A}_i$, the actual state trajectory and the predicted nominal one satisfy the following:*

$$\|x_i(s;t_k) - \hat{x}_i^*(s;t_k)\|_{P_i} \leqslant \bar{\lambda}(P_i^{\frac{1}{2}})\rho_i(s - t_k)e^{L_i(s-t_k)}, s \in [t_k, t_k + T]. \tag{6.10}$$

Proof. Consider the P_i-weighted norm of $x_i(s;t_k) - \hat{x}_i^*(s;t_k)$, $s \in [t_k, t_k + T]$ as

$$\begin{aligned}
&\|x_i(s;t_k) - \hat{x}_i^*(s;t_k)\|_{P_i} \\
=&\|x_i(t_k;t_k) + \int_{t_k}^{s} f_i(x_i(\tau;t_k), \hat{u}_i^*(\tau,t_k)) + \omega_i(\tau;t_k)\mathrm{d}\tau \\
&- \hat{x}_i^*(t_k;t_k) - \int_{t_k}^{s} f_i(\hat{x}_i^*(\tau;t_k), \hat{u}_i^*(\tau;t_k))\mathrm{d}\tau\|_{P_i} \\
\leqslant& \int_{t_k}^{s} \|\omega_i(\tau;t_k)\|_{P_i}\mathrm{d}\tau + \int_{t_k}^{s} \|f_i(x_i(\tau;t_k), \hat{u}_i^*(\tau,t_k)) - f_i(\hat{x}_i^*(\tau;t_k), \hat{u}_i^*(\tau;t_k))\|_{P_i}\mathrm{d}\tau,
\end{aligned}$$

where the triangle inequality is used in obtaining the last step. Applying (6.6) and considering the bound of the disturbance in the above inequality result in

$$\|x_i(s;t_k) - \hat{x}_i^*(s;t_k)\|_{P_i} \leqslant \rho_i(s - t_k)\bar{\lambda}(P_i^{\frac{1}{2}}) + L_i \int_{t_k}^{s} \|x_i(s;t_k) - \hat{x}_i^*(s;t_k)\|_{P_i}\mathrm{d}\tau.$$

By using Gronwall-Bellman inequality, we get (6.10). This completes the proof. □

Based on Lemma 6.2, the following Lemma 6.3 provides the conditions such that the terminal state of the feasible state trajectory candidate can satisfy the terminal constraint in (6.4), i.e., $\tilde{x}_i(t_{k+1} + T; t_{k+1}) \in \Omega(\alpha_i\varepsilon_i)$.

Lemma 6.3. *For each agent $\mathcal{A}_i$, suppose that: Assumption 6.1, 6.2, and 6.3 hold;* **Problem 6.2** *is feasible at time t_k; $\tilde{u}_i(s;t_{k+1})$ is applied at time t_{k+1}. Given the disturbance bound with $\rho_i \leqslant \rho_i^1$, if the sampling period satisfies*

$$-2\frac{\bar{\lambda}(P_i)}{\underline{\lambda}(Q_i^*)}\ln\alpha_i \leqslant \delta \leqslant \frac{(1-\alpha_i)\varepsilon_i}{\rho_i e^{L_i T}\bar{\lambda}(P_i^{\frac{1}{2}})}, \tag{6.11}$$

then the terminal state satisfies the terminal constraint as $\tilde{x}_i(t_{k+1}+T;t_{k+1}) \in \Omega(\alpha_i\varepsilon_i)$, where ρ_i^1 is defined as $\rho_i^1 \triangleq -\underline{\lambda}(Q_i^*)(1-\alpha_i)\varepsilon_i/[2\bar{\lambda}(P_i^{0.5})\bar{\lambda}(P_i)e^{L_i T}\ln\alpha_i]$.

Proof. By considering the deviation between $\hat{x}_i^*(s;t_k)$ and $\tilde{x}_i(s;t_{k+1})$ for $s \in [t_{k+1}, t_k +$

$T]$, we have

$$\begin{aligned}
&\|\tilde{x}_i(s;t_{k+1}) - \hat{x}_i^*(s;t_k)\|_{P_i} \\
=&\|x_i(t_{k+1};t_{k+1}) + \int_{t_{k+1}}^{s} f_i(\tilde{x}_i(\tau;t_{k+1}), \hat{u}_i^*(\tau;t_k))\mathrm{d}\tau \\
&- \hat{x}_i^*(t_{k+1};t_k) - \int_{t_{k+1}}^{s} f_i(\hat{x}_i^*(\tau;t_k), \hat{u}_i^*(s;t_k))\mathrm{d}\tau\|_{P_i} \\
\leqslant&\|x_i(t_{k+1}) - \hat{x}_i^*(t_{k+1};t_k)\|_{P_i} + L_i \int_{t_{k+1}}^{s} \|\tilde{x}_i(\tau;t_{k+1}) - \hat{x}_i^*(\tau;t_k)\|_{P_i}\mathrm{d}\tau,
\end{aligned}$$

where the triangle inequality and the inequality in (6.6) have been used. According to Lemma 6.2, we readily have $\|x_i(t_{k+1}) - \hat{x}_i^*(t_{k+1};t_k)\|_{P_i} \leqslant \bar{\lambda}(P_i^{\frac{1}{2}})\rho_i\delta e^{L_i\delta}$. Therefore, we get

$$\|\tilde{x}_i(s;t_{k+1}) - \hat{x}_i^*(s;t_k)\|_{P_i} \leqslant \bar{\lambda}(P_i^{\frac{1}{2}})\rho_i\delta e^{L_i\delta} + L_i \int_{t_{k+1}}^{s} \|\tilde{x}_i(\tau;t_{k+1}) - \hat{x}_i^*(\tau;t_k)\|_{P_i}\mathrm{d}\tau.$$

In light of Gronwall-Bellman inequality, we have the following

$$\|\tilde{x}_i(s;t_{k+1}) - \hat{x}_i^*(s;t_k)\|_{P_i} \leqslant \bar{\lambda}(P_i^{\frac{1}{2}})\rho_i\delta e^{L_i\delta}e^{(L_i(s-t_{k+1}))}. \tag{6.12}$$

Plugging $s = t_k + T$ into (6.12) results in $\|\tilde{x}_i(t_k+T;t_{k+1}) - \hat{x}_i^*(t_k+T;t_k)\|_{P_i} \leqslant \bar{\lambda}(P_i^{\frac{1}{2}})\rho_i\delta e^{L_iT}$. By considering $\|\hat{x}_i^*(t_k+T;t_k)\|_{P_i} \leqslant \alpha_i\varepsilon_i$ and the constraint in (6.4), we get $\|\tilde{x}_i(t_k+T;t_{k+1})\|_{P_i} \leqslant \bar{\lambda}(P_i^{\frac{1}{2}})\rho_i\delta e^{L_iT} + \alpha_i\varepsilon_i$. Since $\delta \leqslant (1-\alpha_i)\varepsilon_i/(\rho_i e^{L_iT}\bar{\lambda}(P_i^{0.5}))$, we obtain the following

$$\|\tilde{x}_i(t_k+T;t_{k+1})\|_{P_i} \leqslant \varepsilon_i. \tag{6.13}$$

That is, $\tilde{x}_i(t_k+T;t_{k+1}) \in \Omega_i(\varepsilon_i)$. Note that the feasible state trajectory candidate is given by $\dot{\tilde{x}}_i(s;t_{k+1}) = f_i(\tilde{x}_i(s;t_{k+1}), K_i\tilde{x}_i(s;t_{k+1}))$, for $s \in [t_k+T, t_{k+1}+T]$. According to Lemma 6.1, the following holds: $\dot{V}_i(\tilde{x}_i(s;t_{k+1})) \leqslant -\|\tilde{x}_i(s;t_{k+1})\|_{Q_i^*}^2 \leqslant -\frac{\underline{\lambda}(Q_i^*)}{\bar{\lambda}(P_i)}V_i(\tilde{x}_i(s;t_{k+1}))$, where $s \in [t_k+T, t_{k+1}+T]$. By applying the comparison principle [64], we can derive

$$V_i(\tilde{x}_i(s;t_{k+1})) \leqslant V_i(\tilde{x}_i(t_k+T;t_{k+1}))e^{-\frac{\underline{\lambda}(Q_i^*)}{\bar{\lambda}(P_i)}(s-t_k-T)} \leqslant \varepsilon_i^2 e^{-\frac{\underline{\lambda}(Q_i^*)}{\bar{\lambda}(P_i)}(s-t_k-T)}. \tag{6.14}$$

Since $\delta \geqslant -2\bar{\lambda}(P_i)/\underline{\lambda}(Q_i^*)\ln\alpha_i$ in the given conditions, we have $V_i(\tilde{x}_i(t_{k+1}+T;t_{k+1}))$ $\leqslant \varepsilon_i^2 e^{-\frac{\underline{\lambda}(Q_i^*)}{\bar{\lambda}(P_i)}\delta} \leqslant \alpha_i\varepsilon_i$. That is, $\tilde{x}_i(t_{k+1}+T;t_{k+1}) \in \Omega_i(\alpha_i\varepsilon_i)$. The proof is completed. □

Remark 6.2. *It is worth noting that Lemma 6.3 plays an important role in analyzing both feasibility and stability. In the following analysis, the result* $\tilde{x}_i(t_{k+1}+T;t_{k+1}) \in \Omega_i(\alpha_i\varepsilon_i)$ *will be used to prove the satisfaction of the robustness constraint in (6.4); the intermediate result in (6.13) will be applied to prove the fulfillment of the control input constraint.*

Remark 6.3. *The upper bound of* δ *is determined when* $s \in [t_{k+1}, t_k+T]$*. In this interval, due to the external disturbances,* $\tilde{x}_i(s;t_{k+1})$ *actually deviates away from* $\hat{x}_i(s;t_{k+1})$ *as time evolves. Thus, in order to guarantee that* $\tilde{x}_i(t_k+T;t_{k+1})$ *does not go too "far away" from the predicted state trajectory, the sampling period* δ *cannot be too "large". The lower bound of* δ *is determined when* $s \in [t_k+T, t_{k+1}+T]$*. In this interval, the feasible state trajectory candidate* $\tilde{x}_i(s;t_{k+1})$ *begins to converge towards the origin from the terminal set* $\Omega_i(\varepsilon_i)$*. Thus, the sampling period* δ *should not be too "small" such that* $\tilde{x}_i(t_{k+1}+T;t_{k+1})$ *has enough time to enter the terminal set.*

6.4.3 Feasibility of the Robust Dual-mode Distributed MPC

Based on the feasibility of the terminal constraint, we develop sufficient conditions to render the robustness constraint in (6.4) being satisfied. This result is summarized in the following Lemma 6.4.

Lemma 6.4. *For each agent* $\mathcal{A}_i$*, assume that: Assumption 6.1, 6.2 and 6.3 hold;* **Problem 6.2** *is feasible at time* t_k*; the control trajectory* $\tilde{u}_i(s;t_{k+1})$*,* $s \in [t_{k+1}, t_{k+1}+T]$ *is applied at time* t_{k+1}*. Given the constant* α_i *with* $1 > \alpha_i \geqslant 1/2$ *and* $\bar{\lambda}(P_i)/\underline{\lambda}(Q_i^*) \leqslant -\alpha_i T/(2\ln\alpha_i)$*, and the disturbance bound with* $\rho_i \leqslant \min\{\rho_i^1, \rho_i^2\}$*, if the sampling period satisfies (6.11) and also the following:*

$$(1-\alpha_i)T \leqslant \delta \leqslant \min\left\{\alpha_i T, \varsigma_i\right\}, \tag{6.15}$$

where $\varsigma_i \triangleq \frac{2\bar{\lambda}(P_i)}{-\underline{\lambda}(Q_i^*)} \ln \frac{\underline{\lambda}(Q_i^*)\alpha_i T}{2\bar{\lambda}(P_i)}$*, then the robustness constraint in (6.4) is satisfied. Here,* $\rho_i^2 \triangleq \varepsilon_i/[Te^{L_i T}\bar{\lambda}(P_i^{0.5})]$.

Proof. Since $\tilde{x}_i(s;t_{k+1})$, $s \in [t_{k+1}, t_{k+1}+T]$ depends on the value of the sampling period, the proof is derived by considering two cases. In the first case, the sampling period δ is relatively small such that $t_k+T \in [t_{k+1}+\delta, t_{k+1}+T]$. In the second case, the sampling period δ is relatively large so that $t_{k+1}+\delta \in [t_k+T, t_{k+1}+T]$.

Case I: $(1-\alpha_i)T \leqslant \delta < T/2$. In this case, $t_{k+1}+\delta \leqslant t_k+T < t_{k+1}+T$. Let us first consider $\tilde{x}_i(s;t_{k+1})$ within $[t_{k+1}+\delta, t_k+T]$. On the one hand, according to (6.12) in Lemma 6.3, we have $\|\tilde{x}_i(s;t_{k+1})\|_{P_i} \leqslant \|\hat{x}_i^*(s;t_k)\|_{P_i} + \bar{\lambda}(P_i^{\frac{1}{2}})\rho_i\delta e^{L_i\delta}e^{(L_i(s-t_{k+1}))}$. Since **Problem 6.2** is feasible at time t_k, it can be obtained that $\|\hat{x}_i^*(s;t_k)\|_{P_i} \leqslant T\alpha_i\varepsilon_i/(s-t_k)$. Thus,

$$\|\tilde{x}_i(s;t_{k+1})\|_{P_i} \leqslant \frac{T\alpha_i\varepsilon_i}{s-t_k} + \bar{\lambda}(P_i^{\frac{1}{2}})\rho_i\delta e^{L_i\delta}e^{(L_i(s-t_{k+1}))}. \tag{6.16}$$

On the other hand, according to (6.11), we can derive $\delta\bar{\lambda}(P_i^{0.5})\rho_i e^{L_iT} \leqslant (1-\alpha_i)\varepsilon_i$. Since $\delta \leqslant T/2$ and $1 > \alpha_i \geqslant 1/2$, it follows $\frac{T\alpha_i\varepsilon_i}{2\delta} \geqslant (1-\alpha_i)\varepsilon_i$. As a result, the following holds: $\delta\bar{\lambda}(P_i^{\frac{1}{2}})\rho_i e^{L_i\delta}e^{L_i(T-\delta)} \leqslant \frac{T\alpha_i\varepsilon_i}{2\delta}$. It can be seen that the above inequality implies $\delta\bar{\lambda}(P_i^{\frac{1}{2}})\rho_i e^{L_i\delta}e^{L_i(s-t_{k+1})} \leqslant \frac{\delta T\alpha_i\varepsilon_i}{(s-t_k)(s-t_{k+1})}$, for $s \in [t_{k+1}+\delta, t_k+T]$. Therefore, we can obtain $\delta\bar{\lambda}(P_i^{\frac{1}{2}})\rho_i e^{L_i\delta}e^{L_i(s-t_{k+1})} + \frac{T\alpha_i\varepsilon_i}{s-t_k} \leqslant \frac{T\alpha_i\varepsilon_i}{s-t_{k+1}}$, for $s \in [t_{k+1}+\delta, t_k+T]$. In terms of (6.16), we get $\|\tilde{x}_i(s;t_{k+1})\|_{P_i} \leqslant \frac{T\alpha_i\varepsilon_i}{s-t_{k+1}}$, $s \in [t_{k+1}+\delta, t_k+T]$. Next, let us move on to consider the time interval $[t_k+T, t_{k+1}+T]$. Define three functions $\Gamma_i(s) \triangleq e^{-\underline{\lambda}(Q_i^*)(s-t_k-T)/(2\bar{\lambda}(P_i))}$, $\Gamma_i^o(s) \triangleq T\alpha_i/(s-t_{k+1})$, $s \in [t_k+T, t_{k+1}+T]$, $\Delta\Gamma(t) = \alpha_i T e^{\underline{\lambda}(Q_i^*)t/(2\bar{\lambda}(P_i))} - t - T + \delta$, $t \in [0,\delta]$. Since $\delta \geqslant (1-\alpha_i)\varepsilon_i$, we have $\Delta\Gamma(0) \geqslant 0$. Because of the upper bounds in (6.15), it can be shown that $\Delta\Gamma(t)$ is decreasing for $t \in [0,\delta]$. Therefore, $\Delta\Gamma(t) \geqslant 0$ for $t \in [0,\delta]$. On the other hand, we have

$$\begin{aligned}&\Gamma_i^o(s) - \Gamma_i(s), \quad s \in [t_k+T, t_{k+1}+T]\\ =&\frac{\varepsilon_i\Delta\Gamma_i(t)}{(t+T-\delta)e^{\underline{\lambda}(Q_i^*)t/(2\bar{\lambda}(P_i))}} \geqslant 0, t \in [0,\delta].\end{aligned}$$

Thus, $\Gamma_i(s) \leqslant \Gamma_i^o(s)$, $s \in [t_k+T, t_{k+1}+T]$. Furthermore, according to Lemma 6.3, we get $\tilde{x}_i(t_k+T;t_{k+1}) \in \Omega_i(\varepsilon_i)$, and (6.14) holds. Therefore, $\|\tilde{x}_i(s;t_{k+1})\|_{P_i} \leqslant \Gamma_i(s)\varepsilon_i \leqslant \Gamma_i^o(s)\varepsilon_i = \frac{T\alpha_i\varepsilon_i}{s-t_{k+1}}$, for $s \in [t_k+T, t_{k+1}+T]$.

Case II: $T/2 \leqslant \delta \leqslant \alpha_i T$. In this case, $t_k+T \leqslant t_{k+1}+\delta \leqslant t_{k+1}+T$. According to Lemma 6.3, $\tilde{x}_i(t_k+T;t_{k+1}) \in \Omega_i(\varepsilon_i)$. Thus, the feasible state trajectory candidate always satisfies (6.14) for $s \in [t_{k+1}+\delta, t_{k+1}+T]$, i.e.,

$$\|\tilde{x}_i(s;t_{k+1})\|_{P_i} \leqslant \varepsilon_i e^{-\frac{\underline{\lambda}(Q_i^*)}{2\bar{\lambda}(P_i)}(s-t_k-T)}. \tag{6.17}$$

Since $\delta \leqslant \alpha_i T$, $\Gamma_i(t_{k+1}+\delta) \leqslant \Gamma_i^o(t_{k+1}+\delta)$. Similarly, by virtue of the lower bound in (6.11), we get $\Gamma_i(t_{k+1}+T) \leqslant \Gamma_i^o(t_{k+1}+T)$. By following the same line of Case I, it can

be obtained that $\Gamma_i(s) \leqslant \Gamma_i^o(s)$, $s \in [t_{k+1}, t_{k+1}+T]$. By combing the above inequality with the inequality in (6.17), we have $\|\tilde{x}_i(s;t_{k+1})\|_{P_i} \leqslant \frac{T\alpha_i\varepsilon_i}{s-t_{k+1}}$, $s \in [t_{k+1}, t_{k+1}+T]$. By summarizing Case I and Case II, the proof is completed. □

Based on Lemma 6.2–6.4, the feasibility result of the robust dual-mode distributed MPC algorithm for the overall agent system is presented in the following Theorem 6.1.

Theorem 6.1. *For the overall agent system* $\{\mathcal{A}_i, i = 1, \cdots, M\}$*, suppose that Assumption 6.1–6.4 hold. Given the constant* α_i*,* $i = 1 \cdots, M$*, satisfying* $1 > \alpha_i \geqslant 1/2$ *and* $\alpha_i \geqslant \bar{\alpha}$ *and the disturbance bounds with* $\rho_i \leqslant \underline{\rho}_i$*,* $i = 1, \cdots, M$*, if the sampling period satisfies* $\max_i \left\{\bar{\delta}_i\right\} \leqslant \delta \leqslant \min_i \left\{\underline{\delta}_i\right\}$*, then the robust dual-mode distributed MPC algorithm (***Algorithm 4***) is feasible in the set* $\mathcal{Z} \triangleq \mathcal{Z}_1 \times \cdots \times \mathcal{Z}_M$*. Here,*

$$
\begin{aligned}
\bar{\delta}_i &\triangleq \max\left\{(1-\alpha_i)T, -2\frac{\bar{\lambda}(P_i)}{\underline{\lambda}(Q_i^*)}\ln\alpha_i\right\},\\
\underline{\delta}_i &\triangleq \min\left\{\alpha_i T, \frac{(1-\alpha_i)\varepsilon_i}{\rho_i e^{L_i T}\bar{\lambda}(P_i^{0.5})}, \varsigma_i\right\},\\
\underline{\rho}_i &\triangleq \min_{j=1,\cdots,M}\left\{\min\left\{\rho_i^1, \rho_i^2\right\}\right\},\\
\bar{\alpha} &\triangleq \max_{j=1,\cdots,M}\left\{\max\left\{1-\alpha_j, \frac{-2\lambda(\bar{P}_j)}{\underline{\lambda}(Q_j^*)T}\ln\alpha_j\right\}\right\}.
\end{aligned}
$$

Proof. The proof is conducted by the induction principle. First, according to Assumption 6.4 there exists a feasible control input for the overall agent system for $x_0 \in \mathcal{Z}$ at time t_0. Second, assume that the robust distributed MPC algorithm 4 is feasible at time t_k, $k \geqslant 0$. Third, it needs to prove the robust distributed MPC algorithm 4 is feasible at time t_{k+1}.

1) Since the sampling period is set as $\max_i \left\{\bar{\delta}_i\right\} \leqslant \delta \leqslant \min_i \left\{\underline{\delta}_i\right\}$ for the overall agent system, Lemma 6.2–6.4 hold for all the agents simultaneously. As a result, by applying Lemma 6.4 for all the agents, the robustness constraint of the overall agent system is satisfied at time t_{k+1}.

2) Since $\hat{u}^*(s;t_k) \in \mathcal{U}_1 \times \cdots \times \mathcal{U}_M$, we have $\tilde{u}(s;t_{k+1}) \in \mathcal{U}_1 \times \cdots \times \mathcal{U}_M$, for $s \in [t_{k+1}, t_k + T]$. By applying the result in (6.13) for all the agents, we have $\tilde{x}(t_k + T; t_{k+1}) \in \Omega_1(\varepsilon_1) \times \cdots \times \Omega_M(\varepsilon_M)$. According to Lemma 6.1, it can be obtained that $\tilde{u}(s;t_{k+1}) = [K_1, \cdots, K_M]\tilde{x}(s;t_{k+1}) \in \mathcal{U}_1 \times \cdots \times \mathcal{U}_M$ for $s \in$

$[t_k+T, t_{k+1}+T]$. Thus, $\tilde{u}(s;t_{k+1})$, $s \in [t_{k+1}, t_{k+1}+T]$ satisfies the control input constraint at time t_{k+1} for the overall agent system.

By induction, for any initial state in $\mathcal{Z}$, the robust dual-mode distributed MPC algorithm (**Algorithm 4**) is feasible for all $k \geqslant 0$. The proof is completed. □

Remark 6.4. *In Theorem 6.1, the bounds are imposed on α_i and ρ_i to prevent the sampling period interval $[\max_i \{\bar{\delta}_i\}, \min_i \{\underline{\delta}_i\}]$ from being an empty set. Accordingly, for each agent system $\mathcal{A}_i$, the external disturbance should be bounded as $\rho_i \leqslant \underline{\rho}_i$ in order to preserve the feasibility.*

6.5 Stability Analysis

This section presents the stability conditions under which the overall agent system is stabilized. The scrutiny on the robust stability is divided into two steps. In the first step, when the system state is outside the terminal set, the optimal control objective function will be proven to be an appropriate Lyapunov function under certain conditions. In the second step, when the system state enters the terminal set, the local Lyapunov function in Lemma 6.1 will be used and the robust stability will be proven.

Let us start by considering that the system state is outside the terminal set. Before proving that the optimal control objective function is qualified as a Lyapunov function, three propositions are established, which will facilitate the derivations. The first one is to establish the upper bound on the deviation between the feasible state trajectory and the optimal nominal state trajectory during the time interval $[t_{k+1}, t_k+T]$.

Proposition 6.1. *For the overall agent system $\{\mathcal{A}_i,\ i=1,\cdots,M\}$, if Assumption 6.3 holds and the sampling period is chosen by satisfying $\delta \leqslant \min_i\{(1-\alpha_i)[\bar{\lambda}(P_i^{0.5})]^{-1}\ \varepsilon_i\rho_i^{-1}e^{-L_iT}, \varsigma_i\}$ for all agents, then for each agent $\mathcal{A}_i$, $\int_{t_{k+1}}^{t_k+T} \|\tilde{x}_i(s;t_{k+1})\|_{Q_i}^2 - \|\hat{x}_i^*(s;t_k)\|_{Q_i}^2\ ds \leqslant \lambda^2(Q_i,P_i)\varepsilon_i^2(1-\alpha_i)[(T-\delta)(1-\alpha_i)+2T\alpha_i\ln\frac{T}{\delta}]$, where $\lambda(Q_i,P_i) \triangleq \bar{\lambda}(Q_i^{0.5})/\underline{\lambda}(P_i^{0.5})$.*

Proof. Since $\|\tilde{x}_i(s;t_{k+1})\|_{Q_i} \leqslant \lambda(Q_i,P_i)\ \|\tilde{x}_i(s;t_{k+1})\|_{P_i}$ and that the result in (6.12) holds, we have

$$\begin{aligned}\|\tilde{x}_i(s;t_{k+1})\|_{Q_i} + \|\hat{x}_i^*(s;t_k)\|_{Q_i} \leqslant& \lambda(Q_i,P_i)[\|\tilde{x}_i(s;t_{k+1})\|_{P_i} + \|\hat{x}_i^*(s;t_k)\|_{P_i}] \\ \leqslant& \lambda(Q_i,P_i)\left[\bar{\lambda}(P_i^{\frac{1}{2}})\rho_i\delta e^{L_i\delta}e^{(L_i(s-t_{k+1}))} + 2\|\hat{x}_i^*(s;t_k)\|_{P_i}\right],\end{aligned}$$

$s \in [t_{k+1}, t_k+T]$. Plugging the robustness constraint in (6.4) into the above inequality gives rise to

$$\|\tilde{x}_i(s;t_{k+1})\|_{Q_i} + \|\hat{x}_i^*(s;t_k)\|_{Q_i} \leqslant \lambda(Q_i,P_i)\left[\bar{\lambda}(P_i^{\frac{1}{2}})\rho_i\delta e^{L_i\delta}e^{(L_i(s-t_{k+1}))} + 2\frac{T\alpha_i}{s-t_k}\right].$$

On the other hand, by applying the result in (6.12), we have $\|\tilde{x}_i(s;t_{k+1})-\hat{x}_i^*(s;t_k)\|_{Q_i} \leqslant \lambda(Q_i,P_i)\|\tilde{x}_i(s;t_{k+1})-\hat{x}_i^*(s;t_k)\|_{P_i} \leqslant \bar{\lambda}(P_i^{\frac{1}{2}})\rho_i\delta e^{L_i\delta}e^{(L_i(s-t_{k+1}))}$. According to the triangle inequality, we get

$$\begin{aligned}
&\int_{t_{k+1}}^{t_k+T} \|\tilde{x}_i(s;t_{k+1})\|_{Q_i}^2 - \|\tilde{x}_i(s;t_{k+1})\|_{Q_i}^2 ds\\
\leqslant &\int_{t_{k+1}}^{t_k+T} [\|\tilde{x}_i(s;t_{k+1})\|_{Q_i} + \|\tilde{x}_i(s;t_{k+1})\|_{Q_i}][\|\tilde{x}_i(s;t_{k+1}) - \tilde{x}_i(s;t_{k+1})\|_{Q_i}]ds\\
\leqslant &\lambda(Q_i,P_i)\int_{t_{k+1}}^{t_k+T} \bar{\lambda}(P_i^{\frac{1}{2}})\rho_i\delta e^{L_i\delta}e^{(L_i(s-t_{k+1}))}\left[\bar{\lambda}(P_i^{\frac{1}{2}})\rho_i\delta e^{L_i\delta}e^{(L_i(s-t_{k+1}))} + 2\frac{T\alpha_i}{s-t_k}\right]ds\\
\leqslant &\lambda(Q_i,P_i)\int_{t_{k+1}}^{t_k+T} \bar{\lambda}(P_i^{\frac{1}{2}})\rho_i\delta e^{L_iT}\left[\bar{\lambda}(P_i^{\frac{1}{2}})\rho_i\delta e^{L_iT} + 2\frac{T\alpha_i}{s-t_k}\right]ds\\
\leqslant &\lambda^2(Q_i,P_i)\varepsilon_i^2(1-\alpha_i)\left[(T-\delta)(1-\alpha_i) + 2T\alpha_i\ln\frac{T}{\delta}\right],
\end{aligned}$$

where the inequality $\bar{\lambda}(P_i^{0.5})\delta \leqslant (1-\alpha_i)\varepsilon_i\rho_i^{-1}e^{-L_iT}$ has been utilized in the last step. The proof is completed. □

In the second proposition, the upper bound on the deviation between the feasible state trajectory of each agent $\mathcal{A}_i$ and its neighbor's assumed state trajectory during $[t_k+T, t_{k+1}+T]$ is established.

Proposition 6.2. *For the overall agent system* $\{\mathcal{A}_i,\ i=1,\cdots,M\}$*, suppose that: Assumption 6.1, 6.2, 6.3 are satisfied;* **Problem 6.2** *is feasible at time* t_k*; the feasible control trajectory* $\tilde{u}_i(s;t_{k+1})$ *is applied at time* t_{k+1} *for each agent. Given the constant* α_i *with* $1 > \alpha_i \geqslant \bar{\alpha}$ *and the disturbance bound satisfying* $\rho_i \leqslant \underline{\rho}_i$*, if the sampling period satisfies the condition in (6.11) simultaneously for all the agents, then the following*

relationship holds:

$$\begin{aligned}
&\int_{t_{k+1}}^{t_{k+1}+T} \|\tilde{x}_i(s;t_{k+1}) - \hat{x}_j^a(s;t_{k+1})\|_{Q_{ij}}^2 ds \\
\leqslant &(T-\delta)\left[\lambda(Q_{ij},P_i)(1+\frac{T-\delta}{\delta}\alpha_i)\varepsilon_i + \lambda(Q_{ij},P_j)\frac{T}{\delta}\alpha_j\varepsilon_j\right]^2 \\
&+ \delta\left[\lambda(Q_{ij},P_i)\varepsilon_i + \lambda(Q_{ij},P_j)\alpha_j\varepsilon_j\right]^2,
\end{aligned}$$

where $j \in \mathcal{N}_i$.

Proof. By calculating $\int_{t_{k+1}}^{t_k+T} \|\tilde{x}_i(s;t_{k+1})\|_{Q_{ij}} ds$ and using the result in (6.12), we get

$$\begin{aligned}
\int_{t_{k+1}}^{t_k+T} \|\tilde{x}_i(s;t_{k+1})\|_{Q_{ij}} ds \leqslant &\lambda(Q_{ij},P_i) \int_{t_{k+1}}^{t_k+T} \|\tilde{x}_i(s;t_{k+1})\|_{P_i} ds \\
\leqslant &\lambda(Q_{ij},P_i) \int_{t_{k+1}}^{t_k+T} \bar{\lambda}(P_i^{\frac{1}{2}})\rho_i\delta e^{L_i\delta} e^{(L_i(s-t_{k+1}))} + \frac{T\alpha_i}{s-t_k} ds.
\end{aligned}$$

By taking the maximum value in interval $[t_{k+1}, t_k+T]$ and applying (6.11), we obtain

$$\begin{aligned}
\int_{t_{k+1}}^{t_k+T} \|\tilde{x}_i(s;t_{k+1})\|_{Q_{ij}} ds \leqslant &\lambda(Q_{ij},P_i) \int_{t_{k+1}}^{t_k+T} \bar{\lambda}(P_i^{\frac{1}{2}})\rho_i\delta e^{L_iT} + \frac{T\alpha_i}{\delta} ds \\
\leqslant &(T-\delta)\lambda(Q_{ij},P_i)\varepsilon_i\left[(1-\alpha_i) + \frac{T}{\delta}\alpha_i\right].
\end{aligned} \tag{6.18}$$

Next, since $\hat{x}_j^a(s;t_{k+1}) = \hat{x}_j^*(s;t_k)$, $s \in [t_{k+1}, t_k+T]$, we get

$$\begin{aligned}
\int_{t_{k+1}}^{t_k+T} \|\hat{x}_j^a(s;t_{k+1})\|_{Q_{ij}} ds \leqslant &\lambda(Q_{ij},P_j) \int_{t_{k+1}}^{t_k+T} \|\hat{x}_j^*(s;t_k)\|_{P_j} ds \\
\leqslant &\lambda(Q_{ij},P_j) \int_{t_{k+1}}^{t_k+T} \frac{T\alpha_j\varepsilon_j}{s-t_k} ds \leqslant (T-\delta)\lambda(Q_{ij},P_j)\frac{T\alpha_j\varepsilon_j}{\delta}.
\end{aligned} \tag{6.19}$$

Furthermore, due to $\tilde{x}_i(s;t_{k+1}) \in \Omega_i(\alpha_i\varepsilon_i)$, for $s \in [t_k+T, t_{k+1}+T]$, Lemma 6.3 can be applied. As a result,

$$\int_{t_k+T}^{t_{k+1}+T} \|\tilde{x}_i(s;t_{k+1})\|_{Q_{ij}} ds \leqslant \lambda(Q_{ij},P_i)\varepsilon_i\delta. \tag{6.20}$$

By virtue of the generation mechanism of the assumed state trajectory in (6.5) and

(6.9), we obtain

$$\int_{t_k+T}^{t_{k+1}+T} \|\hat{x}_j^a(s;t_{k+1})\|_{Q_{ij}} ds \leqslant \lambda(Q_{ij},P_j)\alpha_j\varepsilon_j\delta. \tag{6.21}$$

Finally, by applying the triangle inequality, we derive

$$\begin{aligned}
&\int_{t_{k+1}}^{t_{k+1}+T} \|\tilde{x}_i(s;t_{k+1}) - \hat{x}_j^a(s;t_{k+1})\|_{Q_{ij}}^2 ds \\
\leqslant &\int_{t_{k+1}}^{t_{k+1}+T} [\|\tilde{x}_i(s;t_{k+1})\|_{Q_{ij}} + \|\hat{x}_j^a(s;t_{k+1})\|_{Q_{ij}}]^2 ds \\
\leqslant &\int_{t_{k+1}}^{t_k+T} [\|\tilde{x}_i(s;t_{k+1})\|_{Q_{ij}} + \|\hat{x}_j^a(s;t_{k+1})\|_{Q_{ij}}]^2 ds \\
&+ \int_{t_k+T}^{t_{k+1}+T} [\|\tilde{x}_i(s;t_{k+1})\|_{Q_{ij}} + \|\hat{x}_j^a(s;t_{k+1})\|_{Q_{ij}}]^2 ds.
\end{aligned}$$

By substituting (6.18)–(6.21) into the above inequality, the result can be readily derived. The proof is completed. □

The third proposition provides the lower bound of the term $\int_{t_k}^{t_{k+1}} \|\hat{x}_i^*(s;t_k)\|_{Q_i}^2 ds$, when the system state of $\mathcal{A}_i$ is outside the terminal set.

Proposition 6.3. *For the overall agent system $\{\mathcal{A}_i,\ i = 1,\cdots,M\}$, suppose that Assumption 6.3 holds and the sampling period satisfies*

$$\delta \leqslant \min_i\{(1-\alpha_i)[\bar{\lambda}(P_i^{0.5})]^{-1}\varepsilon_i\rho_i^{-1}e^{-L_iT}\}$$

*for all the agents. If the robust dual-mode distributed MPC algorithm (***Algorithm 4***) is applied and the system state $x_i(s;t_k) \notin \Omega_i(\varepsilon_i)$ for $s \in [t_k, t_k+\delta]$, then the following holds for each agent $\mathcal{A}_i$: $\int_{t_k}^{t_{k+1}} \|\hat{x}_i^*(s;t_k)\|_{Q_i}^2 ds > \delta\frac{\underline{\lambda}(Q_i)}{\bar{\lambda}(P_i)}\alpha_i^2\varepsilon_i^2$.*

Proof. According to Lemma 6.2, it can be obtained that $\|\hat{x}_i^*(s;t_k)\|_{P_i} \geqslant \|x_i(s;t_k)\|_{P_i} - \bar{\lambda}(P_i^{\frac{1}{2}})\rho_i(s-t_k)e^{L_i(s-t_k)}$ for all $s \in [t_k, t_k+T]$. Since $x_i(s;t_k) \notin \Omega_i(\varepsilon_i)$, we get

$\|\hat{x}_i^*(s;t_k)\|_{P_i} > \varepsilon_i - \bar{\lambda}(P_i^{\frac{1}{2}})\rho_i(s-t_k)e^{L_i(s-t_k)}$. As a result, we have

$$\begin{aligned}
&\int_{t_k}^{t_{k+1}} \|\hat{x}_i^*(s;t_k)\|_{Q_i}^2 ds \geqslant \frac{\underline{\lambda}(Q_i)}{\bar{\lambda}(P_i)} ds \int_{t_k}^{t_{k+1}} \|\hat{x}_i^*(s;t_k)\|_{P_i}^2 \\
>&\delta\frac{\underline{\lambda}(Q_i)}{\bar{\lambda}(P_i)}\left(\varepsilon_i - \bar{\lambda}(P_i^{\frac{1}{2}})\rho_i\delta e^{L_i(\delta)}\right)^2 \\
>&\delta\frac{\underline{\lambda}(Q_i)}{\bar{\lambda}(P_i)}\left(\varepsilon_i - e^{L_i(\delta-T)}(1-\alpha_i)\varepsilon_i\right)^2 > \delta\frac{\underline{\lambda}(Q_i)}{\bar{\lambda}(P_i)}\delta\alpha_i^2\varepsilon_i^2,
\end{aligned}$$

where the condition $\bar{\lambda}(P_i^{0.5})\delta \leqslant (1-\alpha_i)\varepsilon_i\rho_i^{-1}e^{-L_iT}$ has been used. The proof is completed. □

Based on these three propositions, the optimal control objective function will be proven to be qualified as a Lyapunov function under appropriate conditions. Using this Lyapunov function, it can be shown that the system state which is outside the terminal set will enter the terminal set in finite time. These results are summarized in the following Lemma 6.5.

Lemma 6.5. *For the overall multi-agent system $\{\mathcal{A}_i, i = 1, \cdots, M\}$, with initial state $x_0 \in \mathcal{Z}$, suppose that: Assumption 6.1–6.3 hold; the constant α_i is given as $1 \geqslant \alpha_i \geqslant \max\{1/2, \bar{\alpha}\}$; the disturbance bound satisfies $\rho_i \leqslant \underline{\rho}_i$. If the sampling period is designed as $\delta = pT$, and the cooperation weight r_{ij} is taken such that*

$$\sum_{j\in\mathcal{N}_i} r_{ij}\Xi_{ij} \leqslant (1-\beta_i-\zeta_i)pT\alpha_i^2\varepsilon_i^2\frac{\underline{\lambda}(Q_i)}{\bar{\lambda}(P_i)}, \tag{6.22}$$

where β_i, ζ_i are constants with $\beta_i + \zeta_i \in (0,1)$, $p \in (0,1)$ satisfies

$$\frac{(1-p)(1-\alpha_i)^2 - 2\alpha_i(1-\alpha_i)\ln p + (1-\alpha_i^2)\lambda^{-2}(Q_i,P_i)}{pT\beta_i\alpha_i^2} \leqslant \frac{\underline{\lambda}(Q_i)\underline{\lambda}(P_i)}{\bar{\lambda}(P_i)\bar{\lambda}(Q_i)}, \tag{6.23}$$

$$\bar{\delta}_i T^{-1} \leqslant p \leqslant \underline{\delta}_i T^{-1}, \tag{6.24}$$

for all $i = 1, \ldots, M$, simultaneously, and Ξ_{ij} is defined as

$$\begin{aligned}
\Xi_{ij} \triangleq& pT[\lambda(Q_{ij},P_i)\varepsilon_i + \lambda(Q_{ij}\alpha_j\varepsilon_j)]^2 \\
&+ (1-p)T[\lambda(Q_{ij},P_i)(1-\alpha_i+p^{-1})\varepsilon_i + \lambda(Q_{ij},P_j)p^{-1}\alpha_j\varepsilon_j]^2,
\end{aligned}$$

then the system state of each agent $\mathcal{A}_i$ with the initial state $x_i^0 \in \mathcal{Z} \setminus \Omega_i(\varepsilon_i)$ will enter the terminal set $\Omega_i(\varepsilon_i)$ in finite time.

Proof. For each agent $\mathcal{A}_i$ with the feasible control input at time t_{k+1}, we will calculate the upper bound of an auxiliary term $\Delta(J_i)$ defined as

$$\Delta(J_i) \triangleq J_i(\tilde{x}_i(s;t_{k+1}), \tilde{u}_i(s;t_{k+1}), \tilde{x}^a_{-i}(s;t_{k+1})) - J_i(\hat{x}^*_i(s;t_k), \hat{u}^*_i(s;t_k), \hat{x}^a_{-i}(s;t_k)),$$

where $\tilde{x}^a_{-i}(s;t_{k+1})$, $s \in [t_{k+1}, t_{k+1}+T]$, is the feasible assumed state trajectory of the neighbors of agent $\mathcal{A}_i$, which is equal to $\hat{x}^a_{-i}(s;t_{k+1})$ according to the generation mechanism for the assumed state trajectory in **Algorithm 4**. By splitting the interval of integral in $\Delta(J_i)$, we obtain

$$\begin{aligned}
\Delta(J_i) = &\int_{t_{k+1}}^{t_k+T} \|\tilde{x}_i(s;t_{k+1})\|^2_{Q_i} + \|\tilde{u}_i(s;t_{k+1}\|^2_{R_i} - \|\hat{x}^*_i(s;t_k)\|^2_{Q_i} - \|\hat{u}^*_i(s;t_k)\|^2_{R_i} ds \\
&+ \int_{t_k+T}^{t_{k+1}+T} \|\tilde{x}_i(s;t_{k+1})\|^2_{Q_i} + \|\tilde{u}_i(s;t_{k+1})\|^2_{R_i} ds \\
&- \int_{t_k}^{t_{k+1}} \|\hat{x}^*_i(s;t_k)\|^2_{Q_i} + \|\hat{u}^*_i(s;t_k)\|^2_{R_i} ds \\
&+ \|\tilde{x}_i(t_{k+1}+T;t_{k+1})\|^2_{P_i} - \|\hat{x}^*_i(t_k+T;t_k)\|^2_{P_i} \\
&+ \int_{t_{k+1}}^{t_{k+1}+T} \sum_{j\in\mathcal{N}_i} r_{ij} \|\tilde{x}_i(s;t_{k+1}) - \hat{x}^a_j(s;t_{k+1})\|^2_{Q_{ij}} ds \\
&- \int_{t_k}^{t_k+T} \sum_{j\in\mathcal{N}_i} r_{ij} \|\hat{x}^*_i(s;t_k) - \hat{x}^a_j(s;t_k)\|^2_{Q_{ij}} ds.
\end{aligned}$$

In the right-hand side the above equation, we first consider the term

$$\int_{t_{k+1}}^{t_k+T} \|\tilde{x}_i(s;t_{k+1})\|^2_{Q_i} + \|\tilde{u}_i(s;t_{k+1})\|^2_{R_i} - \|\hat{x}^*_i(s;t_k)\|^2_{Q_i} - \|\hat{u}^*_i(s;t_k)\|^2_{R_i} ds.$$

Since $\tilde{u}_i(s;t_{k+1}) = \hat{u}^*_i(s;t_k)$, for $s \in [t_{k+1}, t_k+T]$, we have

$$\begin{aligned}
&\int_{t_{k+1}}^{t_k+T} \|\tilde{x}_i(s;t_{k+1})\|^2_{Q_i} + \|\tilde{u}_i(s;t_{k+1}\|^2_{R_i} - \|\hat{x}^*_i(s;t_k)\|^2_{Q_i} - \|\hat{u}^*_i(s;t_k)\|^2_{R_i} ds \\
=&\int_{t_{k+1}}^{t_k+T} \|\tilde{x}_i(s;t_{k+1})\|^2_{Q_i} - \|\hat{x}^*_i(s;t_k)\|^2_{Q_i} ds.
\end{aligned}$$

For the term $\int_{t_k+T}^{t_{k+1}+T} \|\tilde{x}_i(s;t_{k+1})\|^2_{Q_i} + \|\tilde{u}_i(s;t_{k+1})\|^2_{R_i} ds$, since $\tilde{u}_i(s;t_{k+1}) = K_i \tilde{x}_i(s;t_{k+1})$,

$s \in [t_k + T, t_{k+1} + T]$, we get

$$\int_{t_k+T}^{t_{k+1}+T} \|\tilde{x}_i(s;t_{k+1})\|_{Q_i}^2 + \|\tilde{u}_i(s;t_{k+1})\|_{R_i}^2 ds = \int_{t_k+T}^{t_{k+1}+T} \|\tilde{x}_i(s;t_{k+1})\|_{Q_i^*}^2 ds.$$

According to Lemma 6.3, we have $\tilde{x}_i(s;t_{k+1}) \in \Omega_i(\varepsilon_i)$, $s \in [t_k + T, t_{k+1} + T]$. From Lemma 6.1, it can be obtain that

$$\begin{aligned}
&\int_{t_k+T}^{t_{k+1}+T} \|\tilde{x}_i(s;t_{k+1})\|_{Q_i}^2 + \|\tilde{u}_i(s;t_{k+1})\|_{R_i}^2 ds \\
\leqslant &\int_{t_k+T}^{t_{k+1}+T} -\frac{\mathrm{d}V_i(\tilde{x}_i(s;t_{k+1}))}{ds} ds \\
\leqslant &\|\tilde{x}_i(t_k+T;t_{k+1})\|_{P_i}^2 - \|\tilde{x}_i(t_{k+1}+T;t_{k+1})\|_{P_i}^2 \\
\leqslant &\|\hat{x}_i^*(t_k+T;t_k)\|_{P_i}^2 - \|\tilde{x}_i(t_{k+1}+T;t_{k+1})\|_{P_i}^2 \\
\leqslant &(1-\alpha_i^2)\varepsilon_i^2.
\end{aligned}$$

By collectively considering the terms in $\Delta(J_i)$, we have

$$\begin{aligned}
\Delta(J_i) \leqslant &\int_{t_{k+1}}^{t_k+T} \|\tilde{x}_i(s;t_{k+1})\|_{Q_i}^2 - \|\hat{x}_i^*(s;t_k)\|_{Q_i}^2 ds - \int_{t_k}^{t_{k+1}} \|\hat{x}_i^*(s;t_k)\|_{Q_i}^2 + \|\hat{u}_i^*(s;t_k)\|_{R_i}^2 ds \\
&+ \sum_{j\in\mathcal{N}_i} \int_{t_{k+1}}^{t_{k+1}+T} r_{ij} \|\tilde{x}_i(s;t_{k+1}) - \hat{x}_j^a(s;t_{k+1})\|_{Q_{ij}}^2 ds.
\end{aligned}$$

Furthermore, by using the results of Proposition 6.1–6.3, we obtain

$$\begin{aligned}
\Delta(J_i) < &-\frac{\underline{\lambda}(Q_i)}{\bar{\lambda}(P_i)} pT\alpha_i^2\varepsilon_i^2 + \lambda^2(Q_i,P_i)[(1-p)(1-\alpha_i)^2 - 2\alpha_i(1-\alpha_i)\ln p]T\varepsilon_i^2 \\
&+ \sum_{j\in\mathcal{N}_i} r_{ij}\Xi_{ij},
\end{aligned}$$

where the condition $\delta = pT$ has been used. By applying the conditions in (6.22) and (6.23), we get $\Delta(J_i) < -\zeta_i \frac{\underline{\lambda}(Q_i)}{\bar{\lambda}(P_i)} pT\alpha_i^2\varepsilon_i^2 \triangleq -\epsilon_i$. According to the sub-optimality of the feasible control input at time t_{k+1}, it can be obtained that

$$\begin{aligned}
&J_i(\hat{x}_i^*(s;t_{k+1}), \hat{u}_i^*(s;t_{k+1}), \hat{x}_{-i}^a(s;t_{k+1})) - J_i(\hat{x}_i^*(s;t_k), \hat{u}_i^*(s;t_k), \hat{x}_{-i}^a(s;t_k)) \\
\leqslant &\Delta(J_i) < -\epsilon_i. \qquad (6.25)
\end{aligned}$$

By applying the same arguments as in [21, 97] and using (6.25), it can be concluded

that the system state of each agent $\mathcal{A}_i$ with the initial state $x_i^0 \in \mathcal{Z}_i \setminus \Omega_i(\varepsilon_i)$ will enter the terminal set $\Omega_i(\varepsilon_i)$ in finite time. The proof is completed. □

Remark 6.5. *It is worth noting that the roles of the two constants β_i and ζ_i are different. From conditions in (6.22) and (6.23), it can be seen that the constant β_i is related with the design of the sampling period and the cooperation weights. In fact, an appropriate β_i should be chosen by considering a tradeoff between the design of the cooperation weight and the sampling period. A smaller β_i will result in a larger cooperation weight, which is better for cooperation. However, according to the condition in (6.23), the smaller β_i will lead to a narrower range of the sampling period, which may violate the condition in (6.24). The constant ζ_i affects the cooperation weight and the convergence performance. By observing (6.22), it can be seen that a larger ζ_i will produce a smaller cooperation weight, which weakens the cooperation. But a larger ζ_i may speed up the convergence of the system state from outside to the terminal set, according to (6.25). In addition, there is a coupling between ζ_i and β_i due to $0 < \zeta_i + \beta_i < 1$. By comprehensively considering these effects from ζ_i and β_i , we, first of all, need to determine the constant β_i because the stability depends on the non-pathological sampling period range which is determined by β_i.*

Based on Lemma 6.5, the main result on the robust stability of the overall multi-agent system (6.1) using **Algorithm 4**, is presented in the following Theorem 6.2.

Theorem 6.2. *For the multi-agent system in (6.1) using Algorithm 4 with the initial state $x_0 \in \mathcal{Z}$, suppose that Assumption 6.1–6.4 hold, and that the constant α_i is designed as $1 > \alpha_i \geqslant \max\{1/2, \bar{\alpha}\}$, $i = 1, \cdots, M$. Given the prediction horizon T, if (a) the sampling period is designed as $\delta = pT$, where $p \in (0, 1)$ satisfies (6.23) and (6.24) simultaneously for all $i = 1, \cdots, M$; (b) the cooperation weight r_{ij} satisfies (6.22); (c) the disturbance bound satisfies $\rho_i \leqslant \rho_i^{\max} \leqslant \underline{\rho}_i$, where $\rho_i^{\max} \triangleq \frac{\beta_i' \underline{\lambda}(Q_i^*)\varepsilon_i}{2\bar{\lambda}(P_i^{\frac{1}{2}})\bar{\lambda}(P_i)}$, and $\beta_i' \in (0, 1)$; then the system state will converge to the set $\Omega_i(\sqrt{\beta_1'}\varepsilon_1) \times \cdots \times \Omega_M(\sqrt{\beta_M'}\varepsilon_M)$.*

Proof. According to the proposed robust dual-mode distributed MPC **Algorithm 4**, we consider two cases in the following proof.

Case I: For each agent $\mathcal{A}_i$, the state is in the terminal set i.e., $x_i(t) \in \Omega_i(\varepsilon_i)$. First, let us prove that the system state of each agent $\mathcal{A}_i$ will enter $\Omega_i(\sqrt{\beta_i'}\varepsilon_i)$ in finite time when $x_i(t) \in \Omega_i(\varepsilon_i) \setminus \Omega_i(\sqrt{\beta_i'}\varepsilon_i)$. According to Algorithm 4 for each agent $\mathcal{A}_i$, the control input will be switched to the state feedback control $u_i(t) = K_i x_i(t)$

when $x_i(t) \in \Omega_i(\varepsilon_i)$. In particular, in case of $x_i(t) \in \Omega_i(\varepsilon_i) \backslash \Omega_i(\eta\varepsilon_i)$ with $\eta \in (\sqrt{\beta_i'}, 1)$, by considering the Lyapunov function $V_i(x_i(t))$ for each agent $\mathcal{A}_i$, we have

$$\begin{aligned}\dot{V}_i(x_i(t)) =& - x_i^{\mathrm{T}}(t)Q_i^* x_i(t) + 2x_i^{\mathrm{T}}(t)P_i\omega_i(t) \\ \leqslant& - \frac{\underline{\lambda}(Q_i^*)}{\bar{\lambda}(P_i)}\|x_i(t)\|_{P_i}^2 + 2\|P_i^{\frac{1}{2}}x_i(t)\|\|P_i^{\frac{1}{2}}\|\|\omega_i(t)\|.\end{aligned}$$

Since $x_i(t) \in \Omega_i(\varepsilon_i) \setminus \Omega_i(\eta\varepsilon_i)$ and $\rho_i \leqslant \rho_i^{\max}$, we get

$$\dot{V}_i(x_i(t)) \leqslant (-\eta^2 + \beta_i')\frac{\underline{\lambda}(Q_i^*)}{\bar{\lambda}(P_i)}\varepsilon_i^2 < 0. \tag{6.26}$$

Based on (6.26), using the same arguments in [21, 97], it can be obtained that the state of each agent $\mathcal{A}_i$ will enter $\Omega_i(\sqrt{\beta_i'}\varepsilon_i)$ in finite time.

Second, let us prove that the set $\Omega_i(\sqrt{\beta_i'}\varepsilon_i)$ is a robust invariant set for the agent $\mathcal{A}_i$ when the state feedback $u_i(t) = K_i x_i(t)$ is applied, i.e., $x_i(t_0) \in \Omega_i(\sqrt{\beta_i'}\varepsilon_i)$ implies $x_i(t) \in \Omega_i(\sqrt{\beta_i'}\varepsilon_i), \forall t \geqslant t_0$. This can be proven by contradiction as in[143]. Assume that $x_i(t_0) \in \Omega_i(\sqrt{\beta_i'}\varepsilon_i)$ does not imply $x_i(t) \in \Omega_i(\sqrt{\beta_i'}\varepsilon_i), t \geqslant t_0$. That is, for $x_i(t_0) \in \Omega_i(\sqrt{\beta_i'}\varepsilon_i)$, there exist $t > t_0$ and some $\bar{\epsilon}_i > 0$ such that $\varepsilon_i^2 > V_i(x_i(t)) > \beta_i'\varepsilon_i^2 + \bar{\epsilon}_i$. Let $\underline{t} = \inf\{t \geqslant t_0 : V_i(x_i(t)) \geqslant \beta_i'\varepsilon_i^2 + \bar{\epsilon}_i\}$. Then $x_i(\underline{t}) \in \Omega_i(\varepsilon_i) \setminus \Omega_i(\sqrt{\beta_i'}\varepsilon_i)$. By following the same procedure as deriving (6.26), we have $\dot{V}_i(x_i(\tau))|_{\tau=\underline{t}} \leqslant -\bar{\epsilon}_i\frac{\underline{\lambda}(Q_i^*)}{\bar{\lambda}(P_i)} < 0$. As a result, it can be inferred that $V_i(x_i(t')) > V_i(x_i(\underline{t})) \geqslant \beta_i'\varepsilon_i^2 + \bar{\epsilon}_i$, for some $t' \in (t_0, \underline{t})$. This contradicts the minimality of $\underline{t}$. Thus, we have proven that the set $\Omega_i(\sqrt{\beta_i'}\varepsilon_i)$ is a robust invariant set for the agent $\mathcal{A}_i$.

By summarizing the above results, it has been proven that the state of each agent $\mathcal{A}_i$ will converge to the set $\Omega_i(\sqrt{\beta_i'}\varepsilon_i)$, for all $x_i(t) \in \Omega_i(\varepsilon_i)$.

Case II: For each agent $\mathcal{A}_i$, the state is outside the terminal set, i.e., $x_i(t) \in \mathcal{Z}_i \setminus \Omega_i(\varepsilon_i)$. In this case, according to Lemma 6.5, the state $x_i(t)$ will enter the terminal set $\Omega_i(\varepsilon_i)$ in finite time. Furthermore, in terms of the discussion of Case I, it is concluded that the state $x_i(t)$ will converge to the set $\Omega_i(\sqrt{\beta_i'}\varepsilon_i)$.

By summarizing the results in Case I and Case II, we complete the proof. □

6.6 Simulation Studies

In this section, in order to verify the developed theoretical results, we demonstrate the design procedure by applying the proposed robust distributed MPC scheme to a

multi-agent system consisting of three nonlinear cart-damper-spring subsystems.

The system model of each cart-damper-spring system $\mathcal{A}_i$, $i = 1, 2, 3$, is given as

$$\begin{cases} \dot{x}_{i1}(t) = x_{i2}(t), \\ \dot{x}_{i2}(t) = -\frac{k_i}{M_i} e^{-x_{i1}(t)} x_{i1}(t) - \frac{h_i}{M_i} x_{i2}(t) + \frac{u_i(t)}{M_i} + \frac{\omega_i(t)}{M_i}, \end{cases}$$

where x_{i1} is the displacement of the cart, x_{i2} is its velocity, k_i is the linear spring factor, h_i is the damper factor, M_i is the mass of the cart, $u_i(t)$ is the control force and $\omega_i(t)$ is the external disturbance. Such a system model has been used in [89] for a single nonlinear system using the conventional MPC. For simplicity, each agent $\mathcal{A}_i$, $i = 1, 2, 3$, has the same system parameters which are given as $h_i = 1.1$ Ns/s; $M_i = 1.5$kg; $k_i = 0.25$N/m and the control force is required to be bounded as $u_i(t) \in [-2, 2]$. The communication links are as follows: Agent $\mathcal{A}_1$ is able to receive information from agents $\mathcal{A}_2$ and $\mathcal{A}_3$; agent $\mathcal{A}_2$ is able to receive information from agents $\mathcal{A}_1$ and $\mathcal{A}_3$; agent $\mathcal{A}_3$ is able to receive information from agents $\mathcal{A}_1$ and $\mathcal{A}_2$.

The control objective is to design the robust dual-mode distributed model predictive controllers for the three-agent system according to **Algorithm 4**. For each agent, the parameters of the distributed control objective function are the same. In what follows, let us determine these parameters according to the developed theoretical results. Set $Q_i = I$, $R_i = 0.1$ and $Q_{ij} = 0.1I$, $j \in \mathcal{N}_i$. The local state feedback control gain is given by $K_i = [-4.2291, -4.7221]$. According to Lemma 6.1, the matrix P_i is determined as $P_i = [4.5619, -2.2731; -2.2731, 2.4026]$ and the terminal set level is $\varepsilon_i = 0.31$. The parameter α_i is set as $\alpha_i = 0.98$ which satisfies the requirements in Theorem 6.1 and in Theorem 6.2, where the lower bound $\bar{\alpha}$ is calculated as 0.0303. The prediction horizon is designed as $T = 0.4$s. By solving conditions in (6.23) and (6.24), the interval of the sampling period is determined as $[0.1212, 0.1658]$. Thus, we set $\delta = 0.16$s, which satisfies the conditions in Theorem 6.1 and Theorem 6.2. The constants β_i and ζ_i are given as 0.9 and 0.001, respectively. The parameters r_{ij} and Ξ_{ij} are designed as $r_{ij} = 0.0038$ and $\Xi_{ij} = 0.1281$, $j \in \mathcal{N}_i$, which meet the requirements in (6.22). The bound of the disturbance is set as $\rho_i = 0.005$ which is less than the theoretical disturbance bound $\underline{\rho}_i = 0.0068$ according to Theorem 6.1 and Theorem 6.2. The parameter β_i' is calculated as $\beta_i' = 0.3351$.

Base on these designed parameters, the robust dual-mode distributed MPC **Algorithm 4** is executed by using MATLAB. The simulation results are as follows. The displacements and velocities of the three-agent system are illustrated in Figure

7.3 and Figure 6.2, respectively. The control inputs are demonstrated in Figure 7.5.

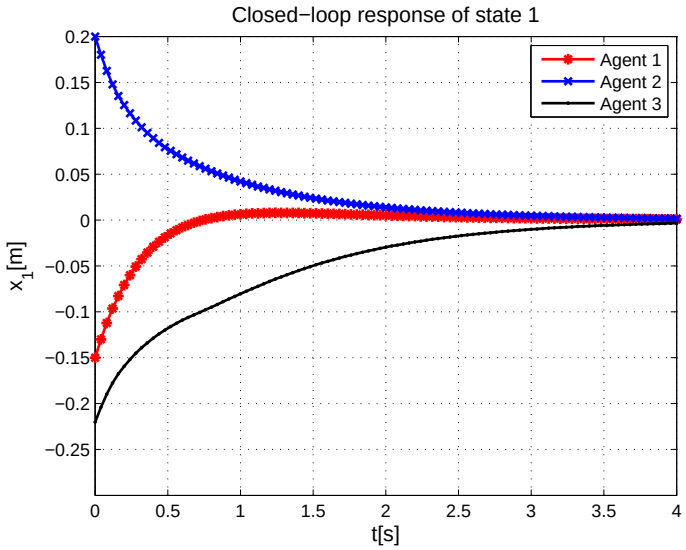

Figure 6.1: Control performance for the displacements of three agents.

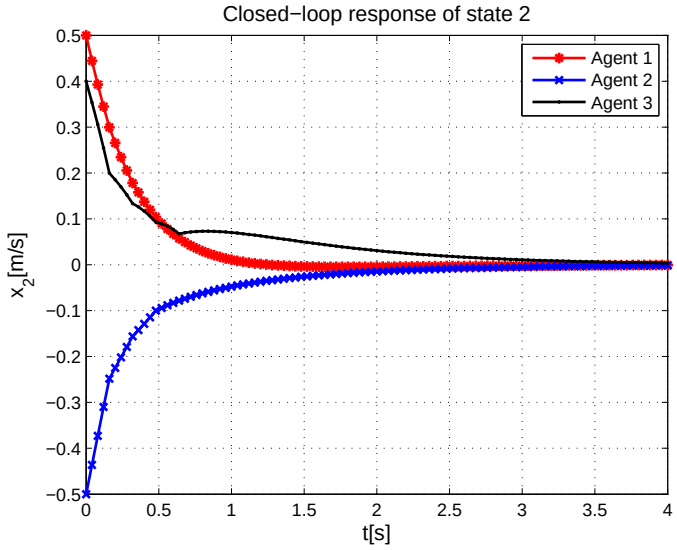

Figure 6.2: Control performance of the velocities of three agents.

From Figure 6.1 and 6.2, it can be seen that the robust dual-mode distributed MPC algorithm robustly stabilizes the three-agent system. Figure 6.3 reveals that the control input constraints are satisfied and the designed **Algorithm 4** is feasible.

Furthermore, to verify Theorem 6.2, we demonstrate the trajectory of each agent

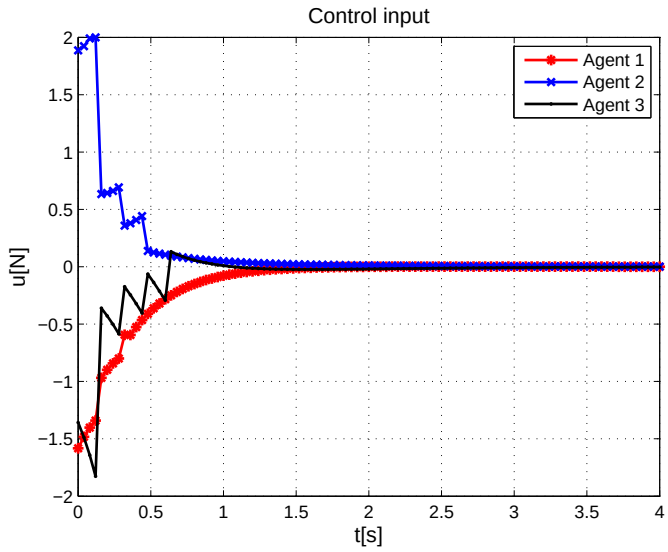

Figure 6.3: Control inputs of three agents.

and its convergence set in Figure 6.4 [1], 6.5 [2] and 6.6[3], respectively. By observing these figures, it can be seen that each agent system is robustly stabilized and converges to the theoretical convergence set.

6.7 Conclusion

In this chapter, we have investigated the robust distributed MPC problem for a group of decoupled constrained nonlinear agent systems with external disturbances. By introducing a robustness constraint, we design a novel robust dual-mode distributed MPC algorithm which can deal with bounded external disturbances. Based on the triangle inequality and the Gronwall-Bellman inequality, it has been proved that the feasibility of the robust dual-mode distributed MPC algorithm can be guaranteed if the sampling period is appropriately chosen according to the established condition and the external disturbances are bounded by some critical values. Furthermore, it has been shown that, the overall agent system can be stabilized into a robustly invariant set, provided that the sampling period, the disturbances and the cooperation weights

[1]The blue line represents the trajectory of agent $\mathcal{A}_1$ which is derived by the simulation and the area of the light green ellipsoid is the convergent set calculated according to Theorem 6.2.

[2]The blue line represents the trajectory of agent $\mathcal{A}_2$ which is derived by the simulation and the area of the light green ellipsoid is the convergent set calculated according to Theorem 6.2.

[3]The blue line represents the trajectory of agent $\mathcal{A}_3$ which is derived by the simulation and the area of the light green ellipsoid is the convergent set calculated according to Theorem 6.2.

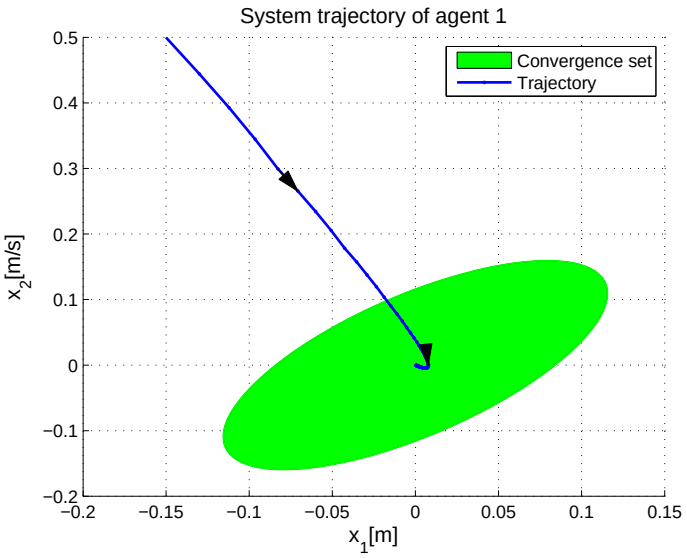

Figure 6.4: Trajectory of agent $\mathcal{A}_1$ and its convergence set.

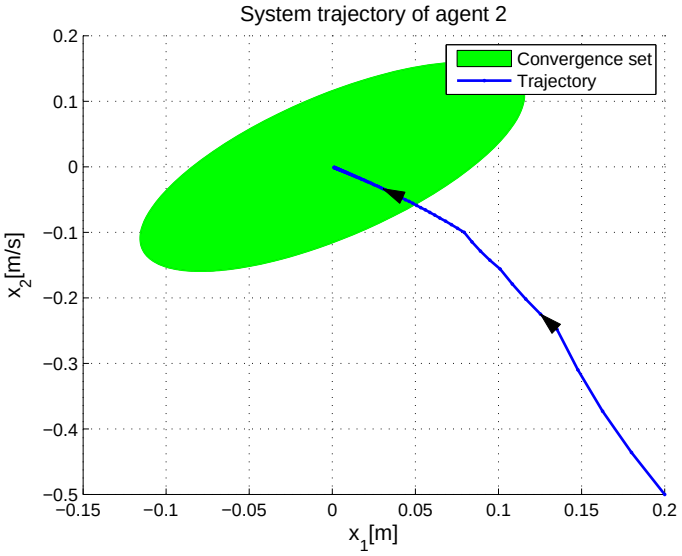

Figure 6.5: Trajectory of agent $\mathcal{A}_2$ and its convergence set.

satisfy the designed conditions.

Interesting future work will concern the following aspects: (1) The distributed MPC relies heavily on communications among subsystems. In practice, the communication networks may not be reliable, so the design of a robust distributed MPC considering communication constraints is to be pursued. (2) In this study, only the information on the bound of disturbances is used, but the distribution and statistical

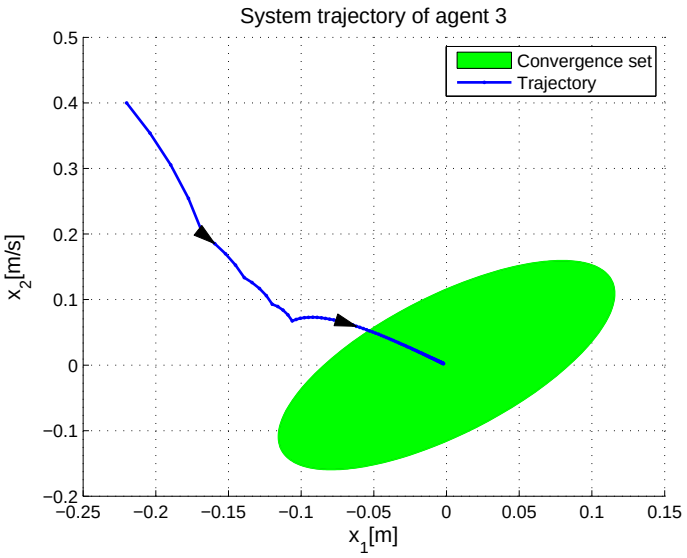

Figure 6.6: Trajectory of agent $\mathcal{A}_3$ and its convergence set.

information of disturbances is not incorporated into the analysis. Therefore, it is desirable to develop a stochastic distributed MPC to incorporate the statistical properties of the disturbances. (3) This study is focused on the large-scale system with decoupled subsystems. An extension can be made by tackling large-scale systems with coupled subsystems. These topics require further investigation.

Chapter 7

Distributed MPC of Large-scale Nonlinear Systems with Communication Delays

7.1 Introduction

Chapter 6 designs a novel distributed MPC algorithm to deal with the external disturbances by implicitly assuming that the communication networks are perfectly reliable. But this assumption may not hold in practice. The hardware constraints and/or network congestions are apt to induce communication imperfections such as time delays, especially when the communication networks shared by large-scale systems. The communication delays, resulting in delayed information exchange among subsystems, may inhibit the use of the existing distributed MPC strategies and render the results invalid. This motivates this chapter to consider communication delays when designing the distributed MPC for large-scale systems.

It is worthwhile to note that the distributed MPC problem for a class of decoupled discrete-time nonlinear systems with delayed system state has been investigated in [31], where the delayed information is dealt with by bounded disturbances. Unlike the work in [31], this chapter will investigate the distributed MPC problem for a class of decoupled continuous-time nonlinear systems, by explicitly incorporating the communication delays into the MPC design and rigorously analyzing its effect to the system performance. In addition, the communication delays considered in this chapter can be time-varying. To focus the attention to the issue of communication

delays, the external disturbances will not be considered in this chapter, but they will be further dealt with in next chapter. The main contributions of this chapter are two-fold:

- A robust distributed MPC scheme is designed. Based on the robustness constraint [70], and by proposing the waiting mechanism, a novel distributed MPC strategy is designed such that it can deal with bounded time-varying communication delays.

- The feasibility and stability analysis are conducted. In particular, the iterative feasibility of the proposed scheme is proved and the sufficient conditions for guaranteeing the closed-loop system stability are developed. We show that, the stability of the overall closed-loop systems is related to the upper bound of the communication delays, the sampling period and the cooperation weights. We believe that these results not only provide a rigorous tool for theoretical analysis, but also facilitate the design of distributed MPC with communication delays.

The rest of this chapter is organized as follows. In Section 7.2, the design problem is formulated and the preliminary assumption is presented. The delay-involved distributed MPC strategy is designed in Section 7.3. In Section 7.4, the feasibility and stability are analyzed. The theoretical result is verified in Section 7.5. Finally, the conclusion remarks are presented in Section 7.6.

The following notations will be used throughout the chapter. The real space is denoted by the symbol $\mathbb{R}$ and the collection of the integers $1, \cdots, M$, is represented as $\{M\}$. Given a matrix S, the transpose and inverse (if invertible) are denoted as S^{T} and S^{-1}, respectively. For a column vector v, the notation $\|v\|$ stands for the Euclidean norm and $\|v\|_S \triangleq \sqrt{v^{\mathrm{T}} S v}$ represents the S-weighted norm with respect to the matrix S. For a given matrix S, by $S > 0$ ($S \geqslant 0$) it means that the matrix S is positive definite (semi-positive definite); the notation $\lambda(S)$ stands for the eigenvalues of the matrix S; the maximum eigenvalue is denoted as $\bar{\lambda}(S)$ and the minimum one is denoted as $\underline{\lambda}(S)$. The column operation $[v_1^{\mathrm{T}}, v_2^{\mathrm{T}}, \cdots, v_n^{\mathrm{T}}]^{\mathrm{T}}$ is written as $\mathrm{col}\{v_1, v_2, \cdots, v_n\}$ for column vectors $v_1, v_2, \cdots, v_n$. Given two sets $A_2 \subseteq A_1 \subseteq \mathbb{R}^n$, the difference between the two sets is defined as $A_1 \setminus A_2 \triangleq \{x | x \in A_1, x \notin A_2\}$.

7.2 Problem Formulation and Preliminaries

Consider the large-scale nonlinear system that comprises M subsystems:

$$\dot{x}_i(t) = f_i(x_i(t), u_i(t)) \quad t \geqslant 0, x_i(0) = x_i^0, \tag{7.1}$$

where $i \in \{M\}$, is the subsystem index; $x_i(t) \in \mathbb{R}^n$ is the subsystem state; $u_i(t) \in \mathbb{R}^n$ is the control input; $f_i : \mathbb{R}^n \times \mathbb{R}^m \to \mathbb{R}^n$ is a twice continuously differentiable function with $f_i(0, 0) = 0$. Due to the actuator saturation, for each subsystem i, the control input $u_i(t)$ is constrained in a compact set $\mathcal{U}_i$ including the origin as an interior point. Assume that for any $x_i^0 \in \mathbb{R}^n$ and any piecewise continuous control input $u_i(t) \in \mathcal{U}_i$, the differential equation in (7.1) has an unique solution. The overall agent system can be characterized as:

$$\dot{x}(t) = f(x(t), u(t)) \quad t \geqslant 0, x(0) = x_0, \tag{7.2}$$

where $x(t) = \text{col}\{x_1(t), \cdots, x_M(t)\}$, $u(t) = \text{col}\{u_1(t), \cdots, u_M(t)\}$, $x_0 = \text{col}\{x_1^0, \cdots, x_M^0\}$, and $f(x(t), u(t)) = \text{col}\{f_1(x_1(t), u_1(t)), \cdots, f_M(x_M(t), u_M(t))\}$.

Suppose that each subsystem i can receive information from its neighboring subsystems (neighbors) whose indices are denoted by $\mathcal{N}_i$ with $\mathcal{N}_i \subseteq \{M\}$ and $\mathcal{N}_i \neq \emptyset$. The cooperation among the subsystems is achieved by designing the cooperation weights and the control objective function in (7.4). The cooperation weights from the subsystem i to its neighbors are designated as $r_{ij} > 0$, where $j \in \mathcal{N}_i$. Note that the described large-scale system associated with the communication topology/structure has been used for modeling many systems such as a group of vehicles [130], a team of robots [23, 31] and power generation systems [150].

In the existing frameworks of the distributed MPC [23, 31, 61], it is implicitly assumed that all the information can be transmitted successfully among the subsystems during the sampling period. In this study, we consider a more practical scenario. That is, for each subsystem, the information transmitted from its neighbors to itself will be subject to time-varying communication delays. The objective of this chapter is to design a distributed MPC strategy which explicitly takes into account the communication delays.

In what follows, some well-developed results are recalled. Consider the linearized

dynamics of each subsystem i:

$$\dot{x}_i(t) = A_i x_i(t) + B_i u_i(t), x_i(0) = x_i^0, \tag{7.3}$$

where $A_i = \partial f_i(x_i, u_i)/\partial x_i|_{(0,0)}$ and $B_i = \partial f_i(x_i, u_i)/\partial u_i|_{(0,0)}$.

Assumption 7.1. *[21, 11, 23] For the system in (7.3), there exists a state feedback control law $u_i(t) = K_i x_i(t)$ such that the closed-loop system $\dot{x}_i(t) = A_i^c x_i(t)$ is stable, where $A_i^c \triangleq A_i + K_i B_i$.*

Lemma 7.1. *[97, 11, 21, 70] Suppose that Assumption 7.1 is satisfied. For the subsystem in (7.1) with two matrices $R_i > 0$ and $Q_i > 0$, there exist a constant $\varepsilon_i > 0$, a stable state feedback control gain K_i and a matrix $P_i > 0$ such that: (1) The set $\Omega_i(\varepsilon_i) \triangleq \{x_i(t) : V_i(x_i(t)) \leqslant \varepsilon_i^2\}$ is an invariant set for the system $\dot{x}_i(t) = f_i(x_i(t), K_i x_i(t))$; (2) for any $x_i(t) \in \Omega_i(\varepsilon_i)$, the control input constraint is satisfied as $u_i(t) = K_i x_i(t) \in \mathcal{U}_i$ and it has $\dot{V}_i(x_i(t)) \leqslant -\|x_i(t)\|_{Q_i^*}^2$. Here, $V_i(x_i(t)) = \|x_i(t)\|_{P_i}^2$ and $Q_i^* = Q_i + K_i^{\mathrm{T}} R_i K_i$.*

7.3 Distributed MPC with Communication Delays

In this section, the modeling of the communication delays and a waiting mechanism are first presented. Then the constrained optimization problem and the delayed-involved distributed MPC scheme are proposed.

In order to describe the communication delays, let us first divide the time domain by the time instants t_k, $k = 0, 1 \cdots$. Assume that at the time instant t_k, all the subsystems generate the control signals simultaneously and send their state information to the subsystems that are connected to them. At the time $t_k + \delta$, each subsystem measures its system state, where δ is the sampling period. There are communication delays occurred for the transmitted information among the communication networks. As a result, each subsystem may not be able to receive its neighbors' information at the time $t_k + \delta$.

For each subsystem i, the communication delay of the transmitted information from its neighbor j to it, is denoted by τ_k^{ij} at time instant t_k, and it is assumed that $\tau_k^{ij} \leqslant \bar{\tau}$. Due to the communication delays, the information from the neighbor j will be received at $t_k + \delta + \tau_k^{ij}$ by the subsystem i. Define $\tau_k^i = \max_{j \in \mathcal{N}_i}\{\tau_k^{ij}\}$ and $\tilde{t}_k^i$ as the time instant when the subsystem i receives all the information from its neighbors.

It can be seen that $\tilde{t}^i_{k+1} = t_k + \delta + \tau^i_k$. Furthermore, define $\tau_k = \max_{i\in\{M\}}\{\tau^i_k\}$ and the time instant t_{k+1} that is used to synchronize all the subsystems, is determined as $t_{k+1} = t_k + \delta + \tau_k$. Note that the subsystem i could generate the control signal at time $\tilde{t}^i_{k+1}$ on its own, since it has already received all the information from its neighbors and sampled the system state. However, in order to keep the overall system synchronized, it will not generate the new control signal until the time t_{k+1} when all the subsystems receive their neighbors' information and the overall system can generate the new control signals simultaneously. This strategy on dealing with communication delays is referred to as the waiting mechanism. See an example in Figure 7.1 for more details [1].

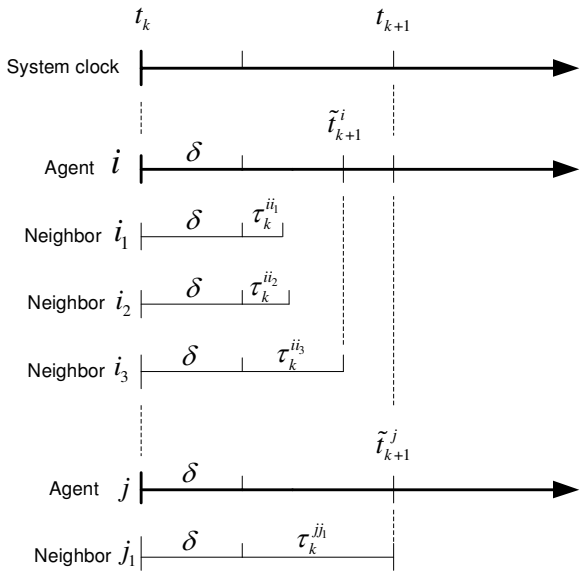

Figure 7.1: Example of applying the control actions according to the communication delays

.

For each subsystem i at time instant t_k, the cooperative control objective function

[1] In this example, there are two subsystems. One is the subsystem i with three neighbors i_1, i_2 and i_3, and the other is the subsystem j with one neighbor j_1. At time t_k, the overall system is synchronized and the optimal control inputs are applied for the subsystem i and j, and the assumed state information begins being transmitted from their neighbors to the subsystems i and j. The system states are measured at time instant $t_k + \delta$. For the subsystem i, the time delays from its neighbors to itself are $\tau^{ii_1}_k$, $\tau^{ii_2}_k$ and $\tau^{ii_3}_k$, respectively. Since $\tau^{ii_1}_k < \tau^{ii_2}_k < \tau^{ii_3}_k$, it has $\tau^i_k = \tau^{ii_3}_k$ and all the neighbors' information has been received at time $\tilde{t}^i_{k+1} = t_k + \delta + \tau^i_k$. For the subsystem j, the time delay from its neighbor to itself is $\tau^{jj_1}_k$. So $\tilde{t}^j_{k+1} = t_k + \delta + \tau^j_k = t_k + \delta + \tau^{jj_1}_k$. Since $\tau^j_k > \tau^i_k$, the synchronized time of the subsystem i and j will be at $t_{k+1} = t_k + \delta + \tau^{jj_1}_k$, and the subsystems i and j will generate and apply the new control signals at the time t_{k+1}.

is defined as:

$$J_i(\hat{x}_i(s;t_k),\hat{u}_i(s;t_k),\hat{x}^a_{-i}(s;t_k)) \triangleq \int_{t_k}^{t_k+T} \|\hat{x}_i(s;t_k)\|^2_{Q_i} + \|\hat{u}_i(s;t_k)\|^2_{R_i} + \sum_{j\in\mathcal{N}_i} r_{ij}\|\hat{x}_i(s;t_k)-\hat{x}^a_j(s;t_k)\|^2_{Q_{ij}}ds + \|\hat{x}_i(t_k+T;t_k)\|^2_{P_i}, \tag{7.4}$$

where $\hat{x}_i(s;t_k)$ is the state trajectory governed by $\dot{\hat{x}}_i(s;t_k) = f_i(\hat{x}_i(s;t_k),\ \hat{u}_i(s;t_k))$; $\hat{u}_i(s;t_k)$ is the control trajectory to be designed; $\hat{x}^a_j(s;t_k)$, $j\in\mathcal{N}_i$, are the assumed state trajectories of the neighbors of the subsystem i, which will be specified in **Problem** $\mathcal{P}_i$; the matrices P_i, Q_i and R_i are determined by satisfying Lemma 7.1; $Q_{ij}>0$, $j\in\mathcal{N}_i$ are the given cooperation matrices; $r_{ij}, j\in\mathcal{N}_i$ are the cooperation weights to be designed; T is the prediction horizon satisfying $T\geqslant\delta+\bar{\tau}$. Note that the similar control objective function has been used in many works, such as [23, 31, 61], to achieve cooperation. However, there are two differences for the control objective function in (7.4) because of the communication delays. In general, the prediction horizon is required as $T>\delta$ and the relationship $t_{k+1}-t_k=\delta$ holds. But in this study, it is required that $T\geqslant\delta+\bar{\tau}$ and we have $t_{k+1}-t_k=\delta+\tau_k$.

For each subsystem i at time t_k, the control trajectory is generated by solving the following optimization problem:

$$\begin{aligned} \textit{Problem } \mathcal{P}_i: \hat{u}^*_i(s;t_k) =& \arg\min_{\hat{u}_i(s;t_k)} J_i(\hat{x}_i(s;t_k),\hat{u}_i(s;t_k),\hat{x}_{-i}(s;t_k)), \text{subject to:}\\ & \dot{\hat{x}}_i(s;t_k) = f_i(\hat{x}_i(s;t_k),\hat{u}_i(s;t_k)), s\in[t_k,t_k+T]\\ & \dot{\hat{x}}^a_j(s;t_k) = f_j(\hat{x}^a_j(s;t_k),\hat{u}^a_j(s;t_k)), s\in[t_k,t_k+T]\\ & \hat{u}_i(s;t_k)\in\mathcal{U}_i, s\in[t_k,t_k+T]\\ & \|\hat{x}_i(s;t_k)\|_{P_i}\leqslant\frac{T\alpha_i}{s-t_k}\varepsilon_i, s\in[t_k+\delta,t_k+T]. \end{aligned} \tag{7.5}$$

Here, $\hat{u}^a_j(s;t_k)$, $j\in\mathcal{N}_i$, is the assumed control trajectory, $\hat{x}^a_j(s;t_k)$ is called the assumed state trajectory for the neighboring subsystem j, $\hat{u}^*_j(s;t_k)$ is the optimal control trajectory, $\hat{x}^*_i(s;t_k)$ is the optimal state trajectory, the parameter α_i $(1>\alpha_i>0)$ is a constant used to adjust the robustness constraint in (7.5), ε_i is the parameter of the terminal set which can be determined from Lemma 7.1.

It is noted that the robustness constraint (7.5) in Problem $\mathcal{P}_i$ has been used to

deal with the effect of the external disturbance in [70]. In this study, this robustness constraint is adopted to render the state trajectory bounded by a decreasing function, enhancing the stability of the closed-loop system, so that it is capable of tolerating the communication delays.

For each subsystem i at time t_k, the assumed state trajectory to be used at time t_{k+1} is generated by $\dot{\hat{x}}_i^a(s;t_{k+1}) = f_i(\hat{x}_i^a(s;t_{k+1}), \hat{u}_i^a(s;t_{k+1}))$, $s \in [t_{k+1},\, t_{k+1}+T]$, with $\hat{x}_i^a(t_{k+1};t_{k+1}) = \hat{x}_i^*(t_{k+1},t_k)$. The assumed control trajectory $\hat{u}_i^a(s;t_{k+1})$ is generated similarly as in [23, 21, 31]:

$$\hat{u}_i^a(s;t_{k+1}) = \begin{cases} \hat{u}_i^*(s;t_k), & \text{if} \quad s \in [t_{k+1}, t_k+T] \\ K_i\hat{x}_i^a(s;t_{k+1}), & \text{if} \quad s \in [t_k+T, t_{k+1}+T]. \end{cases} \tag{7.6}$$

Here, we also employ the so-called dual-mode MPC scheme for each subsystem i [97, 21, 70]. Specifically, the control signal is generated by solving Problem $\mathcal{P}_i$ when the state of the subsystem i is not in the terminal set $\Omega_i(\varepsilon_i)$; the control signal is switched to the state feedback control law $u_i(t) = K_i x_i(t)$ when the state is in the terminal set.

By integrating the control signal generation mechanism, the generation of the assumed state trajectories, and the dual-mode MPC mechanism, the delay-involved distributed MPC scheme can be described as follows:

Step 1 For each subsystem i, at time t_k, if the state is in the terminal set $\Omega_i(\varepsilon_i)$, go to **Step 5**; otherwise, generate the optimal control trajectory $\hat{u}_i^*(s;t_k)$, $s \in [t_k, t_k+T]$ by solving the optimization problem $\mathcal{P}_i$; generate the assumed state trajectory $\hat{x}_i^a(s;t_{k+1})$, $s \in [t_{k+1}, t_{k+1}+T]$ and send it out.

Step 2 During the time interval $[t_k, t_k+\delta+\tau_k^i]$, apply the control input $\hat{u}_i^*(s;t_k)$; measure its state at time $t_k+\delta$ and receive all the assumed states of its neighbors at time $t_k+\delta+\tau_k^i$.

Step 3 During the time interval $[t_k+\delta+\tau_k^i, t_k+\delta+\tau_k]$, still apply the control input $\hat{u}_i^*(s;t_k)$; at time t_{k+1}, synchronize the subsystem i according to the system clock.

Step 4 Repeat **Step 1** to **Step 3**.

Step 5 Generate the control input as $u_i(s;t_k) = K_i x_i(s;t_k)$ and the assumed state trajectory $\hat{x}_i^a(s;t_{k+1})$ as $x_i(s;t_{k+1})$ by $\dot{x}_i(s;t_{k+1}) = f_i(x_i(s;t_{k+1}),\, K_i x_i(s;t_{k+1}))$

and send the assumed state trajectory out.

Remark 7.1. *It is worthwhile to note that all the subsystems are likely to become asynchronous due to the communication delays, so they need to be synchronized at each time t_k as in* **Step 3**. *This is different from the scheme in [70, 23, 61] where all the subsystems only need to be synchronized at the initial time instant and will be automatically synchronized in the following time instants. In addition, the delay-involved MPC scheme amounts to the classic MPC scheme with time-varying sampling periods if a sampling period $\delta_k^{'}$ is re-defined as $\delta_k^{'} = \delta + \tau_k$ (this is because $t_{k+1} - t_k = \delta + \tau_k$ and τ_k is time-varying). Therefore, the feasibility and stability analysis of the distributed MPC with communication delays is more challenging, yet necessary.*

7.4 Analysis

In this section, we first study the iterative feasibility problem for the delay-involved distributed MPC scheme. Then the stability of the closed-loop system is analyzed. Accordingly, the stability conditions including the bound of the communication delays are established.

7.4.1 Feasibility Analysis

In order to prove the iterative feasibility of the delay-involved distributed MPC scheme, an assumption for the initial feasibility is made.

Assumption 7.2. *For each subsystem i, given the prediction horizon $T > \delta + \bar{\tau}$, there exists a feasible solution to Problem $\mathcal{P}_i$ for some initial state x_i^0 and the initial assumed state trajectories $x_j(s; t_0) = 0$, where $j \in \mathcal{N}_i$ and $s \in [t_0, t_1]$.*

It is noted that Assumption 7.2 is fairly standard. The similar assumption has been made in [23, 21, 61] for the distributed MPC. For each subsystem i with the given prediction horizon T, we denote the set consisting of all the initial states in which Problem $\mathcal{P}_i$ admits a feasible solution as the feasible set $\mathcal{Z}_i$. The feasible set for the overall system is defined as $\mathcal{Z} \triangleq \mathcal{Z}_1 \cdots \times \cdots \mathcal{Z}_M$.

Theorem 7.1. *For the system in (7.2), suppose that Assumption 7.1 and 7.2 hold for each subsystem. Then the proposed delay-involved distributed MPC scheme is iteratively feasible in the feasible set $\mathcal{Z}$.*

Proof. The proof is derived by induction. Firstly, according to Assumption 7.2, the constrained optimization problem $\mathcal{P}_i$ associated with each subsystem i is feasible at time t_0 for any $x_i^0 \in \mathcal{Z}_i$. Second, we assume that the constrained optimization problem $\mathcal{P}_i$ is feasible at time t_k, $k \geqslant 1$, for each subsystem i. Third, we need to prove that there exists a feasible solution to Problem $\mathcal{P}_i$ at time t_{k+1} base on the optimal solution at time t_k. Similar to [97, 23, 21], for each subsystem i at time t_{k+1}, we choose the conventional feasible solution (control trajectory) candidate as

$$\tilde{u}_i(s;t_{k+1}) = \begin{cases} \hat{u}_i^*(s;t_k), & \text{if} \quad s \in [t_{k+1}, t_k + T], \\ K_i\tilde{x}_i(s;t_{k+1}), & \text{if} \quad s \in [t_k + T, t_{k+1} + T]. \end{cases} \tag{7.7}$$

where $\tilde{x}_i(s;t_{k+1})$ is the system state trajectory generated by the feasible control trajectory candidate $\tilde{u}_i(s;t_{k+1})$. In what follows, we shall prove that the candidate $\tilde{u}_i(s;t_{k+1})$, $s \in [t_{k+1}, t_{k+1} + T]$ is indeed a feasible solution at time t_{k+1}.

S1) The control input constraint is satisfied. Since $\hat{u}_i^*(s;t_k)$ is the optimal solution to Problem $\mathcal{P}_i$ at time t_k, it can be seen that $\tilde{u}_i(s;t_{k+1}) \in \mathcal{U}_i$ for $s \in [t_{k+1}, t_k+T]$. According to the robustness constraint in (7.5) and $\tilde{x}_i(t_k + T;t_{k+1}) = \hat{x}_i^*(t_k + T;t_k)$, one has $\hat{x}_i^*(t_k + T;t_k) \in \Omega_i(\varepsilon_i)$. Therefore, in terms of Lemma 7.1, we have $\tilde{u}_i(s;t_{k+1}) = K_i\tilde{x}_i(s;t_{k+1}) \in \mathcal{U}_i$ for $s \in [t_k + T, t_{k+1} + T]$. That is, the control trajectory candidate $\tilde{u}_i(s;t_{k+1})$, $s \in [t_{k+1}, t_{k+1} + T]$, satisfies the control input constraint.

S2) The robustness constraint in (7.5) is satisfied. Firstly, we derive an upper bound of the feasible state candidate $\tilde{x}_i(s;t_{k+1})$, $s \in [t_k + T, t_{k+1} + T]$. Since the state feedback control law $K_i\tilde{x}_i(s;t_{k+1})$ is applied during this interval, we have $V_i(\tilde{x}_i(s;t_{k+1})) \leqslant -\|\tilde{x}_i(s;t_{k+1})\|_{Q_i^*}^2$ according to Lemma 7.1. Similar to [70, 21], by applying the comparison principle [64], we can obtain

$$\|\tilde{x}_i(s;t_{k+1})\|_{P_i} \leqslant F_1(s), s \in [t_k + T, t_{k+1} + T], \tag{7.8}$$

where $F_1(s) \triangleq \alpha_i\varepsilon_i e^{-\underline{\lambda}(Q_i^*)(s-t_k-T)/(2\bar{\lambda}(P_i))}$. Second, we complete the proof by discussing three cases.

- Case I: $\delta+\tau_k \leqslant T < 2\delta+\tau_k$. In this situation, one has $t_{k+1} \leqslant t_k+T < t_{k+1}+\delta$. According to (7.8), we have $\|\tilde{x}_i(s;t_{k+1})\|_{P_i} \leqslant F_1(s) \leqslant T\alpha_i\varepsilon_i/(s - t_{k+1})$, $s \in [t_{k+1} + \delta, t_{k+1} + T]$.

- Case II: $2\delta + \tau_k \leqslant T < 2\delta + \tau_k + \tau_{k+1}$. In this case, one has $t_{k+1} + \delta \leqslant t_k + T < t_{k+1} + \delta + \tau_{k+1}$. For $s \in [t_{k+1} + \delta, t_k + T]$, we have $\|\tilde{x}_i(s; t_{k+1})\|_{P_i} = \|\hat{x}_i^*(s; t_k)\|_{P_i} \leqslant T\alpha_i\varepsilon_i/(s - t_k) \leqslant T\alpha_i\varepsilon_i/(s - t_{k+1})$. For $s \in [t_k + T, t_{k+1} + T]$, we can obtain $\|\tilde{x}_i(s; t_{k+1})\|_{P_i} \leqslant F_1(s) \leqslant T\alpha_i\varepsilon_i/(s - t_{k+1})$ in terms of (7.8).
- Case III: $2\delta + \tau_k + \tau_{k+1} \leqslant T < T + \tau_k + \delta$. In this case, one has $t_{k+1} + \delta + \tau_{k+1} \leqslant t_k + T < t_{k+1} + T$. The similar result of Case II can be applied to derive $\|\tilde{x}_i(s; t_{k+1})\|_{P_i} \leqslant T\alpha_i\varepsilon_i/(s - t_{k+1})$, $s \in [t_{k+1} + \delta, t_{k+1} + T]$.

By summarizing S1) and S2), we have shown that the robustness constraint and the control input constraint are satisfied at time t_{k+1}, i.e., $\tilde{u}_i(s; t_{k+1})$, $s \in [t_{k+1}, t_{k+1} + T]$, is a feasible solution to Problem $\mathcal{P}_i$. The proof is completed. □

7.4.2 Stability Analysis and Delay Bounds

In order to prove the stability of the overall system, we first present an important result in the following lemma.

Lemma 7.2. *For the overall system in (7.2) by implementing the delay-involved distributed MPC scheme, suppose that Assumption 7.1 and 7.2 hold. For each subsystem i, if the system state $x_i(s; t_k) \in \mathcal{Z}_i \setminus \Omega_i(\varepsilon_i)$, $s \in [t_k, t_{k+1}]$, then the following holds:*

$$\begin{aligned}\Delta J_i(x_i^*(s; t_k)) < & -(\delta + \tau_k)\frac{\underline{\lambda}(Q_i)}{\bar{\lambda}(P_i)}\varepsilon_i^2 \\ & + \sum_{j \in \mathcal{N}_i} r_{ij} \int_{t_{k+1}}^{t_k + T} [\lambda(Q_{ij}, P_i)\alpha_i\varepsilon_i + \lambda(Q_{ij}, P_j)\alpha_j\varepsilon_j]^2 \frac{T^2}{(s - t_k)^2} ds \\ & + (\delta + \tau_k) \sum_{j \in \mathcal{N}_i} r_{ij} [\lambda(Q_{ij}, P_i)\alpha_i\varepsilon_i + \lambda(Q_{ij}, P_j)\alpha_j\varepsilon_j]^2,\end{aligned}$$

where

$$\begin{aligned}\Delta J_i(x_i^*(s; t_k)) \triangleq & J_i(\hat{x}_i^*(s; t_{k+1}), \hat{u}_i^*(s; t_{k+1}), \hat{x}_{-i}^a(s; t_{k+1})) \\ & - J_i(\hat{x}_i^*(s; t_k), \hat{u}_i^*(s; t_k), \hat{x}_{-i}^a(s; t_k)).\end{aligned}$$

Proof. Let us start by considering $\Delta\tilde{J}_i(x_i^*(s; t_k))$, which is defined by $J_i(\tilde{x}_i(s; t_{k+1}),$

$\tilde{u}_i(s;t_{k+1})$, $\hat{x}^a_{-i}(s;t_{k+1}))$ $-J_i(\hat{x}^*_i(s;t_k)$, $\hat{u}^*_i(s;t_k), \hat{x}^a_{-i}(s;t_k))$. Specifically, we have

$$
\begin{aligned}
&\Delta\tilde{J}_i(x^*_i(s;t_k))\\
=&\int_{t_k+T}^{t_{k+1}+T} \|\tilde{x}_i(s;t_{k+1})\|^2_{Q_i} + \|\tilde{u}_i(s;t_{k+1})\|^2_{R_i} + r_{ij}\sum_{j\in\mathcal{N}_i}\|\tilde{x}_i(s;t_{k+1})\\
&-\hat{x}^a_j(s;t_{k+1})\|^2_{Q_{ij}}ds + \int_{t_{k+1}}^{t_k+T} \|\tilde{x}_i(s;t_{k+1})\|^2_{Q_i} + \|\tilde{u}_i(s;t_{k+1})\|^2_{R_i}\\
&+ r_{ij}\sum_{j\in\mathcal{N}_i}\|\tilde{x}_i(s;t_{k+1}) - \hat{x}^a_j(s;t_{k+1})\|^2_{Q_{ij}}ds\\
&-\int_{t_{k+1}}^{t_k+T} \|\hat{x}^*_i(s;t_k)\|^2_{Q_i} + \|\hat{u}^*_i(s;t_k)\|^2_{R_i} + r_{ij}\sum_{j\in\mathcal{N}_i}\|\hat{x}^*_i(s;t_k) - \hat{x}^a_j(s;t_k)\|^2_{Q_{ij}}ds\\
&-\int_{t_k}^{t_{k+1}} \|\hat{x}^*_i(s;t_k)\|^2_{Q_i} + \|\hat{u}^*_i(s;t_k)\|^2_{R_i} + r_{ij}\sum_{j\in\mathcal{N}_i}\|\hat{x}^*_i(s;t_k) - \hat{x}^a_j(s;t_k)\|^2_{Q_{ij}}ds\\
&+\|\tilde{x}_i(t_{k+1}+T;t_{k+1})\|^2_{P_i} - \|x^*_i(t_k+T;t_k)\|^2_{P_i}.
\end{aligned}
$$

According to the feasible control trajectory in (7.7), one has $\hat{u}^*_i(s;t_k) = \tilde{u}_i(s;t_{k+1})$ and $\tilde{x}_i(s;t_{k+1}) = \hat{x}^*_i(s;t_k)$ for $s \in [t_{k+1}, t_k+T]$. By plugging these results into $\Delta\tilde{J}_i(x^*_i(s;t_k))$, we obtain

$$
\begin{aligned}
&\Delta\tilde{J}_i(x^*_i(s;t_k))\\
\leqslant&\int_{t_k+T}^{t_{k+1}+T} \|\tilde{x}_i(s;t_{k+1})\|^2_{Q_i} + \|\tilde{u}_i(s;t_{k+1})\|^2_{R_i}ds + \|\tilde{x}_i(t_{k+1}+T;t_{k+1})\|^2_{P_i}\\
&-\|x^*_i(t_k+T;t_k)\|^2_{P_i} + \int_{t_{k+1}}^{t_{k+1}+T} r_{ij}\sum_{j\in\mathcal{N}_i}\|\tilde{x}_i(s;t_{k+1}) - \hat{x}^a_j(s;t_{k+1})\|^2_{Q_{ij}}ds\\
&-\int_{t_k}^{t_{k+1}} \|\hat{x}^*_i(s;t_k)\|^2_{Q_i} + \|\hat{u}^*_i(s;t_k)\|^2_{R_i}ds.
\end{aligned}
$$

Since $\tilde{x}_i(t_k+T;t_{k+1}) = \hat{x}^*_i(t_k+T;t_k) \in \Omega_i(\varepsilon_i)$ and $\tilde{u}_i(s;t_{k+1}) = K_i\tilde{x}_i(s;t_{k+1})$, for $s \in [t_k+T, t_{k+1}+T]$, Lemma 7.1 can be utilized. As a result, $\|\tilde{x}_i(s;t_{k+1})\|^2_{Q_i}$ $+\|\tilde{u}_i(s;t_{k+1})\|^2_{R_i} \leqslant -\dot{V}_i(\tilde{x}_i(s;t_{k+1}))$. Thus,

$$
\begin{aligned}
\Delta\tilde{J}_i(x^*_i(s;t_k)) \leqslant&\int_{t_{k+1}}^{t_{k+1}+T} r_{ij}\sum_{j\in\mathcal{N}_i}\|\tilde{x}_i(s;t_{k+1}) - \hat{x}^a_j(s;t_{k+1})\|^2_{Q_{ij}}ds\\
&-\int_{t_k}^{t_{k+1}} \|\hat{x}^*_i(s;t_k)\|^2_{Q_i} + \|\hat{u}^*_i(s;t_k)\|^2_{R_i}ds.
\end{aligned}
$$

Due to $x_i(s;t_k) \in \mathcal{Z}_i \setminus \Omega_i(\varepsilon_i), s \in [t_k, t_{k+1}]$, it can be obtained

$$\begin{aligned}\Delta\tilde{J}_i(x_i^*(s;t_k)) <& r_{ij}\sum_{j\in\mathcal{N}_i}\int_{t_{k+1}}^{t_{k+1}+T}[\|\tilde{x}_i(s;t_{k+1})\|_{Q_{ij}} + \|\hat{x}_j^a(s;t_{k+1})\|_{Q_{ij}}]^2 ds \\ & - (\delta+\tau_k)\frac{\underline{\lambda}(Q_i)}{\bar{\lambda}(P_i)}\varepsilon_i^2. \end{aligned} \tag{7.9}$$

In terms of the satisfaction of the robustness constraint in (7.5), one gets

$$\|\tilde{x}_i(s;t_{k+1})\|_{Q_{ij}} \leqslant \lambda(Q_{ij},P_i)\|\tilde{x}_i(s;t_{k+1})\|_{P_i} \leqslant \lambda(Q_{ij},P_i)\frac{T\alpha_i}{s-t_k}\varepsilon_i, s \in [t_k, t_k+T]. \tag{7.10}$$

Analogously, one has

$$\|\hat{x}_j^a(s;t_{k+1})\|_{Q_{ij}} \leqslant \lambda(Q_{ij},P_j)\|\hat{x}_j^a(s;t_{k+1})\|_{P_j} \leqslant \lambda(Q_{ij},P_j)\frac{T\alpha_j}{s-t_k}\varepsilon_j, s \in [t_k, t_k+T]. \tag{7.11}$$

In addition, since $\tilde{x}_i(t_k+T;t_{k+1}) = \hat{x}_i^*(t_k+T;t_k) \in \Omega_i(\alpha_i\varepsilon_i)$ and $\tilde{u}_i(s;t_{k+1}) = K_i\tilde{x}_i(s;t_{k+1})$ is applied for $s \in [t_k+T, t_{k+1}+T]$, it can be obtained

$$\|\tilde{x}_i(s;t_{k+1})\|_{Q_{ij}} \leqslant \lambda(Q_{ij},P_i)\|\tilde{x}_i(s;t_{k+1})\|_{P_i} \leqslant \lambda(Q_{ij},P_i)\alpha_i\varepsilon_i, s \in [t_k+T, t_{k+1}+T]. \tag{7.12}$$

Using the same line of reasoning as (7.12), for $s \in [t_k+T, t_{k+1}+T]$, we have

$$\|\hat{x}_j^a(s;t_{k+1})\|_{Q_{ij}} \leqslant \lambda(Q_{ij},P_j)\|\hat{x}_j(s;t_{k+1})\|_{P_j} \leqslant \lambda(Q_{ij},P_j)\alpha_j\varepsilon_j, . \tag{7.13}$$

By substituting (7.11)–(7.13) into (7.9) and applying $\Delta J_i(x_i^*(s;t_k)) \leqslant \Delta\tilde{J}_i(x_i^*(s;t_k))$, the result in Lemma 7.2 can be obtained. This completes the proof. □

Based on Lemma 7.2, the stability result is summarized in the following Theorem 7.2.

Theorem 7.2. *For the overall system in (7.2) with initial state $x_0 \in \mathcal{Z}$, suppose that Assumption 7.1 and 7.2 hold and the delay-involved distributed MPC scheme is used. Then the state of the overall system is stabilized to the equilibrium point, if the communication delays are bounded as*

$$\tau_k \leqslant \frac{b_i + \sqrt{4b_i - 3b_i^2}}{2(b_i-1)}T - \delta, \quad i = 1, \cdots, M, \tag{7.14}$$

the parameter b_i is designed as $b_i \in (1, 4/3)$ and the sampling period is designed as

$$\delta \in \left[\frac{(b_i - \sqrt{4b_i - 3b_i^2})T}{2(b_i - 1)}, \frac{(b_i + \sqrt{4b_i - 3b_i^2})T}{2(b_i - 1)} \right], \quad i = 1, \cdots, M,$$

where $b_i \triangleq \sum_{j \in \mathcal{N}_i} r_{ij}[\lambda_{ij}\alpha_i + \bar{\lambda}_{ij}\varepsilon_j\varepsilon_i^{-1}\alpha_j]^2$, $\lambda_{ij} \triangleq \lambda(Q_{ij}, P_i)\sqrt{\bar{\lambda}(P_i)}(\underline{\lambda}(Q_i))^{-0.5}$, $\bar{\lambda}_{ij} \triangleq \lambda(Q_{ij}, P_j)\ \sqrt{\bar{\lambda}(P_i)}(\underline{\lambda}(Q_i))^{-0.5}$ and $j \in \mathcal{N}_i$.

Proof. Consider each subsystem i, $i \in \mathcal{M}$. If $x_i^0 \in \Omega_i(\varepsilon_i)$, then the state feedback control law $u_i(t) = K_i x_i(t)$ will be used because of the dual-mode mechanism. According to Lemma 7.1, one has $\dot{V}_i(x_i(t)) \leqslant -\|x_i(t)\|^2_{Q_i^*}$. By the Lyapunov theory, the system state of the subsystem i converges to zero. If $x_i^0 \in \mathcal{Z}_i \setminus \Omega_i(\varepsilon_i)$, the control signal will be generated by solving Problem $\mathcal{P}_i$. In particular, if $k \geqslant 0$, $\hat{x}_i^*(s; t_k) \in \mathcal{Z}_i \setminus \Omega_i(\varepsilon_i)$ for $s \in [t_k, t_{k+1}]$, the result in Lemma 7.2 holds. As a result, we have

$$\begin{aligned}
\Delta J_i(x_i^*(s; t_k)) < & -(\delta + \tau_k)\frac{\underline{\lambda}(Q_i)}{\bar{\lambda}(P_i)}\varepsilon_i^2 \\
& + \sum_{j \in \mathcal{N}_i} r_{ij}[\lambda(Q_{ij}, P_i)\alpha_i\varepsilon_i T + \lambda(Q_{ij}, P_j)\alpha_j\varepsilon_j T]^2 \left[\frac{1}{\delta + \tau_k} - \frac{1}{T} \right] \\
& + (\delta + \tau_k) \sum_{j \in \mathcal{N}_i} r_{ij}[\lambda(Q_{ij}, P_i)\alpha_i\varepsilon_i + \lambda(Q_{ij}, P_j)\alpha_j\varepsilon_j]^2,
\end{aligned}$$

Substituting the delay bound (7.14) into the above inequality, one gets $\Delta J_i(x_i^*(s; t_k)) < 0$. By using the same argument in [97], it can be obtained that the subsystem state will enter the terminal state in some time $\bar{t}_i < \infty$, i.e., $x_i^*(\bar{t}_i) \in \Omega_i(\varepsilon_i)$. According to the dual-mode mechanism, the state feedback signal $u_i(t) = K_i x_i(t)$ will be applied for all $t > \bar{t}_i$. Therefore, the system state of the subsystem i will converge to zero. The proof is completed. □

Remark 7.2. *From the proof of Theorem 7.2, it can be observed that the system state will first enter the terminal set under the control signal generated by solving optimization problem. Then it will be driven into the origin by the state feedback control signal. Theorem 7.2 provides sufficient conditions for ensuring stability, and it reals that the stability of the closed-loop system is affected by the bound of the communication delays, the sampling period and the parameter b_i which is determined by the cooperation weights.*

7.5 Simulation

In order to test the proposed distributed MPC scheme and verify the theoretical result, the simulation studies are conducted in this section.

7.5.1 System Setup

The system to be tested is a mechanical system consisting of three cart-damper-spring subsystems. For each cart-damper-spring subsystem i, $i = 1, 2, 3$, the system dynamics is described as follows:

$$\begin{cases} \dot{x}_{i,1}(t) = x_{i,2}(t), \\ \dot{x}_{i,2}(t) = -\frac{\kappa}{M_c} e^{-x_{i,1}(t)} x_{i,1}(t) - \frac{h_d}{M_c} x_{i,2}(t) + \frac{u_i(t)}{M_c}, \end{cases}$$

where $x_{i,1}(t)$ is the displacement of the cart, $x_{i,2}(t)$ denotes its velocity, $\kappa = 0.25$N/m is the spring factor, $M_c = 1.5$kg is the mass of the cart, $h_d = 0.25$ N.s/m is the damper factor and $u_i(t)$ is the control input. Note that the same model has been used in [124] for testing the classic MPC and in [70] for the robust distributed MPC without communication delays. In the overall system, each subsystem is connected with its neighbors according to the following communication links: the neighboring indices for the subsystem $1, 2, 3$ are $\mathcal{N}_1 = \{2, 3\}$, $\mathcal{N}_2 = \{1, 3\}$ and $\mathcal{N}_3 = \{1, 2\}$, respectively.

In designing the distributed MPC, the matrices $Q_i = I$, $R_i = 0.1$ and $Q_{ij} = 0.1I$, where $i = 1, 2, 3$ and $j \in \mathcal{N}_i$. The matrix P_i is designed as $P_i = [4.5619, -2.2731; -2.2731, 2.4026]$ and the level set value ε_i of the terminal set is determined as $\varepsilon_i = 0.31$ using the approaches in [11, 97]; the shrinkage rates of the terminal set are $\alpha_1 = 0.9$, $\alpha_1 = 0.8$ and $\alpha_1 = 0.85$, respectively. The cooperation weights are designed as $r_{12} = 0.7032$, $r_{13} = 0.7032$, $r_{21} = 0.7343$, $r_{23} = 0.7343$, $r_{31} = 0.6957$ and $r_{32} = 0.6957$. The prediction horizon is $T = 2$sec. The constants b_i, $i = 1, 2, 3$ are determined as $b_1 = 1.3$, $b_2 = 1.28$ and $b_3 = 1.25$, respectively. It can be seen that the cooperation weights satisfy the condition in Theorem 7.2. The sampling period is designed as $\delta = 0.8$sec, which is in the bound $[0.7226, 1.2774]$ determined in Theorem 7.2. Furthermore, in terms of Theorem 7.2, the bound of communication delays is determined as $\tau = 1.2774 - \delta = 0.4774$sec.

The initial states of each subsystem are given as $x_1^0 = [0.6, -0.2]$, $x_2^0 = [-0.6, 0.2]$ and $x_3^0 = [-0.2, -0.2]$, respectively. The communication delays are generated ran-

domly with the specified bound $\tau \leqslant 0.4$sec, which satisfies Theorem 7.2. The delays occurring for subsystems are illustrated in Figure 7.2.

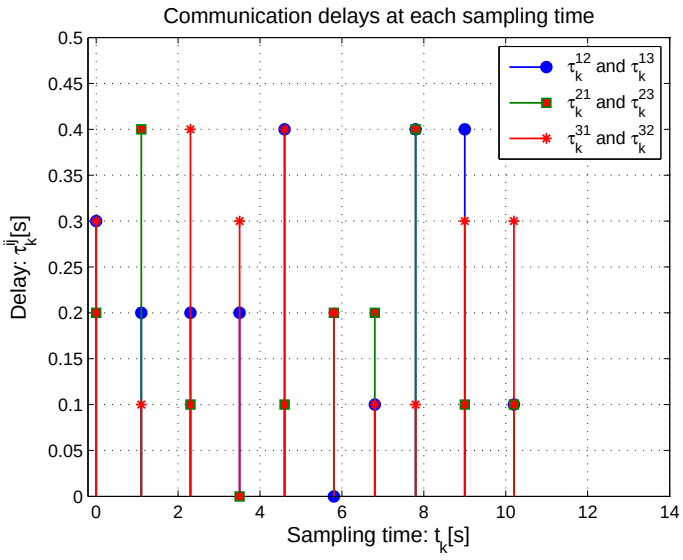

Figure 7.2: Delays of each subsystem and delays for overall system.

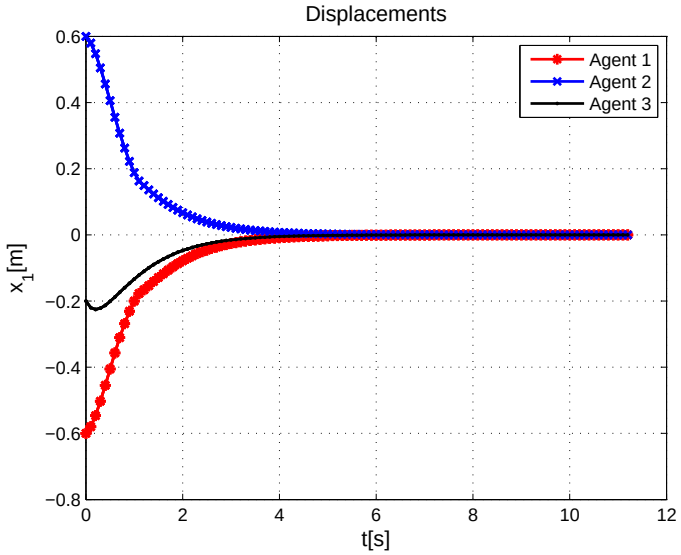

Figure 7.3: Displacements of the closed-loop system.

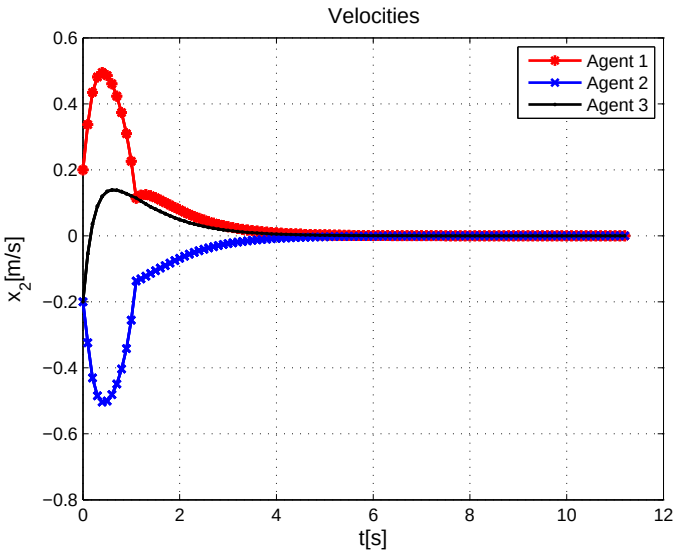

Figure 7.4: Velocities of the closed-loop system.

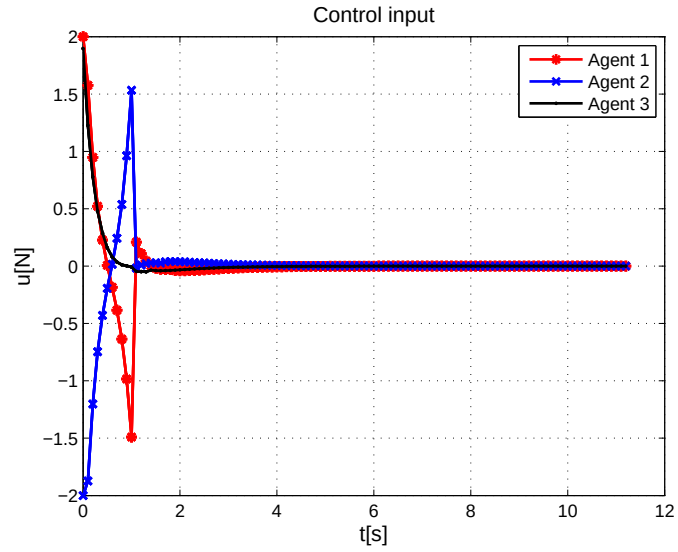

Figure 7.5: Control inputs of the overall system.

7.5.2 Simulation Results

By applying the proposed delay-involved distributed MPC to the multi-agent system consisting of three cart-damper-spring subsystems, the displacements and velocities are illustrated in Figure 7.3 and Figure 7.4, respectively. The control input is depicted in Figure 7.5. From Figure 7.3 and 7.4, it can be seen that the system state converges to zero, which verifies Theorem 7.2. By observing the control inputs in Figure 7.5, it

reveals that the control input constraints are satisfied and the proposed distributed MPC scheme is feasible.

7.6 Conclusion

In this work, a distributed MPC scheme has been proposed for large-scale decoupled nonlinear systems by addressing the communication delays. By employing the robustness constraint and waiting mechanism, the proposed distributed MPC scheme is capable of dealing with bounded communication delays. The iterative feasibility of the proposed scheme is proven and the stability conditions including the delay bounds and the design of the cooperation weights are developed. These conditions provide a useful criterion for practitioners to design distributed MPC strategy of large-scale nonlinear systems.

Chapter 8

Robust Distributed MPC of Large-Scale Nonlinear Systems: Handling Communication Delays and Disturbances

8.1 Introduction

In previous two chapters, two issues, i.e., external disturbances and communication delays, are dealt with separately. It is well recognized that the design of the distributed MPC strategy for practical large-scale systems is apt to encounter the two main issues simultaneously. This chapter will further research by considering a more practical case: Large-scale nonlinear systems simultaneously subject to bounded disturbances and communication delays. Due to the co-existence of communication delays and external disturbances, the system state used as an initial value for the optimization problem is not available. Thus, the system state trajectory needs to be estimated when communication delays occur, and a new robust distributed MPC scheme needs to be designed accordingly. The novel robust distributed MPC also necessitates the investigation of the feasibility and stability issues, especially by considering the co-effect of communication delays and external disturbances. Extensions to jointly consider communication delays and external disturbances in distributed MPC design bring essential technical difficulties which are resolved in this chapter. The main contributions of this study are three-fold.

- A dual-mode robust distributed MPC strategy, being capable of handling the communication delays and external disturbances simultaneously, is proposed. In order to address the co-effect of the communication delays and external disturbances, the robustness constraint [70, 69] is incorporated into the optimization problem. In addition, a post-predicted state trajectory (which is defined in (8.11)) is generated when communication delays occur, and the post-prediction state is designed as the initial system state for the optimization Problem 8.1.

- The feasibility of the proposed robust distributed MPC is analyzed and the feasible conditions are developed. We show that the iterative feasibility of the distributed MPC is related to the bounds of the disturbances, the sampling period and the upper bound of the communication delays, given the initial feasibility. The specific bounds of these parameters on ensuring the feasibility, are proposed.

- The robust stability of the closed-loop large-scale system is established and the sufficient conditions on ensuring the robust stability are developed. We show that, the stability of the closed-loop system is affected by the upper bounds of the disturbances, the sampling period, the upper bound of the communication delays and the minimum eigenvalues of the cooperation matrices. Under the developed conditions, the large-scale system can be stabilized into a robustly invariant set.

It is believed that the developed results not only give insights into understanding how the disturbances and communication delays affect the control performance, but also provide a feasible robust distributed MPC approach for practitioners.

The rest of this chapter is organized as follows. The notations used in the chapter will be presented at the end of this section, and the problem formulation and some preliminary results are given in Section 8.2. In Section 8.3, the new optimization problem and the robust dual-mode distributed MPC are designed. The feasibility analysis is presented in Section 8.4 and the stability analysis is developed in Section 8.5. In Section 8.6, a simulation study is reported and the concluding remarks are summarized in Section 8.7.

The notations used in this chapter are as follows. The symbol $\mathbb{N}$ represents the set of all positive integers; the symbol $\mathcal{M}$ is defined as the collection $\{1, 2, \cdots, M\}$, $M \in \mathbb{N}$, and $\mathbb{R}^n$ stands for the n-dimensional real space. The subscript "T" and

"-1" denote the transpose and the inverse operation of a matrix, respectively. Given a matrix P, $P > 0$ ($P \geqslant 0$) means the matrix is positive definite (positive semi-definite). The 2-norm of a given column vector v is denoted by $\|v\|$ and the P-weighted norm is defined as $\|v\|_P \triangleq \sqrt{v^{\mathrm{T}} P v}$, where P is a given matrix with appropriate dimension. Given two matrices Q_1 and Q_2, $\bar{\lambda}(Q_1)$ and $\underline{\lambda}(Q_1)$ represent the maximum and minimum of the absolute values of the eigenvalues for the matrix Q_1; the notation $\lambda(Q_1, Q_2)$ is defined as $\lambda(Q_1, Q_2) \triangleq \underline{\lambda}(Q_1)/\bar{\lambda}(Q_2)$, where $\bar{\lambda}(Q_2) \neq 0$.

8.2 Problem Statement and Preliminaries

Consider the distributed MPC problem for a large-scale nonlinear system in which each subsystem (agent) $\mathcal{A}_i$, $i \in \mathcal{M}$, is described as:

$$\dot{x}_i(t) = f_i(x_i(t), u_i(t)) + \omega_i(t), \tag{8.1}$$

where $x_i(t) \in \mathbb{R}^n$ is the system state, $u_i(t) \in \mathbb{R}^m$ is the control input, $\omega_i(t) \in \mathbb{R}^n$ is the external disturbance. For each agent $\mathcal{A}_i$, the control input is constrained as $u_i(t) \in \mathcal{U}_i \subset \mathbb{R}^m$, where $\mathcal{U}_i$ is a compact set which contains the origin as an interior point. $\omega_i(t)$ belongs to a compact set $\mathcal{W}_i$ and is bounded as $\rho_i \triangleq \sup_{\omega_i(t) \in \mathcal{W}_i} \|\omega_i(t)\|$. The nominal system of the system in (8.1) can be characterized as:

$$\dot{\bar{x}}_i(t) = f_i(\bar{x}_i(t), u_i(t)). \tag{8.2}$$

By defining $x(t) = \mathrm{col}(x_1(t), \cdots, x_M(t))$, $u(t) = \mathrm{col}(u_1(t), \cdots, u_M(t))$, $\omega(t) = \mathrm{col}(\omega_1(t), \cdots, \omega_M(t))$, $f(x, u) = \mathrm{col}(f_1(x_1, u_1(t)), \cdots, f_M(x_M, u_M))$, $\mathcal{U} = \mathcal{U}_1 \times \cdots \times \mathcal{U}_M$ and $\mathcal{W} = \mathcal{W}_1 \times \cdots \times \mathcal{W}_M$, the large-scale nonlinear system can be characterized as:

$$\dot{x}(t) = f(x(t), u(t)) + \omega(t), \tag{8.3}$$

where $u(t) \in \mathcal{U}$ and $\omega(t) \in \mathcal{W}$.

In the large-scale system, each agent $\mathcal{A}_i$ is able to communicate with some agents according to their physical distances. The neighbors of the agent $\mathcal{A}_i$ are defined as the agents from which it can receive information. The indices for the neighbors of agent $\mathcal{A}_i$ is denoted as $\mathcal{N}_i$ and the concatenated state vector of neighbors of the agent $\mathcal{A}_i$ is denoted as $x_{-i}(t)$. There are time delays of the transmitted information among the communication links deployed in each agent and its neighbors. The system states

of the large-scale system in (8.3) are coupled in the objective (or cost) function. The objective of this chapter is to design a robust distributed MPC scheme for the large-scale system in (8.3) subject to communication delays and external disturbances, such that the overall system is robustly stabilized.

Before proceeding, some standard assumptions associated with the system dynamics are made. The same assumptions have been made in [23, 21, 70, 69].

Assumption 8.1. *For each agent $\mathcal{A}_i$, $i \in \mathcal{M}$, with the system dynamics in (8.1), assume that: (a) $f_i(0,0) = 0$ and $f_i : \mathbb{R}^n \times \mathbb{R}^m \to \mathbb{R}^n$ is a twice continuously differentiable function, and has a Lipschitz constant l_i with respect to the first argument; (b) for any initial value $x_i(0) \in \mathbb{R}^n$, piecewise right-continuous control input $u_i(t) \in \mathcal{U}_i$ and external disturbance $\omega_i(t) \in \mathcal{W}_i$, $t \geqslant 0$, the differential equation admits a unique solution.*

In terms of Assumption 8.1, the nominal system in (8.2) can be linearized at $(0,0)$ and the linearized system can be derived as:

$$\dot{\bar{x}}_i(t) = A_i\bar{x}_i(t) + B_iu_i(t), \tag{8.4}$$

where $A_i = \partial f_i/\partial x_i|_{(0,0)}$ and $B_i = \partial f_i/\partial u_i|_{(0,0)}$.

Assumption 8.2. *The linearized system in (8.4) is controllable, i.e., there exists a state feedback control law $u_i(t) = K_i\bar{x}_i(t)$ such that $\bar{A}_i \triangleq A_i + B_iK_i$ is stable.*

In addition, we recall a well-developed result of the classical MPC (such as [11, 97]) on computing the terminal set, which will be used for feasibility and stability analysis.

Lemma 8.1. *For the system in (8.2), suppose that Assumption 8.1 and 8.2 hold. There exist a constant $\varepsilon_i > 0$ and a matrix $P_i > 0$, such that, when $\bar{x}_i(t) \in \Omega_i(\varepsilon_i)$,*

(1) $V_i(\bar{x}_i(t))$ is a Lyapunov function to the system $\dot{\bar{x}}_i(t) = f_i(\bar{x}_i(t), K_i\bar{x}_i(t))$, in particular, $\dot{V}_i(\bar{x}_i(t)) \leqslant -\|\bar{x}_i(t)\|^2_{Q_i^*}$ holds;

(2) $u_i(t) = K_i\bar{x}_i(t) \in \mathcal{U}_i$, i.e., the control input constraint is satisfied.

Here, $V_i(\bar{x}_i(t)) \triangleq \|\bar{x}_i(t)\|^2_{P_i}$, the terminal set is defined as $\Omega_i(\varepsilon_i) \triangleq \{\bar{x}_i(t) : V_i(\bar{x}_i(t)) \leqslant \varepsilon_i^2\}$, $Q_i^* = Q_i + K_i^{\mathrm{T}}R_iK_i$, where K_i is a given stable state feedback gain, and the parameters $Q_i > 0$ and $R_i > 0$ are two given matrices with appropriate dimensions.

8.3 Robust Dual-mode Distributed MPC with Delays

In this section, the mechanism to deal with the communication delays is first introduced. Then the constrained optimization problem is proposed to generate control inputs. Finally, the robust distributed MPC scheme is designed to address the communication delays and external disturbances.

8.3.1 Communication Delays and Optimization Problem

For the large-scale system in (8.3), let us define the sequence $\{t_k\}, k \in \mathbb{N}$ as the time instants that all the agents are synchronized and the control signals are applied. At each time instant t_k, each agent also sends its state information to the agents connected to it by the communication networks. At time instants $\{t_k + \delta\}, k \in \mathbb{N}$, each agent samples its system state, where the constant $\delta > 0$ is called the sampling period. There is information delayed in the communication links, so each agent may not receive the information from its neighbors during the time interval $[t_k, t_k + \delta]$. For each agent i, the communication delay of the transmitted information from its neighbor $\mathcal{A}_j$, $j \in \mathcal{N}_i$, is denoted by τ_k^{ji} at time instant t_k. Specifically, τ_k^{ji} can be determined as follows: If the agent $\mathcal{A}_i$ receives the information from its neighbor $\mathcal{A}_j$ within the time interval $[t_k, t_k + \delta]$, then $\tau_k^{ji} = 0$; otherwise, τ_k^{ji} is equal to the length of the time period between $t_k + \delta$ and the time instant when the agent $\mathcal{A}_i$ receives the information from its neighbor $\mathcal{A}_j$. Define $\tau_k^i \triangleq \max_{j\in\mathcal{N}_i}\{\tau_k^{ji}\}$, which is the maximum delay for agent $\mathcal{A}_i$'s neighbors, i.e., at time $t_k+\tau_k^i$, agent $\mathcal{A}_i$ receives all the information from its neighbors. But the agent $\mathcal{A}_i$ will not solve the optimization problem to generate a new control signal until all the other agents receive their information. This strategy is used to facilitate synchronizing the overall agent system. Define $\tau_k = \max_{i\in\mathcal{M}}\{\tau_k^i\}$, which is the maximum delay for the overall agent system, i.e., at time $t_k+\tau_k$, all the agents receive their information. Assume that $\tau_k \leqslant \tau$, where τ is a positive constant. Since all the information is available for the overall system at time instants $\{t_k+\delta+\tau_k\}$, all the agents are synchronized to solve the optimization problems to generate the control signals at such time instants. We thus set $t_{k+1} = t_k + \delta + \tau_k$.

For each agent $\mathcal{A}_i$, we design an optimization problem as follows:

Problem 8.1. *Minimize the objective function* $J_i(\hat{x}_i(s;t_k), \hat{u}_i(s;t_k), \hat{x}_{-i}^a(s;t_k))$ *with*

respect to $\hat{u}_i(s;t_k)$*, and subject to:*

$$\begin{aligned}
\dot{\hat{x}}_i(s;t_k) =& f_i(\hat{x}_i(s;t_k),\hat{u}_i(s;t_k)), s\in[t_k,t_k+T],\\
\dot{\hat{x}}^a_j(s;t_k) =& f_j(\hat{x}^a_j(s;t_k),\hat{u}^a_j(s;t_k)), j\in\mathcal{N}_i, s\in[t_k,t_k+T],\\
\hat{u}_i(s;t_k) \in& \mathcal{U}_i, s\in[t_k,t_k+T],\\
\|\hat{x}_i(s;t_k)\|_{P_i} \leqslant& \frac{T\alpha_i}{s-t_k}\varepsilon_i, s\in[t_k+\delta,t_k+T],\\
\hat{x}_i(t_k;t_k) =& x^p_i(t_k;t_{k-1}+\delta), \hat{x}^a_j(t_k;t_k)=\hat{x}^*_j(t_k;t_{k-1}),
\end{aligned} \tag{8.5}$$

where $\hat{x}_i(s;t_k)$ *is called the predicted nominal system trajectory, which is generated by the control trajectory* $\hat{u}_i(s;t_k)$*,* $\hat{u}^a_j(s;t_k)$ *is called the assumed control trajectory of the neighbor* $\mathcal{A}_j$ *of agent* $\mathcal{A}_i$*, which is used to produce the assumed state trajectory* $\hat{x}^a_j(s;t_k)$*.* $T>\delta+\tau$ *is the optimization horizon;* $1>\alpha_i>0$ *is called the constraint shrinkage rate. Here, the objective function is defined as*

$$\begin{aligned}
J_i(\hat{x}(s;t_k),\hat{u}_i(s;t_k),\hat{x}^a_{-i}(s;t_k)) =& \int_{t_k}^{t_k+T} \|\hat{x}_i(s;t_k)\|^2_{Q_i}+\|\hat{u}_i(s;t_k)\|^2_{R_i}\\
&+\sum_{j\in\mathcal{N}_i}\|\hat{x}_i(s;t_k)-\hat{x}^a_j(s;t_k)\|^2_{Q_{ij}}\mathrm{d}s\\
&+\|\hat{x}_i(t_k+T;t_k)\|^2_{P_i},
\end{aligned} \tag{8.6}$$

where $\hat{x}^a_{-i}(s;t_k)$ *is the collection of the assumed states of agent* $\mathcal{A}_i$*'s neighbors,* $Q_i>0$ *and* $P_i>0$ *are the parameters designed according to Lemma 8.1,* $Q_{ij}>0$ *is called the cooperation matrix.*

In Problem 8.1, the optimal solution is denoted as $\hat{u}^*_i(s;t_k)$, $s\in[t_k,t_k+T]$, and the assumed control trajectory $\hat{u}^a_j(s;t_k)$ is generated as follows [23, 97]:

$$\hat{u}^a_i(s;t_k)=\begin{cases}\hat{u}^*_i(s;t_{k-1}), & \text{if} \quad s\in[t_k,t_{k-1}+T]\\ K_i\hat{x}^a_i(s;t_k), & \text{if} \quad s\in[t_{k-1}+T,t_k+T].\end{cases} \tag{8.7}$$

The post-predicted state trajectory is evolved as follows:

$$\dot{x}^p_i(s;t_k+\delta)=f_i(x^p_i(s;t_k+\delta),\hat{u}^*_i(s;t_k)), s\in[t_k+\delta,t_k+T], \tag{8.8}$$

where $x^p_i(t_k+\delta;t_k+\delta)=x_i(t_k+\delta)$. For each agent $\mathcal{A}_i$, the control input is applied as $u(t)=\hat{u}^*_i(t;t_k)$ for $t\in[t_k,t_{k+1}]$.

Remark 8.1. *It is noted that, the constraint in (8.5) is the robustness constraint which has been proposed in [69, 70]. This constraint is used to constrain the system state trajectory by following an upper and a lower bound in order for providing stability margins, so that the effects of the communication delays and disturbances can be well addressed. Furthermore, unlike the delay-free distributed MPC in [23, 21, 70, 61], the initial system state for Problem 8.1 is the post-predicted state* $x_i^p(t_k; t_{k-1}+\delta)$ *at time* t_k*. It is the best choice by considering the collective effects of the communication delays and disturbances. This is because the actual state* $x_i(t_k)$ *cannot be used due to the communication delays, and the post-predicted state* $x_i^p(t_k; t_{k-1}+\delta)$ *is closer to* $x_i(t_k)$ *compared to the distance between* $x_i(t_k)$ *and* $\hat{x}_i^*(t_k; t_{k-1})$ *owing to the disturbances.*

8.3.2 Dual-mode Distributed MPC Strategy

Like robust MPC schemes in [97, 21, 70], we also adopt the dual-mode MPC mechanism to robustly stabilize the overall agent system. That is, the control generation strategy is different according to two phases. In the first phase, when the system state is out of the terminal set, i.e., $x(t) \notin \Omega(\varepsilon)$, where $\Omega(\varepsilon) \triangleq \{x_1 \times \cdots \times x_M \in \mathbb{R}^{nM} | V_1(x_1) \leqslant \varepsilon_1, \cdots, V_M(x_M) \leqslant \varepsilon_M\}$, the control input is taken from the optimal control trajectory by solving Problem 8.1. Specifically, for each agent $\mathcal{A}_i$ at time instant t_k, the control input is applied as $u_i(s; t_k) = u_i^*(s; t_k)$, $s \in [t_k, t_{k+1}]$. In the second phase, when the system state enters the terminal set, i.e., $x(t) \in \Omega(\varepsilon)$, the control input is applied by the nominal control law as derived in Lemma 8.1. In particular, for each agent $\mathcal{A}_i$, the control input is designed as

$$u_i(s; t_k) = K_i \hat{x}_i(s; t_k), \quad s \in [t_k, t_{k+1}), \tag{8.9}$$

where $\hat{x}_i(s; t_k)$ is generated as $\dot{\hat{x}}_i(s; t_k) = f_i(\hat{x}_i(s; t_k), K_i \hat{x}_i(s; t_k))$ with $\hat{x}_i(t_k; t_k) = x_i(t_k)$.

The specific robust dual-mode distributed MPC strategy with communication delays and disturbances is described by the following two stages.

Stage I: $x(t_k) \notin \Omega(\varepsilon), k = 0, 1, \cdots, k_e - 1$

I.1 For each agent $\mathcal{A}_i$, $i \in \mathcal{M}$, at time t_k, its neighbors' assumed state trajectories $x_j^a(s; t_k)$, $j \in \mathcal{N}_i$ are received; the post-predicted system state $x_i^p(t_k; t_{k-1})$ is calculated; the control input $\hat{u}_i^*(s; t_k)$ is generated by solving Problem 8.1 and

applied to the actuator; the assumed state trajectory $\hat{x}_i^a(s;t_k)$ is generated and sent through the communication networks.

I.2 For each agent $\mathcal{A}_i$, $i \in \mathcal{M}$, at time $t_k + \delta$, the system state is measured.

I.3 The overall system is synchronized at time $t_k + \delta + \tau_k$. Go to the step I.1.

Stage II: $x(t_k) \in \Omega(\varepsilon), k = k_e, k_e + 1, \cdots$

II.1 For each agent $\mathcal{A}_i$, $i \in \mathcal{M}$, at time instant t_k, the system state $x_i(t_k)$ is measured; the control input as in (8.9) is generated and applied to the actuator for $[t_k, t_{k+1})$.

8.4 Feasibility Analysis

In this section, the iterative feasibility of the robust distributed MPC scheme is analyzed using the induction principle, and the sufficient conditions on ensuring the feasibility are developed. First of all, a feasible solution candidate is constructed and an assumption is made to render the distributed MPC scheme feasible at the initial time instant. Second, some auxiliary results are developed to facilitate the derivations for the last subsection. Finally, the conditions are proposed to guarantee that the feasible solution candidate is indeed a feasible solution, and the induction principle is applied to prove the feasibility.

8.4.1 Feasible Control Trajectory and Initial Feasibility

In order to prove the iterative feasibility, we need to construct a feasible control trajectory (i.e., a feasible solution to Problem 8.1) at time t_{k+1} based on the optimal control trajectory at time t_k. The feasible control trajectory at time t_{k+1} is denoted as $\tilde{u}_i(s;t_{k+1})$ for each agent $\mathcal{A}_i$, and it is designed as follows:

$$\tilde{u}_i(s;t_{k+1}) = \begin{cases} \hat{u}_i^*(s;t_k), & \text{if} \quad s \in [t_{k+1}, t_k + T], \\ K_i\tilde{x}_i(s;t_{k+1}), & \text{if} \quad s \in [t_k + T, t_{k+1} + T], \end{cases} \tag{8.10}$$

where $\tilde{x}_i(s;t_{k+1})$, $s \in [t_{k+1}, t_{k+1}+T]$ is the feasible state trajectory, which is generated as:

$$\dot{\tilde{x}}_i(s;t_{k+1}) = f_i(\tilde{x}_i(s;t_{k+1}), \tilde{u}_i(s;t_{k+1})), s \in [t_{k+1}, t_{k+1} + T],$$

with $\tilde{x}_i(t_{k+1};t_{k+1}) = x_i^p(t_{k+1};t_k + \delta)$.

Remark 8.2. *Note that the way of generating the feasible control trajectory is similar to [23, 21, 70, 69, 31], but the dynamics of the feasible control trajectory and state trajectory used in this study are different. In [23, 21, 70, 69], the initial value for generating the feasible state trajectory is precisely the system state $x_i(t_{k+1})$. But the initial value in present study is the post-predicted state $x_i^p(t_{k+1}; t_k + \delta)$ due to the communication delays, which make the analysis essentially different and more challenging.*

Before utilizing the induction principle, it is required that the distributed MPC scheme is feasible at the initial time instant. The initial feasibility problem or the calculation of initial feasible set is a difficult problem (even for classic nonlinear MPC algorithms), which deserves further study. Like some existing MPC schemes in [23, 21, 69, 70], we make an assumption on the initial feasibility and focus on the main topic.

Assumption 8.3. *For each agent $\mathcal{A}_i$, $i \in \mathcal{M}$, given the prediction horizon T, the initial system state $x_i(t_0)$ and the initial assumed trajectories $x_j^a(s; t_0)$, $s \in [t_0, t_0+T]$, $j \in \mathcal{N}_i$, there exists a solution to the optimization Problem 8.1 at time t_0.*

8.4.2 Auxiliary Results

In order to prove that the designed feasible control trajectory is indeed feasible, we need to show that it fulfills the control input constraint and the resultant feasible state trajectory satisfies the robustness constraint. Further, several results related to $x_i(s; t_k)$, $\hat{x}_i^*(s; t_k)$, $x_i^p(s; t_k + \delta)$ and $\tilde{x}_i(s; t_{k+1})$ are developed. These results also play instrumental roles in the stability analysis. Firstly, an upper bound of the distance between $x_i(s; t_k)$ and $x_i^p(s; t_k + \delta)$ are developed.

Lemma 8.2. *For each agent $\mathcal{A}_i$, $i \in \mathcal{M}$, with the system dynamics in (8.1), if Assumption 8.1 holds, then the following holds:*

$$\|x_i(s; t_k) - x_i^p(s; t_k + \delta)\|_{P_i} \leqslant (s - t_k - \delta)\sqrt{\bar{\lambda}(P_i)}\rho_i e^{l_i(s-t_k-\delta)}, s \in [t_k + \delta, t_{k+1}]. \quad (8.11)$$

Proof. According to the generation of $x_i^p(s; t_k + \delta)$ in (8.8), we get

$$\begin{aligned}\|x_i(s; t_k) - x_i^p(s; t_k + \delta)\|_{P_i} =& \|x_i(t_k + \delta; t_k) + \int_{t_k+\delta}^{s} f_i(x_i(t; t_k), \hat{u}_i^*(t; t_k)) + \omega_i(t; t_k)dt \\ & - x_i^p(t_k + \delta; t_k + \delta) - \int_{t_k+\delta}^{s} f_i(x_i^p(t; t_k + \delta), \hat{u}_i^*(t; t_k))dt\|_{P_i}.\end{aligned}$$

By using $x_i^p(t_k+\delta;t_k+\delta)=x_i(t_k;t_k)$ and applying the triangle inequality, we have

$$\begin{aligned}\|x_i(s;t_k)-x_i^p(s;t_k+\delta)\|_{P_i}\leqslant&\|\int_{t_k+\delta}^{s}\omega_i(t;t_k)dt\|_{P_i}\\&+\int_{t_k+\delta}^{s}\|f_i(x_i^p(t;t_k+\delta),\hat{u}_i^*(t;t_k))\\&-f_i(x_i^p(t;t_k+\delta),\hat{u}_i^*(t;t_k))\|_{P_i}dt.\end{aligned}$$

In terms of Assumption 8.1, the following can be obtained

$$\begin{aligned}\|x_i(s;t_k)-x_i^p(s;t_k+\delta)\|_{P_i}\leqslant&(s-t_k-\delta)\sqrt{\bar{\lambda}(P_i)}\rho_i\\&+l_i\int_{t_k+\delta}^{s}\|x_i(t;t_k)-x_i^p(t;t_k+\delta))\|_{P_i}dt.\end{aligned}$$

Finally, the result in (8.11) follows by using the Gronwall-Bellman inequality. □

Based on Lemma 8.2, an upper bound of the distance between $x_i(s;t_k)$ and $\hat{x}_i^*(s;t_k)$ is developed in the following lemma.

Lemma 8.3. *For each agent $\mathcal{A}_i$, $i\in\mathcal{M}$, with the system dynamics in (8.1), if Assumption 8.1 holds, then the distance between $x_i(s;t_k)$ and $\hat{x}_i^*(s;t_k)$ are bounded as*

$$\|x_i(s;t_k)-\hat{x}_i^*(s;t_k)\|_{P_i}\leqslant[\tau_{k-1}e^{l_i\tau_{k-1}}+(s-t_k)]\sqrt{\bar{\lambda}(P_i)}\rho_i e^{l_i(s-t_k)},s\in[t_k,t_{k+1}]. \quad (8.12)$$

Proof.

$$\begin{aligned}\|x_i(s;t_k)-\hat{x}_i^*(s;t_k)\|_{P_i}=&\|x_i(t_k;t_k)-\hat{x}_i^*(t_k;t_k)+\int_{t_k}^{s}f_i(x_i(t;t_k),\hat{u}_i^*(t;t_k))+\omega_i(t;t_k)dt\\&-\int_{t_k}^{s}f_i(\hat{x}_i^*(t;t_k),\hat{u}_i^*(t;t_k))dt\|_{P_i}\\\leqslant&\|x_i(t_k;t_k)-\hat{x}_i^*(t_k;t_k)\|_{P_i}+(s-t_k)\sqrt{\bar{\lambda}(P_i)}\rho_i\\&+l_i\int_{t_k}^{s}\|x_i(t;t_k)-\hat{x}_i^*(t;t_k))\|_{P_i}dt,\end{aligned}$$

where the conditions in Assumption 8.1 and the triangle inequality have been applied

in the last step. According to Lemma 8.2, we have

$$\begin{aligned}\|x_i(s;t_k)-\hat{x}_i^*(s;t_k)\|_{P_i} \leqslant \tau_{k-1}\sqrt{\bar{\lambda}(P_i)}\rho_i e^{l_i\tau_{k-1}} + (s-t_k)\sqrt{\bar{\lambda}(P_i)}\rho_i \\ + l_i\int_{t_k}^{s}\|x_i(t;t_k)-\hat{x}_i^*(t;t_k))\|_{P_i}dt.\end{aligned}$$

By applying the Gronwall-Bellman inequality, the result in Lemma 8.3 follows. □

Inspecting the generation of the feasible control trajectory in (8.10), it can be seen that the feasible control trajectory $\tilde{u}_i^*(s;t_{k+1})$ will fulfill the control input constraint for $s\in[t_k+T,t_{k+1}+T]$, if the feasible state is in the terminal set at t_k+T according to Lemma 8.1. With the help of Lemma 8.2 and Lemma 8.3, the sufficient condition that guarantees $\tilde{x}_i(t_k+T;t_{k+1})\in\Omega_i(\varepsilon_i)$, is presented in the following theorem.

Theorem 8.1. *For each agent $\mathcal{A}_i$, $i\in\mathcal{M}$, suppose that Assumption 8.1 is satisfied. Given the prediction horizon T, the sampling period δ and the disturbance bound $\rho_i\leqslant(1-\alpha_i)\varepsilon_i/(\sqrt{\bar{\lambda}(P_i)}\delta e^{l_iT})$, if the communication delays are bounded as*

$$\sqrt{\bar{\lambda}(P_i)}\rho_i[\tau_k e^{l_i(T-\delta)}+(\tau_{k-1}e^{l_i\tau_{k-1}}+\delta+\tau_k)e^{l_iT}]\leqslant(1-\alpha_i)\varepsilon_i, \tag{8.13}$$

then $\tilde{x}_i(t_k+T;t_{k+1})\in\Omega_i(\varepsilon_i)$.

Proof. According to Problem 8.1, we have that $\hat{x}_i^*(t_k+T;t_k)\in\Omega_i(\alpha_i\varepsilon_i)$. To proceed, we consider the distance between $\tilde{x}_i(s;t_{k+1})$ and $\hat{x}_i^*(s;t_k)$ as:

$$\begin{aligned}&\|\tilde{x}_i(s;t_{k+1})-\hat{x}_i^*(s;t_k)\|_{P_i}, s\in[t_{k+1},t_k+T],\\ =&\|\tilde{x}_i(t_{k+1};t_{k+1})+\int_{t_{k+1}}^{s}f_i(\tilde{x}_i(t;t_{k+1}),\tilde{u}_i(t;t_{k+1}))dt\\ &-\hat{x}_i^*(t_{k+1};t_k)-\int_{t_{k+1}}^{s}f_i(\hat{x}_i^*(t;t_k),\hat{u}_i^*(t;t_k))dt\|_{P_i}\\ \leqslant&\|\tilde{x}_i(t_{k+1};t_{k+1})-x_i(t_{k+1})\|_{P_i}+\|x_i(t_{k+1})-\hat{x}_i^*(t_{k+1};t_k)\|_{P_i}\\ &+l_i\int_{t_{k+1}}^{s}\|\tilde{x}_i(t;t_{k+1})-\hat{x}_i^*(t;t_k)\|_{P_i}dt,\end{aligned}$$

where the triangle inequality has been used in the last step. In terms of Lemma 8.2, we get $\|\tilde{x}_i(t_{k+1};t_{k+1})-x_i(t_{k+1})\|_{P_i}\leqslant\tau_k\sqrt{\bar{\lambda}(P_i)}\rho_i e^{l_i\tau_k}$. By using Lemma 8.3, it can be obtained that $\|x_i(t_{k+1})-\hat{x}_i^*(t_{k+1};t_k)\|_{P_i}\leqslant[\tau_{k-1}e^{l_i\tau_{k-1}}+(\delta+\tau_k)]\sqrt{\bar{\lambda}(P_i)}\rho_i e^{l_i(\delta+\tau_k)}$.

Substituting these two results into the above inequality gives rise to

$$\begin{aligned}&\|\tilde{x}_i(s;t_{k+1}) - \hat{x}_i^*(s;t_k)\|_{P_i}, s \in [t_{k+1}, t_k + T],\\ \leqslant&\tau_k\sqrt{\bar{\lambda}(P_i)}\rho_i e^{l_i\tau_k} + [\tau_{k-1}e^{l_i\tau_{k-1}} + (\delta + \tau_k)]\sqrt{\bar{\lambda}(P_i)}\rho_i e^{l_i(\delta+\tau_k)}\\ &+ l_i\int_{t_{k+1}}^{s}\|\tilde{x}_i(t;t_{k+1}) - \hat{x}_i^*(t;t_k)\|_{P_i}dt.\end{aligned}$$

By applying the Gronwall-Bellman inequality, we get

$$\begin{aligned}&\|\tilde{x}_i(s;t_{k+1}) - \hat{x}_i^*(s;t_k)\|_{P_i}, s \in [t_{k+1}, t_k + T],\\ \leqslant&\sqrt{\bar{\lambda}(P_i)}\rho_i\left[\tau_k e^{l_i(s-t_{k+1}+\tau_k)} + \left(\tau_{k-1}e^{l_i\tau_{k-1}} + \delta + \tau_k\right)e^{l_i(s+\delta+\tau_k-t_{k+1})}\right].\end{aligned} \tag{8.14}$$

Plugging $s = t_k + T$ into (8.14) gives

$$\begin{aligned}&\|\tilde{x}_i(t_k + T;t_{k+1}) - \hat{x}_i^*(t_k + T;t_k)\|_{P_i}\\ \leqslant&\sqrt{\bar{\lambda}(P_i)}\rho_i[\tau_k e^{l_i(T-\delta)} + (\tau_{k-1}e^{l_i\tau_{k-1}} + \delta + \tau_k)]e^{l_iT}].\end{aligned}$$

By using $\hat{x}_i^*(t_k + T;t_k) \in \Omega_i(\alpha_i\varepsilon_i)$ and the condition in (8.13), it can be obtained $\|\tilde{x}_i(t_k + T;t_{k+1})\|_{P_i} \leqslant \varepsilon_i$. The proof is completed. □

Remark 8.3. *It is noted that the requirement imposed on the disturbance bound in Theorem 8.1 provides a necessary condition for satisfying (8.13). That is, only for such bounded disturbances, the condition in (8.13) can possibly be satisfied with some communication delays, and $\tilde{x}_i(t_k + T;t_{k+1})$ can be driven to the terminal set $\Omega_i(\varepsilon_i)$.*

Remark 8.4. *Theorem 8.1 indicates that, both the communication delays τ_{k-1} and τ_k cannot be too large in order to steer the feasible state into the terminal set at $t_k + T$. The insights into such a requirement on τ_{k-1} and τ_k are in two aspects. On the one hand, due to the external disturbance, the larger τ_{k-1}, the further the post-predicted state $x_i^p(t_k;t_{k-1} + \delta)$ will deviate away from the system state $x_i(t_k)$. This results in a larger error in the initial value $\hat{x}_i^*(t_k;t_k)$ for generating the optimal state trajectory since $\hat{x}_i^*(t_k;t_k) = x_i^p(t_k;t_{k-1} + \delta)$. Both the larger error in the initial value $\hat{x}_i^*(t_k;t_k)$ and the larger τ_k may cause an increased distance between $x_i(t_{k+1})$ and $x_i^*(t_{k+1};t_k)$. On the other hand, the larger τ_k will also increase the distance between $x_i^p(t_{k+1};t_k + \delta)$ and $x_i(t_{k+1})$ due to the external disturbance. That is, the distance between $\tilde{x}_i(t_{k+1};t_{k+1})$ and $x_i(t_{k+1})$ will be increased. Therefore, the distance between*

$\tilde{x}_i(t_{k+1};t_{k+1})$ and $x_i^*(t_{k+1};t_k)$ will be affected both by τ_{k-1} and τ_k. In summary, the larger τ_{k-1} and/or τ_k will enlarge the distance between $\tilde{x}_i(t_k+T;t_{k+1})$ and $x_i^*(t_k+T;t_k)$, which may result in $\tilde{x}_i(t_k+T;t_{k+1}) \notin \Omega_i(\varepsilon_i)$. Thus, the condition in (8.13) should be satisfied.

In particular, if the communication delays are uniform with respect to the time instants, i.e., $\tau_k = \tau_{k+1}$, $k \in \mathbb{N}$, then an upper bound of the communication delays can be derived as $\tau_k \leqslant \min_{i\in\{\mathcal{M}\}}\{\bar{\tau}_i\}$, where $\bar{\tau}_i$ is the solution to the following equation:

$$\bar{\tau}_i[e^{l_i(T-\delta)} + e^{l_i T} + e^{l_i\bar{\tau}_i}] = \frac{(1-\alpha_i)\varepsilon_i}{\sqrt{\bar{\lambda}(P_i)}\rho_i} - \delta e^{l_i T}.$$

Finally, we develop a sufficient condition which renders $\tilde{x}_i(t_{k+1};t_k) \in \Omega_i(\alpha_i\varepsilon_i)$. This result will be used to prove that the robustness constraint is fulfilled.

Lemma 8.4. *For each agent $\mathcal{A}_i$, $i \in \mathcal{M}$, suppose that Assumption 8.1 and 8.2 hold, that the sampling period is designed as $T > \delta \geqslant -2\frac{\underline{\lambda}(Q_i^*)}{\bar{\lambda}(P_i)}\ln\alpha_i$, and that the disturbance is bounded as $\rho_i \leqslant (1-\alpha_i)\varepsilon_i/(\sqrt{\bar{\lambda}(P_i)}\delta e^{l_i T})$. If the communication delay satisfies the condition in (8.13), then $\tilde{x}_i(t_{k+1}+T;t_{k+1}) \in \Omega_i(\alpha_i\varepsilon_i)$.*

Proof. According to Theorem 8.1, we have $\tilde{x}_i(t_k+T;t_{k+1}) \in \Omega_i(\varepsilon_i)$. Since the feasible control trajectory is given as $\tilde{u}_i(s;t_{k+1}) = K_i\tilde{x}_i(s;t_{k+1})$, $s \in [t_k+T, t_{k+1}+T]$, the result in Lemma 8.1 can be used. In particular, we have

$$\begin{aligned}\dot{V}_i(\tilde{x}_i(s;t_{k+1})) =& -(\tilde{x}_i(s;t_{k+1}))^{\mathrm{T}}Q_i^*\tilde{x}_i(s;t_{k+1}), s \in [t_k+T, t_{k+1}+T],\\ \leqslant& -\frac{\underline{\lambda}(Q_i^*)}{\bar{\lambda}(P_i)}V_i(\tilde{x}_i(s;t_{k+1})).\end{aligned}$$

By applying the comparison principle [64], it can be obtained that

$$\|\tilde{x}_i(s;t_{k+1})\|_{P_i} \leqslant \varepsilon_i e^{-\frac{\underline{\lambda}(Q_i^*)}{\bar{\lambda}(P_i)}\frac{s-t_k-T}{2}}, s \in [t_k+T, t_{k+1}+T]. \tag{8.15}$$

Substituting $s = t_{k+1}+T$ into (8.15) results in $\|\tilde{x}_i(t_{k+1}+T;t_{k+1})\|_{P_i} \leqslant \varepsilon_i e^{-\frac{\underline{\lambda}(Q_i^*)}{\bar{\lambda}(P_i)}\frac{\tau_k+\delta}{2}}$. Since $\tau_k \geqslant 0$ and $\delta \geqslant -2\underline{\lambda}(Q_i^*)/\bar{\lambda}(P_i)\ln\alpha_i$, we get $\|\tilde{x}_i(t_{k+1}+T;t_{k+1})\|_{P_i} \leqslant \alpha_i\varepsilon_i$. The proof is completed. □

Remark 8.5. *Since $\tilde{x}_i(t_k+T;t_{k+1}) \in \Omega_i(\varepsilon_i)$, and the feasible control input is applied as $\tilde{u}_i(s;t_{k+1}) = K_i\tilde{x}_i(s;t_{k+1})$, $\tilde{x}_i(s;t_{k+1})$ converges toward $\Omega_i(\alpha_i\varepsilon_i)$ as time involves.*

But it needs enough time to drive the feasible state to enter the set $\Omega_i(\alpha_i\varepsilon_i)$. That is, the sampling period should be lower bounded as in Lemma 8.4.

8.4.3 Delay Bound for Guaranteeing Feasibility

To verify that the designed feasible control trajectory is indeed feasible at time t_{k+1}, it suffices to show that the generated feasible state trajectory satisfies the robustness constraint. In the following lemma, it is shown that if the sampling period is designed appropriately, and the communication delays are bounded by a given value, then the generated feasible state trajectory satisfies the robustness constraint.

Lemma 8.5. *For each agent $\mathcal{A}_i$, $i \in \mathcal{M}$, suppose that Assumption 8.1 and 8.2 hold, and that the optimal control trajectory $\hat{u}_i^*(s;t_k)$, $s \in [t_k, t_k+T]$ exists at time t_k. If the sampling period is designed as*

$$\max\left\{(1-\alpha_i)T, -2\frac{\underline{\lambda}(Q_i^*)}{\bar{\lambda}(P_i)}\ln\alpha_i\right\} \leqslant \delta \leqslant \frac{2\bar{\lambda}(P_i)}{\underline{\lambda}(Q_i^*)}\ln\left(\frac{2\bar{\lambda}(P_i)}{\underline{\lambda}(Q_i^*)T\alpha_i}\right), \tag{8.16}$$

the disturbance is bounded as $\rho_i \leqslant (1-\alpha_i)\varepsilon_i/(\sqrt{\bar{\lambda}(P_i)}\delta e^{l_iT})$, and the communication delay satisfies (8.13) as well as the following condition:

$$\tau_k \leqslant \frac{2\bar{\lambda}(P_i)}{\underline{\lambda}(Q_i^*)}\ln\left(\frac{2\bar{\lambda}(P_i)}{\underline{\lambda}(Q_i^*)T\alpha_i}\right) - \delta, \tag{8.17}$$

then the designed feasible state trajectory satisfies the robustness constraint at time t_{k+1}, i.e., $\|\tilde{x}_i(s;t_{k+1})\|_{P_i} \leqslant T\alpha_i\varepsilon_i/(s-t_{k+1})$, $s \in [t_{k+1}+\delta, t_{k+1}+T]$.

Proof. The proof is derived from discussing two cases with respect to the value of $2\delta+\tau_k$.

- **Case I:** The sampling period and the communication delays satisfy the conditions in Lemma 8.5, and $2\delta+\tau_k > T$. In this situation, $t_k+T \leqslant t_{k+1}+\delta \leqslant t_{k+1}+T$. According to Lemma 8.4, it can be obtained that $\|\tilde{x}_i(s;t_{k+1})\|_{P_i} \leqslant \varepsilon_i e^{-\frac{\underline{\lambda}(Q_i^*)}{2\bar{\lambda}(P_i)}\frac{s-t_k-T}{2}}, s \in [t_{k+1}+\delta, t_{k+1}+T]$. Based on this, let us define a function $F(s) = \frac{T\alpha_i\varepsilon_i}{s-t_{k+1}} - \varepsilon_i e^{-\frac{\underline{\lambda}(Q_i^*)}{2\bar{\lambda}(P_i)}\frac{s-t_k-T}{2}}$, $s \in [t_{k+1}+\delta, t_{k+1}+T]$. By changing variable $t = s-t_{k+1}+\delta$, we get $F(t) = \frac{G(t)}{(t+\delta)}e^{-\frac{\underline{\lambda}(Q_i^*)}{2\bar{\lambda}(P_i)}(t+2\delta+\tau_k-T)}$, where $G(t) = T\alpha_i e^{\frac{\underline{\lambda}(Q_i^*)}{2\bar{\lambda}(P_i)}(t+2\delta+\tau_k-T)} - t - \delta$ and $t \in [0, T-\delta]$. It can be shown that the function $G(t)$ monotonically decreases for $t \in [0, \frac{2\bar{\lambda}(P_i)}{\underline{\lambda}(Q_i^*)}\ln\left(\frac{2\bar{\lambda}(P_i)}{\underline{\lambda}(Q_i^*)T\alpha_i}\right)+T-2\delta-\tau_k]$.

Therefore, it also monotonically decreases for $t \in [0, T-\delta]$ due to $\tau_k \leqslant \frac{2\bar{\lambda}(P_i)}{\underline{\lambda}(Q_i^*)} \ln\left(\frac{2\bar{\lambda}(P_i)}{\underline{\lambda}(Q_i^*)T\alpha_i}\right) - \delta$. Furthermore, it can be verified that $G(T-\delta) \geqslant 0$ because of the upper bounds of δ in (8.16). Thus, we have $G(t) \geqslant 0$ for $t \in [0, T-\delta]$, which implies $F(s) \geqslant 0$ for $s \in [t_{k+1}+\delta, t_{k+1}+T]$. As a result, $\|\tilde{x}_i(s; t_{k+1})\|_{P_i} \leqslant \frac{T\alpha_i\varepsilon_i}{s-t_{k+1}}$, $s \in [t_{k+1}+\delta, t_{k+1}+T]$, i.e., the robustness constraint is satisfied.

- **Case II:** The sampling period and the communication delays satisfy the proposed conditions, but $0 < 2\delta + \tau_k \leqslant T$. This results in that $t_{k+1}+\delta \leqslant t_k + T \leqslant t_{k+1}+T$. We divide the interval $[t_{k+1}+\delta, t_{k+1}+T]$ into two subintervals $[t_{k+1}+\delta, t_k+T]$ and $[t_k+T, t_{k+1}+T]$ to conduct the proof. When $s \in [t_{k+1}+\delta, t_k+T]$, according to (8.14) in Theorem 8.1, we have

$$\begin{aligned}\|\tilde{x}_i(s; t_{k+1})\|_{P_i} \leqslant & \|\hat{x}_i^*(s; t_k)\|_{P_i} + \sqrt{\bar{\lambda}(P_i)}\rho_i \left[\tau_k e^{l_i(s-t_{k+1}+\tau_k)}\right. \\ & \left. + \left(\tau_{k-1}e^{l_i\tau_{k-1}} + \delta + \tau_k\right) e^{l_i(s+\delta+\tau_k-t_{k+1})}\right].\end{aligned}$$

Based on this result, to show the robustness constraint is satisfied, for all $s \in [t_{k+1}+\delta, t_k+T]$, it suffices to prove the following:

$$\begin{aligned}&\sqrt{\bar{\lambda}(P_i)}\rho_i \left[\tau_k e^{l_i(s-t_{k+1}+\tau_k)} + \left(\tau_{k-1}e^{l_i\tau_{k-1}} + \delta + \tau_k\right) e^{l_i(s+\delta+\tau_k-t_{k+1})}\right] \\ &\leqslant \frac{T\alpha_i\varepsilon_i(\delta+\tau_k)}{(s-t_{k+1})(s-t_k)}, s \in [t_{k+1}+\delta, t_k+T]. \end{aligned} \tag{8.18}$$

Since $\delta > (1-\alpha_i)T$, the right-hand side of (8.18) can be bounded as

$$\frac{T\alpha_i\varepsilon_i(\delta+\tau_k)}{(s-t_{k+1})(s-t_k)} \geqslant \frac{\delta+\tau_k}{T-\delta-\tau_k}\alpha_i\varepsilon_i \geqslant (1-\alpha_i)\varepsilon_i, s \in [t_{k+1}+\delta, t_k+T].$$

In terms of (8.13) in Theorem 8.1, it can be shown that (8.18) holds. Therefore, the feasible state trajectory satisfies the robustness constraint for $s \in [t_{k+1}+\delta, t_k+T]$. Next, we consider the feasible state trajectory when $s \in [t_k+T, t_{k+1}+T]$. According to Lemma 8.4, we have $\|\tilde{x}_i(s; t_{k+1})\|_{P_i} \leqslant \varepsilon_i e^{-\frac{\underline{\lambda}(Q_i^*)}{2\bar{\lambda}(P_i)}\frac{s-t_k-T}{2}}, s \in [t_k+T, t_{k+1}+T]$. By following the similar line of **Case I**, it can be obtained that $\varepsilon_i e^{-\frac{\underline{\lambda}(Q_i^*)}{2\bar{\lambda}(P_i)}\frac{s-t_k-T}{2}} \leqslant \frac{T\alpha_i\varepsilon_i}{s-t_{k+1}}$, for $s \in [t_k+T, t_{k+1}+T]$. Therefore, $\|\tilde{x}_i(s; t_{k+1})\|_{P_i} \leqslant \frac{T\alpha_i\varepsilon_i}{s-t_{k+1}}$ as well, for $s \in [t_k+T, t_{k+1}+T]$.

By summarizing **Case I** and **Case II**, we show that the designed feasible state

trajectory satisfies the robustness constraint. This completes the proof. □

Remark 8.6. *It is worth noting that if the communication delays are uniform with respect to the time instants, a specific bound of the communication delays of each agent $\mathcal{A}_i$, can be derived as $\tau_i^m \triangleq \min\{\bar{\tau}_i, \frac{2\bar{\lambda}(P_i)}{\underline{\lambda}(Q_i^*)} \ln\left(\frac{2\bar{\lambda}(P_i)}{\underline{\lambda}(Q_i^*)T\alpha_i}\right) - \delta\}$, $i \in \mathcal{M}$.*

In Lemma 8.5, we have developed conditions (i.e., the sampling period and the bound of communication delays) for rendering the feasible state trajectory satisfying the robustness constraint for each agent individually. But in order to establish the feasibility for the distributed MPC of the overall system, these conditions are required to be satisfied simultaneously. Furthermore, we also need to prove that the designed feasible control trajectory satisfies the control input constraint. By considering these aspects, the result on ensuring the feasibility of the distributed MPC scheme is presented in the following theorem.

Theorem 8.2. *For the overall agent system in (8.3) with the designed distributed MPC, suppose that Assumption 8.1, 8.2 and 8.3 hold for each agent $\mathcal{A}_i$, $i \in \mathcal{M}$. If the sampling period is designed*

$$\max_{i\in\mathcal{M}}\{\underline{\delta}_i\} \leqslant \delta \leqslant \min_{i\in\mathcal{M}}\{\bar{\delta}_i\}, \tag{8.19}$$

the disturbance is bounded as $\rho_i \leqslant (1-\alpha_i)\varepsilon_i/(\sqrt{\bar{\lambda}(P_i)}\delta e^{l_i T})$ and the communications delay is uniform and bounded as $\tau_k \leqslant \min_{i\in\mathcal{M}}\{\tau_i^m\}$, where

$$\underline{\delta}_i \triangleq \max\left\{(1-\alpha_i)T, -2\frac{\underline{\lambda}(Q_i^*)}{\bar{\lambda}(P_i)}\ln\alpha_i\right\},$$
$$\bar{\delta}_i \triangleq \frac{2\bar{\lambda}(P_i)}{\underline{\lambda}(Q_i^*)}\ln\left(\frac{2\bar{\lambda}(P_i)}{\underline{\lambda}(Q_i^*)T\alpha_i}\right),$$

then the designed distributed MPC scheme is iteratively feasible.

Proof. The proof is developed by the induction principle. According to Assumption 8.3, there exist optimal control trajectories to all the agents $\mathcal{A}_i$, $i \in \mathcal{M}$, at time $t = t_0$. Assume that there exist optimal control trajectories for all the agents at time $t = t_k$, $k \in \mathbb{N}, k \geqslant 0$ and take the control trajectory as (8.10) at time t_{k+1} for each agent $\mathcal{A}_i$. In what follows, we shall prove that the designed feasible control trajectory is feasible for each agent $\mathcal{A}_i$. Let us first prove that it satisfies the control input constraint. Due to $\hat{u}_i^*(s;t_k) \in \mathcal{U}_i$, $s \in [t_{k+1}, t_k + T]$ and (8.10), for each agent

$\mathcal{A}_i$, we get $\tilde{u}_i(s;t_{k+1}) \in \mathcal{U}_i$, $s \in [t_{k+1}, t_k + T]$. Furthermore, because of (8.19) and $\tau_k \leqslant \min_{i\in\mathcal{M}}\{\tau_i^m\}$, Theorem 8.1 holds for all the agents simultaneously. For each agent $\mathcal{A}_i$, we have $\tilde{x}_i(t_k + T; t_{k+1}) \in \Omega_i(\varepsilon_i)$. Thus, Lemma 8.1 can be applied, which implies $\tilde{u}_i(s;t_{k+1}) \in \mathcal{U}_i$, $s \in [t_k+T, t_{k+1}+T]$. That is, the control input constraints are satisfied for all the agents. Next, let us prove that the feasible state trajectories fulfill the robustness constraints at time t_{k+1}. Since the sampling period is designed as (8.19) and the communication delays satisfy $\tau_k \leqslant \min_{i\in\mathcal{M}}\{\tau_i^m\}$, the result of Lemma 8.5 is valid for all the agents simultaneously. As a result, all the designed feasible state trajectories satisfy the robustness constraints at time t_{k+1}. Therefore, the control trajectory in (8.10) is feasible at time t_{k+1} as desired. By the induction principle, we conclude that the designed distributed MPC scheme is iteratively feasible. □

8.5 Stability Analysis

This section develops sufficient conditions that guarantee the system state of the overall closed-loop system is stabilized into a robustly invariant set. According to the dual-mode strategy, the derivation has been divided into two steps. In the first step, it is shown that the system state will enter the terminal set in finite time if the parameters are appropriately designed, and the communication delays and disturbances are small enough. In the second step, the system state that is in the terminal set, will be proven to converge to the robustly invariant set.

Firstly, let us develop the conditions that will render the system state of the overall system entering the terminal set. Further, an upper bound of the difference between the optimal objective functions at two adjacent steps is developed in the following lemma.

Lemma 8.6. *For the overall system in (8.3), suppose that Assumption 8.1, 8.2 and 8.3 hold. If the sampling period is designed as (8.19), the disturbance is bounded as* $\rho_i \leqslant (1-\alpha_i)\varepsilon_i/(\sqrt{\bar{\lambda}(P_i)}\delta e^{l_i T})$ *and the communication delay is bounded as in Theorem*

8.2, then for each agent $\mathcal{A}_i$, $i \in \mathcal{M}$, the following holds:

$$
\begin{aligned}
&J(\hat{x}_i^*(s;t_{k+1}),\hat{u}_i^*(s;t_{k+1}),\hat{x}_{-i}^a(s;t_{k+1}))-J(\hat{x}_i^*(s;t_k),\hat{u}_i^*(s;t_k),\hat{x}_{-i}^a(s;t_k))\\
\leqslant&-\int_{t_k}^{t_{k+1}}\|\hat{x}_i^*(s;t_k)\|_{Q_i}^2ds+\lambda^2(Q_i,P_i)\left[(T-\delta-\tau_k)\Lambda_i^2(\delta,\tau_k)\right.\\
&\left.+2T\alpha_i\varepsilon_i\Lambda_i(\delta,\tau_k)\ln\frac{T}{\delta+\tau_k}\right]+(T-\delta-\tau_k)\sum_{j\in\mathcal{N}_i}\left[\lambda(Q_{ij},P_i)\Lambda_i(\delta,\tau_k)+\frac{\lambda_{ij}T}{\delta+\tau_k}\right]^2\\
&+(1-\alpha_i^2)\varepsilon_i^2+\sum_{j\in\mathcal{N}_i}(\delta+\tau_k)\bar{\lambda}_{ij}^2,
\end{aligned}
$$

where $\Lambda_i(\delta,\tau_k)\triangleq\sqrt{\lambda(\bar{P}_i)}\rho_i[\tau_k e^{l_i(T-\delta)}+(\tau_k e^{l_i\tau_k}+\delta+\tau_k)e^{l_iT}]$, $\lambda_{ij}\triangleq\lambda(Q_{ij},P_i)\alpha_i\varepsilon_i+\lambda(Q_{ij},P_j)\alpha_j\varepsilon_j$ *and* $\bar{\lambda}_{ij}\triangleq\lambda(Q_{ij},P_i)\varepsilon_i+\lambda(Q_{ij},P_j)\alpha_j\varepsilon_j$.

Proof. In order to calculate an upper bound of $J(\hat{x}_i^*(s;t_{k+1}),\hat{u}_i^*(s;t_{k+1}),\hat{x}_j^a(s;t_{k+1}))$ $-J(\hat{x}_i^*(s;t_k),\hat{u}_i^*(s;t_k),\hat{x}_j^a(s;t_k))$, we first evaluate $J(\tilde{x}_i(s;t_{k+1}),\tilde{u}_i(s;t_{k+1}),\hat{x}_j^a(s;t_{k+1}))$ $-J(\hat{x}_i^*(s;t_k),\hat{u}_i^*(s;t_k),\hat{x}_j^a(s;t_k))$. That is,

$$
\begin{aligned}
&J(\tilde{x}_i(s;t_{k+1}),\tilde{u}_i(s;t_{k+1}),\hat{x}_j^a(s;t_{k+1}))-J(\hat{x}_i^*(s;t_k),\hat{u}_i^*(s;t_k),\hat{x}_j^a(s;t_k))\\
=&\int_{t_{k+1}}^{t_{k+1}+T}\|\tilde{x}_i(s;t_{k+1})\|_{Q_i}^2+\|\tilde{u}_i(s;t_{k+1})\|_{R_i}^2+\sum_{j\in\mathcal{N}_i}\|\tilde{x}_i(s;t_{k+1})-\hat{x}_j^a(s;t_{k+1})\|_{Q_{ij}}^2\mathrm{d}s\\
&-\int_{t_k}^{t_k+T}\|\hat{x}_i^*(s;t_k)\|_{Q_i}^2+\|\hat{u}_i^*(s;t_k)\|_{R_i}^2+\sum_{j\in\mathcal{N}_i}\|\hat{x}_i^*(s;t_k)-\hat{x}_j^a(s;t_k)\|_{Q_{ij}}^2\mathrm{d}s\\
&+\|\tilde{x}_i(t_{k+1}+T;t_{k+1})\|_{P_i}^2-\|\hat{x}_i^*(t_k+T;t_k)\|_{P_i}^2. \qquad (8.20)
\end{aligned}
$$

Next, we divide the terms in (8.20) into four parts and consider them part by part. The first part to be considered is $\Delta_i^1\triangleq\int_{t_{k+1}}^{t_k+T}\|\tilde{x}_i(s;t_{k+1})\|_{Q_i}^2+\|\tilde{u}_i(s;t_{k+1})\|_{R_i}^2\mathrm{d}s-\int_{t_{k+1}}^{t_k+T}\|\hat{x}_i^*(s;t_k)\|_{Q_i}^2+\|\hat{u}_i^*(s;t_k)\|_{R_i}^2\mathrm{d}s$. Since $\tilde{u}_i(s;t_{k+1})=\hat{u}_i^*(s;t_k)$, for $s\in[t_{k+1},t_k+T]$, we have

$$
\begin{aligned}
\Delta_i^1&=\int_{t_{k+1}}^{t_k+T}\|\tilde{x}_i(s;t_{k+1})\|_{Q_i}^2-\|\hat{x}_i^*(s;t_k)\|_{Q_i}^2\mathrm{d}s\\
&\leqslant\int_{t_{k+1}}^{t_k+T}\|\tilde{x}_i(s;t_{k+1})-\hat{x}_i^*(s;t_k)\|_{Q_i}[\|\tilde{x}_i(s;t_{k+1})\|_{Q_i}+\|\hat{x}_i^*(s;t_k)\|_{Q_i}]\mathrm{d}s.
\end{aligned}
$$

According to (8.14) in Theorem 8.1 and because of the uniform delay, it can be

obtained

$$\begin{aligned}&\|\tilde{x}_i(s;t_{k+1})-\hat{x}_i^*(s;t_k)\|_{Q_i}, s\in[t_{k+1},t_k+T]\\ \leqslant&\lambda(Q_i,P_i)\sqrt{\bar{\lambda}(P_i)}\rho_i\left[\tau_k e^{l_i(s-t_{k+1}+\tau_k)}+\left(\tau_k e^{l_i\tau_k}+\delta+\tau_k\right)e^{l_i(s+\delta+\tau_k-t_{k+1})}\right].\end{aligned}$$

Due to the triangle inequality and the robustness constraint, we get

$$\begin{aligned}&\|\tilde{x}_i(s;t_{k+1})\|_{Q_i}+\|\hat{x}_i^*(s;t_k)\|_{Q_i}, s\in[t_{k+1},t_k+T]\\ \leqslant&\lambda(Q_i,P_i)\left\{\sqrt{\bar{\lambda}(P_i)}\rho_i\left[\tau_k e^{l_i(s-t_{k+1}+\tau_k)}+\left(\tau_k e^{l_i\tau_k}+\delta+\tau_k\right)e^{l_i(s+\delta+\tau_k-t_{k+1})}\right]+\frac{2T\alpha_i\varepsilon_i}{s-t_k}\right\}.\end{aligned}$$

Therefore, we can obtain

$$\Delta_i^1\leqslant\lambda^2(Q_i,P_i)\left[(T-\delta-\tau_k)\Lambda_i^2(\delta,\tau_k)+2T\alpha_i\varepsilon_i\Lambda_i(\delta,\tau_k)\ln\frac{T}{\delta+\tau_k}\right]. \tag{8.21}$$

The second part to be dealt with is $\Delta_i^2\triangleq\int_{t_k+T}^{t_{k+1}+T}\|\tilde{x}_i(s;t_{k+1})\|_{Q_i}^2+\|\tilde{u}_i(s;t_{k+1})\|_{R_i}^2\mathrm{d}s+\|\tilde{x}_i(t_{k+1}+T;t_{k+1})\|_{P_i}^2-\|\hat{x}_i^*(t_k+T;t_k)\|_{P_i}^2$. Since $\tilde{u}_i(s;t_{k+1})=K_i\tilde{x}_i(s;t_{k+1})$, $s\in[t_k+T,t_{k+1}+t]$, it can be obtained

$$\Delta_i^2=\int_{t_k+T}^{t_{k+1}+T}\|\tilde{x}_i(s;t_{k+1})\|_{Q_i^*}^2\mathrm{d}s+\|\tilde{x}_i(t_{k+1}+T;t_{k+1})\|_{P_i}^2-\|\hat{x}_i^*(t_k+T;t_k)\|_{P_i}^2.$$

According to Theorem 8.1, we get $\tilde{x}_i(s;t_k+T)\in\Omega_i(\varepsilon_i)$. Thus, the results in Lemma 8.1 hold, i.e., $\|\tilde{x}_i(s;t_{k+1})\|_{Q_i^*}^2\leqslant-\dot{V}_i(\tilde{x}_i(s;t_{k+1}))$, $s\in[t_k+T,t_{k+1}+t]$. As a result,

$$\Delta_i^2\leqslant\|\tilde{x}_i(t_k+T;t_{k+1})\|_{P_i}^2-\|\hat{x}_i^*(t_k+T;t_k)\|_{P_i}^2\leqslant(1-\alpha_i^2)\varepsilon_i^2. \tag{8.22}$$

Let us resume to consider the third part

$$\Delta_i^3\triangleq\int_{t_{k+1}}^{t_{k+1}+T}\sum_{j\in\mathcal{N}_i}\|\tilde{x}_i(s;t_{k+1})-\hat{x}_j^a(s;t_{k+1})\|_{Q_{ij}}^2\mathrm{d}s$$

. By using the triangle inequality, we have

$$\Delta_i^3\leqslant\sum_{j\in\mathcal{N}_i}\int_{t_{k+1}}^{t_{k+1}+T}[\|\tilde{x}_i(s;t_{k+1})\|_{Q_ij}+\|\hat{x}_j^a(s;t_{k+1})\|_{Q_{ij}}]^2\mathrm{d}s. \tag{8.23}$$

According to (8.14), we get

$$\|\tilde{x}_i(s;t_{k+1})\|_{Q_{ij}} \leqslant \lambda(Q_{ij},P_i)\left[\Lambda_i(\delta,\tau_k)+\frac{T\alpha_i\varepsilon_i}{s-t_k}\right], s\in[t_{k+1},t_k+T].$$

By applying Lemma 8.4, we have

$$\|\tilde{x}_i(s;t_{k+1})\|_{Q_{ij}} \leqslant \lambda(Q_{ij},P_i)\varepsilon_i, s\in[t_k+T,t_{k+1}+T].$$

Furthermore, due to the robustness constraint, it can be obtained

$$\begin{aligned}\|\hat{x}_j^a(s;t_{k+1})\|_{Q_{ij}} \leqslant&\lambda(Q_{ij},P_j)\|\hat{x}_j^*(s;t_k)\|_{P_i}, s\in[t_{k+1},t_k+T]\\ \leqslant&\lambda(Q_{ij},P_j)\frac{T\alpha_j\varepsilon_j}{s-t_k}.\end{aligned}$$

With the help of Lemma 8.1, it can be obtained $\|\hat{x}_j^a(s;t_{k+1})\|_{Q_{ij}} \leqslant \lambda(Q_{ij},P_j)\alpha_j\varepsilon_j$, for $s\in[t_k+T,t_{k+1}+t]$. Plugging the above results into (8.23) yields

$$\Delta_i^3 \leqslant (T-\delta-\tau_k)\sum_{j\in\mathcal{N}_i}\left[\lambda(Q_{ij},P_i)\Lambda_i(\delta,\tau_k)+\frac{\lambda_{ij}T}{\delta+\tau_k}\right]^2+\sum_{j\in\mathcal{N}_i}(\delta+\tau_k)\bar{\lambda}_{ij}^2. \tag{8.24}$$

For the last part, we have

$$\int_{t_k}^{t_{k+1}}\|\hat{x}_i^*(s;t_k)\|_{Q_i}^2+\|\hat{u}_i^*(s;t_k)\|_{R_i}^2\mathrm{d}s \geqslant \int_{t_k}^{t_{k+1}}\|\hat{x}_i^*(s;t_k)\|_{Q_i}^2\mathrm{d}s. \tag{8.25}$$

Finally, by substituting (8.21), (8.22), (8.24) and (8.25) into (8.20) and applying the fact that $J(\hat{x}_i^*(s;t_k),\ \hat{u}_i^*(s;t_{k+1}),\hat{x}_j^a(s;t_{k+1})) \leqslant J(\tilde{x}_i(s;t_{k+1}),\tilde{u}_i(s;t_{k+1}),\hat{x}_j^a(s;t_{k+1}))$, the result in Lemma 8.6 is obtained. This completes the proof. □

Lemma 8.6 reveals an upper bound of the decrease on the optimal objective function from t_k to t_{k+1}, for each agent $\mathcal{A}_i$. But in order to analyze the trajectory of the overall system, we need construct a control Lyapunov function for the whole system. Based on the optimal objective function of each agent, we define a new overall objective function as $J(\hat{x}^*(s;t_k),\hat{u}^*(s;t_k)) \triangleq \sum_{i=0}^{M}J_i(\hat{x}_i^*(s;t_k),\hat{u}_i^*(s;t_k),\hat{x}_{-i}^a(s;t_k))$. We will prove $J(\hat{x}^*(s;t_k),\hat{u}^*(s;t_k))$ is qualified as a control Lyapunov function if the some conditions are satisfied. As a result, the system state will enter the terminal set in finite time if they are not in the terminal set. These results are summarized in the following theorem.

Theorem 8.3. *For the overall system in (8.3), suppose that Assumption 8.1, 8.2 and 8.3 hold for each agent $\mathcal{A}_i$. Given three sets of constants $\bar{\alpha}_i \in (0,1)$, $\beta_i \in (0,1)$ and $\gamma_i \in (0,1)$, with $\beta_i + \gamma_i \in (0,1)$ and $i \in \mathcal{M}$, and the initial system state is out of the terminal set, i.e., $x_0 \notin \Omega(\varepsilon)$, if (1) the sampling period is designed as:*

$$\max_{i\in\mathcal{M}}\{\max\{\underline{\delta}_i, T_i\}\} \leqslant \delta \leqslant \min_{i\in\mathcal{M}}\{\bar{\delta}_i\}, \tag{8.26}$$

where T_i is the positive solution to the following equation: $[\frac{\underline{\lambda}(Q_i)}{\bar{\lambda}(P_i)}\beta_i(1-\bar{\alpha}_i)^2\varepsilon_i^2 + \sum_{j=1}^{M}(\underline{\lambda}(Q_j)\bar{\lambda}^{-1}(P_j))^2(1-\alpha_j)^2\varepsilon_j^2]T_i^2 - [T\sum_{j=1}^{M}(\underline{\lambda}(Q_j)\bar{\lambda}^{-1}(P_j))^2(1-\alpha_j)^2\varepsilon_j^2 + M(1-\alpha_i^2)\varepsilon_i^2]T_i - 2T^2\sum_{j=1}^{M}(\underline{\lambda}(Q_j)\bar{\lambda}^{-1}(P_j))^2\alpha_j(1-\alpha_j)\varepsilon_j^2 = 0$, $\forall i \in \mathcal{M}$; (2) the disturbance is bounded as $\rho_i \leqslant (1-\alpha_i)\varepsilon_i/(\sqrt{\bar{\lambda}(P_i)}\delta e^{l_i T})$; (3) the communication delay is bounded as

$$\tau_k \leqslant \min_{i\in\mathcal{M}}\{\tau_i^m, \tilde{\tau}_i\}, \tag{8.27}$$

where $\tilde{\tau}_i$ satisfies the inequality equation $\sqrt{\bar{\lambda}(P_i)}\rho_i e^{l_i(\delta+\tilde{\tau}_i)}(\tilde{\tau}_i e^{l_i\tilde{\tau}_i} + \delta + \tilde{\tau}_i) \leqslant \bar{\alpha}_i\varepsilon_i$, $\forall i \in \mathcal{M}$; (4) the cooperation matrices Q_{ij}, $\forall i \in \mathcal{M}$, $j \in \mathcal{N}_i$ are designed such that the following inequalities hold:

$$\begin{aligned}
&(T-\delta-\tau_k)\sum_{j\in\mathcal{N}_i}\left[\lambda(Q_{ij},P_i)\Lambda_i(\delta,\tau_k) + \frac{\lambda_{ij}T}{\delta+\tau_k}\right]^2 + \sum_{j\in\mathcal{N}_i}(\delta+\tau_k)\bar{\lambda}_{ij}^2 \\
\leqslant&\gamma_{j'}\frac{\underline{\lambda}(Q_{j'})}{\bar{\lambda}(P_{j'})}(\delta+\tau_k)(1-\bar{\alpha}_{j'})^2\varepsilon_{j'}^2, \forall j' \in \mathcal{M},
\end{aligned} \tag{8.28}$$

then the system state will enter the terminal set in finite time.

Proof. According to Lemma 8.6, we have

$$\begin{aligned}
&J(\hat{x}^*(s;t_{k+1}),\hat{u}^*(s;t_{k+1})) - J(\hat{x}^*(s;t_k),\hat{u}^*(s;t_k)) \\
\leqslant&-\sum_{i=1}^{M}\int_{t_k}^{t_{k+1}}\|\hat{x}_i^*(s;t_k)\|_{Q_i}^2 ds \\
&+\sum_{i=1}^{M}\lambda^2(Q_i,P_i)\left[(T-\delta-\tau_k)\Lambda_i^2(\delta,\tau_k) + 2T\alpha_i\varepsilon_i\Lambda_i(\delta,\tau_k)\ln\frac{T}{\delta+\tau_k}\right] + (1-\alpha_i^2)\varepsilon_i^2 \\
&+\sum_{i=1}^{M}\left\{(T-\delta-\tau_k)\sum_{j\in\mathcal{N}_i}\left[\lambda(Q_{ij},P_i)\Lambda_i(\delta,\tau_k) + \frac{\lambda_{ij}T}{\delta+\tau_k}\right]^2 + \sum_{j\in\mathcal{N}_i}(\delta+\tau_k)\bar{\lambda}_{ij}^2\right\}.
\end{aligned}$$

Since $x(s;t_k) \notin \Omega(\varepsilon)$, then there exists at least one agent whose state trajectory is not

in its terminal set. Without loss of generality, denote such an agent as $\mathcal{A}_{j'}$, $j' \in \mathcal{M}$. Then it can be obtained $x_{j'}(s;t_k) \notin \Omega_{j'}(\varepsilon_{j'})$. According to Lemma 8.3 and the triangle inequality, we obtain:

$$\|\hat{x}^*_{j'}(s;t_k)\|_{P_{j'}} \geqslant \varepsilon_{j'} - \left(\tau_k e^{l_{j'}\tau_k} + \delta + \tau_k\right)\sqrt{\bar{\lambda}(P_{j'})}\rho_{j'}e^{l_{j'}(\delta+\tau_k)}.$$

Therefore, we arrives at

$$\begin{aligned}
&J(\hat{x}^*(s;t_{k+1}),\hat{u}^*(s;t_{k+1})) - J(\hat{x}^*(s;t_k),\hat{u}^*(s;t_k))\\
\leqslant&-(\delta+\tau_k)\frac{\underline{\lambda}(Q_{j'})}{\bar{\lambda}(P_{j'})}\left[\varepsilon_{j'} - (\tau_k e^{l_{j'}\tau_k}+\delta+\tau_k)\sqrt{\bar{\lambda}(P_{j'})}\rho_{j'}e^{l_{j'}(\delta+\tau_k)}\right]^2\\
&+\sum_{i=1}^{M}\lambda^2(Q_i,P_i)\left[(T-\delta-\tau_k)\Lambda_i^2(\delta,\tau_k) + 2T\alpha_i\varepsilon_i\Lambda_i(\delta,\tau_k)\ln\frac{T}{\delta+\tau_k}\right] + (1-\alpha_i^2)\varepsilon_i^2\\
&+\sum_{i=1}^{M}\left\{(T-\delta-\tau_k)\sum_{j\in\mathcal{N}_i}\left[\lambda(Q_{ij},P_i)\Lambda_i(\delta,\tau_k) + \frac{\lambda_{ij}T}{\delta+\tau_k}\right]^2 + \sum_{j\in\mathcal{N}_i}(\delta+\tau_k)\bar{\lambda}_{ij}^2\right\}.
\end{aligned}$$

On the one hand, by exploiting the conditions $\delta \geqslant \max\{T_i\}$ and $\tau_k \geqslant 0$, one can obtain

$$\begin{aligned}
&\sum_{i=1}^{M}\lambda^2(Q_i,P_i)\left[(T-\delta-\tau_k)(1-\alpha_i)^2\varepsilon_i^2 + 2T\alpha_i(1-\alpha_i)\varepsilon_i^2\frac{T}{\delta+\tau_k}\right] + (1-\alpha_i^2)\varepsilon_i^2\\
\leqslant&\beta_{j'}\frac{\underline{\lambda}(Q_{j'})}{\bar{\lambda}(P_{j'})}(\delta+\tau_k)(1-\bar{\alpha}_{j'})^2\varepsilon_{j'}^2, \forall j' \in \mathcal{M}.
\end{aligned}$$

On the other hand, according to (8.13), we get $\Lambda_i(\delta,\tau_k) \leqslant (1-\alpha_i)\varepsilon_i$. In addition, $\ln\frac{T}{\delta+\tau_k} < \frac{T}{\delta+\tau_k}$. Therefore, it follows

$$\begin{aligned}
&J(\hat{x}^*(s;t_{k+1}),\hat{u}^*(s;t_{k+1})) - J(\hat{x}^*(s;t_k),\hat{u}^*(s;t_k))\\
<&-(\delta+\tau_k)\frac{\underline{\lambda}(Q_{j'})}{\bar{\lambda}(P_{j'})}\left[\varepsilon_{j'} - (\tau_k e^{l_{j'}\tau_k}+\delta+\tau_k)\sqrt{\bar{\lambda}(P_{j'})}\rho_{j'}e^{l_{j'}(\delta+\tau_k)}\right]^2\\
&+\beta_{j'}\frac{\underline{\lambda}(Q_{j'})}{\bar{\lambda}(P_{j'})}(\delta+\tau_k)(1-\bar{\alpha}_{j'})^2\varepsilon_{j'}^2\\
&+\sum_{i=1}^{M}\left\{(T-\delta-\tau_k)\sum_{j\in\mathcal{N}_i}\left[\lambda(Q_{ij},P_i)(1-\alpha_i)\varepsilon_i + \frac{\lambda_{ij}T}{\delta+\tau_k}\right]^2 + \sum_{j\in\mathcal{N}_i}(\delta+\tau_k)\bar{\lambda}_{ij}^2\right\}.
\end{aligned}$$

Since the communication delay is bounded as (8.27) and the cooperation matrices are

designed to make (8.28) hold, we obtain

$$\begin{aligned} & J(\hat{x}^*(s;t_{k+1}),\hat{u}^*(s;t_{k+1})) - J(\hat{x}^*(s;t_k),\hat{u}^*(s;t_k)) \\ < & -(1-\gamma_{j'}-\beta_{j'})(\delta+\tau_k)\frac{\underline{\lambda}(Q_{j'})}{\bar{\lambda}(P_{j'})}(1-\bar{\alpha}_{j'})^2\varepsilon_{j'}^2. \end{aligned}$$

By applying the same argument in [97], it can be shown that the system state will enter the terminal set in finite time. □

Remark 8.7. *It is noted that, Theorem 8.3 imposes several conditions in order to drive the system state into the terminal set. Most of these conditions have been used for guaranteeing the feasibility (in Theorem 8.2). There are also two newly-imposed conditions. The lower bound T_i in (8.26) imposed on the sampling period is used to account for the effect of individual objective function to the overall objective function. That is, in order that the overall optimal control objective function is decreased, the sampling period should not be too small. The cooperation matrices need to be designed as (8.28), because the couplings among agents cannot be too strong in order for making the overall optimal control objective function decrease.*

Remark 8.8. *It is worthwhile to point out that the three sets of constants $\bar{\alpha}_i$, β_i and γ_i affect different parameters. In particular, $\bar{\alpha}_i$ affects the bound of the communication delays. The larger $\bar{\alpha}_i$ allows a larger bound of the communication delays. β_i affects T_i, i.e., the lower bound of the sampling period. The larger β_i results in a smaller T_i, which might enlarge the design range of the sampling period. γ_i affects the design of the cooperation matrices. The larger γ_i might allow the larger eigenvalues of the cooperation matrices, which is beneficial for the cooperation.*

According to the dual-mode strategy, once the system state enters the terminal set, the control input will be switched to (8.9). Under this control input, we show that the overall system state will be stabilized into a robustly invariant set if the external disturbances are not too large. The detailed results are reported in the following theorem.

Theorem 8.4. *For the overall system in (8.3), suppose that Assumption 8.1, 8.2 and 8.3 hold, and that the conditions on the sampling period, the communication delays and the cooperation matrices are satisfied as Theorem 8.3. For each agent $\mathcal{A}_i$, $i \in \mathcal{M}$,*

if the disturbance is bounded as

$$\rho_i = \min\left\{\frac{(1-e^{-\frac{\underline{\lambda}(Q_i^*)\delta}{2\bar{\lambda}(P_i)}})\bar{\beta}_i\varepsilon_i}{\bar{\lambda}(\sqrt{P_i})\delta e^{l_i\delta}}, \frac{(1-\alpha_i)\varepsilon_i}{(\sqrt{\bar{\lambda}(P_i)}\delta e^{l_iT})e^{l_i\delta}}\right\},$$

then the overall system state will be stabilized into the robustly invariant set $\Omega_1(\bar{\beta}_1\varepsilon_1)\times\cdots\times\Omega_M(\bar{\beta}_M\varepsilon_M)$*, where* $\bar{\beta}_i\in(0,1)$.

Proof. According to Theorem 8.3, the system state will enter the terminal set in finite time. In terms of the dual-mode strategy, the control input will be applied as (8.9) for each agent $\mathcal{A}_i$ when the system state enters the terminal set. Without loss of generality, we denote such a time instant as t_{k_e}. To prove the result, we next need to prove that, for each agent $\mathcal{A}_i$, $i\in\mathcal{M}$, the system state will be stabilized into the robustly invariant set $\Omega_i(\bar{\beta}_i\varepsilon_i)$ under the control input as (8.9). To that end, two facts should be proved: (1) The system state converges to $\Omega_i(\bar{\beta}_i\varepsilon_i)$; (2) the set $\Omega_i(\bar{\beta}_i\varepsilon_i)$ is robustly invariant for the agent $\mathcal{A}_i$.

Let us first prove that the system state of the agent $\mathcal{A}_i$ converges to the set $\Omega_i(\bar{\beta}_i\varepsilon_i)$. By taking the Lyapunov function as $\bar{V}_i(x_i(s;t_k))=\|x_i(t_k)\|_{P_i}^2$, $s\in[t_k,t_{k+1}]$ for the agent $\mathcal{A}_i$, we have

$$\begin{aligned}
&\bar{V}_i(x_i(s;t_{k+1}))-\bar{V}_i(x_i(s;t_k))\\
=&\left[\|x_i(t_{k+1})\|_{P_i}-\|x_i(t_k)\|_{P_i}\right]\left[\|x_i(t_{k+1})\|_{P_i}+\|x_i(t_k)\|_{P_i}\right]\\
\leqslant&\left[\|\hat{x}_i(t_{k+1};t_k)\|_{P_i}+\bar{\lambda}(\sqrt{P_i})\rho_i\delta e^{l_i\delta}-\|x_i(t_k)\|_{P_i}\right]\left[\|x_i(t_{k+1})\|_{P_i}+\|x_i(t_k)\|_{P_i}\right],
\end{aligned}$$

where the result

$$\|x_i(s;t_k)-\hat{x}_i(s;t_k)\|_{P_i}\leqslant\bar{\lambda}(\sqrt{P_i})\rho_i(s-t_k)e^{l_i(s-t_k)}, s\in[t_k,t_{k+1}] \tag{8.29}$$

has been used. By following the similar line of deriving (8.15), we get

$$\|\hat{x}_i(t_{k+1};t_k)\|_{P_i}\leqslant\|\hat{x}_i(t_k;t_k)\|_{P_i}e^{-\frac{\underline{\lambda}(Q_i^*)(s-t_k)}{2\bar{\lambda}(P_i)}}. \tag{8.30}$$

Therefore, we obtain

$$\begin{aligned}&\bar{V}_i(x_i(s;t_{k+1}))-\bar{V}_i(x_i(s;t_k))\\&\leqslant\left[(e^{-\frac{\underline{\lambda}(Q_i^*)\delta}{2\lambda(P_i)}}-1)\|x_i(t_k)\|_{P_i}+\bar{\lambda}(\sqrt{P_i})\rho_i\delta e^{l_i\delta}\right]\left[\|x_i(t_{k+1})\|_{P_i}+\|x_i(t_k)\|_{P_i}\right].\end{aligned}\tag{8.31}$$

Suppose that $x_i(t_k)$ never converges to $\Omega_i(\bar{\beta}_i\varepsilon_i)$, i.e., $\|x_i(t_k)\|_{P_i}>\bar{\beta}_i\varepsilon_i$ for $k\geqslant k_e$. Without loss of generality, it can be written that $\|x_i(t_k)\|_{P_i}=\bar{\beta}_i\varepsilon_i+h(t_k)$, where $h(t_k)>0$ and $\lim_{k\to\infty}h(t_k)\neq 0$, for $k\geqslant k_e$. Thus, according to (8.31), we get

$$\bar{V}_i(x_i(s;t_{k+1}))-\bar{V}_i(x_i(s;t_k))\leqslant -2(1-e^{-\frac{\underline{\lambda}(Q_i^*)\delta}{2\lambda(P_i)}})\bar{\beta}_i\varepsilon_i h(t_k).$$

Since $\lim_{k\to\infty}h(t_k)\neq 0$, it is easy to obtain that $\lim_{k\to\infty}\bar{V}_i(x_i(s;t_k))=-\infty$. This contradicts the fact that $0<\bar{V}_i(x_i(s;t_k))<\infty$, for $k\geqslant k_e$. Therefore, the state $x_i(t_k)$ will converge to the set $\Omega_i(\bar{\beta}_i\varepsilon_i)$.

Second, we will prove that the set $\Omega_i(\bar{\beta}_i\varepsilon_i)$ is robustly invariant for the agent $\mathcal{A}_i$. That is, if $x_i(t_k)\in\Omega_i(\bar{\beta}_i\varepsilon_i)$, then $x_i(t)\in\Omega_i(\bar{\beta}_i\varepsilon_i)$, for all $t\geqslant t_k$. By using (8.31), it can be obtained that

$$\begin{aligned}&\|x_i(t_{k+1})\|_{P_i}^2-\|(x_i(t_k))\|_{P_i}^2\\&\leqslant\left[(e^{-\frac{\underline{\lambda}(Q_i^*)\delta}{2\lambda(P_i)}}-1)\|x_i(t_k)\|_{P_i}+\bar{\lambda}(\sqrt{P_i})\rho_i\delta e^{l_i\delta}\right]\left[(e^{-\frac{\underline{\lambda}(Q_i^*)\delta}{2\lambda(P_i)}}+1)\|x_i(t_k)\|_{P_i}+\bar{\lambda}(\sqrt{P_i})\rho_i\delta e^{l_i\delta}\right],\end{aligned}$$

where the results in (8.29) and (8.30) are utilized. That is,

$$\begin{aligned}\|x_i(t_{k+1})\|_{P_i}^2\leqslant&e^{-\frac{\underline{\lambda}(Q_i^*)\delta}{\lambda(P_i)}}\|(x_i(t_k))\|_{P_i}^2\\&+2e^{-\frac{\underline{\lambda}(Q_i^*)\delta}{2\lambda(P_i)}}\bar{\lambda}(\sqrt{P_i})\rho_i\delta e^{l_i\delta}\|(x_i(t_k))\|_{P_i}+\left(\bar{\lambda}(\sqrt{P_i})\rho_i\delta e^{l_i\delta}\right)^2.\end{aligned}\tag{8.32}$$

Plugging $\|x_i(t_k)\|_{P_i}\leqslant\bar{\beta}_i\varepsilon_i$ into (8.32) results in $\|x_i(t_{k+1})\|_{P_i}^2\leqslant\bar{\beta}_i^2\varepsilon_i^2$. Thus, $x_i(t_k)\in\Omega_i(\bar{\beta}_i\varepsilon_i)$ implies $x_i(t_{k+1})\in\Omega_i(\bar{\beta}_i\varepsilon_i)$ for all $k\geqslant k_e$. Furthermore, according to (8.29), we have

$$\begin{aligned}\|x_i(s;t_k)\|_{P_i}\leqslant&\|\hat{x}_i(s;t_k)\|_{P_i}+\bar{\lambda}(\sqrt{P_i})\rho_i(s-t_k)e^{l_i(s-t_k)},s\in[t_k,t_{k+1}]\\\leqslant&\|x_i(t_k)\|_{P_i}e^{-\frac{\underline{\lambda}(Q_i^*)\delta}{2\lambda(P_i)}}+\bar{\lambda}(\sqrt{P_i})\rho_i\delta e^{l_i\delta}.\end{aligned}\tag{8.33}$$

From (8.33), it can be verified that $\|x_i(s;t_k)\|_{P_i}\leqslant\bar{\beta}_i\varepsilon_i$, $s\in[t_k,t_{k+1}]$, if $\|x_i(t_k)\|_{P_i}\leqslant$

$\bar{\beta}_i\varepsilon_i$ for all $k \geqslant k_e$. Therefore, $x_i(t_k) \in \Omega_i(\bar{\beta}_i\varepsilon_i)$ implies $x_i(t) \in \Omega_i(\bar{\beta}_i\varepsilon_i)$ for $t \geqslant t_k$. That is, the set $\Omega_i(\bar{\beta}_i\varepsilon_i)$ is robustly invariant. The proof is completed. □

8.6 Simulation Studies

In this section, the distributed control of a group of mechanical systems is utilized to verify the proposed theoretical results.

8.6.1 System Model

Consider three identical nonlinear spring-damping-cart systems. Each system $\mathcal{A}_i$, $i = 1, 2, 3$, is described as follows:

$$\begin{cases} \dot{x}_1^i(t) = x_2^i(t), \\ \dot{x}_2^i(t) = -\frac{\kappa}{M_c} e^{-x_1^i(t)} x_1^i(t) - \frac{h_d}{M_c} x_2^i(t) + \frac{u_i(t)}{M_c} + \omega_i(t), \end{cases}$$

where $x_1^i(t)$ and $x_2^i(t)$ are system states, representing the displacement and velocity of the cart, respectively, $u_i(t)$ is the control input, standing for the control force, which is constrained as $-3\text{N} \leqslant u_i(t) \leqslant 3\text{N}$, $\omega_i(t)$ is the external disturbance. The parameters are given as follows: $M_c = 1.8\text{kg}$, $\kappa = 1.2\text{N/m}$, $h_d = 0.25\text{Ns/m}$. This mechanical system has been used to test nonlinear MPC schemes in many studies such as [89, 124, 69, 70].

For the overall system, the indices of the neighbors of $\mathcal{A}_1$ are $\mathcal{N}_1 = \{2, 3\}$; similarly, $\mathcal{N}_2 = \{1, 3\}$ and $\mathcal{N}_3 = \{1, 2\}$. In the objective function (8.6) of each agent $\mathcal{A}_i$, the matrices $Q_1 = Q_2 = Q_3 = \text{diag}(1, 1)$ and $R_1 = R_2 = R_3 = 0.1$. The prediction horizon $T = 0.2\text{sec}$. The state feedback gain in Assumption 8.2 is given as $K_1 = K_2 = K_3 = [-4.2291, -4.8551]$. In Lemma 8.1, the matrices are designed as $P_1 = P_2 = P_3 = [5.0511, -2.2731; -2.2731, 2.4586]$. According to the methods in [11, 97, 95], the terminal set levels can be calculated as $\varepsilon_1 = \varepsilon_2 = \varepsilon_3 = 0.50$.

8.6.2 Theoretical Bounds of Parameters

The constraint shrinkage rates are given as $\alpha_1 = \alpha_2 = \alpha_3 = 0.99$. The constants in Theorem 8.3 are given as follows: $\bar{\alpha}_1 = \bar{\alpha}_2 = \bar{\alpha}_3 = 0.01$, $\beta_1 = \beta_2 = \beta_3 = 0.9$ and $\gamma_1 = \gamma_2 = \gamma_3 = 0.09$. The constants in Theorem 8.4 are given as $\bar{\beta}_1 = \bar{\beta}_2 = \bar{\beta}_3 = 0.2$. Firstly, according to Theorem 8.2, the bounds of the sampling period to guarantee

the feasibility are calculated as $\delta \geqslant 0.063$ and $\delta < 0.28$. The upper bound of the communication delays is calculated as $\tau_k \leqslant 0.0303$. The external disturbance bounds are evaluated as $\rho_1 = \rho_2 = \rho_3 = 0.004$, respectively. Second, in terms of (8.26) in Theorem 8.3, the bounds of the sampling for guaranteeing the stability is calculated as $\delta \geqslant 0.2398$ and $\delta < 0.28$. The upper bound of the communication delay is still $\tau_k \leqslant 0.0384$. In Theorem 8.4, the external disturbance bounds are determined as $\rho_1 = \rho_2 = \rho_3 = 0.0033$.

8.6.3 Simulation Results

In order to ensure the feasibility and stability, we choose the following design parameters. The sampling period is designed as $\delta = 0.24$sec, $\tau_k = 0.02$sec, and the external disturbances are generated as three independent and uniformly distributed stochastic processed confined between $[-0.003, 0.003]$. Note these parameters satisfy Theorem 8.1 - 8.4. The cooperation matrices are designed as $Q_{12} = Q_{13} = [0.2, 0.5; 0, 0.1364]$, $Q_{21} = Q_{23} = [0.2, 0.5; 0, 0.1364]$ and $Q_{31} = Q_{32} = [0.2, 0.5; 0, 0.1364]$. It can be verified that they satisfy (8.28) in Theorem 8.3.

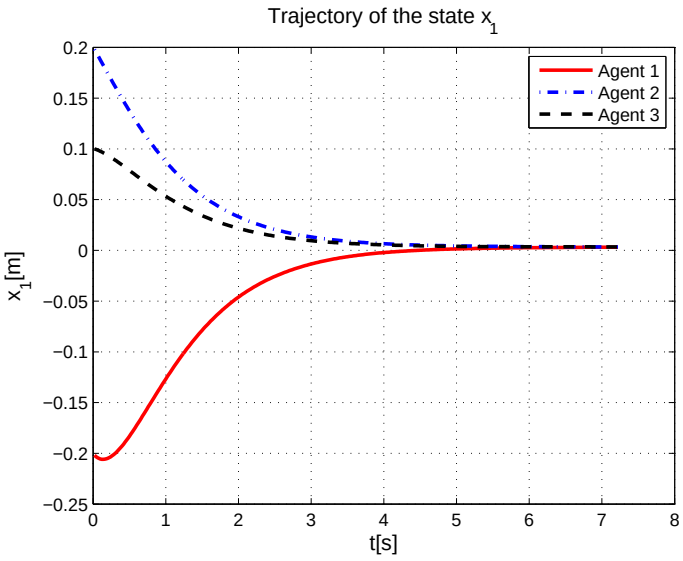

Figure 8.1: The trajectories of the displacements.

By executing the robust distributed MPC algorithm with the designed parameters, the simulation results are as follows. The trajectories of three displacements are presented in Figure 8.1; the trajectories of the velocities are depicted in Figure 8.2 and the control inputs are illustrated in Figure 8.3. From Figure 8.1 and Figure 8.2,

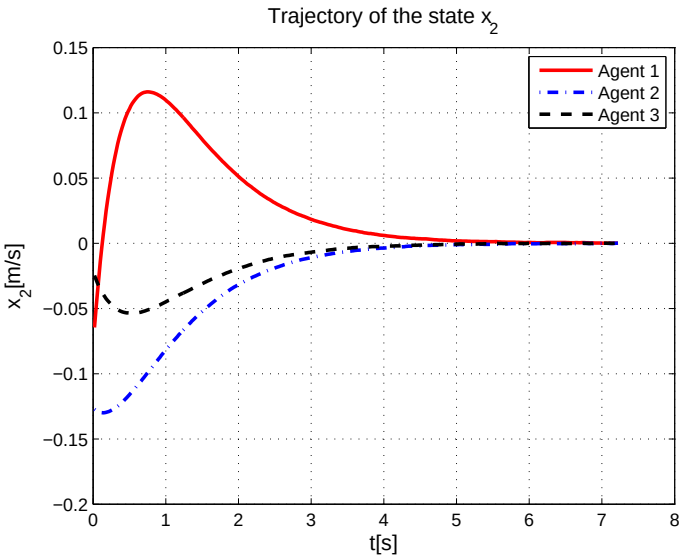

Figure 8.2: The trajectories of the velocities.

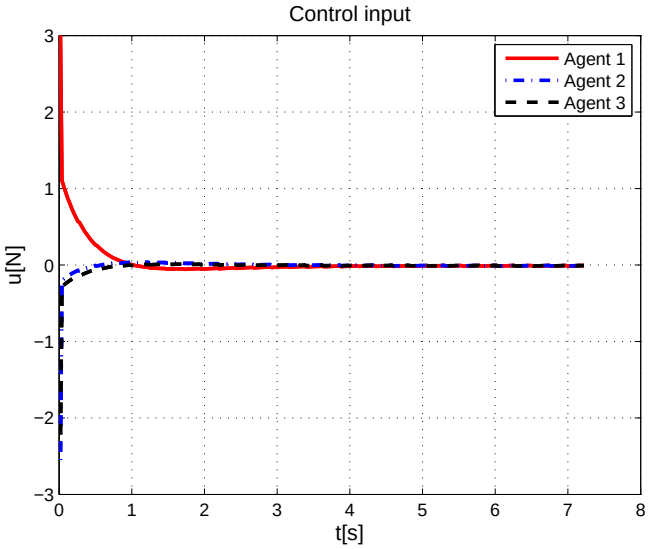

Figure 8.3: The control inputs.

it can be seen that the system state of the three subsystems converges in a robustly invariant set. Figure 8.3 implies that the distributed MPC is feasible and the control input constraints are satisfied.

8.7 Conclusion

This chapter studies the robust distributed MPC problem for a group of nonlinear systems subject to communication delays and external disturbances. By using the robustness constraint, the novel dual-model robust distributed MPC strategy is designed for simultaneously addressing the communication delays and external disturbances. The feasibility of the designed distributed MPC and the stability of the overall closed-loop system are analyzed. The conditions on ensuring the feasibility and robust stability are developed. It is shown that (1) the feasibility can be guaranteed if the external disturbances and communication delays are small enough, and the sampling period is appropriately designed; (2) the system state converges to a robustly invariant set, if the external disturbances and communication delays are bounded by given values, and the sampling period and the cooperation matrices are designed properly.

Chapter 9

Conclusions and Future Work

9.1 Conclusions

In the dissertation, three important issues in nonlinear NCSs have been addressed, namely, the robust filtering problem, the robust MPC problem, and the distributed MPC problem of large-scale nonlinear systems.

The robust filtering problem of uncertain nonlinear NCSs has been studied in **Chapter 2**, where the model uncertainties, external disturbances and measurement time delays modeled by a Markov process have been considered. The robust $\mathcal{H}_\infty$ nonlinear filter has been designed for such systems and the filtering performance has been analyzed. It is shown that the resulting filtering system is stochastic stable in the sense of mean square and achieves the prescribed disturbance attenuation level, if the Markov-chain dependent HJI is satisfied.

The robust MPC problem of NCSs has been explored in **Chapter 3, 4 and 5**, focusing on three different aspects. In **Chapter 3**, the nonlinear NCS with input and state constraints, external disturbances and two-channel packet dropouts has been studied. The robust networked MPC scheme has been proposed to reduce the communication load by designing an efficient compensation strategy. A novel Lyapunov function has been designed to prove the ISpS of the closed-loop system. In **Chapter 4**, the nonlinear NCS investigated is subject to input and state constraints, external disturbances, and two-channel packet dropouts as well as time delays. To improve the robustness and control performance, a networked min-max MPC strategy has been developed by incorporating the characteristics of disturbances into the optimization problem design. The ISpS of the closed-loop system is established by

constructing a new ISpS-Lyapunov function. In **Chapter 5**, to deal with the issue that the system state is not directly measurable, the robust output feedback MPC problem of NCSs has been investigated. The system is linear but subject to input and state constraints, intermittent measurement dropouts and external disturbances. A novel networked output feedback MPC algorithm has been designed by augmenting and tightening the constraints. The stability and feasibility conditions have been established, and the system state is regulated into some convergence sets.

The distributed MPC problem of large-scale nonlinear systems has been dealt with in **Chapter 6, 7 and 8** step by step. **Chapter 6** has focused on subsystems with input constraints and external disturbances, but without considering the communication delays among them. The robustness constraint is invented to handle the external disturbances, and the novel robust distributed MPC algorithm has been designed for such systems. Sufficient conditions have been developed to guarantee the feasibility of the proposed algorithm and the stability of the closed-loop system. **Chapter 7** has studied subsystems subject to input constraints and communication delays, but without disturbances. The delay-involved distributed MPC algorithm has been developed by designing a waiting mechanism. The corresponding feasibility and stability issues have been thoroughly investigated. Based on the results in **Chapter 6 and 7**, **Chapter 8** has designed the robust distributed MPC algorithm of large-scale systems subject to input constraints, external disturbances and communication delays. The feasibility and stability properties have been established: If the bounds of the disturbances and communication delays are small enough and the sampling period is chosen appropriately, then the feasibility can be established; if, in addition to these conditions, the minimum eigenvalues of the cooperation matrices are designed properly, the system state is stabilized into a robustly invariant set.

9.2 Future Work

Since NCSs are emerging and vibrant research area spawning a lot of challenging topics, there are many interesting issues deserving studies in the future. Here, three potential future directions most closely related with this dissertation are suggested as follows.

- **Distributed nonlinear filtering of NCSs**. In the dissertation, a robust $\mathcal{H}_\infty$ filter is designed for a class of nonlinear NCSs. But it may not be applicable

for large-scale nonlinear systems and/or multi-agent systems which finds many applications in modern industrial systems. This is because, in such large-scale systems, a filtering center is generally not available due to distributed system structures and/or limited computation resources. Thus, a robust distributed filtering scheme needs to be designed such that the system state can be estimated. The distributed filter can generally be synthesized by designing local filters of subsystems and the information exchange strategy. Note that the quality of information exchange among subsystems, being essential to make the states of distributed filters converge to an equilibrium point or reach a consensus point, is dependent on communication networks. In practice, however, it is likely that the communication networks are not always reliable, especially in wireless networks shared by a large number of subsystems. Therefore, the robust filtering problems of large-scale nonlinear systems subject to communication constraints such as time delays, packet dropouts and quantization errors is of great practical interest, which deserves further study.

- **Robust output feedback MPC of nonlinear NCSs**. A robust output feedback MPC algorithm has been proposed for a class of NCSs in this dissertation. However, the designed MPC algorithm is only valid for linear systems with measurements subject to periodical dropouts. There are still many important issues needed to be considered in practice. For example, most of the industrial control systems are essentially nonlinear; the measurements are likely to be subject to random time delays and/or packet dropouts. Hence, there is much work to be done towards a robust output feedback MPC approach to nonlinear NCSs that are able to deal with different types of communication constraints. It is worth noting that the separation principle is generally not valid even for designing MPC of linear systems, thus the design of output MPC of nonlinear NCSs is a very challenging topic which needs much effort. One tentative solution to this problem consists of two parts: Firstly, a nonlinear networked observer is required to be designed for estimating the system state when the measurements are subject to communication constraints. Secondly, treating the estimation error as an extra disturbance, a nonlinear robust state feedback MPC strategy can be designed based on the state estimation.

- **Distributed moving horizon estimation (MHE) of large-scale nonlinear systems**. The distributed MHE problem has not been studied in this

dissertation. In comparison with other nonlinear estimation approaches, the distributed MHE offers two desired features for practical applications: (1) it is able to achieve optimal system state estimation even for nonlinear systems subject to unknown disturbances; (2) it is very efficient to deal with system constraints by incorporating the constraint information into system state estimation, and the estimation accuracy might be improved. These two features make the distributed MHE a desired choice in many industrial systems such as sensor networks [26] and process control systems [25]. To design an applicable distributed MHE algorithm for large-scale industrial nonlinear systems, several issues need to be investigated. For example, how to design the local MHEs and their communication topologies and information exchange schemes such that the distributed MHE can estimate system state or achieve a consensus estimation? How to design a robust distributed MHE considering communication constraints including time delays, packet dropouts and quantization errors simultaneously? In addition, the study of the stability and convergence properties of the distributed MHE under different network topologies and communication constraints is also a worthwhile yet challenging topic.

Bibliography

[1] P. Antsaklis and J. Baillieul. Guest editorial special issue on networked control systems. *IEEE Transactions on Automatic Control*, 49(9):1421–1423, 2004.

[2] J. Baillieul and P. J. Antsaklis. Control and communication challenges in networked real-time systems. *Proceedings of the IEEE*, 95(1):9–28, 2007.

[3] A. Bemporad, F. Borrelli, and M. Morari. Min-max control of constrained uncertain discrete-time linear systems. *IEEE Transactions on Automatic Control*, 48(9):1600–1606, 2003.

[4] A. Bemporad and A. Garulli. Output-feedback predictive control of constrained linear systems via set-membership state estimation. *International Journal of Control*, 73(8):655–665, 2000.

[5] N. Berman and U. Shaked. H_∞ control for discrete-time nonlinear stochastic systems. *IEEE Transactions on Automatic Control*, 51(6):1041–1046, 2006.

[6] F. Blanchini. Set invariance in control. *Automatica*, 35(11):1747–1767, 1999.

[7] E. Camponogara, D. Jia, B. H. Krogh, and S. Talukdar. Distributed model predictive control. *IEEE Control Systems Magazine*, 22(1):44–52, 2002.

[8] M. Cannon, B. Kouvaritakis, and V. Deshmukh. Enlargement of polytopic terminal region in NMPC by interpolation and partial invariance. In *Proceedings of the American Control Conference*, pages 4287–4292, Denver, Colorado, 2003.

[9] A. Casavola, E. Mosca, and M. Papini. Predictive teleoperation of constrained dynamic systems via internet-like channels. *IEEE Transactions on Control Systems Technology*, 14(4):681–694, 2006.

[10] D. Chatterjee. *Studies on Stability and Stabilization of Randomly Switched Systems*. PhD thesis, University of Illinois, 2007.

[11] H. Chen and F. Allgöwer. A quasi-infinite horizon nonlinear model predictive control scheme with guaranteed stability. *Automatica*, 34(10):1205–1217, 1998.

[12] I.-R. Chen, A.P. Speer, and M. Eltoweissy. Adaptive fault-tolerant qos control algorithms for maximizing system lifetime of query-based wireless sensor networks. *IEEE Transactions on Dependable and Secure Computing*, 8(2):161–176, 2011.

[13] J. Chen, G. W. Irwin, and A. McKernan. Packet-based robust mpc for wireless networked control using co-design. In *American Control Conference*, pages 1829–1834, Marriott Waterfront, Baltimore, MD, USA, 2010.

[14] L. Chisci, J. A. Rossiter, and G. Zappa. Systems with persistent disturbances: predictive control with restricted constraints. *Automatica*, 37(7):1019–1028, 2001.

[15] L. Chisci and G. Zappa. Feasibility in predictive control of constrained linear systems: the output feedback case. *International Journal of Robust and Nonlinear Control*, 12(5):465–487, 2002.

[16] C. E. de Souza, K. A. Barbosa, and A. T. Neto. Robust H_∞ filtering for discrete-time linear systems with uncertain time-varying parameters. *IEEE Transactions on Signal Processing*, 54(6):2110–2118, 2006.

[17] D. Ding, Z. Wang, B. Shen, and H. Shu. H_∞ state estimation for discrete-time complex networks with randomly occurring sensor saturations and randomly varying sensor delays. *IEEE Transactions on Neural Networks and Learning Systems*, 23(5):725–736, 2012.

[18] H. Dong, Z. Wang, and H. Gao. Distributed H_∞ filtering for a class of markovian jump nonlinear time-delay systems over lossy sensor networks. *IEEE Transactions on Industrial Electronics, In press.*

[19] H. Dong, Z. Wang, D. W. C. Ho, and H. Gao. Robust H_∞ filtering for a class of nonlinear networked systems with multiple stochastic communication delays and packet dropouts. *IEEE Transactions on Signal Processing*, 58(4):1957–1966, 2010.

[20] H. Dong, Z. Wang, D. W. C. Ho, and H. Gao. Robust H_∞ filtering for markovian jump systems with randomly occurring nonlinearities and sensor saturation: the finite-horizon case. *IEEE Transactions on Signal Processing*, 59(7):3048–3057, 2011.

[21] W. B. Dunbar. Distributed receding horizon control of dynamically coupled nonlinear systems. *IEEE Transactions on Automatic Control*, 52(7):1249–1263, 2007.

[22] W. B. Dunbar and D. S. Caveney. Distributed receding horizon control of vehicle platoons: Stability and string stability. *IEEE Transactions on Automatic Control*, 57(3):620–633, 2012.

[23] W. B. Dunbar and R. M. Murray. Distributed receding horizon control for multi-vehicle formation stabilization. *Automatica*, 42(4):549–558, 2006.

[24] D. Famularo and G. Franzè. Output feedback model predictive control of uncertain norm-bounded linear systems. *International Journal of Robust and Nonlinear Control*, 21(8):838–862, 2011.

[25] M. Farina, G. Ferrari-Trecate, C. Romani, and R. Scattolini. Moving horizon estimation for distributed nonlinear systems with application to cascade river reaches. *Journal of Process Control*, 21(5):767–774, 2011.

[26] M. Farina, G. Ferrari-Trecate, and R. Scattolini. Distributed moving horizon estimation for sensor networks. In *Proceeding of 1st IFAC Workshop on Estimation and Control of Networked Systems*, pages 126–131, 2009.

[27] M. Farina and R. Scattolini. Distributed predictive control: a non-cooperative algorithm with neighbor-to-neighbor communication for linear systems. *Automatica*, 48(6):1088–1096, 2012.

[28] G. Ferrari-Trecate, L. Galbusera, M.P.E. Marciandi, and R. Scattolini. Model predictive control schemes for consensus in multi-agent systems with single- and double-integrator dynamics. *IEEE Transactions on Automatic Control*, 54(11):2560–2572, 2009.

[29] J. N. Fidalgo, J. A. Pecas Lopes, and V. Miranda. Neural networks applied to preventive control measures for the dynamic security of isolated power systems with renewables. *IEEE Transactions on Power Systems*, 11(4):1811–1816, 1996.

[30] R. Findeisen and P. Varutti. Stabilizing nonlinear predictive control over nondeterministic communication networks. In *Nonlinear Model Predictive Control*, volume 384, pages 167–179. Springer Berlin / Heidelberg, 2009.

[31] E. Franco, L. Magni, T. Parisini, M. M. Polycarpou, and D. M. Raimondo. Cooperative constrained control of distributed agents with nonlinear dynamics and delayed information exchange: A stabilizing receding-horizon approach. *IEEE Transactions on Automatic Control*, 53(1):324–338, 2008.

[32] E. Franco, T. Parisini, and M. M. Polycarpou. Design and stability analysis of cooperative receding-horizon control of linear discrete-time agents. *International Journal of Robust and Nonlinear Control*, 17(10-11):982–1001, 2007.

[33] H. Gao and T. Chen. H_∞ estimation for uncertain systems with limited communication capacity. *IEEE Transactions on Automatic Control*, 52(10):2070–2084, 2007.

[34] H. Gao, X. Meng, and T. Chen. A parameter-dependent approach to robust H_∞ filtering for time-delay systems. *IEEE Transactions on Automatic Control*, 53(10):2420–2425, 2008.

[35] H. Gao and C. Wang. A delay-dependent approach to robust H_∞ filtering for uncertain discrete-time state-delayed systems. *IEEE Transactions on Signal Processing*, 52(6):1631–1640, 2004.

[36] A. Germani, C. Manes, and P. Palumbo. Filtering of stochastic nonlinear differential systems via a carleman approximation approach. *IEEE Transactions on Automatic Control*, 52(11):2166–2172, 2007.

[37] G. C. Goodwin, H. Haimovich, D. E. Quevedo, and J. S. Welsh. A moving horizon approach to networked control system design. *IEEE Transactions on Automatic Control*, 49(9):1427–1445, 2004.

[38] K. Gopalsamy and X.-Z. He. Delay-independent stability in bidirectional associative memory networks. *IEEE Transactions on Neural Networks*, 5(6):998–1002, 1994.

[39] G. Grimm, M. J. Messina, S. E. Tuna, and A. R. Teel. Examples when nonlinear model predictive control is nonrobust. *Automatica*, 40(10):1729–1738, 2004.

[40] L. Grüne and J. Pannek. *Nonlinear Model Predictive Control: Theory and Algorithms*. Springer-London, 2011.

[41] L. Grüne, J. Pannek, and K. Worthmann. A prediction based control scheme for networked systems with delays and packet dropouts. In *in the Proceedings of the 48th IEEE Conference on Decision and Control and 28th Chinese Control Conference*, pages 537–542, 2009.

[42] R. A. Gupta and C. Mo-Yuen. Networked control system: overview and research trends. *IEEE Transactions on Industrial Electronics*, 57(7):2527–2535, 2010.

[43] Y. He, M. Wu, and J. H. She. Delay-dependent exponential stability of delayed neural networks with time-varying delay. *IEEE Transactions on Circuits and Systems II: Express Briefs*, 53(7):553–557, 2006.

[44] W. P. M. H. Heemels, A. R. Teel, N. van de Wouw, and D. Nesic. Networked control systems with communication constraints: tradeoffs between transmission intervals, delays and performance. *IEEE Transactions on Automatic Control*, 55(8):1781–1796, 2010.

[45] M. Heidarinejad, J. Liu, D. Muñoz de la Peña, J. F. Davis, and P. D. Christofides. Handling communication disruptions in distributed model predictive control. *Journal of Process Control*, 21(1):173–181, 2011.

[46] M. Heidarinejad, J. Liu, D. Muñoz de la Peña, J. F. Davis, and P. D. Christofides. Multirate Lyapunov-based distributed model predictive control of nonlinear uncertain systems. *Journal of Process Control*, 21(9):1231–1242, 2011.

[47] J. P. Hespanha, P. Naghshtabrizi, and Y. Xu. A survey of recent results in networked control systems. *Proceedings of the IEEE*, 95(1):138–162, 2007.

[48] L. Hetel, J. Daafouz, and C. Iung. Stabilization of arbitrary switched linear systems with unknown time-varying delays. *IEEE Transactions on Automatic Control*, 51(10):1668–1674, 2006.

[49] S. Hirche, T. Matiakis, and M. Buss. A distributed controller approach for delay-independent stability of networked control systems. *Automatica*, 45(8):1828–1836, 2009.

[50] Y.-C. Ho. On centralized optimal control. *IEEE Transactions on Automatic Control*, 50(4):537–538, 2005.

[51] S. H. Hong. Bandwidth allocation scheme for cyclic-service fieldbus networks. *IEEE/ASME Transactions on Mechatronics*, 6(2):197–204, 2001.

[52] J. Hu, Z. Wang, H. Gao, and L. K. Stergioulas. Extended kalman filtering with stochastic nonlinearities and multiple missing measurements. *Automatica*, 48(9):2007–2015, 2012.

[53] D. Huang and S. K. Nguang. State feedback control of uncertain networked control systems with random time delays. *IEEE Transactions on Automatic Control*, 53(3):829–833, 2008.

[54] M. Huang and S. Dey. Stability of kalman filtering with markovian packet losses. *Automatica*, 43(4):598–607, 2007.

[55] O. C. Imer, S. Yükel, and T. BaÇar. Optimal control of lti systems over unreliable communication links. *Automatica*, 42(9):1429–1439, 2006.

[56] Y. Ji and W. Gao. Nonlinear H_∞-control and estimation of optimal H_∞-gain. *Systems & Control Letters*, 24(5):321–332, 1995.

[57] D. Jia and B. Krogh. Min-max feedback model predictive control for distributed control with communication. In *Proceedings of the 2002 American Control Conference*, volume 6, pages 4507–4512, 2002.

[58] X. Jiang, Q.-L. Han, S. Liu, and A. Xue. A new H_∞ stabilization criterion for networked control systems. *IEEE Transactions on Automatic Control*, 53(4):1025–1032, 2008.

[59] Z. Jiang and Y. Wang. Input-to-state stability for discrete-time nonlinear systems. *Automatica*, 37(6):857–869, 2001.

[60] B. Johansson, A. Speranzon, M. Johansson, and K. H. Johansson. On decentralized negotiation of optimal consensus. *Automatica*, 44(4):1175–1179, 2008.

[61] T. Keviczky, F. Borrelli, and G. J. Balas. Decentralized receding horizon control for large scale dynamically decoupled systems. *Automatica*, 42(12):2105–2115, 2006.

[62] T. Keviczky, F. Borrelli, K. Fregene, D. Godbole, and G. J. Balas. Decentralized receding horizon control and coordination of autonomous vehicle formations. *IEEE Transactions on Control Systems Technology*, 16(1):19–33, 2008.

[63] T. Keviczky and K. H. Johansson. A study on distributed model predictive consensus. *arXiv preprint arXiv:0802.4450*, 2008.

[64] H. K. Khalil. *Nonlinear Systems*. Prentice hall, 3 edition, 2002.

[65] S. Kluge, K. Reif, and M. Brokate. Stochastic stability of the extended kalman filter with intermittent observations. *IEEE Transactions on Automatic Control*, 55(2):514–518, 2010.

[66] I. Kolmanovsky and E. G. Gilbert. Theory and computation of disturbance invariant sets for discrete-time linear systems. *Mathematical Problem in Engineering*, 4(4):317–367, 1998.

[67] B. Kouvaritakis, J. A. Rossiter, and J. Schuurmans. Efficient robust predictive control. *IEEE Transactions on Automatic Control*, 45(8):1545–1549, 2000.

[68] Y. I. Lee and B. Kouvaritakis. Receding horizon output feedback control for linear systems with input saturation. *IEE Proceedings - Control Theory and Applications*, 148(2):109–115, 2001.

[69] H. Li and Y. Shi. Distributed model predictive control of constrained constinuous-time nonlinear systems with communication delays. *Submitted to Systems & Control Letters*, 2012.

[70] H. Li and Y. Shi. Robust distributed model predictive control of constrained constinuous-time nonlinear systems: A robustness constraint approach. *Submitted to IEEE Transactions on Automatic Control*, 2012.

[71] H. Li and Y. Shi. Robust H_∞ filtering for nonlinear stochastic systems with uncertainties and markov delays. *Automatica*, 48(1):159–166, 2012.

[72] H. Li and Y. Shi. Output feedback model predictive control for constrained linear systems with intermittent measurement. *Systems & Control Letters*, 62(4):345–354, 2013.

[73] H. Li and Y. Shi. Network-based predictive control for constrained nonlinear systems with two-channel packet dropouts. *IEEE Transactions on Industrial Electronics*, accepted, April 2013.

[74] H. Li and Y. Shi. Networked min-max model predictive control of constrained nonlinear systems with delays and packet dropouts. *International Journal of Control*, pages 610–624, DOI:10.1080/00207179.2012.751628, 2013.

[75] L. Li and Y. Xia. Stochastic stability of the unscented kalman filter with intermittent observations. *Automatica*, (5):978–981, 2012.

[76] Z. Li, W. Wang, and Y. Jiang. Brief paper: Intelligent scheduling and optimisation for resource-constrained networks. *IET Control Theory & Applications*, 4(12):2982–2992, 2010.

[77] D. Limon, T. Alamo, F. Salas, and E. F. Camacho. Input to state stability of min-max MPC controllers for nonlinear systems with bounded uncertainties. *Automatica*, 42(5):797–803, 2006.

[78] G.-P. Liu. Predictive controller design of networked systems with communication delays and data loss. *IEEE Transactions on Circuits and Systems II: Express Briefs*, 57(6):481–485, 2010.

[79] G.-P. Liu, S. Chai, J. Mu, and D. Rees. Networked predictive control of systems with random delay in signal transmission channels. *International Journal of Systems Science*, 39(11):1055–1064, 2008.

[80] G.-P. Liu, Y. Xia, J. Chen, D. Rees, and W. Hu. Networked predictive control of systems with random network delays in both forward and feedback channels. *IEEE Transactions on Industrial Electronics*, 54(3):1282–1297, 2007.

[81] J. Liu, X. Chen, D. M. de la Peña, and P. D. Christofides. Sequential and iterative architectures for distributed model predictive control of nonlinear process systems. *AIChE Journal*, 56(8):2137–2149, 2010.

[82] J. Liu, X. Chen, D. M. de la Peña, and P. D. Christofides. Iterative distributed model predictive control of nonlinear systems: Handling asynchronous, delayed measurements. *IEEE Transactions on Automatic Control*, 57(2):528–534, 2012.

[83] J. Liu, D. M. de la Peña, and P. D. Christofides. Distributed model predictive control of nonlinear process systems. *AIChE Journal*, 55(5):1171–1184, 2009.

[84] J. Liu, D. Muñoz de la Peña, and P. D. Christofides. Distributed model predictive control of nonlinear systems subject to asynchronous and delayed measurements. *Automatica*, 46(1):52–61, 2010.

[85] J. Liu, D. Muñoz de la Peña, P. D. Christofides, and J. F. Davis. Lyapunov-based model predictive control of nonlinear systems subject to time-varying measurement delays. *International Journal of Adaptive Control and Signal Processing*, 23(8):788–807, 2009.

[86] C. Løvaas, M. M. Seron, and G. C. Goodwin. Robust output-feedback model predictive control for systems with unstructured uncertainty. *Automatica*, 44(8):1933–1943, 2008.

[87] W.J. Ma and V. Gupta. Input-to-state stability of hybrid systems with receding horizon control in the presence of packet dropouts. *Automatica*, 48(8):1920–1923, 2012.

[88] J. M. Maestre, D. M. de la Peña, and E. F. Camacho. Distributed model predictive control based on a cooperative game. *Optimal Control Applications and Methods*, 32(2):153–176, 2011.

[89] L. Magni, G. De Nicolao, R. Scattolini, and F. Allgöwer. Robust model predictive control for nonlinear discrete-time systems. *International Journal of Robust and Nonlinear Control*, 13(4):229–246, 2003.

[90] L. Magni, D. M. Raimondo, and R. Scattolini. Regional input-to-state stability for nonlinear model predictive control. *IEEE Transactions on Automatic Control*, 51(9):1548–1553, 2006.

[91] X. Mao. Robustness of stability of nonlinear systems with stochastic delay perturbations. *Systems & Control Letters*, 19(5):391–400, 1992.

[92] T. Matiakis, S. Hirche, and M. Buss. Control of networked systems using the scattering transformation. *IEEE Transactions on Control Systems Technology*, 17(1):60–67, 2009.

[93] D. Q. Mayne, S. V. Raković, R. Findeisen, and F. Allgöwer. Robust output feedback model predictive control of constrained linear systems. *Automatica*, 42(7):1217–1222, 2006.

[94] D. Q. Mayne, S. V. Raković, R. Findeisen, and F. Allgöwer. Robust output feedback model predictive control of constrained linear systems: Time varying case. *Automatica*, 45(9):2082–2087, 2009.

[95] D. Q. Mayne, J. B. Rawlings, C. V. Rao, and P. O. Scokaert. Constrained model predictive control: Stability and optimality. *Automatica*, 36(6):789–814, 2000.

[96] D. Q. Mayne, M. M. Seron, and S. V. Raković. Robust model predictive control of constrained linear systems with bounded disturbances. *Automatica*, 41(2):219–224, 2005.

[97] H. Michalska and D. Q. Mayne. Robust receding horizon control of constrained nonlinear systems. *IEEE Transactions on Automatic Control*, 38(11):1623–1633, 1993.

[98] T. Mori, N. Fukuma, and M. Kuwahara. Delay-independent stability criteria for discrete-delay systems. *IEEE Transactions on Automatic Control*, 27(4):964–966, 1982.

[99] N. Motee and B. Sayyar-Rodsari. Optimal partitioning in distributed model predictive control. In *Proceedings of the 2003 American Control Conference*, volume 6, pages 5300–5305, 2003.

[100] D. Muñoz de la Peña and P. D. Christofides. Lyapunov-based model predictive control of nonlinear systems subject to data losses. *IEEE Transactions on Automatic Control*, 53(9):2076–2089, 2008.

[101] D. Muñoz de la Peña and P. D. Christofides. Lyapunov-based model predictive control of nonlinear systems subject to data losses. *IEEE Transactions on Automatic Control*, 53(9):2076–2089, 2008.

[102] D. Muñoz de la Peña and P. D. Christofides. Output feedback control of nonlinear systems subject to sensor data losses. *Systems & Control Letters*, 57(8):631–642, 2008.

[103] D. Nešić and D. Liberzon. A unified framework for design and analysis of networked and quantized control systems. *IEEE Transactions on Automatic Control*, 54(4):732–747, 2009.

[104] D. Nešić and A. R. Teel. Input-to-state stability of networked control systems. *Automatica*, 40(12):2121–2128, 2004.

[105] S. K. Nguang and P. Shi. Nonlinear H_∞ filtering of sampled-data systems. *Automatica*, 36(2):303–310, 2000.

[106] S.-I. Niculescu, C. E. de Souza, L. Dugard, and J.-M. Dion. Robust exponential stability of uncertain systems with time-varying delays. *IEEE Transactions on Automatic Control*, 43(5):743–748, 1998.

[107] J. Nilsson. *Real-time Control Systems With Delays*. PhD thesis, Lund Institute of Technology, Lund, Sweden, 1998.

[108] J. Nilsson, B. Bernhardsson, and B. Wittenmark. Stochastic analysis and control of real-time systems with random time delays. *Automatica*, 34(1):57–64, 1998.

[109] C.-J. Ong and E. G. Gilbert. The minimal disturbance invariant set: Outer approximations via its partial sums. *Automatica*, 42(9):1563–1568, 2006.

[110] C.-J. Ong, D. Sui, and E. G. Gilbert. Enlarging the terminal region of nonlinear model predictive control using the support vector machine method. *Automatica*, 42(6):1011–1016, 2006.

[111] R. M. Palhares, C. E. de Souza, and P. L. D. Peres. Robust H_∞ filtering for uncertain discrete-time state-delayed systems. *IEEE Transactions on Signal Processing*, 49(8):1696–1703, 2001.

[112] A. W. Pila, U. Shaked, and C. E. de Souza. H_∞ filtering for continuous-time linear systems with delay. *IEEE Transcations on Automatic Control*, 44(7):1412–1417, 1999.

[113] G. Pin and T. Parisini. Networked predictive control of uncertain constrained nonlinear systems: recursive feasibility and input-to-state stability analysis. *IEEE Transactions on Automatic Control*, 56(1):72–87, 2011.

[114] I. G. Polushin, P. X. Liu, and C.-H. Lung. On the model-based approach to nonlinear networked control systems. *Automatica*, 44(9):2409–2414, 2008.

[115] S. J. Qin and T. A. Badgwell. An overview of nonlinear model predictive control applications. In *Nonlinear Predictive Control*. Verlag, 2000.

[116] S. J. Qin and T. A. Badgwell. A survey of industrial model predictive control technology. *Control Engineering Practice*, 11(7):733–764, 2003.

[117] J. Qiu, G. Feng, and J. Yang. Improved delay-dependent H_∞ filtering design for discrete-time polytopic linear delay systems. *IEEE Transactions on Circuits and Systems-II: Express Briefs*, 55(2):178–182, 2008.

[118] D. E. Quevedo and D. Nešić. On stochastic stability of packetized predictive control of non-linear systems over erasure channels. In *8th IFAC Symposium on Nonlinear Control Systems*, Bologna, Italy, 2010.

[119] D. E. Quevedo and D. Nešić. Input-to-state stability of packetized predictive control over unreliable networks affected by packet-dropouts. *Automatic Control, IEEE Transactions on*, 56(2):370–375, 2011.

[120] D. E. Quevedo and D. Nešić. Input-to-state stability of packetized predictive control over unreliable networks affected by packet-dropouts. *IEEE Transactions on Automatic Control*, 56(2):370–375, 2011.

[121] D. E. Quevedo and D. Nešić. Robust stability of packetized predictive control of nonlinear systems with disturbances and markovian packet losses. *Automatica*, to appear.

[122] D. E. Quevedo, J. Østergaard, and D. Nešić. Packetized predictive control of stochastic systems over bit-rate limited channels with packet loss. *IEEE Transactions on Automatic Control*, 56(12):2854–2868, 2011.

[123] D. M. Raimondo. *Nonlinear Model Predictive Control Stability, Robustness and Applications*. PhD thesis, 2008.

[124] D. M. Raimondo, L. Magni, and R. Scattolini. Decentralized MPC of nonlinear systems: An input-to-state stability approach. *International Journal of Robust and Nonlinear Control*, 17(17):1651–1667, 2007.

[125] S. V. Raković, E. C. Kerrigan, K. I. Kouramas, and D. Q. Mayne. Invariant approximations of the minimal robust positively invariant set. *IEEE Transactions on Automatic Control*, 50(3):406–410, 2005.

[126] S. V. Raković, E. C. Kerrigan, D. Q. Mayne, and K. I. Kouramas. Optimized robust control invariance for linear discrete-time systems: Theoretical foundations. *Automatica*, 43(5):831–841, 2007.

[127] J. B. Rawlings and B. T. Stewart. Coordinating multiple optimization-based controllers: New opportunities and challenges. *Journal of Process Control*, 18(9):839–845, 2008.

[128] M. Reble, D. E. Quevedo, and F. Allgöwer. Stochastic stability and performance estimates of packetized unconstrained model predictive control for networked control systems. In *9th IEEE International Conference on Control and Automation (ICCA)*, pages 171–176, 2011.

[129] M. Reble, D. E. Quevedo, and F. Allgöwer. Control over erasure channels: stochastic stability and performance of packetized unconstrained model predictive control. *International Journal of Robust and Nonlinear Control*, 2012, in press.

[130] A. Richards and J. P. How. Robust distributed model predictive control. *International Journal of Control*, 80(9):1517–1531, 2007.

[131] S. M. Ross. *Introduction to Probability Models*. Academic Press, Inc., 2006.

[132] L. Schenato, B. Sinopoli, M. Franceschetti, K. Poolla, and S. S. Sastry. Foundations of control and estimation over lossy networks. *Proceedings of the IEEE*, 95(1):163–187, 2007.

[133] P. O. M. Scokaert and D. Q. Mayne. Min-max feedback model predictive control for constrained linear systems. *IEEE Transactions on Automatic Control*, 43(8):1136–1142, 1998.

[134] U. Shaked and N. Berman. H_∞ nonlinear filtering of discrete-time processes. *IEEE Transactions on Signal Processing*, 43(9):2205–2209, 1995.

[135] B. Shen, Z. Wang, Y. S. Hung, and G. Chesi. Distributed H_∞ filtering for polynomial nonlinear stochastic systems in sensor networks. *IEEE Transactions on Industrial Electronics*, 58(5):1971–1979, 2011.

[136] B. Shen, Z. Wang, H. Shu, and G. Wei. On nonlinear H_∞ filtering for discrete-time stochastic systems with missing measurements. *IEEE Transactions on Automatic Control*, 53(9):2170–2180, 2008.

[137] B. Shen, Z. Wang, H. Shu, and G. Wei. H_∞ filtering for nonlinear discrete-time stochastic systems with randomly varying sensor delays. *Automatica*, 45(4):1032–1037, 2009.

[138] B. Shen, Z. Wang, H. Shu, and G. Wei. H_∞ filtering for uncertain time-varying systems with multiple randomly occurred nonlinearities and successive packet dropouts. *International Journal of Robust and Nonlinear Control*, 21(14):1693–1709, 2010.

[139] B. Shen, Z. Wang, H. Shu, and G. Wei. Robust H_∞ finite-horizon filtering with randomly occurred nonlinearities and quantization effects. *Automatica*, 46(11):1743–1751, 2010.

[140] Y. Shi and B. Yu. Output feedback stabilization of networked control systems with random delays modeled by markov chains. *IEEE Transactions on Automatic Control*, 54(7):1668–1674, 2009.

[141] Y. Shi and B. Yu. Robust mixed H_2/H_∞ control of networked control systems with random time delays in both forward and backward communication links. *Automatica*, 47(4):754–760, 2011.

[142] B. Sinopoli, L. Schenato, M. Franceschetti, K. Poolla, M. I. Jordan, and S. S. Sastry. Kalman filtering with intermittent observations. *IEEE Transactions on Automatic Control*, 49(9):1453–1464, 2004.

[143] E. D. Sontag and Y. Wang. On characterizations of the input-to-state stability property. *Systems & Control Letters*, 24(5):351–359, 1995.

[144] E. D. Sontag and Y. Wang. New characterizations of input-to-state stability. *IEEE Transactions on Automatic Control*, 41(9):1283–1294, 1996.

[145] B. T. Stewart, A. N. Venkat, J. B. Rawlings, S. J. Wright, and G. Pannocchia. Cooperative distributed model predictive control. *Systems & Control Letters*, 59(8):460–469, 2010.

[146] B. T. Stewart, S. J. Wright, and J. B. Rawlings. Cooperative distributed model predictive control for nonlinear systems. *Journal of Process Control*, 21(5):698–704, 2011.

[147] M. Tabbara, D. Nešić, and A. R. Teel. Networked control systems: Emulation-based design. In *Networked Control Systems*, pages 57–94. Springer London, 2008.

[148] P. L. Tang and C. W. de Silva. Compensation for transmission delays in an ethernet-based control network using variable-horizon predictive control. *IEEE Transactions on Control Systems Technology*, 14(4):707–718, 2006.

[149] K. Tsumura, H. Ishii, and H. Hoshina. Tradeoffs between quantization and packet loss in networked control of linear systems. *Automatica*, 45(12):2963–2970, 2009.

[150] A. N. Venkat, I. A. Hiskens, J. B. Rawlings, and S. J. Wright. Distributed MPC strategies with application to power system automatic generation control. *IEEE Transactions on Control Systems Technology*, 16(6):1192–1206, 2008.

[151] G. C. Walsh, O. Beldiman, and L. G. Bushnell. Asymptotic behavior of nonlinear networked control systems. *IEEE Transactions on Automatic Control*, 46(7):1093–1097, 2001.

[152] G. C. Walsh, Y. Hong, and L. G. Bushnell. Stability analysis of networked control systems. *IEEE Transactions on Control Systems Technology*, 10(3):438–446, 2002.

[153] R. Wang, G.-P. Liu, W. Wang, D. Rees, and Y. Zhao. H_∞ control for networked predictive control systems based on the switched lyapunov function method. *IEEE transactions on industrial electronics*, 57(10):3565, 2010.

[154] R. Wang, G.-P. Liu, W. Wang, D. Rees, and Y. Zhao. Guaranteed cost control for networked control systems based on an improved predictive control method. *IEEE Transactions on Control Systems Technology*, 18(5):1226–1232, 2010.

[155] R. Wang, G.-P. Liu, W. Wang, D. Rees, and Y.-B. Zhao. H_∞ control for networked predictive control systems based on the switched Lyapunov function method. *IEEE Transactions on Industrial Electronics*, 57(10):3565–3571, 2010.

[156] W. Wang, D. E. Rivera, and K. G. Kempf. Centralized model predictive control strategies for inventory management in semiconductor manufacturing supply chains. In *Proceedings of the 2003 American Control Conference*, pages 585–590, 2003.

[157] Z. Wang, D. W. C. Ho, Y. Liu, and X. Liu. Robust H_∞ control for a class of nonlinear discrete time-delay stochastic systems with missing measurements. *Automatica*, 45:684–691, 2009.

[158] Z. Wang, B. Huang, and H. Unbehauenc. Robust H_∞ observer design of linear time-delay systems with parametric uncertainty. *Systems & Control Letters*, 42(4):303–312, 2001.

[159] Z. Wang, B. Shen, and X. Liu. H_∞ filtering with randomly occurring sensor saturations and missing measurements. *Automatica*, 43(8):556–562, 2012.

[160] Z. Wang, B. Shen, H. Shu, and G. Wei. Quantized H_∞ control for nonlinear stochastic time-delay systems with missing measurements. *IEEE Transactions on Automatic Control*, 57(6):1431–1444, 2012.

[161] G. Wei, Z. Wang, and H. Shu. Robust filtering with stochastic nonlinearities and multiple missing measurements. *Automatica*, 45(3):836–841, 2009.

[162] J. Wu, L. Zhang, and T. Chen. Model predictive control for networked control systems. *International Journal of Robust and Nonlinear Control*, 19(9):1016–1035, 2008.

[163] Y. Xia, G.-P. Liu, M. Fu, and D. Rees. Predictive control of networked systems with random delay and data dropout. *IET Control Theory & Applications*, 3(11):1476–1486, 2009.

[164] L. Xie. Control over communication networks: Trend and challenges in integrating control theory and information theory. In *Proceedings of the 30th Chinese Control Conference (CCC)*, pages 35–39, 2011.

[165] L. Xie, L. Liu, D. Zhang, and H. Zhang. Improved robust H_2 and H_∞ filtering for uncertain discrete-time systems. *Automatica*, 40(5):873–880, 2004.

[166] S. Xu. Robust H_∞ filtering for a class of discrete-time uncertain nonlinear systems with state delay. *IEEE Transactions on Circuits and Systems-I: Fundamental Theory and Applications*, 49(12):1853–1859, 2002.

[167] B. Xue, N. Li, S. Li, and Q. Zhu. Robust model predictive control for networked control systems with quantisation. *IET Control Theory & Applications*, 4(12):2896–2906, 2010.

[168] R. Yang, P. Shi, and G. Liu. Filtering for discrete-time networked nonlinear systems with mixed random delays and packet dropouts. *IEEE Transactions on Automatic Control,*, 56(11):2655–2660, 2011.

[169] T. C. Yang. Networked control system: A brief survey. *IEE Proceedings of Control Theory and Applications*, 153(4):403–412, 2006.

[170] B. Yu. Networked control system design and parameter estimation. Master thesis, University of Saskatchewan, 2008.

[171] B. Yu, Y. Shi, and J. Huang. Modified generalized predictive control of networked systems with application to a hydraulic position control system. *ASME Journal of Dynamic Systems, Measurement, and Control*, 133(3), 2011.

[172] D. Yue, C. Peng, and G. Y. Tang. Guaranteed cost control of linear systems over networks with state and input quantisations. *IEE Proceedings of Control Theory and Applications*, 153(6):658–664, 2006.

[173] S. Zampieri. Trends in networked control systems. In *17th IFAC World Congress*, pages 2886–2894, 2008.

[174] H. Zhang. *Robust tracking control and signal estimation for networked control systems*. PhD Thesis, University of Victoria, 2012.

[175] H. Zhang, Y. Shi, and A. Saadat Mehr. Robust energy-to-peak filtering for networked systems with time-varying delays and randomly missing data. *IET Control Theory & Applications*, 4(12):2921–2936, 2010.

[176] H. Zhang, D. Zhang, and L. Xie. An innovation approach to H_∞ prediction with application to systems with delayed measurements. *Automatica*, 40(7):1253–1261, 2004.

[177] L. Zhang, Y. Shi, T. Chen, and B. Huang. A new method for stabilization of networked control systems with random delays. *IEEE Transactions on Automatic Control*, 50(8):1177–1181, 2005.

[178] W. Zhang, M. S. Branicky, and S. M. Phillips. Stability of networked control systems. *IEEE Control Systems Magazine*, 21(1):84–99, 2001.

[179] W. Zhang, B.-S. Chen, and C.-S. Tseng. Robust H_∞ filtering for nonlinear stochastic systems. *IEEE Transactions on Signal Processing*, 53(2):589–598, 2005.

[180] X. Zhang and Q. Han. Delay-dependent robust H_∞ filtering for uncertain discrete-time systems with time-varying delay based on a finite sum inequality. *IEEE Transactions on Circuits and Systems-II: Express Briefs*, 53(12):1466–1470, 2006.

Appendix A

Publications

- **Refereed Journal Papers**

  1. **H. Li** and Y. Shi, "Network-based predictive control for constrained nonlinear systems with two-channel packet dropouts," *IEEE Transactions on Industrial Electronics*, accepted, April 2013.
  2. **H. Li** and Y. Shi, "Robust output feedback model predictive control for constrained linear systems with intermittent measurement," *Systems & Control Letters*, vol. 62, no. 4, pp. 345-354, 2013.
  3. **H. Li** and Y. Shi, "Networked min-max model predictive control of constrained nonlinear systems with delays and packet dropouts," *International Journal of Control*, DOI:10.1080/00207179.2012.751628, pp. 610-624, 2012.
  4. **H. Li** and Y. Shi, "State-feedback H_∞ control for stochastic time-delay nonlinear systems with state and disturbance-dependent noise," *International Journal of Control*, vol. 85, no.10, pp. 1515-1531, 2012.
  5. **H. Li** and Y. Shi, "Robust H_∞ filtering for nonlinear stochastic systems with uncertainties and random delays modeled by Markov chains," *Automatica*, vol. 48, no. 1, pp. 159-166, 2012.

- **Journal Papers Under Review/Revision**

  6. **H. Li** and Y. Shi, "Event-triggered robust model predictive control of nonlinear systems with disturbances," submitted to *Automatica*, 2013.

7. **H. Li** and Y. Shi, "Robust distributed model predictive control of continuous-time nonlinear systems: Handling communication delays and disturbances," submitted to *Automatica*, under revision for the first-round review, 2012.
8. **H. Li** and Y. Shi, "Distributed model predictive control of continuous-time nonlinear systems with communication delays," submitted to *Systems & Control Letters*, under revision for the first-round review, 2012.
9. **H. Li** and Y. Shi, "Robust distributed model predictive control of constrained continuous-time nonlinear systems," submitted to *IEEE Transactions on Automatic Control*, under revision for the first-round review, 2012.
10. **H. Li** and Y. Shi, "Dissipation-based output feedback control of stochastic nonlinear time-delay systems," submitted to *International Journal of Control*, under revision for the first-round review, 2012.

- **Refereed Conference Papers**

1. **H. Li** and Y. Shi, "Consensus-based distributed receding horizon estimation of sensor networks," in Proceedings of *The 2013 Chinese Control Conference*, Xi'an, China, July 2013.
2. **H. Li** and Y. Shi, "Distributed receding horizon control of constrained linear systems with communication delays," in Proceedings of *The 2013 American Control Conference*, Washington DC, USA, June 2013.
3. **H. Li** and Y. Shi, "Delay-dependent state-feedback H_∞ control for nonlinear stochastic systems with time-varying delays," in Proceedings of *the 51st IEEE Conference on Decision and Control*, Maui, Hawaii, USA, December 2012, pp. 4279-4284.
4. **H. Li** and Y. Shi, "Dissipativity based H_∞ control for nonlinear stochastic systems with time-varying delays," in Proceedings of *the 50th IEEE Conference on Decision and Control and European Control Conference*, Orland, USA, December 2011, pp. 3240-3245.